

Instituto de Investigaciones Químicas
Departamento de Química Inorgánica



**Tautomería de heterociclos nitrogenados mediante
complejos de iridio(III) con formación de carbenos
N-heterocíclicos**

Ana Rita Guerreiro De Brito Petronilho

Sevilla, 2010

Tautomería de heterociclos nitrogenados mediante complejos de iridio(III) con formación de carbenos N-heterocíclicos

por

Ana Rita Guerreiro de Brito Petronilho

Trabajo presentado para aspirar al

Título de Doctora en Química

Sevilla, 2010

Fdo: Ana Rita Guerreiro de Brito Petronilho

Los Directores:

Ernesto Carmona Guzmán
Catedrático de Química Inorgánica
(Universidad de Sevilla)

Manuel López Poveda
Profesor de Investigación
(CSIC)

Margarita Paneque Sosa
Profesora de Investigación
(CSIC)

Aos meus pais



René Magritte, *La Clairvoyance*, 1936

Utopía: Plan, proyecto, doctrina o sistema optimista que aparece como irrealizable en el momento de su formulación.

Agradecimientos

La realización de esta tesis doctoral hubiera sido imposible sin la contribución valiosa de algunas personas, a quien deseo agradecer:

En primer lugar, a mis Directores: al Profesor Ernesto Carmona, que con su entusiasmo, dedicación y preocupación es una fuente de inspiración y ejemplo para quienes tenemos el privilegio de convivir de su cordialidad, sabiduría y capacidad de trabajo; al Dr. Manuel López Poveda, por contribuir enormemente para la mejoría de mi raciocinio químico y por el esfuerzo y la ayuda prestada para que esta tesis llegara a su final; a la Dra. Margarita Paneque, por la preocupación, el apoyo y la confianza prestado durante la realización de esta tesis.

Al Ministerio de Educación y Ciencia por la concesión de una beca FPI y a la Fundação para a Ciência e a Tecnologia por la concesión de una Bolsa de Doutoramento.

Al Dr. Salvador Conejero que ha contribuido en parte de los resultados experimentales que se presentan, y a quien agradezco la enorme paciencia en los inicios de esta tesis y las fructíferas discusiones químicas a lo largo de estos años. Su contribución a mi formación es inestimable, fruto de su gran capacidad científica y paciencia para escuchar mis *carbénicos* planteamientos. Que todo siga descarboxilando...

A los Dres. Eleuterio Álvarez y Celia Maya por los estudios de Difracción de Rayos X. Al Dr. Joaquín López Serrano por la realización de los cálculos teóricos.

A mis compañeros de Laboratório 1-2 por compartir conmigo los buenos ratos y las frustraciones, por alegrarse cuando todo iba bien y preocuparse cuando no iba tan bien. A Amorín, cuya frontalidad mucho aprecio, que además me ha sido de mucha utilidad estos años y por quien guardo una admiración enorme por su *estoicismo temprano*... y al ente llamado “Salva y Amor” por los inmejorables almuerzos. A Laura, Nuria y Margot, que me han introducido al *andalúh* y al *miarmismo* desde aquel ya lejano Erasmus en que el 1-2 era el labo de las niñas. A Patri, mi compañera de tesis, de vitrina y de mesa, inventora del *petrinombramiento*, a quien

todo lo que tengo que agradecer no cabría aquí. A José Enrique, nuestro organizador de eventos, por tu buen carácter que tanto estimo y humor (las arañas no tienen gracia, y no voy a encender la *salsaparrilla*, así que no insistas.). A Flo y Yohar, (la *famiglia piridina*), Cristina (mi compañera de nervios), a Irene y Mario (1º, el monoarilo, 2º...) y Joaquín. A Riccardo, el políglota *bonvivant*, porque aunque te guste la copla, eres un encanto de persona. A Oracio (*sinh*) y a Verónica. A los compañeros del 9, Marta, Jesús, Orestes y Crispín y a los de al *lao*: a Mikael, con quien aprendí que se puede tener siempre la razón, pero hay que leer a Shopenhauer; Mari Ángeles, por su sonrisa constante (tienes que empezar a dar clases de felicidad), Luismi (L.M.R.....) y Antonio (contribución cargador Mac). A las niñas del 11, y también a los compañeros de orgánica, en especial a Ainhoa. A mi querida Marina, mi compañera desde el Erasmus (el C1, el C2...nos queda el griego.).

A mi pandilla sevillana... Cristina (tigres enanos bajo la lluvia... que haría yo sin ti...) y Carmen (tu crema de calabacines = gasolina tesinal), mis niñas del 24; Pepa y Ozecai (los marqueses), Índio, Amparo, Ricardo, Iban, Ema (sí, con m.), Pombinho, Odil y Emilie, con quien compartí mi vida durante estos años... por hacerme sentir en casa, haciendo de esta ciudad la mía también. A la Sirena y sus sirenidos, por mis cafés tardíos postlabo y mis cervecitas de fin de semana.

À Susa e Tânia, Ana Rebeca, Zé, Dani e Mi, a minha segunda família desde os tempos do Liceu, com quem partilhei e partilho tormentas e grandes dias de sol. Dani, continuas comigo. À brigada do reumático do IST, em particular ao Munhá, pelos discussões via skype, e pelo enorme apoio, sem olhar a quilómetros, no meu primeiro ano de tese.

Aos meus pais, pelos esforços e sacrificios para que pudesse obter a formação que desejava. Pelos conselhos e pelo respeito que sempre tiveram pelas minhas escolhas. À minha mãe, por incutir-me desde sempre um espírito de independência, e por ser dona de uma sensatez que algum dia espero ter também. Ao meu pai, por transmitir-me o meu espírito lutador e inquietude para arriscar.

E finalmente à minha irmã Raquel, pela paciência (e eu sei que é muita), pelo carinho, pelas chaves da tua casa cada vez que vou para Lisboa às tantas, e pela quantidade de abraços que mereces e não te dou.

Índice

Consideraciones generales	1
Abreviaturas	9
I. Introducción	15
I.1. Coordinación de las piridinas en complejos de los metales de transición	16
I.1.1. Aspectos generales	16
I.1.2. Modos de coordinación	19
I.2. Activación de enlaces C–H en piridinas	22
I.3. Formación de tautómeros de la piridina	29
I.3.1. Consideraciones generales	29
I.3.2. Formación de carbenos derivados de las piridinas promovida por complejos de los metales de transición	33
I.3.2.1. Métodos clásicos	33
I.3.2.2. Tautomería de piridinas con formación de carbenos N-heterocíclicos promovida por complejos de metales de transición	36
I.3.3. Tautomería de heterociclos derivados del imidazol inducida por complejos de metales de transición	39
I.4. Bibliografía	42

II. Results and Discussion	49
II.1. Reaction of $\text{Tp}^{\text{Me}_2}\text{IrPh}_2(\text{N}_2)$ with Pyridines	52
II.1.1. Reaction of $\text{Tp}^{\text{Me}_2}\text{IrPh}_2(\text{N}_2)$ with 2-Picoline	52
II.1.1.1. Synthesis of the N-Heterocyclic Carbene Complex 2	52
II.1.1.2. Synthesis of the N-Bound Adduct 3	56
II.1.1.3. Isotopic Studies: Exchange Reactions and Determination of the Kinetic Isotopic Effect	59
II.1.2. Reactions of $\text{Tp}^{\text{Me}_2}\text{IrPh}_2(\text{N}_2)$ with 2-Phenylpyridine	61
II.1.2.1. Synthesis of the N-Heterocyclic Carbene Complex 4	61
II.1.2.2. Synthesis of Complex 5. Trapping with H_2O a Plausible Intermediate?	63
II.1.2.3. Reactivity of Complex 5	66
II.1.2.4. Generation of the Carbonyl Derivative 6	67
II.1.3. Reactions of $\text{Tp}^{\text{Me}_2}\text{IrPh}_2(\text{N}_2)$ with other Pyridines	68
II.1.3.1. Reactions with 2-tert-Butylpyridine and 2-Dimethylaminopyridine. Synthesis of N-Heterocyclic Carbenes 7 and 8	68
II.1.3.2. Reactions with Pyridine, 3-Phenylpyridine, 4-Phenylpyridine and 4-Dimethylaminopyridine: Synthesis of complexes 9 - 12	70
II.1.3.3. Variable Temperature ^1H NMR Studies with Complex 9	73
II.1.3.4. Attempts of Synthesis of Carbenes Derived from 9 - 12	76

II.1.3.5. Competition Experiments	77
II.1.3.6. Reaction of 1 with 2,6-Lutidine: Activation of a Pyridine Lacking C–H Bonds Adjacent to Nitrogen	78
II.1.4. Some general comments on the Tautomerization of Pyridines by $[\text{Tp}^{\text{Me}_2}\text{Ir(III)Ph}_2]$ Species	81
II.1.4.1. Mechanism of Carbene Formation with 2-Substituted Pyridines	84
II.1.4.2. Mechanistic Considerations on Somewhat Related Systems	86
II.1.4.3. On the Stability of N-Heterocyclic Carbenes Derived from Pyridines: some considerations	90
II.1.5. Generalization of the Tautomerization Processes to other N-Heterocycles: Studies with Quinolines and Polypyridines	92
II.1.5.1. Reaction of $\text{Tp}^{\text{Me}_2}\text{IrPh}_2(\text{N}_2)$ with Quinolines	92
II.1.5.1.1. Generation of Complexes 14 and 15	92
II.1.5.1.2. Synthesis of Complex 16 . Trapping an Active Intermediate with Quinoline	94
II.1.5.1.3. Reactivity of Complex 16	95
II.1.5.1.4. Reaction of 1 with Isoquinoline	98
II.1.5.2. Study of Polypyridine Reactions	99
II.1.5.2.1. 2,2'-Bipyridine	100
II.1.5.2.2. Phenantroline	103
II.1.5.2.3. Terpyridine	105

II.1.5.2.4.	4,4'-Bypiridine	107
I.2.	Reactivity of the N-heterocyclic Carbenes Derived from Pyridines	109
II.2.1.	Reactivity of Compounds 2 and 4 towards Alkenes	111
II.2.1.1.	Reaction with Ethylene	111
II.2.1.2.	Light Effects on the NMR Spectra of Complex 26	116
II.2.1.3.	Reaction with Propene	120
II.2.1.4.	Selective C–H Bond Activation and C–C Bond Formation: Activation of the Methyl Group of Propene	127
II.2.2.	Reactivity of Carbenes 2 and 4 Towards CO	128
II.2.3.	Reactivity of Carbene 2 Towards NCCH₃	129
II.2.4.	Reactivity of 4 towards 2-Phenylpyridine	130
II.2.5.	Reactivity of 4 towards Alkynes	132
II.2.5.1.	Reactivity of 4 towards Acetylene	132
II.2.5.2.	Reactivity of 4 towards Phenylacetylene	136
II.3.	Bibliography	138
III.	Parte experimental	149
IV.	Apéndice I	225
V.	Conclusiones	257

Consideraciones generales

La Química Organometálica de los metales de transición ha experimentado un desarrollo extraordinario desde mediados del siglo XX. Durante este período los complejos organometálicos de los metales de transición han sido responsables del desarrollo de nuevos procesos sintéticos y catalíticos, de enorme impacto en la calidad de vida de la sociedad actual, debido, entre otros, a descubrimientos tan importantes como la catálisis de polimerización de olefinas, la catálisis asimétrica y la de metátesis de olefinas. Actualmente, la química organometálica se enfrenta a nuevos retos, protagonizando un papel crucial en el descubrimiento de nuevos materiales, nuevas formas de obtención de energía, y en la mejora y desarrollo de procesos industriales. Asimismo, la investigación fundamental en química organometálica es de interés prioritario ya que permite alcanzar un conocimiento detallado de las etapas fundamentales de diferentes transformaciones de interés.

Los resultados que se presentan en esta Memoria se encuadran en una de las líneas de investigación que desarrolla el grupo de Química Organometálica y Catálisis Homogénea del Instituto de Investigaciones Químicas (Centro Mixto Universidad de Sevilla-CSIC), que tiene como objetivo el estudio de las reacciones de ruptura y formación de enlaces C—H, C—O, C—C y otros similares, inducidas de manera selectiva por complejos de metales del grupo 9.

En el presente trabajo se han llevado a cabo diversos estudios fundamentales sobre procesos básicos en Química Organometálica. Las investigaciones realizadas han

permitido profundizar en aspectos de tanta importancia como la funcionalización de algunas moléculas, saturadas o insaturadas, el esclarecimiento de aspectos estructurales y de reactividad, etc. Los experimentos que se describen incluyen la síntesis de compuestos organometálicos derivados de piridinas y polipiridinas, y en particular el estudio de la transformación de estas moléculas en sus tautómeros de tipo carbeno N-heterocíclico, en procesos que implican ruptura de enlaces C—H y la formación de enlaces N—H. Se describe asimismo su reactividad y su caracterización estructural mediante técnicas espectroscópicas y en algunos casos de difracción de rayos X. Estas últimas determinaciones se han llevado a cabo de manera independiente por los Dres. Celia Maya y Eleuterio Álvarez. Se han utilizado complejos estabilizados por ligandos de tipo polipirazolilborato, en concreto el ligando hidrotris(3,5-dimetilpirazolil)borato.¹

Su contenido se presenta siguiendo una estructura clásica: **Introducción, Resultados y Discusión y Parte Experimental**. Para facilitar su lectura, la bibliografía aparece a pie de página y también al final de cada capítulo. La numeración de las ecuaciones es independiente en cada capítulo; asimismo, en la Introducción, las ecuaciones se encuentran numeradas mediante números romanos consecutivos, mientras que en el capítulo “Resultados y Discusión” se numeran con números arábigos. Las figuras, las tablas y los esquemas presentan el número correspondiente a cada capítulo (I ó II), seguido del número arábigo consecutivo correspondiente. La numeración de los compuestos es única para todo el escrito y su identificación se ha realizado mediante números arábigos consecutivos. Dado que el español no es la lengua materna de la autora de esta Tesis Doctoral, y que el inglés es el idioma científico por excelencia, se ha considerado de interés redactar una parte de esta Memoria en dicho idioma.

Las Tablas A1-A30, correspondientes a las distancias y ángulos de enlace seleccionados y a los datos cristalográficos para los compuestos caracterizados mediante difracción de rayos X, aparecen en el Apéndice I.

¹ a) Trofimenko, S. *Chem. Rev.* **1993**, 93, 943. b) Parkin, G. *Adv. Inorg. Chem.* **1995**, 42, 291. c) Kitajima, N.; Tolman, W.B. *Prog. Inorg. Chem.* **1995**, 43, 418. d) Trofimenko, S. *Scorpionates. The Coordination Chemistry of Polypyrazolylborate Ligands*. Imperial College Press: London, **1999**.

El objetivo fundamental de esta Tesis Doctoral es el estudio de la reacción de diversas piridinas con complejos de Ir(III). En estos procesos, se produce la tautomería de piridinas sustituidas por activación múltiple de enlaces C—H, obteniéndose como resultado complejos de tipo carbeno, y también las reacciones de los compuestos anteriores con olefinas y alquinos, con formación de enlaces C—N.

Una parte de los resultados obtenidos se ha publicado en forma preliminar, mientras que otras secciones son todavía inéditas. A continuación se relacionan los artículos derivados de esta Tesis que ya están publicados. A esta relación le sigue la de los nuevos compuestos que se han obtenido y caracterizado, y finalmente la lista de abreviaturas usadas en la Memoria.

General Considerations

The organometallic chemistry of the transition metals accomplished an extraordinary development since the second half of the 20th century. During this period, organometallic complexes have been responsible for the appearance of new synthetic and catalytic processes of immense impact in society, due to important achievements that include, among others, olefin polymerization, asymmetric catalysis and olefin metathesis. Nowadays, organometallic chemistry faces new challenges, having a crucial role in the discovery of new materials, development of new methods for the generation of energy and the improvement and advancement of industrial processes. Thus, basic investigation in the field is of primary interest since it would provide a detailed knowledge of the elemental steps involved in the aforementioned transformations.

The results presented in this Thesis may be viewed as part of one of the research projects developed by the organometallic chemistry group at the Instituto de Investigaciones Químicas (joint center of the Universidad de Sevilla-Consejo Superior de Investigaciones Científicas), namely that dealing with the study of the formation and breaking of C—H, C—O and C—C bonds, induced by complexes of rhodium and iridium stabilized by coordination to bulky polydentate ligands.

In the present work, studies on some fundamental processes in organometallic chemistry have been performed. This research allowed us to gain insight into aspects related to the functionalization of some saturated and unsaturated molecules, and has also permitted to clarify structural and reactivity issues of the investigated systems. The experiments described include the synthesis of organometallic complexes, derived from pyridines and polypyridines and, in particular, the study of the transformation of these molecules into the corresponding N-heterocyclic carbene tautomers. These processes imply the rupture of a C—H bond and generation of a N—H bond. The reactivity of the generated complexes is also described whereas their structural characterization has been performed, by means of spectroscopic techniques and in some cases X-ray diffraction studies. The latter were conducted independently by Dr. Celia Maya and Dr. Eleuterio Álvarez. Complexes stabilized by poly(pyrazolyl)borate ligands were used, in particular hydrotris(3,5-dimethylpyrazolyl)borate.¹

The contents of the Thesis follow the classical structure: **Introduction, Results and Discussion, and Experimental Part**. To facilitate the reading, references are indicated at the end of the page and also at the end of each chapter, when convenient. The numbering of Equations is independent for each chapter. Thus for the **Introduction** section equations follow consecutive Roman numerals, whereas for **Results and Discussion** equations are represented by Arabic consecutive numerals. Figures, tables and schemes are designated with the number of corresponding chapter (I or II), and consecutive Arabic numerals thereafter. With respect to the new compounds, the numbering scheme is the common one and therefore follows consecutive Arabic numerals. Intermediates are referenced by letters **A** to **F**. Since Spanish is not the main language of the author of this manuscript, it was considered of interest to write part of the Thesis in English.

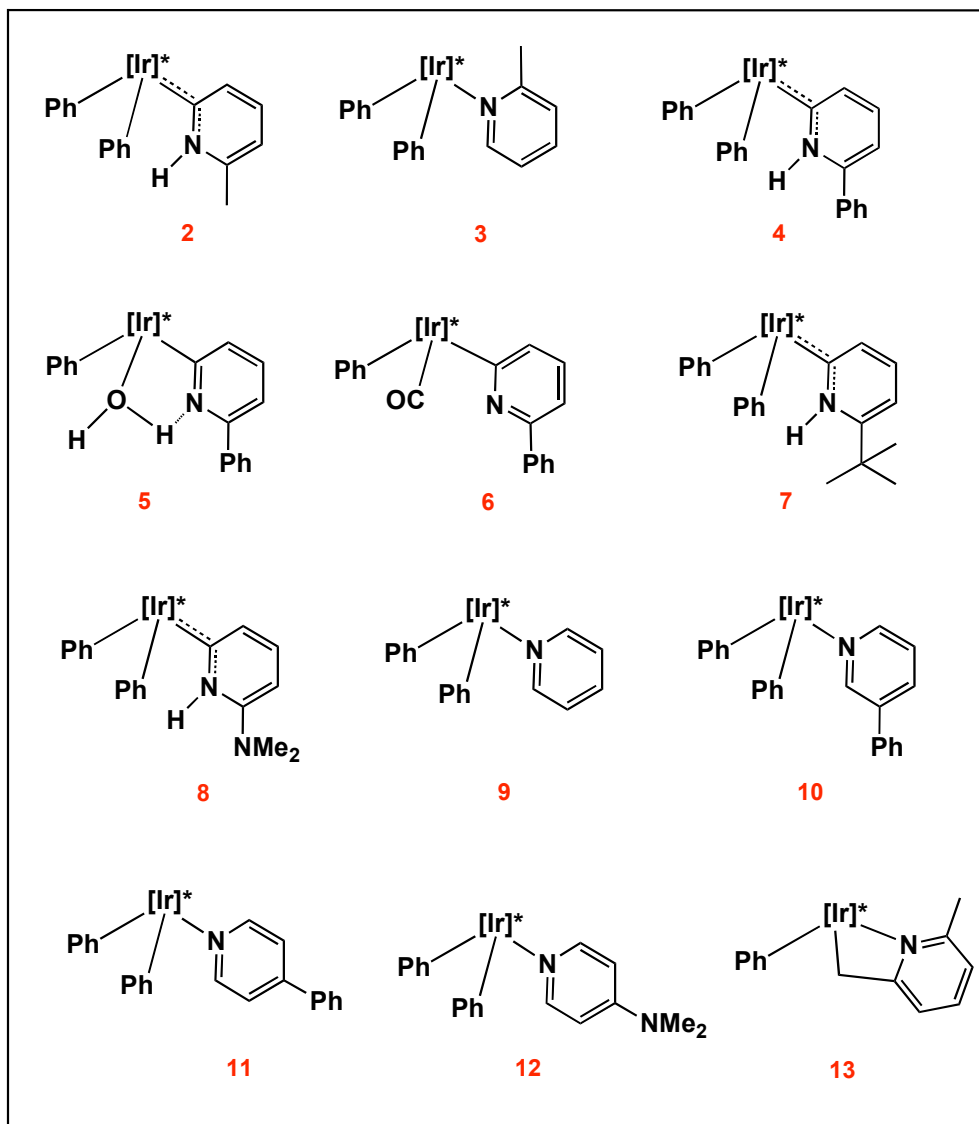
Tables A1-A30, containing selected bond distances and angles as well as the crystallographic data for the compounds characterized by X-ray diffraction studies are shown in Appendix 1.

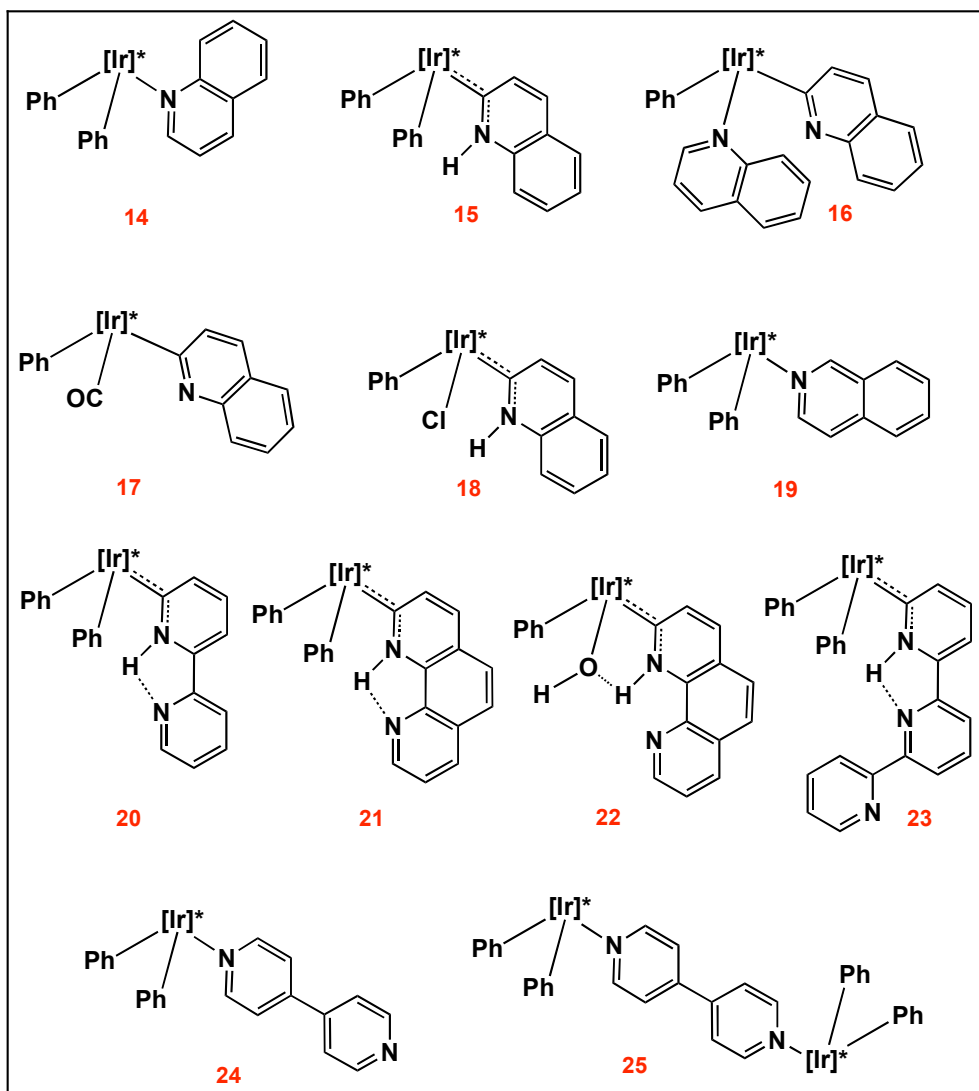
The aim of this Doctoral thesis is the study of the reaction of several pyridines with Ir(III) complexes.

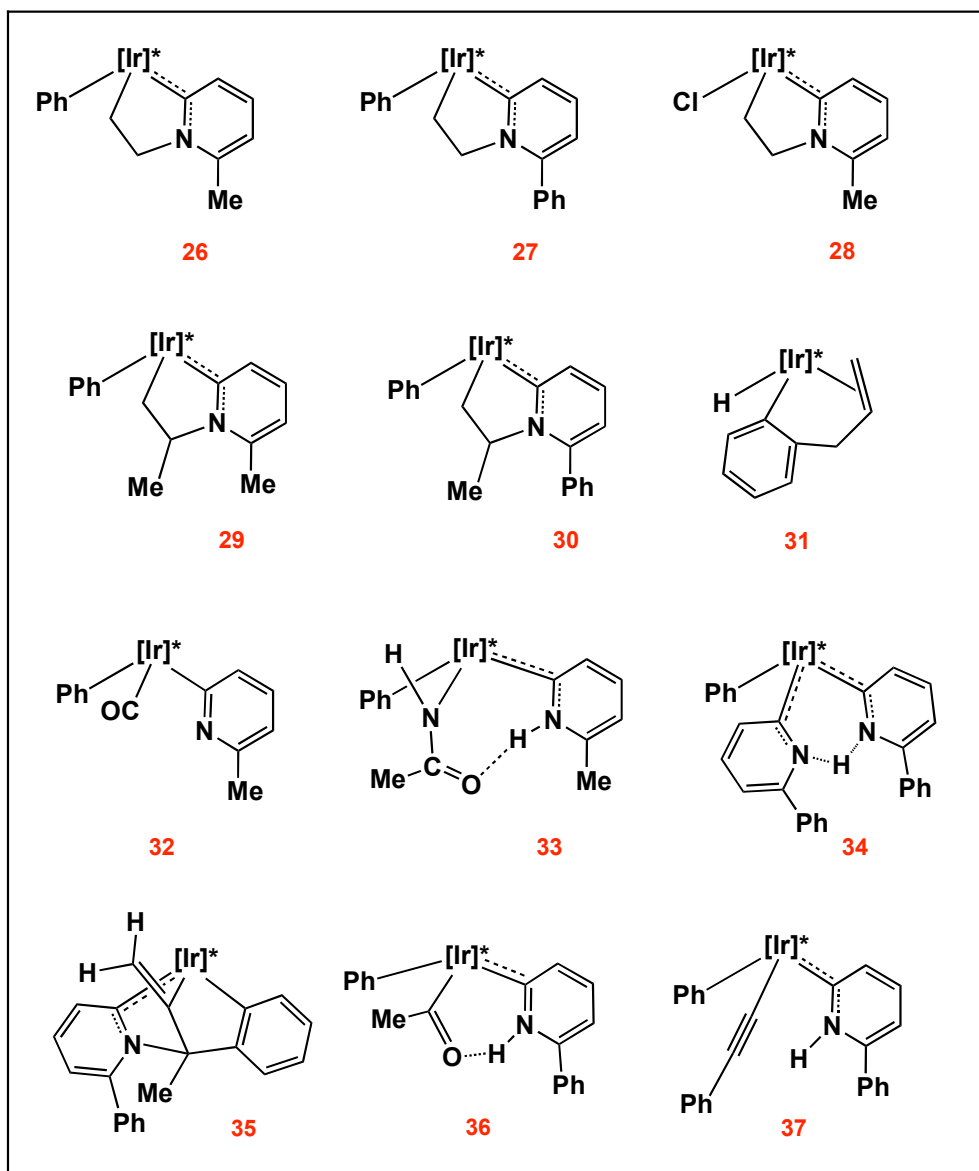
Part of the results described in the Thesis has been already reported in preliminary form. A list of the publications derived from the work developed within this Thesis is indicated bellow. This is followed by the list of new compounds obtained and then by the abbreviations used in the manuscript.

Publicaciones

1. “*Iridium induced Isomerization of 2-substituted Pyridines to N-Heterocyclic Carbenes*” E. Álvarez, S. Conejero, M. Paneque, A. Petronilho, M. L. Poveda, Oracio Serrano, E. Carmona, *J. Am. Chem. Soc.* **2006**, 128, 13060.
2. “*Rearrangement of Pyridine to Its 2-Carbene Tautomer Mediated by Iridium*” E. Álvarez, S. Conejero, P. Lara, J. A. López, M. Paneque, A. Petronilho, M. L. Poveda, D. del Río, O. Serrano, E. Carmona. *J. Am. Chem. Soc.* **2007**, 129, 14131.
3. “*Monodentate, N-Heterocyclic Carbene-Type Coordination of 2,2'-Bipyridine and 1,10-Phenanthroline to Iridium*” S. Conejero, P. Lara, M. Paneque, A. Petronilho, M. L. Poveda, O. Serrano, F. Vattier, E. Álvarez, C. Maya, V. Salazar, E. Carmona, *Angew. Chem. Int. Ed.* **2008**, 47, 4380.
4. “*Metallacyclic Pyridylidene Structures from Reactions of Terminal Pyridylidenes with Alkenes and Acetylene*” E. Álvarez, Y. A. Hernández, J. López-Serrano, C. Maya, M. Paneque, A. Petronilho, M. L. Poveda, V. Salazar, F. Vattier, E. Carmona, *Angew. Chem. Int. Ed.* **2010**, 49, 3496.

Relación de compuestos preparados en esta Tesis Doctoral





Abreviaturas

Me	metilo, -CH ₃
Et	etilo, -CH ₂ CH ₃
Pr	propilo, -CH ₂ CH ₂ CH ₃
Ph	fenilo, -C ₆ H ₅
Ar	arilo
cod	1,5 ciclooctadieno
Coe	cicloocteno
^t Bu	terc-butilo, -CMe ₃
THF	tetrahidrofurano, C ₄ H ₈ O
Et ₂ O	éter etílico
py	piridina, C ₅ H ₅ N
phen	1,10-fenantrolina
bpy	2,2'-bipiridina
terpy	2,2';6',2"-terpiridina
L	ligando donador de 2 electrones
AL	ácido de Lewis
Eq.	ecuación
Fig.	figura
Tp ^{Me2}	hidrotris(3,5-dimetilpirazolil)borato
[Ir]*	Tp ^{Me2} Ir
Tp ^{Ms}	hidrotris(3-mesitilpirazolil)borato
Tp'	cualquier ligando de tipo hidrotris(pirazolil)borato con sustituyentes en el anillo de pirazol
α	indicador de posición (primera) de un átomo o grupo respecto a otro átomo o grupo tomado como punto de referencia.
β	indicador de posición (segunda) de un átomo o grupo respecto a otro átomo o grupo tomado como punto de referencia.

κ	indicador de la denticidad de un ligando; n° de átomos de un ligando polidentado que se encuentran unidos al metal.
η	indicador de la hapticidad de un ligando: número de átomos contiguos implicados en el enlace de un ligando con un metal.
ν	frecuencia de tensión de enlace (en cm^{-1}).
h	horas
eq.	equivalentes
atm.	atmósferas
Anal. Calc.	análisis calculado
Exp.	experimental
Rdto.	rendimiento
d_n	n átomos de deuterio
g	gramos
mmol	milimol
mL	mililitro
cm	centímetro
Å	Angstron
°	grado
C	centígrado
K	Kelvin
ref.	referencia
p	página
vol	volumen
ORTEP	tipo de representación de datos cristalográficos (Oak Ridge Thermal Ellipsoid Program).
IR	infrarrojo
e^-	electrones
HRMS	espectro de masas de alta resolución (High Resolution Mass Spectra)
NHC	carbeno N-heterocíclico

Abreviaturas para RMN

RMN	Resonancia Magnética Nuclear
δ	desplazamiento químico en partes por millón
ppm	partes por millón
NOESY	espectroscopia de efecto nuclear Overhauser.
HETCOR	espectroscopia de correlación heteronuclear ^1H - ^{13}C .
COSY	espectroscopia de correlación ^1H - ^1H .
s	singulete
d	doblete
t	triplete
q	cuartete
m	multiplete
a	ancho
$^nJ_{AB}$	constante de acoplamiento (en Hz) entre los núcleos A y B separados por n enlaces.
Hz	hercios
C_q	átomo de carbono cuaternario
ar	aromático
pz	anillo de pirazolilo

I. Introducción

I. Introducción

Las piridinas son moléculas de reconocida importancia química. Así, se encuentran como unidades básicas en multitud de productos naturales,¹ son productos de partida para la síntesis de moléculas de interés farmacológico² o biológico,³ y constituyen la base de nuevos materiales fotoelectrónicos y supramoleculares,⁴ hechos que reflejan la diversidad de áreas en las cuales las piridinas y compuestos relacionados están presentes.

El estudio de la reactividad de estos heterociclos frente a los complejos de los metales de transición se presenta asimismo como prioritario,⁵ dada la necesidad de alcanzar un mayor conocimiento sobre sus propiedades, modos de interacción, activación y funcionalización. La capacidad de los metales de transición para coordinarse a las moléculas orgánicas y promover la rotura de sus enlaces y la formación de otros nuevos, los convierte en catalizadores potenciales de procesos de interés, y de hecho, no pocos de los métodos más poderosos y selectivos para la síntesis de moléculas orgánicas implican la catálisis organometálica. Los heterociclos nitrogenados son sustratos por excelencia para nuevos y más sencillos métodos sintéticos facilitados por los metales de transición.⁶

¹ E. Brown, *Ring Nitrogen and Key Biomolecules: The Biochemistry of N-Heterocycles*, Kluwer Academic, Boston, **1998**.

² J. S. Carey, D. Laffan, C. Thomson, M. T. Williams, *Org. Biomol. Chem.* **2006**, 4, 2337.

³ V. Balzani, A. Juris, M. Venturi, S. Campagna, S. Serroni, *Chem. Rev.* **1996**, 96, 759.

⁴ K. Matsumoto, *Heterocyclic Supramolecules I, Vol. 17*, Springer-Verlag, Berlin-Heidelberg, **2008**.

⁵ W. Pitt, D. Parry, B. Perry, C. Groom, *J. Med. Chem.* **2009**, 52, 2952.

⁶ H. Davies, C. Bolm, *Chem. Soc. Rev.* **2007**, 36, 1035.

El empleo general de los complejos de los metales de transición en transformaciones de interés técnico o comercial, ha supuesto un gran avance en las aplicaciones industriales de muchos procesos. En la actualidad, el objetivo no es sólo la búsqueda de catalizadores efectivos para diferentes procesos, sino también la mejora del conocimiento de las etapas elementales que constituyen el ciclo catalítico en cada caso. De este modo, estudiando sistemas estequiométricos en los que ocurran transformaciones elementales de forma controlada, se podrá alcanzar una mayor comprensión de los diferentes procesos industriales, y proponer mejoras para ellos.

Uno de los procesos en los que se centra gran parte de la atención en esta Tesis Doctoral es la tautomería de heterociclos nitrogenados, reacción en la que se observa la transformación del heterociclo en su correspondiente tautómero de tipo carbeno N-heterocíclico (NHC), y que transcurre, como se verá más adelante, a través de varios procesos de activación C–H. Esta inusual transformación está íntimamente relacionada con las características estéricas que presenta el heterociclo y el modo en el que influyen en su coordinación, y en este sentido es crucial entender qué factores afectan a la coordinación del heterociclo al centro metálico.

I.1. Coordinación de las piridinas en complejos de los metales de transición

I.1.1. Aspectos generales

Las piridinas pueden coordinarse a los metales de transición como ligandos π ó σ , aunque el modo de coordinación clásico, y el más general, es a través del par electrónico no compartido del átomo de nitrógeno, para formar los correspondientes aductos.⁷ El origen de esta mayor afinidad, en comparación con los análogos carbocíclicos, es debida en parte a la presencia de un átomo de nitrógeno, puesto que el heteroátomo induce una distribución irregular de la densidad electrónica, como

⁷ P. Tomasik, Z. Ratajewicz, *Chemistry of Heterocyclic Compounds: Pyridine Metal Complexes, Part 6, Vol. 14*, John Wiley & Sons, New York, **1985**.

consecuencia de la diferencia entre las electronegatividades de los átomos de nitrógeno y carbono. Así, por su mayor electronegatividad, el átomo de nitrógeno ejerce un efecto atractor sobre la nube π del sistema aromático, lo que hace que el heterociclo posea, por un lado, una aromaticidad inferior a la del benceno, y por otro, un dipolo negativo sobre el heteroátomo, que favorece la coordinación de éste a centros con deficiencia electrónica, como los complejos de los metales de transición (Fig. I – 1).

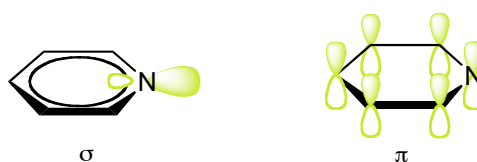


Figura I - 1. Representación del orbital sp^2 sobre el átomo de nitrógeno y sistema orbital π de la piridina.

Lógicamente la geometría del orbital sp^2 que contiene el par electrónico no compartido del átomo de nitrógeno contribuye de forma decisiva a la formación de los aductos N-coordinados, dado que se sitúa en el plano del anillo y por tanto perpendicular al sistema aromático, formando enlaces σ sin pérdida de aromaticidad.

No obstante, el estudio de la reactividad de las piridinas frente a distintos metales de transición, ha desvelado una química de coordinación mucho más extensa, al poner de manifiesto que no siempre se coordinan a través del átomo de nitrógeno, sino que pueden presentar una gran versatilidad en su coordinación a los metales de transición.^{7,8}

La formación de estas especies está condicionada, como por otra parte cabe esperar, por las características electrónicas y estéricas del heterociclo y de las correspondientes al centro metálico. La coordinación del átomo de nitrógeno al metal se ve pues afectada por la presencia de sustituyentes en el anillo aromático,

⁸ A. P. Sadimenko, *Adv. Heterocycl. Chem.* **2005**, 88, 111.

por su posición relativa y por sus características electrónicas.⁹ De modo general (Fig. I – 2), puede decirse que:

- Los sustituyentes atractores de electrones disminuyen la basicidad y nucleofilia del heterociclo, y consecuentemente su capacidad de donación σ .^{7,10}
- Los sustituyentes en las posiciones 2 y 6 dificultan la coordinación del átomo de nitrógeno al centro metálico.

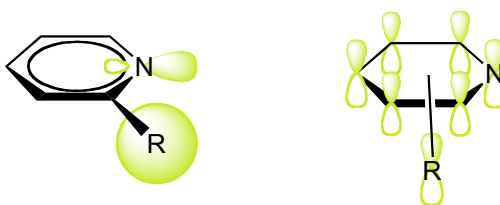


Figura I - 2. Efecto de los sustituyentes sobre el orbital sp^2 del átomo nitrógeno y sobre el sistema orbital π de la piridina.

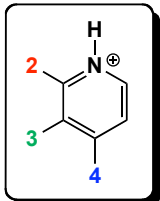
La disponibilidad del par electrónico del átomo de nitrógeno es, por tanto, el resultado de los efectos anteriormente mencionados e influye en el modo de coordinación del heterociclo al metal. La introducción de sustituyentes en las posiciones 2, 3 ó 4 tiene efectos distintos sobre la basicidad y nucleofilia. La Tabla I - 1 recoge los cambios en la acidez del ácido conjugado de las piridinas sustituidas al variar el sustituyente y la posición de sustitución.

⁹ A. Katritzky, A. Pozharskii, *Handbook of Heterocyclic Chemistry*, 2 ed., Pergamon Press, New York, **2000**.

¹⁰ J. J. R. Fraústo Da Silva, J. G. Calado, *J. Inorg. Nucl. Chem.* **1966**, 28, 125.

Tabla I - 1. Valores de ΔpK_a (H_2O) para piridinas monosustituidas.⁹

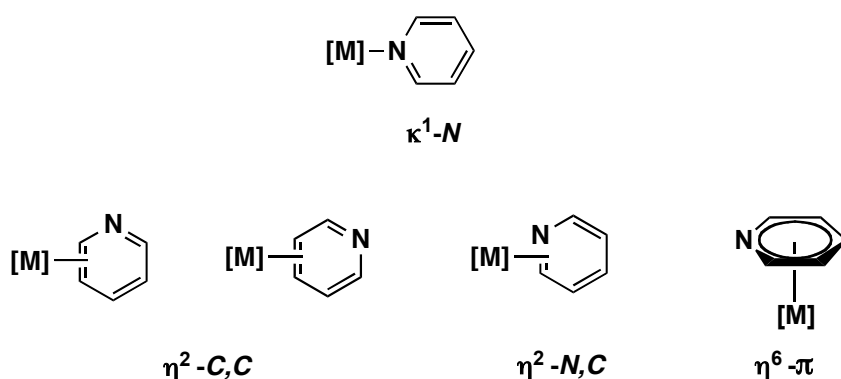
pK_a ión piridinio: 5.3

	Me	^t Bu	NH ₂	Ph	Cl
	2 + 0.8	+ 0.6	+ 1.7	- 0.7	- 4.5
3	+ 0.5	+ 0.7	+ 0.9	- 0.4	- 2.4
4	+ 0.8	+ 0.8	+ 4.0	+ 0.3	- 1.4

Como se aprecia, un determinado sustituyente puede, por una parte, aumentar la basicidad de la piridina, pero al mismo tiempo, si se encuentra en una posición adyacente al átomo de nitrógeno, bloquear la coordinación por efectos estéreos, por lo que no es posible deducir exclusivamente de los valores de pK_a , la capacidad de donación σ de un determinado heterociclo.⁹

I.1.2. Modos de coordinación

Aunque el modo de coordinación clásico de las piridinas es κ^1-N , pueden encontrarse en la literatura química numerosos ejemplos de otros modos de

**Figura I - 3.** Modos de coordinación de las piridinas.

coordinación (Fig. I - 3). La formación de complejos metálicos mediante la utilización del sistema π de las piridinas no es trivial pero, al igual que ocurre en sus análogos carbocíclicos, se pueden formar complejos resultantes de la coordinación η^2-C,C , η^2-N,C y $\eta^6-\pi$. La formación de los complejos η^2-C,C se observa para piridinas impedidas en las posiciones 2 y/o 6, es decir, está favorecida por los efectos estéreos, y también por los grupos donadores de electrones π en la posición 2 (Fig. I - 4).¹¹

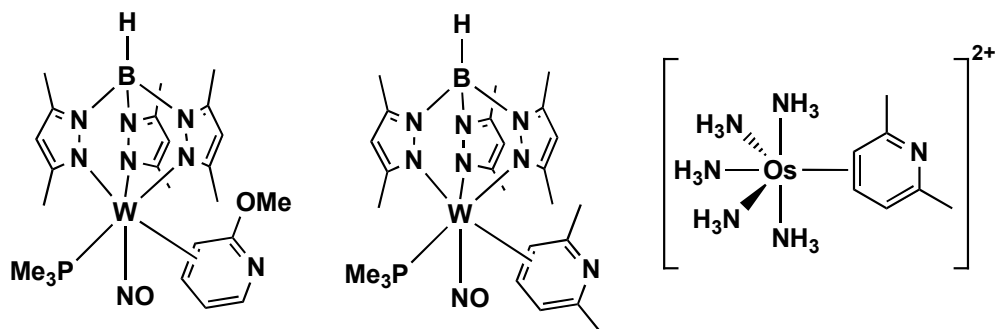


Figura I - 4. Ejemplos de complejos con coordinación η^2-C,C .

La coordinación $\eta^6-\pi$ (Fig. I - 5) se observa predominantemente para piridinas sustituidas en las posiciones 2 y/o 6, es decir, cuando la coordinación N se encuentra

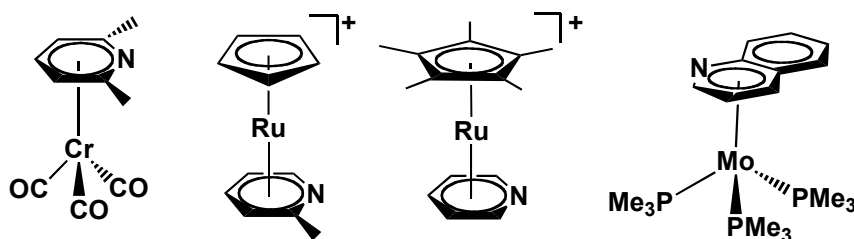


Figura I - 5. Ejemplos de complejos con coordinación $\eta^6-\pi$.

¹¹ a) R. Cordone, W. D. Harman, H. Taube, *J. Am. Chem. Soc.* **1989**, *111*, 2896. b) D. A. Delafuente, G. W. Kosturko, P. M. Graham, W. H. Harman, W. H. Myers, Y. Surendranath, R. C. Klet, K. D. Welch, C. O. Trindle, M. Sabat, W. D. Harman, *J. Am. Chem. Soc.* **2007**, *129*, 406. c) W. D. Harman, *Chem. Rev.* **1997**, *97*, 1953. d) D. Harrison, K. Welch, A. Nichols-Nielander, M. Sabat, W. H. Myers, W. D. Harman, *J. Am. Chem. Soc.* **2008**, *130*, 16844. e) S. Meiere, B. Brooks, T. Gunnoe, E. Carrig, M. Sabat, W. D. Harman, *Organometallics* **2001**, *20*, 3661.

impedida, como en el caso anterior.¹² Sin embargo, si el fragmento metálico tiene una gran afinidad por la coordinación a los arenos (arenofilia)^{12e} se puede observar esta coordinación para la propia piridina. Este efecto suele depender del estado de oxidación del metal, por lo que la alteración de éste puede hacer variar el modo de coordinación del heterociclo.¹³

La coordinación η^2-N,C es de especial importancia dado que puede preceder a la activación de un enlace C–H en posición α al átomo de nitrógeno.^{12h,13,14} Este modo de coordinación (Fig. I – 6) se favorece en aquellos casos en los que se pueden producir repulsiones electrónicas importantes en la interacción del par electrónico no compartido del átomo de nitrógeno y los orbitales d ocupados del metal,^{14c} y suele proponerse como precursor de la activación C₆–H de las piridinas, dado que el átomo H₆ interacciona con el centro metálico con mayor facilidad una vez que se ha coordinado el heterociclo.

¹² **a)** E. Wucherer, E. Muetterties, *Organometallics* **1987**, *6*, 1691. **b)** E. Wucherer, E. Muetterties, *Organometallics* **1987**, *6*, 1696. **c)** R. H. Fish, H. Kim, J. Babin, R. Adams, *Organometallics* **1988**, *7*, 2250. **d)** S. G. Davies, M. R. Shipton, *J. Chem. Soc., Chem. Commun.* **1989**, 995. **e)** R. H. Fish, H. Kim, R. Fong, *Organometallics* **1989**, *8*, 1375. **f)** R. H. Fish, E. Baralt, H. Kim, *Organometallics* **1991**, *10*, 3411. **g)** R. H. Fish, R. Fong, A. Tran, E. Baralt, *Organometallics* **1991**, *10*, 1209. **h)** G. Zhu, J. Tanski, D. Churchill, K. Janak, G. Parkin, *J. Am. Chem. Soc.* **2002**, *124*, 13658.

¹³ K. Allen, M. Bruck, S. Gray, R. Kingsborough, D. Smith, K. Weller, D. E. Wigley, *Polyhedron* **1995**, *14*, 3315.

¹⁴ **a)** D. Neithamer, L. Parkanyi, J. Mitchell, P. T. Wolczanski, *J. Am. Chem. Soc.* **1988**, *110*, 4421. **b)** J. R. Strickler, M. A. Bruck, D. E. Wigley, *J. Am. Chem. Soc.* **1990**, *112*, 2814. **c)** K. Covert, D. Neithamer, M. Zonneville, R. LaPointe, C. Schaller, P. T. Wolczanski, *Inorg. Chem.* **1991**, *30*, 2494. **d)** S. Gray, D. Smith, M. Bruck, D. E. Wigley, *J. Am. Chem. Soc.* **1992**, *114*, 5462. **e)** P. T. Wolczanski, *Polyhedron* **1995**, *14*, 3335. **f)** T. S. Kleckley, J. L. Bennett, P. T. Wolczanski, E. B. Lobkovsky, *J. Am. Chem. Soc.* **1997**, *119*, 247. **g)** A. Veige, T. Kleckley, R. Chamberlin, D. Neithamer, C. Lee, P. T. Wolczanski, E. Lobkovsky, W. Glassey, *J. Organomet. Chem.* **1999**, *591*, 194. **h)** J. B. Bonanno, A. S. Veige, P. T. Wolczanski, E. B. Lobkovsky, *Inorg. Chim. Acta* **2003**, *345*, 173.

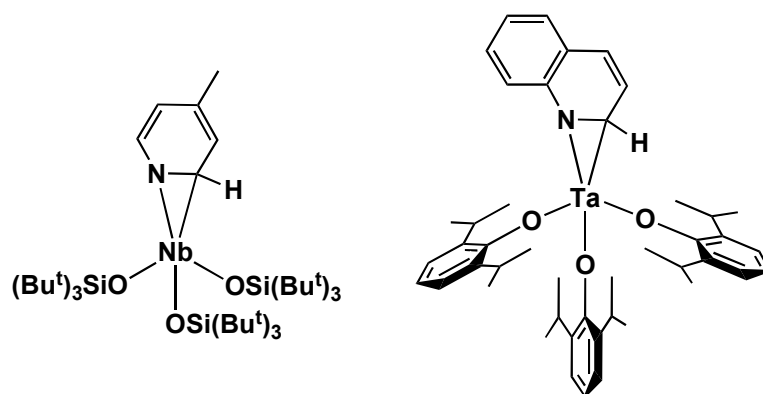


Figura I - 6. Ejemplos de complejos con coordinación $\eta^2 - N,C$.

A pesar de ello, no se conocen muchos complejos de los metales de transición en los que esta forma de coordinación conduzca a complejos estables. Los complejos que resultan de activaciones C–H posteriores son mucho mas comunes y se tratarán en el apartado siguiente, en el marco de la activaciones C–H de las piridinas.

I.2. Activación de enlaces C–H en piridinas

Los distintos modos de coordinación de las piridinas condicionan su reactividad subsiguiente, sobre todo en lo que respecta a la activación de sus enlaces C–H y la

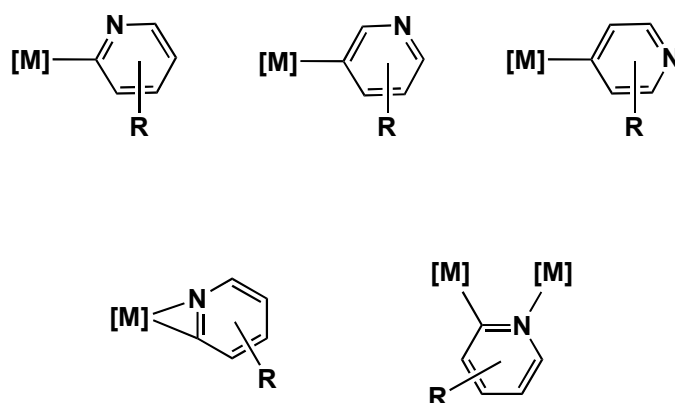


Figura I - 7. Complejos resultantes de la activación C–H de piridinas.

posible funcionalización del anillo aromático. La utilización de los procesos de activación C–H es, por tanto, una herramienta muy útil, puesto que permite la activación selectiva del anillo heterocíclico de forma directa, sin necesidad de modificarlo previamente.¹⁵ La Fig. I – 7 muestra algunas de estas estructuras activadas.^{12,16}

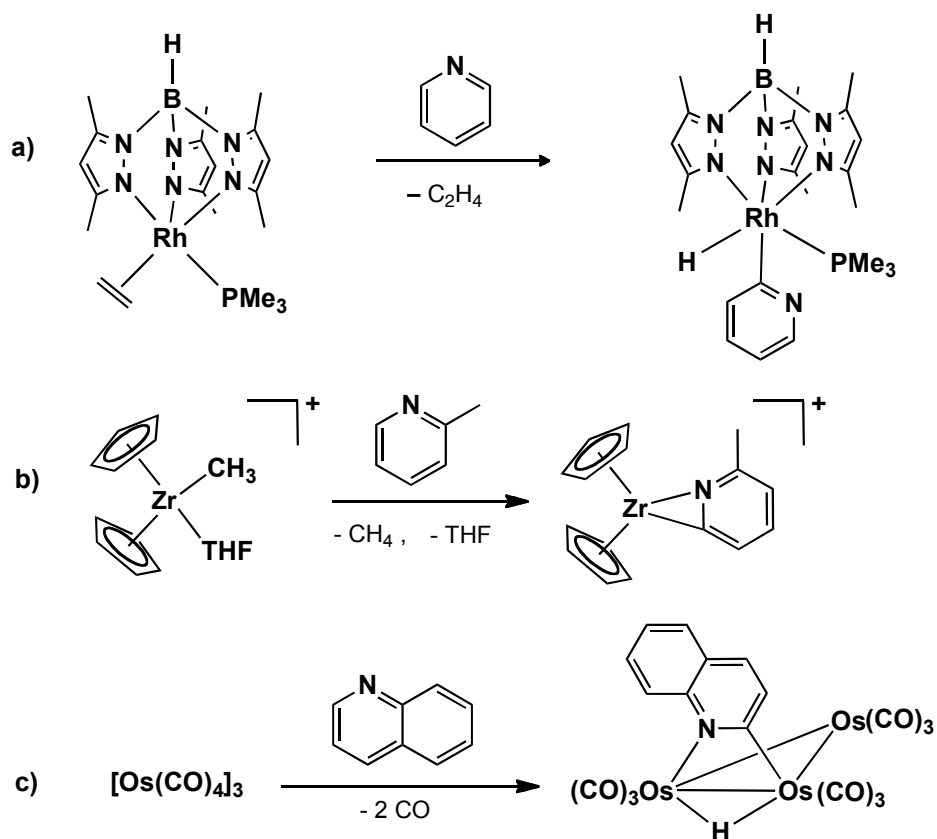
La activación de un enlace C–H de un anillo de piridina conduce normalmente a la formación de un complejo de piridilo (Esquema I – 1a),¹⁶ⁱ que en algunos casos puede implicar la coordinación del átomo de nitrógeno, formando un anillo de tres miembros ($\kappa\text{-N,C}$) con el centro metálico (Esquema I – 1b) o alternativamente complejos de tipo puente (Esquema I – 1c).¹⁷

¹⁵ I. Seregin, V. Gevorgyan, *Chem. Soc. Rev.* **2007**, 36, 1173.

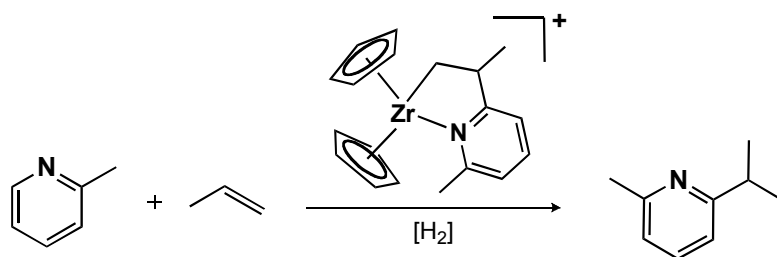
¹⁶ **a)** K. Den Haan, J. De Boer, J. Teuben, A. Spek, B. Kojic-Prodic, G. Hays, R. Huis, *Organometallics* **1986**, 5, 1726. **b)** R. F. Jordan, D. Taylor, *J. Am. Chem. Soc.* **1989**, 111, 778. **c)** R. F. Jordan, D. Taylor, N. Baenziger, *Organometallics* **1990**, 9, 1546. **d)** R. F. Jordan, A. Guram, *Organometallics* **1990**, 9, 2116. **e)** A. Guram, R. F. Jordan, *Organometallics* **1990**, 9, 2190. **f)** A. Guram, R. F. Jordan, *Organometallics* **1991**, 10, 3470. **g)** R. Boaretto, P. Roussel, A. Kingsley, I. Munslow, *Chem. Commun.* **1999**, 1701. **i)** H. Selnau, J. Merola, *Organometallics* **1993**, 12, 1583. **h)** W. Jones, L. Dong, A. Myers, *Organometallics* **1995**, 14, 855. **j)** M. Paneque, P. J. Perez, A. Pizzano, M. L. Poveda, S. Taboada, M. Trujillo, E. Carmona, *Organometallics* **1999**, 18, 4304. **l)** C. Bradley, E. Lobkovsky, P. Chirik, *J. Am. Chem. Soc.* **2003**, 125, 8110. **m)** O. Ozerov, M. Pink, L. Watson, K. Caulton, *J. Am. Chem. Soc.* **2004**, 126, 2105. **n)** S. Arndt, B. R. Elvidge, P. M. Zeimentz, T. P. Spaniol, J. Okuda, *Organometallics* **2006**, 25, 793. **o)** K. Jantunen, B. Scott, J. Gordon, J. Kiplinger, *Organometallics* **2007**, 26, 2777. **p)** J. Kiplinger, B. Scott, E. Schelter, J. A. Pool-Davis-Tournear, *J. Alloys Compd.* **2007**, 444, 477. **q)** D. Krut'ko, R. Kirsanov, S. Belov, M. Borzov, A. Churakov, J. Howard, *Polyhedron* **2007**, 26, 2864. **r)** G. Zhu, K. Pang, G. Parkin, *J. Am. Chem. Soc.* **2008**, 130, 1564.

¹⁷ A. Eisenstadt, C. Giandomenico, M. Frederick, R. Laine, *Organometallics* **1985**, 4, 2033.

Esquema I - 1

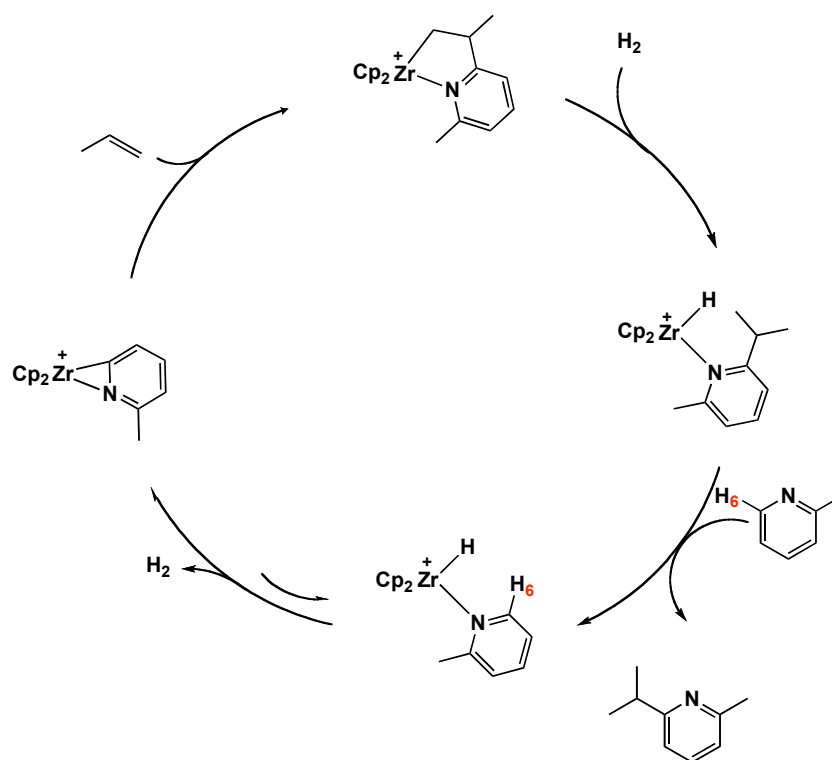


Existen en la bibliografía numerosos ejemplos de sistemas estequiométricos de funcionalización de piridinas a través de procesos de activación C–H. Sin embargo, los sistemas catalíticos que hacen uso de esta metodología son muy escasos. En 1989 Jordan describió el primer proceso catalítico para la activación y



Ecuación I

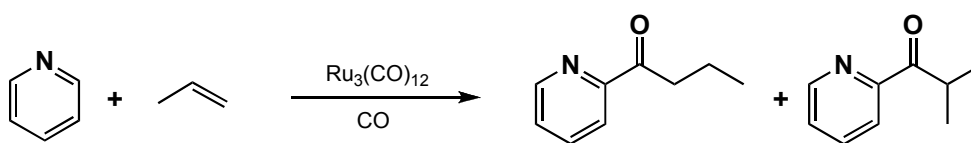
Esquema I - 2



funcionalización selectiva de las piridinas, mediante la utilización de un complejo de zirconio (Ec. I).^{16b} En este sistema, la activación del enlace $\text{C}_6\text{--H}_6$ de la 2-picolina en presencia de propeno, conduce a la formación de un nuevo enlace C--C , que resulta formalmente de la adición 1,2 del enlace C--H de la piridina al carbono olefínico más sustituido. El mecanismo propuesto implica la coordinación de la piridina como aducto N-coordinado, y se sugiere que la activación C--H posterior se facilita por una interacción agóstica con el átomo de H_6 . Esta hipótesis se fundamenta en los desplazamientos químicos hacia campo alto de los núcleos H_6 y C_6 en los espectros de RMN por coordinación al átomo metálico.^{16e} En el Esquema I - 2 se muestra el ciclo catalítico propuesto para esta transformación. La transformación ocurre de forma catalítica únicamente en presencia de H_2 , que actúa

como cocatalizador, y la formación del nuevo enlace C–C se produce en el átomo de carbono olefínico más sustituido, atribuyéndose esta regioselectividad a factores estéreos. Finalmente, la mayor labilidad del complejo que contiene la piridina 2,6-disustituida que se forma, permite su sustitución por la 2-picolina, cerrándose de este modo el ciclo catalítico. La actividad catalítica es moderada, el catalizador presenta una vida media larga y muestra también una elevada selectividad. Estas características indujeron a los autores al estudio exhaustivo de este sistema, a fin de extenderlo a otras piridinas, pero la aplicabilidad encontrada resultó muy limitada.^{16f,18}

En 1992, Moore,¹⁹ encontró un sistema catalítico para el acoplamiento de piridinas y olefinas, con incorporación de una molécula de CO (Ec. II). La elección de los complejos de rutenio como catalizadores se basaba en su capacidad para



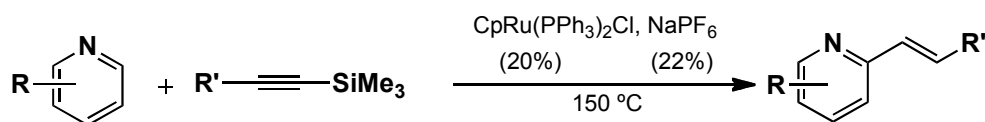
Ecuación II

formar complejos binucleares de piridilo, resultantes de la activación selectiva del enlace $\text{C}_2\text{--H}_2$. La coordinación posterior del propeno en presencia de CO permite el acoplamiento C–C que conduce a las piridinas sustituidas en la posición 2. Tanto el número de sustituyentes en la olefina, como en la piridina son determinantes para el acoplamiento, obteniéndose los mejores resultados con las olefinas terminales, y las piridinas que no poseen sustituyentes en adyacentes al átomo de nitrógeno. Existe, sin embargo, muy poca información mecanicista sobre esta transformación, y por

¹⁸ S. Bi, Z. Lin, R. F. Jordan, *Organometallics* **2004**, 23, 4882.

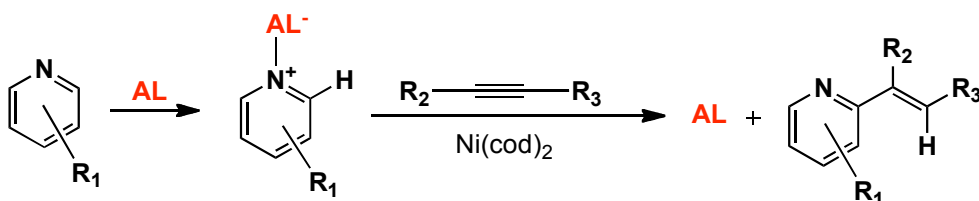
¹⁹ E. Moore, W. Pretzer, T. O'Connell, J. Harris, *J. Am. Chem. Soc.* **1992**, 114, 5888.

otra parte, aunque la capacidad de este complejo de rutenio para promover los procesos de acoplamiento de diversos N-heterociclos fue estudiada por otros grupos, los resultados fueron muy limitados, por requerir condiciones de reacción drásticas y producir rendimientos tan sólo moderados.²⁰



Ecuación III

Más recientemente, Murakami y Hori han descrito un proceso de acoplamiento C-C entre la piridina y algunos alquinos, catalizado por un complejo de rutenio catiónico (Ec. III).²¹ En esta misma línea de trabajo, Nakao y Hiyama han desarrollado un proceso para la alquenilación de diversas piridinas sustituidas,²² que se beneficia del aumento de la acidez del enlace $C_{\alpha}-H_{\alpha}$ observado cuando el átomo de N se coordina a un ácido de Lewis. Como se muestra en la Ec. IV, el aducto de Lewis se acopla con el alquino, en una reacción catalizada por $Ni(cod)_2$, con formación de piridinas sustituidas en la posición 6. El mecanismo propuesto



Ecuación IV

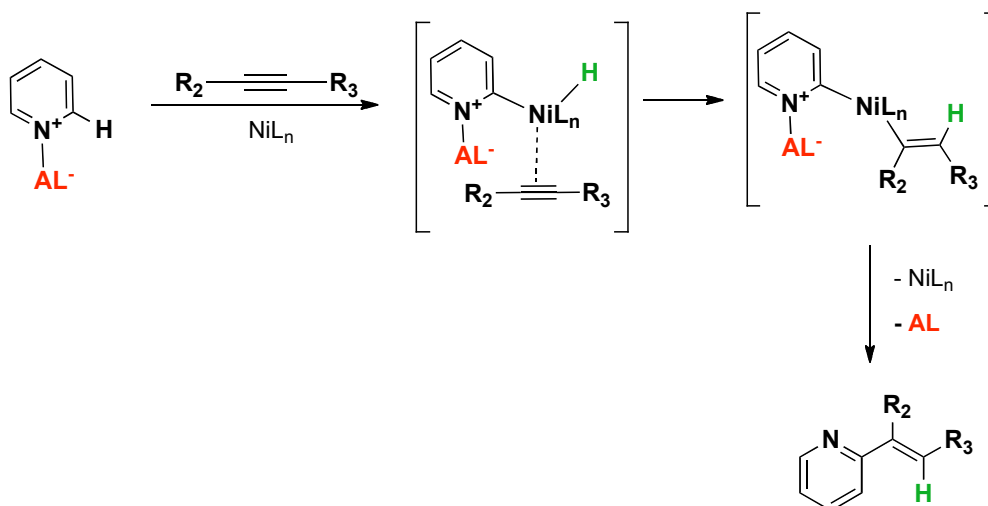
²⁰ a) R. Grigg, V. Savic, *Tetrahedron Lett.* **1997**, 38, 5737. b) T. Fukuyama, N. Chatani, J. Tatsumi, F. Kakiuchi, S. Murai, *J. Am. Chem. Soc.* **1998**, 120, 11522. c) K. Godula, B. Sezen, D. Sames, *J. Am. Chem. Soc.* **2005**, 127, 3648.

²¹ M. Murakami, S. Hori, *J. Am. Chem. Soc.* **2003**, 125, 4720.

²² Y. Nakao, K. Kanyiva, T. Hiyama, *J. Am. Chem. Soc.* **2008**, 130, 2448.

(Esquema I – 3) postula la adición oxidante del enlace $C_{\alpha}-H_{\alpha}$ de la piridina al complejo de Ni(0), seguida de la inserción migratoria del alquino en el enlace Ni–H del compuesto resultante, seguida de la eliminación reductora de la alquénil piridina.

Esquema I – 3



Finalmente, es obligado destacar por su relevancia en este campo los trabajos desarrollados en fechas recientes por Ellman y Bergman, que han proporcionado nuevos y muy eficaces métodos para la funcionalización selectiva de las piridinas y de otros heterociclos mediante procesos de activación C–H, de modo catalítico. Dado que estos trabajos son coincidentes en el tiempo con el desarrollo de esta Tesis Doctoral y que sus aspectos mecanicistas guardan estrecha relación con ella, se ha considerado adecuado discutirlos con el detalle necesario en una sección posterior de esta Memoria.

I.3. Formación de tautómeros de la piridina

I.3.1. Consideraciones generales

La piridina puede presentar tres tautómeros, resultantes de la migración de un átomo de hidrógeno al de nitrógeno, desde las posiciones 2, 3 ó 4 del anillo piridínico. Los tautómeros I y III (Fig. I - 8), se estabilizan por resonancia entre las formas canónicas neutras (de tipo carbeno) y las cargadas (zwitteriónicas o de tipo iluro).

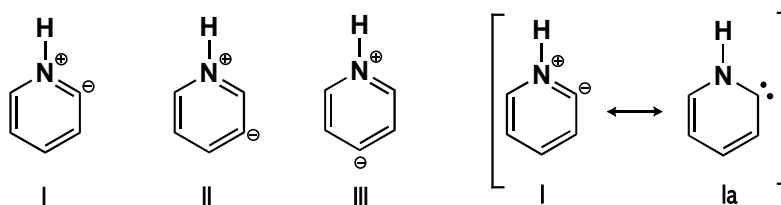
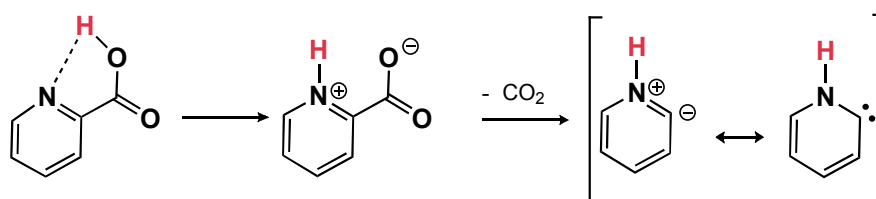


Figura I - 8. Tautómeros de la piridina.

Shevlin²³ obtuvo evidencias sobre la estructura **II** al estudiar la reacción de expansión del anillo de pirrol con carbono atómico, pero el tautómero **I** de la piridina fue propuesto por primera vez por Hammick en 1937²⁴ como responsable de

Esquema I - 4

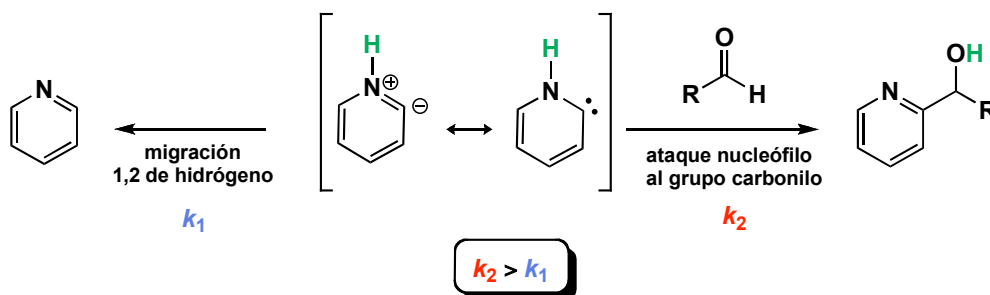


²³ C. J. Emanuel, P. B. Shevlin, *J. Am. Chem. Soc.* **1994**, 116, 5991.

²⁴ a) P. Dyson, D. Hammick, *J. Chem. Soc.* **1937**, 1724. b) M. Ashworth, R. Daffern, D. Hammick, *J. Chem. Soc.* **1939**, 809.

la mayor facilidad de descarboxilación del ácido 2-picolín-carboxílico, en comparación con sus isómeros en las posiciones 3 y 4 del anillo de piridina (Esquema I – 4). Hammick propuso que **I** debe tener cierta estabilidad, y de hecho, fue posteriormente atrapado en disolución, formando alcoholes secundarios cuando se genera en presencia de aldehídos.²⁵ En un trabajo posterior, Breslow propuso que esta estabilidad adicional se puede deber a la formación de la forma neutra de carbeno **Ia**,²⁶ y diversos estudios posteriores^{25a,27} sugirieron la participación de **I** como intermedio de reacción en este tipo de procesos, estudiándose su estabilidad por diferentes métodos.²⁸ En efecto, la reactividad del ácido 2-picolínico frente a los aldehídos indica que **I** debe poseer una vida media significativa, y por lo tanto cierta estabilidad en disolución, que le permite atacar al grupo carbonilo antes de experimentar una migración 1,2 del átomo de hidrógeno para originar la piridina (Esquema I – 5). En otras palabras, la barrera de energía correspondiente a esta transposición 1,2-H debe tener un valor elevado.

Esquema I - 5



²⁵ a) K. Ratts, R. Howe, W. Phillips, *J. Am. Chem. Soc.* **1969**, *91*, 6115. b) E. Brown, M. Shambhu, *J. Org. Chem.* **1971**, *36*, 2002.

²⁶ R. Breslow, *J. Am. Chem. Soc.* **1958**, *80*, 3719.

²⁷ a) B. Brown, D. Hammick, *J. Chem. Soc.* **1949**, 659. b) P. Haake, J. Mantecon, *J. Am. Chem. Soc.* **1964**, *86*, 5230.

²⁸ a) R. Gleiter, R. Hoffmann, *J. Am. Chem. Soc.* **1968**, *90*, 5457. b) R. Grigg, L. Wallace, J. O. Morley, *J. Chem. Soc., Perkin Trans. 2* **1990**, 51.

Sobre la base de estos y otros datos^{28b,29} Schwarz y colaboradores³⁰ han estudiado recientemente mediante cálculos teóricos y espectrometría de masas, la formación de estos tautómeros y las energías necesarias para su formación a partir de la piridina. Los cálculos teóricos (Fig. I – 9) indican que el tautómero **I** de la piridina presenta una energía de aproximadamente 45 kcal·mol⁻¹ más elevada que la de la piridina, mientras que **II** y **III** tienen energías aún superiores, del orden de 60-65 kcal·mol⁻¹. La especie más estable es, como cabe esperar, la piridina.

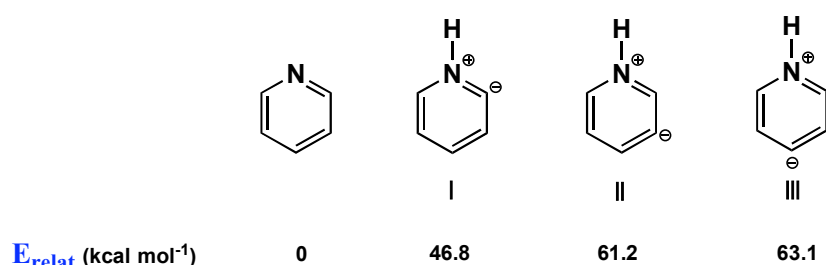


Figura I - 9. Energía relativa de los tautómeros de la piridina.

En lo que se refiere a la interconversión de los tautómeros, la isomerización de la piridina para formar la especie 2-carbeno, es decir **I**, está prohibida por una barrera de energía de nada menos que 85 kcal·mol⁻¹ (Fig. I – 10). Si se recuerda que **I** tiene una energía de aproximadamente 45 kcal·mol⁻¹ superior a la de la piridina, la transformación termodinámicamente muy favorable del 2-carbeno en piridina requiere superar una barrera de 40 kcal·mol⁻¹.

²⁹ P. Chen, *J. Org. Chem.* **1976**, *41*, 2973.

³⁰ **a)** D. Lavorato, J. Terlouw, T. Dargel, W. Koch, G. McGibbon, H. Schwarz, *J. Am. Chem. Soc.* **1996**, *118*, 11898. **b)** D. Lavorato, J. Terlouw, G. McGibbon, T. Dargel, W. Koch, H. Schwarz, *Int. J. Mass Spectrom.* **1998**, *179*, 7.

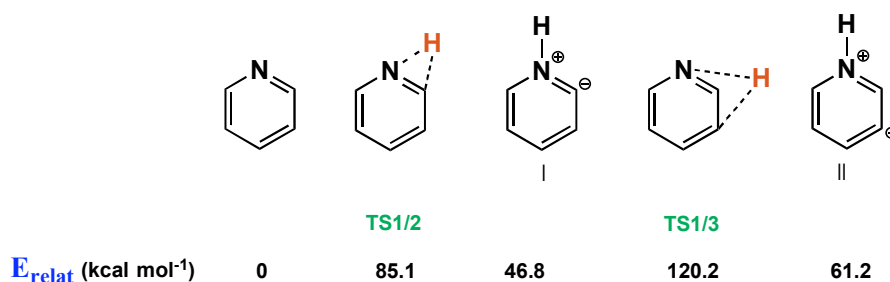


Figura I - 10. Energía relativa de los tautómeros de la piridina y de los estados de transición para la migración 1,2 y 1,3 de hidrógeno.

Insistiendo en estos resultados, Hollóczky y Nyulászi,³¹ han propuesto que **I**, al tratarse de un carbeno N-heterocíclico, se estabiliza por la presencia del átomo de nitrógeno, y también por poseer un sistema aromático de 6 electrones, tal como anteriormente habían apuntado Hoffman y Gleiter.^{28a} En efecto, los cálculos teóricos realizados por estos autores indican que la presencia del átomo de nitrógeno estabiliza electrónicamente al carbeno por el solapamiento orbital entre el orbital p ocupado del nitrógeno y el orbital p vacío del carbono, mientras que el sistema de 6 electrones confiere la estabilidad que deriva de su aromaticidad, y fuerza además la geometría plana del anillo aromático, que permite el solapamiento orbital mencionado, sin pérdida total del carácter aromático (la aromaticidad calculada para **I** con respecto a la piridina es de aproximadamente 80%). No obstante esta limitada estabilidad de la forma **I**, la tautomería de las piridinas promovida por los complejos de los metales de transición encuentra muy pocos precedentes bibliográficos. Se conocen, sin embargo, algunos complejos de tipo carbeno NHC derivados de las piridinas, que se generan de modo indirecto y se discutirán brevemente en el siguiente apartado.

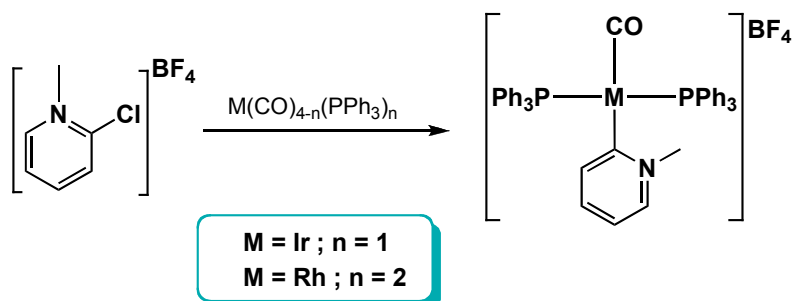
³¹ O. Hollóczki, L. Nyulászi, *J. Org. Chem.* **2008**, 73, 4794.

I.3.2. Formación de carbenos N-heterocíclicos derivados de piridinas promovida por complejos de metales de transición

I.3.2.1. Métodos clásicos

Se encuentran descritos en la bibliografía diversos complejos de tipo carbeno N-heterocíclico derivados de las piridinas, que se han generado a partir de sales de piridinio, mediante la funcionalización del átomo de nitrógeno de complejos de piridilo o por otros procedimientos. La bibliografía específica de este campo ha sido revisada muy recientemente,³² por lo que en este apartado se mencionarán únicamente algunos de los procesos más relevantes.

El empleo de sales de piridinio es una metodología estudiada por distintos grupos de investigación. La utilización de sales de halopiridinas, cuya adición al centro metálico conduce a la formación del carbeno pretendido, ha sido ampliamente estudiada y encuentra aplicaciones en la síntesis de carbenos NHC con varios metales de transición,³³ como se muestra en la Ec. V y en la Fig. I – 11.



Ecuación V

³² O. Schuster, L. Yang, H. Raubenheimer, M. Albrecht, *Chem. Rev.* **2009**, *109*, 3445.

³³ **a)** P. Fraser, W. Roper, F. Stone, *J. Chem. Soc., Dalton Trans.* **1974**, 760. **b)** U. Kirchgaessner, H. Piana, U. Schubert, *J. Am. Chem. Soc.* **1991**, *113*, 2228. **c)** W. Meyer, M. Deetlefs, M. Pohlmann, R. Scholz, M. Esterhuysen, G. Julius, H. Raubenheimer, *Dalton Trans.* **2004**, 413.

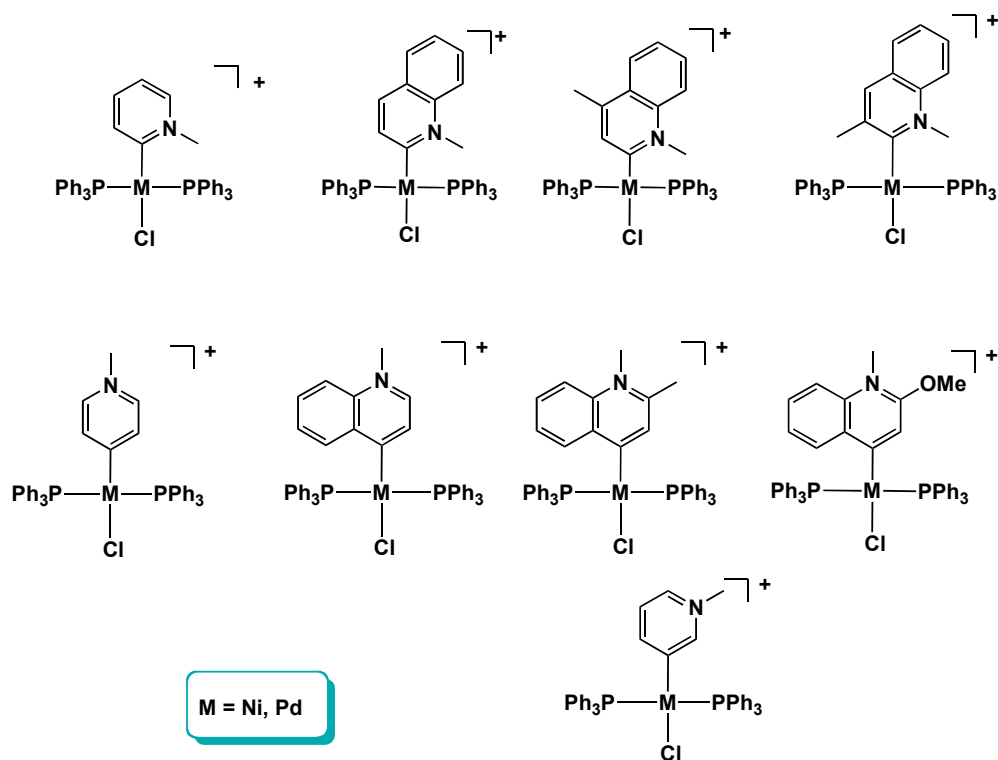


Figura I - 11. Complejos con ligandos NHC derivados de piridinas obtenidos mediante adición oxidante de halopiridinas.

También se pueden utilizar sales de piridinio que no contienen átomos de halógeno, favoreciéndose la formación del carbeno NHC por activación C–H (Fig I - 12) y así recientemente Bercaw y colaboradores³⁴ han aplicado esta

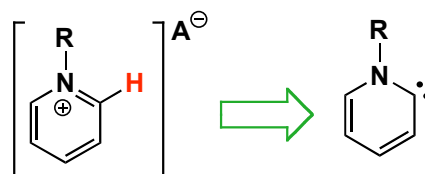
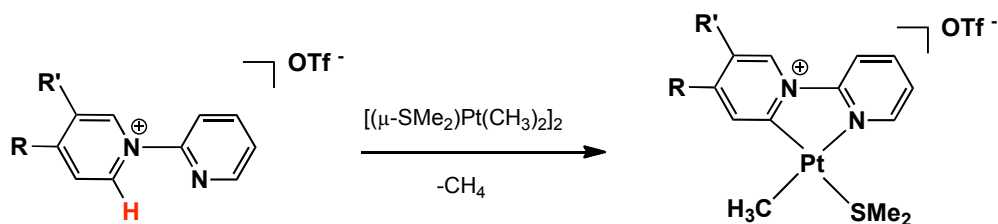


Figura I - 12. Sales de piridinio como precursores de carbenos.

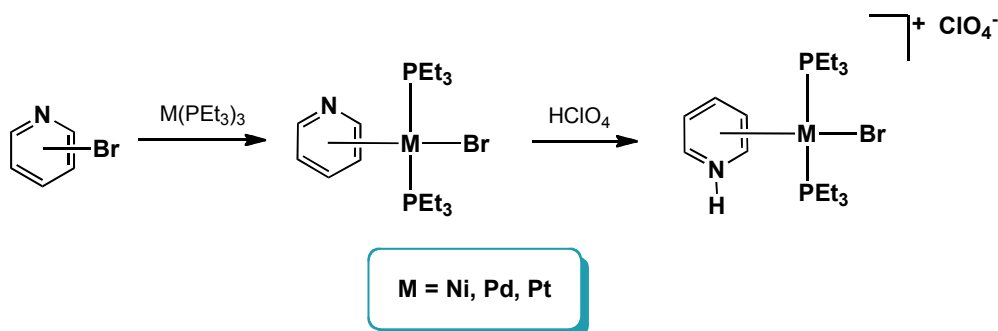
³⁴ a) J. Owen, J. Labinger, J. Bercaw, *J. Am. Chem. Soc.* **2004**, 126, 8247. b) N. Piro, J. Owen, J. Bercaw, *Polyhedron* **2004**, 23, 2797.

metodología mediante la utilización de sales de piridinio con un sustituyente capaz de coordinarse también al metal, induciendo de este modo la activación C–H, y la subsecuente formación del carbeno por ciclometalación (Ec. VI).



Ecuación VI

En otra aproximación experimental diferente se han obtenido carbenos derivados de la piridina utilizando como precursores complejos que contienen un grupo piridilo, procediéndose después a su funcionalización. La formación de los compuestos deseados se puede conseguir, por ejemplo, por adición oxidante de piridinas halogenadas³⁵ (Ec. VII) o por reacción de derivados litiados³⁶ (Esquema I - 6), y los complejos que se generan se protonan o alquilan en el átomo de nitrógeno, originando así los carbenos NHC pretendidos.

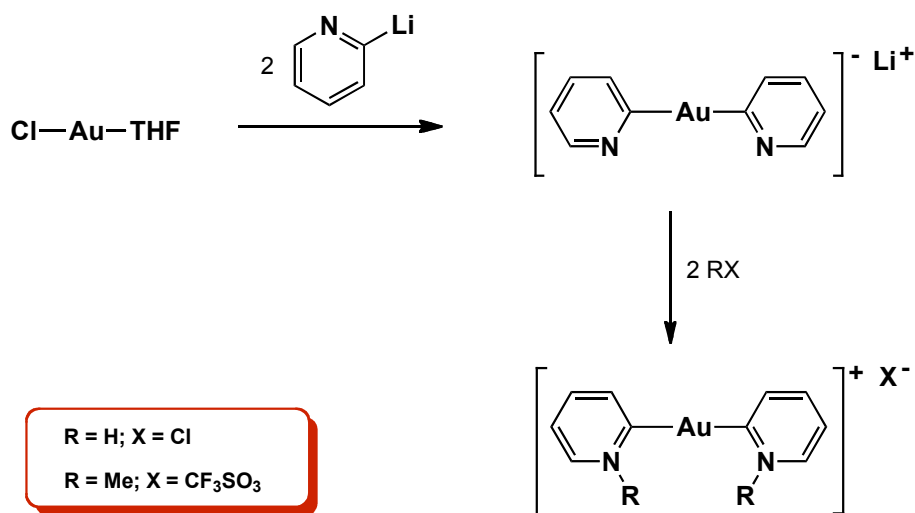


Ecuación VII

³⁵ **a)** K. Nakatsu, K. Kinoshita, H. Kanda, K. Isobe, *Chem. Lett.* **1980**, 913. **b)** K. Isobe, E. Kai, Y. Nakamura, K. Nishimoto, T. Miwa, S. Kawaguchi, K. Kinoshita, K. Nakatsu, *J. Am. Chem. Soc.* **1980**, *102*, 2475. **c)** B. Crociani, F. Di Bianca, A. Giovenco, A. Scrivanti, *J. Organomet. Chem.* **1983**, *251*, 393. **d)** K. Isobe, Y. Nakamura, T. Miwa, S. Kawaguchi, *Bull. Chem. Soc. Jpn.* **1987**, *60*, 149. **e)** B. Crociani, F. Di Bianca, A. Giovenco, A. Berton, R. Bertani, *J. Organomet. Chem.* **1989**, 361, 255. **f)** F. Di Bianca, A. Fontana, R. Bertani, B. Crociani, *J. Organomet. Chem.* **1992**, 425, 155.

³⁶ **a)** H. G. Raubenheimer, J. G. Toerien, G. J. Kruger, R. Otte, W. van Zyl, P. Olivier, *J. Organomet. Chem.* **1994**, 466, 291. **b)** A. Poulain, A. Neels, M. Albrecht, *Eur. J. Inorg. Chem.* **2009**, *13*, 1871.

Esquema I – 6



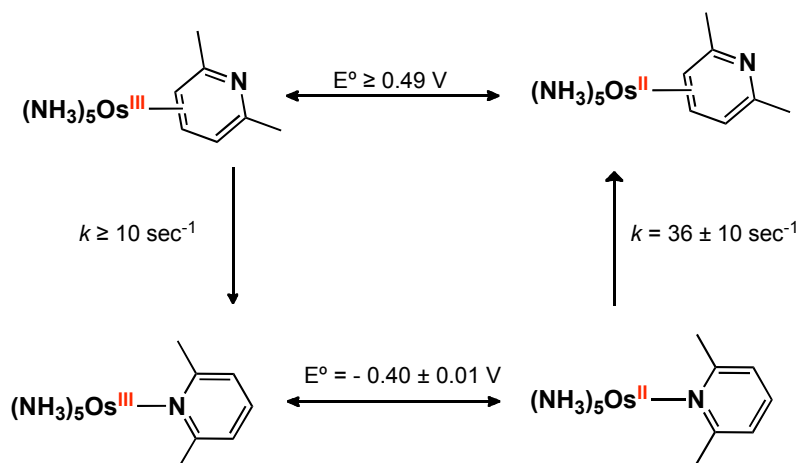
1.3.2.2. Tautomería de piridinas con formación de carbenos N-heterocíclicos promovida por complejos de metales de transición

La interacción de las piridinas con los complejos de los metales de transición que se han descrito en la primera parte de esta introducción hacen referencia a los distintos modos de coordinación a través de los cuales las piridinas se unen al centro metálico. La coordinación de la piridina puede activarla para formar por ejemplo complejos de tipo piridilo, mediante activación C–H. Sin embargo, la coordinación de la piridina en alguna de sus formas tautómeras a un centro metálico, por reacción directa de la piridina con un complejo, tal como, de hecho, se describe en esta Tesis Doctoral, encuentra muy pocos precedentes bibliográficos. En 1987, Taube y Cordone,³⁷ al estudiar la interacción de los fragmentos $\text{Os}^{\text{II}}(\text{NH}_3)_5$ y $\text{Os}^{\text{III}}(\text{NH}_3)_5$ con

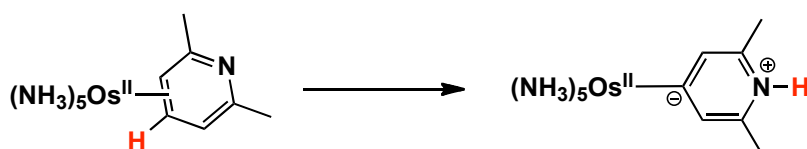
³⁷ R. Cordone, H. Taube, *J. Am. Chem. Soc.* **1987**, *109*, 8101.

la 2,6-dimetilpiridina, observaron la formación, por otra parte esperada, de los correspondientes complejos de areno con coordinación η^2-C, C (Esquema I - 7).³⁸

Esquema I - 7



Como se ilustra en la Ec. VIII, el complejo η^2-C, C de la 2,6-dimetilpiridina y Os(II) se tautomeriza de forma espontánea para dar el correspondiente carbeno NHC en la posición C(4), es decir, el hoy día llamado “carbeno remoto”.³² Formalmente, la redistribución requiere la migración 1,4 del átomo de hidrógeno.

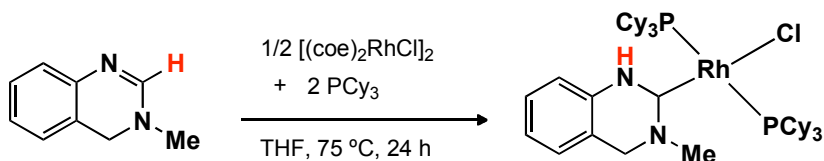


Ecuación VIII

En fechas recientes, Bergman y sus colaboradores han observado la conversión de un derivado de la quinazolina en el correspondiente carbeno N-heterocíclico que se recoge en la Ec. IX. Este complejo resulta formalmente de la migración de 1,2 de un átomo de hidrógeno, y durante la realización de esta Tesis Doctoral, estos autores han estudiado en detalle este sistema tanto en lo que respecta a sus detalles

³⁸ W. D. Harman, H. Taube, *J. Am. Chem. Soc.* **1987**, *109*, 1883.

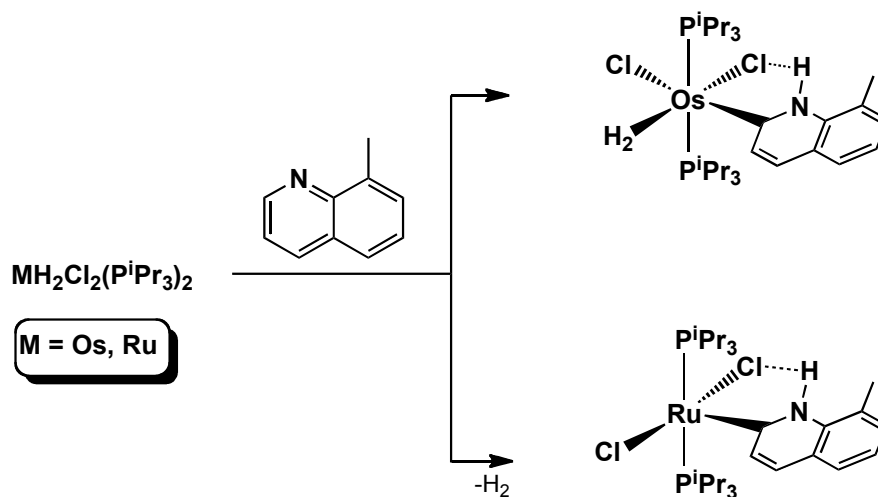
mecanicistas³⁹ que llevan a la formación de esta especie, como en lo que concierne a sus aplicaciones catalíticas para la funcionalización de las piridinas.⁴⁰



Ecuación IX

En 2006, de manera prácticamente simultánea con nuestro trabajo, Esteruelas y colaboradores observaron la tautomería de distintas quinolinas mediante complejos de osmio y rutenio (Esquema I – 8).⁴¹ Por su estrecha relación con los trabajos que se describen en esta Tesis Doctoral, estas investigaciones se analizarán con el detalle debido en el apartado de Resultados y Discusión.

Esquema I - 8



³⁹ S. H. Wiedemann, J. C. Lewis, J. A. Ellman, R. Bergman, *J. Am. Chem. Soc.* **2006**, *128*, 2452.

⁴⁰ a) J. C. Lewis, R. Bergman, J. A. Ellman, *J. Am. Chem. Soc.* **2007**, *129*, 5332. b) A. M. Berman, J. C. Lewis, R. Bergman, J. A. Ellman, *J. Am. Chem. Soc.* **2008**, *130*, 14926.

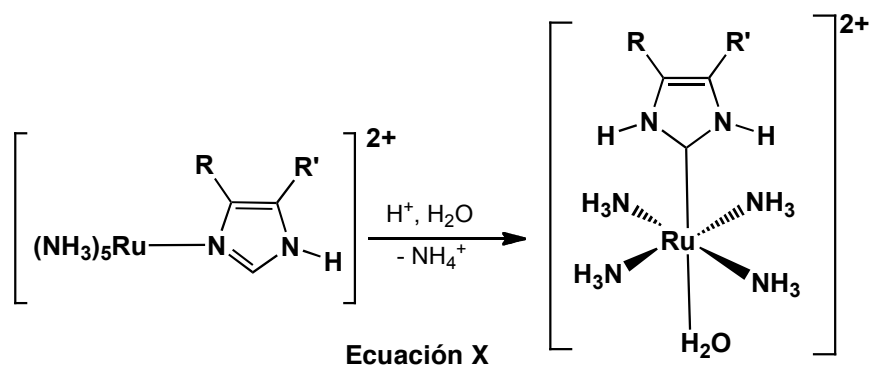
⁴¹ M. A. Esteruelas, F. Fernandez-Álvarez, E. Oñate, *J. Am. Chem. Soc.* **2006**, *128*, 13044.

I.3.3. Tautomería de heterociclos derivados del imidazol inducida por complejos de metales de transición

Se encuentran igualmente descritos en la bibliografía ejemplos de tautomería de imidazol y sus derivados, aunque, tal como ocurre con las piridinas, estos ejemplos son escasos y en su mayoría de observación muy reciente. Del mismo modo que la piridina, para el imidazol la energía del tautómero carbeno es aproximadamente 28 kcal·mol⁻¹ más alta que la del tautómero N-coordinado, y los métodos de síntesis de los carbenos derivados del imidazol no implican procesos de tautomería directos. Los trabajos teóricos desarrollados por Crabtree y Eisenstein, han permitido deducir que la coordinación de los derivados de imidazol para obtener los correspondientes tautómeros C- o N-, depende del fragmento metálico al que se coordinan,⁴² encontrándose que la coordinación C está facilitada para:

- Los metales de la 2ª y 3ª series de transición con buena capacidad de retrodonación π .
- Los ligandos en *trans* a la posición de coordinación que poseen escasa influencia *trans*.
- Los ligandos capaces de estabilizar el grupo NH.

Para estos sistemas deben analizarse los dos procesos de tautomería, es decir, la transformación del tautómero N al correspondiente carbeno ($N \rightarrow C$) y el proceso

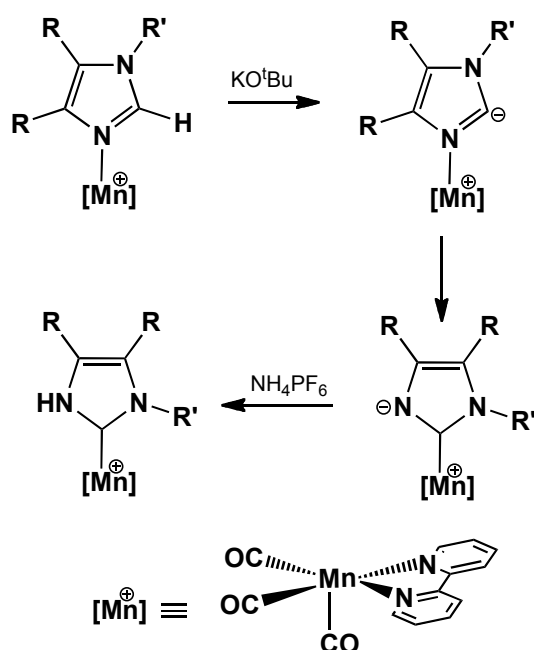


⁴² G. Sini, O. Eisenstein, R. H. Crabtree, *Inorg. Chem.* **2002**, *41*, 602.

contrario ($C \rightarrow N$).

El primer ejemplo de tautomería $N \rightarrow C$ de un imidazol fue descrito por Taube en 1974, al observar la formación del carbeno a partir de un complejo de imidazol coordinado a través de su átomo de nitrógeno, mediante catálisis ácida (Eq. X).⁴³

Esquema I – 9



Muy recientemente, se ha descrito un proceso de tautomería $N \rightarrow C$, que transcurre mediante el auxilio de una base.⁴⁴ En esta transformación (Esquema I – 9), la base desprotona el grupo C–H facilitando la coordinación del átomo de carbono aniónico resultante a través de un proceso de migración 1,2, con transferencia formal de la carga negativa al átomo de nitrógeno. En presencia de una fuente protónica, el proceso no es reversible, y se produce la protonación del átomo de nitrógeno para obtener el carbeno N–heterocíclico. Se ha observado también una transformación relacionada con la anterior para complejos de renio.⁴⁵

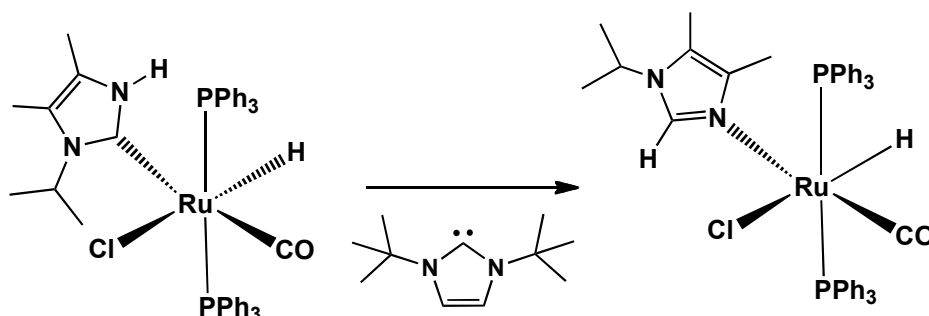
⁴³ R. J. Sundberg, R. F. Bryan, I. F. Taylor Jr., H. Taube, *J. Am. Chem. Soc.* **1974**, 96, 381.

⁴⁴ J. Ruiz, B. F. Perandones, *J. Am. Chem. Soc.* **2007**, 129, 9298.

⁴⁵ M. A. Huertos, J. Pérez, L. Riera, A. Menéndez-Velázquez, *J. Am. Chem. Soc.* **2008**, 130, 13530.

Whittlesey y col. observaron en 2006, al estudiar la reactividad de diversos complejos de rutenio con el 1,3-di-isopropil-4,5-dimetilimidazol-2-ilideno, la formación del tautómero N y la del correspondiente carbeno (Esquema I – 10).⁴⁶

Esquema I - 10



Los estudios encaminados a determinar la estabilidad de estos tautómeros indican que el isómero *N* – resulta tras tiempos prologados de reacción, es decir, es la especie termodinámicamente más estable y se observa que el proceso de tautomerización transcurre en presencia de NHC. Este proceso constituye el primer ejemplo de tautomería $C \rightarrow N$ de un carbeno derivado del imidazol. Dado que el proceso requiere la presencia de un carbeno libre, se propone que transcurre probablemente bajo catálisis básica, aunque los intentos para determinar la proveniencia del protón en el grupo NH han resultado infructuosos. Este resultado, que está de acuerdo con la propuesta de Crabtree y Eisenstein, atribuye a la presencia de un grupo aceptor π en *trans* con respecto al imidazol (CO), la mayor estabilidad del tautómero N.

Todos estos resultados ponen de manifiesto la capacidad de los complejos de los metales de transición para inducir transformaciones que requieren energías muy altas en las moléculas orgánicas libres, y revelan además que los procesos de tautomería de las piridinas y sus derivados son muchos más generales de lo que se creía hasta el presente.

⁴⁶ S. Burling, M. F. Mahon, R. E. Powell, M. K. Whittlesey, J. Williams, *J. Am. Chem. Soc.* **2006**, 128, 13702.

1.4. Bibliografía

1. E. Brown, *Ring Nitrogen and Key Biomolecules: The Biochemistry of N-Heterocycles*, Kluwer Academic, Boston, **1998**.
2. J. S. Carey, D. Laffan, C. Thomson, M. T. Williams, *Org. Biomol. Chem.* **2006**, *4*, 2337.
3. V. Balzani, A. Juris, M. Venturi, S. Campagna, S. Serroni, *Chem. Rev.* **1996**, *96*, 759.
4. K. Matsumoto, *Heterocyclic Supramolecules I, Vol. 17*, Springer-Verlag, Berlin-Heidelberg, **2008**.
5. W. Pitt, D. Parry, B. Perry, C. Groom, *J. Med. Chem.* **2009**, *52*, 2952.
6. H. Davies, C. Bolm, *Chem. Soc. Rev.* **2007**, *36*, 1035.
7. P. Tomasik, Z. Ratajewicz, *Chemistry of Heterocyclic Compounds: Pyridine Metal Complexes, Part 6, Vol. 14*, John Wiley & Sons, New York, **1985**.
8. A. P. Sadimenko, *Adv. Heterocycl. Chem.* **2005**, *88*, 111.
9. A. Katritzky, A. Pozharskii, *Handbook of Heterocyclic Chemistry*, 2 ed., Pergamon Press, New York, **2000**.
10. J. J. R. Fraústo Da Silva, J. G. Calado, *J. Inorg. Nucl. Chem.* **1966**, *28*, 125.
11. a) R. Cordone, W. D. Harman, H. Taube, *J. Am. Chem. Soc.* **1989**, *111*, 2896. b) D. A. Delafuente, G. W. Kosturko, P. M. Graham, W. H. Harman, W. H. Myers, Y. Surendranath, R. C. Klet, K. D. Welch, C. O. Trindle, M. Sabat, W. D. Harman, *J. Am. Chem. Soc.* **2007**, *129*, 406. c) W. D. Harman, *Chem. Rev.* **1997**, *97*, 1953. d) D. Harrison, K. Welch, A. Nichols-Nielander, M. Sabat, W. H. Myers, W. D. Harman, *J. Am. Chem. Soc.* **2008**, *130*, 16844. e) S. Meiere, B. Brooks, T. Gunnoe, E. Carrig, M. Sabat, W. D. Harman, *Organometallics* **2001**, *20*, 3661.
12. a) E. Wucherer, E. Muetterties, *Organometallics* **1987**, *6*, 1691. b) E. Wucherer, E. Muetterties, *Organometallics* **1987**, *6*, 1696. c) R. H. Fish,

- H. Kim, J. Babin, R. Adams, *Organometallics* **1988**, *7*, 2250. **d)** S. G. Davies, M. R. Shipton, *J. Chem. Soc., Chem. Commun.* **1989**, 995. **e)** R. H. Fish, H. Kim, R. Fong, *Organometallics* **1989**, *8*, 1375. **f)** R. H. Fish, E. Baralt, H. Kim, *Organometallics* **1991**, *10*, 3411. **g)** R. H. Fish, R. Fong, A. Tran, E. Baralt, *Organometallics* **1991**, *10*, 1209. **h)** G. Zhu, J. Tanski, D. Churchill, K. Janak, G. Parkin, *J. Am. Chem. Soc.* **2002**, *124*, 13658.
- 13.** K. Allen, M. Bruck, S. Gray, R. Kingsborough, D. Smith, K. Weller, D. E. Wigley, *Polyhedron* **1995**, *14*, 3315.
- 14.** **a)** D. Neithamer, L. Parkanyi, J. Mitchell, P. T. Wolczanski, *J. Am. Chem. Soc.* **1988**, *110*, 4421. **b)** J. R. Strickler, M. A. Bruck, D. E. Wigley, *J. Am. Chem. Soc.* **1990**, *112*, 2814. **c)** K. Covert, D. Neithamer, M. Zonnevylle, R. LaPointe, C. Schaller, P. T. Wolczanski, *Inorg. Chem.* **1991**, *30*, 2494. **d)** S. Gray, D. Smith, M. Bruck, D. E. Wigley, *J. Am. Chem. Soc.* **1992**, *114*, 5462. **e)** P. T. Wolczanski, *Polyhedron* **1995**, *14*, 3335. **f)** T. S. Kleckley, J. L. Bennett, P. T. Wolczanski, E. B. Lobkovsky, *J. Am. Chem. Soc.* **1997**, *119*, 247. **g)** A. Veige, T. Kleckley, R. Chamberlin, D. Neithamer, C. Lee, P. T. Wolczanski, E. Lobkovsky, W. Glassey, *J. Organomet. Chem.* **1999**, *591*, 194. **h)** J. B. Bonanno, A. S. Veige, P. T. Wolczanski, E. B. Lobkovsky, *Inorg. Chim. Acta* **2003**, *345*, 173.
- 15.** I. Seregin, V. Gevorgyan, *Chem. Soc. Rev.* **2007**, *36*, 1173.
- 16.** **a)** K. Den Haan, J. De Boer, J. Teuben, A. Spek, B. Kojic-Prodic, G. Hays, R. Huis, *Organometallics* **1986**, *5*, 1726. **b)** R. F. Jordan, D. Taylor, *J. Am. Chem. Soc.* **1989**, *111*, 778. **c)** R. F. Jordan, D. Taylor, N. Baenziger, *Organometallics* **1990**, *9*, 1546. **d)** R. F. Jordan, A. Guram, *Organometallics* **1990**, *9*, 2116. **e)** A. Guram, R. F. Jordan, *Organometallics* **1990**, *9*, 2190. **f)** A. Guram, R. F. Jordan, *Organometallics* **1991**, *10*, 3470. **g)** R. Boaretto, P. Roussel, A. Kingsley, I. Munslow, *Chem. Commun.* **1999**, 1701. **i)** H. Selnau, J. Merola, *Organometallics* **1993**, *12*, 1583. **h)** W. Jones, L. Dong, A. Myers, *Organometallics* **1995**, *14*, 855. **j)** M. Paneque, P. J. Perez, A. Pizzano, M.

- L. Poveda, S. Taboada, M. Trujillo, E. Carmona, *Organometallics* **1999**, *18*, 4304. **l)** C. Bradley, E. Lobkovsky, P. Chirik, *J. Am. Chem. Soc.* **2003**, *125*, 8110. **m)** O. Ozerov, M. Pink, L. Watson, K. Caulton, *J. Am. Chem. Soc.* **2004**, *126*, 2105. **n)** S. Arndt, B. R. Elvidge, P. M. Zeimentz, T. P. Spaniol, J. Okuda, *Organometallics* **2006**, *25*, 793. **o)** K. Jantunen, B. Scott, J. Gordon, J. Kiplinger, *Organometallics* **2007**, *26*, 2777. **p)** J. Kiplinger, B. Scott, E. Schelter, J. A. Pool-Davis-Tournear, *J. Alloys Compd.* **2007**, *444*, 477. **q)** D. Krut'ko, R. Kirsanov, S. Belov, M. Borzov, A. Churakov, J. Howard, *Polyhedron* **2007**, *26*, 2864. **r)** G. Zhu, K. Pang, G. Parkin, *J. Am. Chem. Soc.* **2008**, *130*, 1564.
- 17.** A. Eisenstadt, C. Giandomenico, M. Frederick, R. Laine, *Organometallics* **1985**, *4*, 2033.
- 18.** S. Bi, Z. Lin, R. F. Jordan, *Organometallics* **2004**, *23*, 4882.
- 19.** E. Moore, W. Pretzer, T. O'Connell, J. Harris, *J. Am. Chem. Soc.* **1992**, *114*, 5888.
- 20.** **a)** R. Grigg, V. Savic, *Tetrahedron Lett.* **1997**, *38*, 5737. **b)** T. Fukuyama, N. Chatani, J. Tatsumi, F. Kakiuchi, S. Murai, *J. Am. Chem. Soc.* **1998**, *120*, 11522. **c)** K. Godula, B. Sezen, D. Sames, *J. Am. Chem. Soc.* **2005**, *127*, 3648.
- 21.** M. Murakami, S. Hori, *J. Am. Chem. Soc.* **2003**, *125*, 4720.
- 22.** Y. Nakao, K. Kanyiva, T. Hiyama, *J. Am. Chem. Soc.* **2008**, *130*, 2448.
- 23.** C. J. Emanuel, P. B. Shevlin, *J. Am. Chem. Soc.* **1994**, *116*, 5991.
- 24.** **a)** P. Dyson, D. Hammick, *J. Chem. Soc.* **1937**, 1724. **b)** M. Ashworth, R. Daffern, D. Hammick, *J. Chem. Soc.* **1939**, 809.
- 25.** **a)** K. Ratts, R. Howe, W. Phillips, *J. Am. Chem. Soc.* **1969**, *91*, 6115. **b)** E. Brown, M. Shambhu, *J. Org. Chem.* **1971**, *36*, 2002.
- 26.** R. Breslow, *J. Am. Chem. Soc.* **1958**, *80*, 3719.
- 27.** **a)** B. Brown, D. Hammick, *J. Chem. Soc.* **1949**, 659. **b)** P. Haake, J. Mantecon, *J. Am. Chem. Soc.* **1964**, *86*, 5230.

-
28. a) R. Gleiter, R. Hoffmann, *J. Am. Chem. Soc.* **1968**, 90, 5457. b) R. Grigg, L. Wallace, J. O. Morley, *J. Chem. Soc., Perkin Trans. 2* **1990**, 51.
29. P. Chen, *J. Org. Chem.* **1976**, 41, 2973.
30. a) D. Lavorato, J. Terlouw, T. Dargel, W. Koch, G. McGibbon, H. Schwarz, *J. Am. Chem. Soc.* **1996**, 118, 11898. b) D. Lavorato, J. Terlouw, G. McGibbon, T. Dargel, W. Koch, H. Schwarz, *Int. J. Mass Spectrom.* **1998**, 179, 7.
31. O. Hollóczki, L. Nyulászi, *J. Org. Chem.* **2008**, 73, 4794.
32. O. Schuster, L. Yang, H. Raubenheimer, M. Albrecht, *Chem. Rev.* **2009**, 109, 3445.
33. a) P. Fraser, W. Roper, F. Stone, *J. Chem. Soc., Dalton Trans.* **1974**, 760. b) U. Kirchgaessner, H. Piana, U. Schubert, *J. Am. Chem. Soc.* **1991**, 113, 2228. c) W. Meyer, M. Deetlefs, M. Pohlmann, R. Scholz, M. Esterhuysen, G. Julius, H. Raubenheimer, *Dalton Trans.* **2004**, 413.
34. a) J. Owen, J. Labinger, J. Bercaw, *J. Am. Chem. Soc.* **2004**, 126, 8247. b) N. Piro, J. Owen, J. Bercaw, *Polyhedron* **2004**, 23, 2797.
35. a) K. Nakatsu, K. Kinoshita, H. Kanda, K. Isobe, *Chem. Lett.* **1980**, 913. b) K. Isobe, E. Kai, Y. Nakamura, K. Nishimoto, T. Miwa, S. Kawaguchi, K. Kinoshita, K. Nakatsu, *J. Am. Chem. Soc.* **1980**, 102, 2475. c) B. Crociani, F. Di Bianca, A. Giovenco, A. Scrivanti, *J. Organomet. Chem.* **1983**, 251, 393. d) K. Isobe, Y. Nakamura, T. Miwa, S. Kawaguchi, *Bull. Chem. Soc. Jpn.* **1987**, 60, 149. e) B. Crociani, F. Di Bianca, A. Giovenco, A. Berton, R. Bertani, *J. Organomet. Chem.* **1989**, 361, 255. f) F. Di Bianca, A. Fontana, R. Bertani, B. Crociani, *J. Organomet. Chem.* **1992**, 425, 155.
36. a) H. G. Raubenheimer, J. G. Toerien, G. J. Kruger, R. Otte, W. van Zyl, P. Olivier, *J. Organomet. Chem.* **1994**, 466, 291. b) A. Poulain, A. Neels, M. Albrecht, *Eur. J. Inorg. Chem.* **2009**, 13, 1871.
37. R. Cordone, H. Taube, *J. Am. Chem. Soc.* **1987**, 109, 8101.
38. W. D. Harman, H. Taube, *J. Am. Chem. Soc.* **1987**, 109, 1883.

- 39. S. H. Wiedemann, J. C. Lewis, J. A. Ellman, R. Bergman, *J. Am. Chem. Soc.* **2006**, *128*, 2452.
- 40. a) J. C. Lewis, R. Bergman, J. A. Ellman, *J. Am. Chem. Soc.* **2007**, *129*, 5332. b) A. M. Berman, J. C. Lewis, R. Bergman, J. A. Ellman, *J. Am. Chem. Soc.* **2008**, *130*, 14926.
- 41. M. A. Esteruelas, F. Fernandez-Álvarez, E. Oñate, *J. Am. Chem. Soc.* **2006**, *128*, 13044.
- 42. G. Sini, O. Eisenstein, R. H. Crabtree, *Inorg. Chem.* **2002**, *41*, 602.
- 43. R. J. Sundberg, R. F. Bryan, I. F. Taylor Jr., H. Taube, *J. Am. Chem. Soc.* **1974**, *96*, 381.
- 44. J. Ruiz, B. F. Perandones, *J. Am. Chem. Soc.* **2007**, *129*, 9298.
- 45. M. A. Huertos, J. Pérez, L. Riera, A. Menéndez-Velázquez, *J. Am. Chem. Soc.* **2008**, *130*, 13530.
- 46. S. Burling, M. F. Mahon, R. E. Powell, M. K. Whittlesey, J. Williams, *J. Am. Chem. Soc.* **2006**, *128*, 13702.

II. Results and Discussion

II. Results and Discussion

Transition metal complexes containing cyclometallated pyridines or other N-heterocycles are known nowadays for their interesting photophysical properties.¹ To date, applications of these properties have been found in several areas, from CO₂ photocatalytic reduction² to phosphorescent doping in OLED's³ and oxidation of water.⁴ In particular, several cyclometallated Ir(III) complexes with 2-phenylpyridines with outstanding luminescent properties are described in the literature,⁵ and the study of their photophysical characteristics remains an area of major interest. Reactivity studies with the 16 e⁻ unsaturated iridium fragment [Tp^{Me2}IrPh₂] (**A**) (Tp^{Me2} = hydrotris(3,5-dimethylpyrazolyl)borate) have demonstrated the capacity of this species to activate C–H bonds.⁶ This intermediate is generated *in situ* both by routes 1 or 2, of Scheme II - 1, and the presence of a vacant site makes it extremely reactive towards a variety of

¹ T. Meyer, *Pure Appl. Chem.* **1986**, 58, 1193.

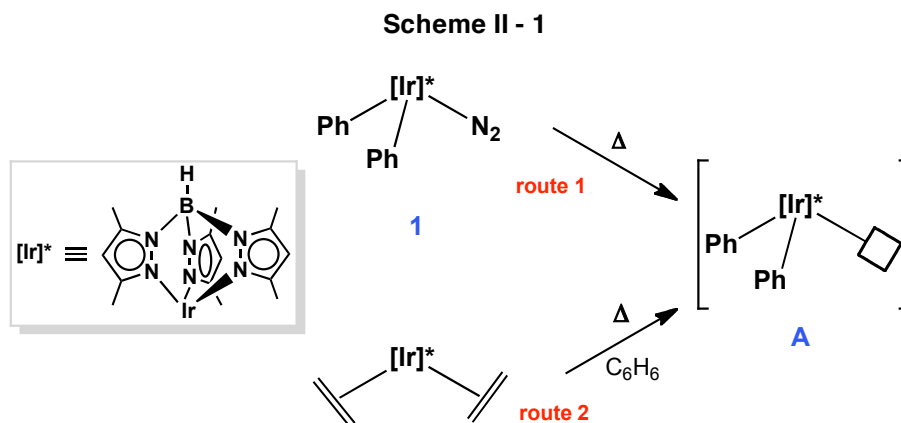
² **a)** C. Kutal, A. Corbin, G. Ferraudi, *Organometallics* **1987**, 6, 553. **b)** J. Van Diemen, R. Hage, J. Haasnoot, H. Lempers, J. Reedijk, J. Vos, L. De Cola, F. Barigelletti, V. Balzani, *Inorg. Chem.* **1992**, 31, 3518. **c)** F. Johnson, M. George, F. Hartl, J. Turner, *Organometallics* **1996**, 15, 3374. **d)** Y. Hayashi, S. Kita, B. Brunschwig, E. Fujita, *J. Am. Chem. Soc.* **2003**, 125, 11976.

³ **a)** E. Holder, B. Langeveld, U. Schubert, *Adv. Mat.* **2005**, 17, 1109. **b)** H. Yersin, *Highly efficient OLEDs with phosphorescent materials*, Wiley-VCH, Weinheim, **2007**.

⁴ **a)** N. McDaniel, F. Coughlin, L. Tinker, S. Bernhard, *J. Am. Chem. Soc.* **2008**, 130, 210. **b)** J. Hull, D. Balcells, J. Blakemore, C. Incarvito, O. Eisenstein, G. Brudvig, R. H. Crabtree, *J. Am. Chem. Soc.* **2009**, 131, 8730.

⁵ **a)** S. Lamansky, P. Djurovich, D. Murphy, F. Abdel-Razzaq, H. E. Lee, C. Adachi, P. E. Burrows, S. R. Forrest, M. E. Thompson, *J. Am. Chem. Soc.* **2001**, 123, 4304. **b)** K. Lo, D. Ng, C. Chung, *Organometallics* **2001**, 20, 4999. **c)** A. B. Tamayo, B. D. Alleyne, P. I. Djurovich, S. Lamansky, I. Tsyba, N. N. Ho, R. Bau, M. E. Thompson, *J. Am. Chem. Soc.* **2003**, 125, 7377. **d)** J. D. Slinker, A. A. Gorodetsky, M. S. Lowry, J. Wang, S. Parker, R. Rohl, S. Bernhard, G. G. Malliaras, *J. Am. Chem. Soc.* **2004**, 126, 2763. **e)** K. Lo, J. Chan, L. Lui, C. Chung, *Organometallics* **2004**, 23, 3108. **f)** T. Sajoto, P. Djurovich, A. Tamayo, M. Yousufuddin, R. Bau, M. Thompson, R. Holmes, S. Forrest, *Inorg. Chem.* **2005**, 44, 7992. **g)** M. Lowry, S. Bernhard, *Chem. Eur. J.* **2006**, 12, 7971. **h)** T. Sajoto, P. Djurovich, A. Tamayo, J. Oxgaard, W. Goddard, M. Thompson, *J. Am. Chem. Soc.* **2009**, 131, 9813.

reagents. Moreover, this and other $[\text{Tp}^{\text{Me}_2}\text{Ir}(\text{R})(\text{R}')]]$ fragments, where R and R' are anionic ligands, are suitable for related reactivity studies. For instance they have been found to strongly stabilize carbene ligands with or without heteroatom substituents, also generated through C–H activation reactions. This complementarity, that may be referred to as carbenophilia, is responsible for the unusual isomerization of aromatic aldehydes to hydroxycarbene ligands,⁷ and of Ir-alkene termini to Ir-alkylidenes,⁸ among other unusual rearrangements.



The work described in the present manuscript started with the study of the reactivity of 2-phenylpyridine with $\text{Tp}^{\text{Me}_2}\text{IrPh}_2(\text{N}_2)$ (**1**). The main purpose was to achieve C–H activation of the pendant phenyl ring, favoured by the chelate effect attained by

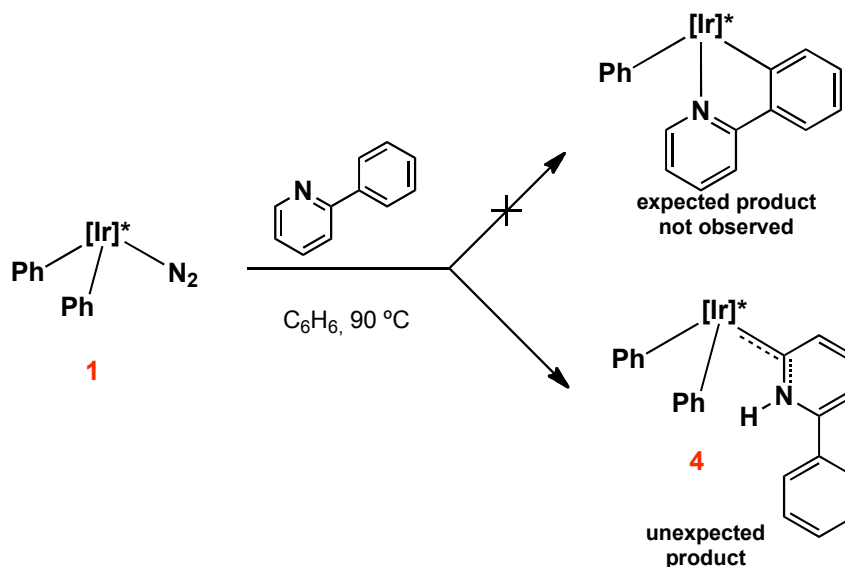
⁶ E. Gutiérrez-Puebla, A. Monge, M. C. Nicasio, P. J. Pérez, M. L. Poveda, E. Carmona, *Chem. Eur. J.* **1998**, *4*, 2225.

⁷ E. Gutiérrez-Puebla, A. Monge, M. Paneque, M. L. Poveda, V. Salazar, E. Carmona, *J. Am. Chem. Soc.* **1999**, *121*, 248.

⁸ **a)** L. Santos, K. Mereiter, M. Paneque, C. Slugovc, E. Carmona, *New J. Chem.* **2003**, *27*, 107. **b)** M. Paneque, M. L. Poveda, L. L. Santos, E. Carmona, A. Lledós, G. Ujaque, K. Mereiter, *Angew. Chem. Int. Ed.* **2004**, *43*, 3708. **c)** P. Lara, M. Paneque, M. L. Poveda, V. Salazar, L. L. Santos, E. Carmona, *J. Am. Chem. Soc.* **2006**, *128*, 3512. **d)** E. Álvarez, M. Paneque, A. Petronilho, M. L. Poveda, L. L. Santos, E. Carmona, K. Mereiter, *Organometallics* **2007**, *26*, 1231. **e)** P. Lara, M. Paneque, M. L. Poveda, L. L. Santos, J. E. V. Valpuesta, V. Salazar, E. Carmona, S. Moncho, G. Ujaque, A. Lledós, C. Maya, K. Mereiter, *Chem. Eur. J.* **2009**, *15*, 9046. **f)** P. Lara, M. Paneque, M. L. Poveda, L. L. Santos, J. E. V. Valpuesta, E. Carmona, S. Moncho, G. Ujaque, A. Lledós, E. Álvarez, K. Mereiter, *Chem. Eur. J.* **2009**, *15*, 9034. **g)** S. Conejero, M. Paneque, M. L. Poveda, L. L. Santos, E. Carmona, *Acc. Chem. Res.* **2010**, *43*, 572.

cyclometallation⁹. It is known that Ir(III) is capable to form mono-, bis- and tris-cyclometallated complexes,^{2d,10} under appropriate conditions, and, moreover, that Cp' Ir(III) organometallic derivatives also afford cyclometallated compounds with 2-phenylpyridine.^{4b,11}

Scheme II - 2



Much to our surprise, when this reaction was carried out, the expected cyclometallation did not take place. Instead, and as revealed by NMR spectroscopic studies, a new Ir species containing two phenyl groups and one pyridine-derived carbene ligand, formally akin to **I** (see Introduction) was the reaction product. Clearly, this ligand is the result of a formal 1,2-hydrogen shift from carbon to nitrogen.

This unexpected reactivity of $[\text{Tp}^{\text{Me}_2}\text{IrPh}_2]$ towards 2-phenylpyridine represented the first observation of the tautomerization of a pyridine mediated by transition metal

⁹ M. Albrecht, *Chem. Rev.* **2009**, *110*, 576.

¹⁰ **a)** S. Sprouse, K. King, P. Spellane, R. Watts, *J. Am. Chem. Soc.* **1984**, *106*, 6647. **b)** K. King, P. Spellane, R. Watts, *J. Am. Chem. Soc.* **1985**, *107*, 1431. **c)** K. King, R. Watts, *J. Am. Chem. Soc.* **1987**, *109*, 1589. **d)** K. Garcés, K. King, R. Watts, *Inorg. Chem.* **1988**, *27*, 3464. **e)** S. Lamansky, P. Djurovich, D. Murphy, F. Abdel-Razzaq, R. Kwong, I. Tsyba, M. Bortz, B. Mui, R. Bau, M. Thompson, *Inorg. Chem.* **2001**, *40*, 1704.

¹¹ **a)** L. Li, W. Brennessel, W. Jones, *Organometallics* **2009**, *28*, 3492. **b)** L. S. Park-Gehrke, J. Freudenthal, W. Kaminsky, A. G. Dipasquale, J. M. Mayer, *Dalton Trans.* **2009**, 1972.

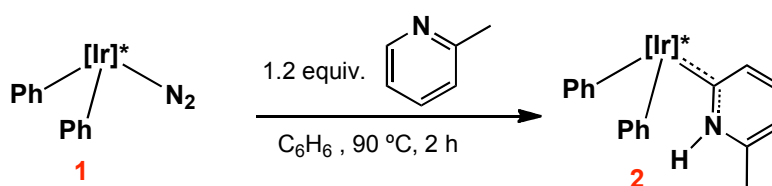
complexes, with the exception of the much more congested 2,6-dimethylpyridine commented in the Introduction section. It was therefore deemed worthwhile to investigate in detail the reactivity of a series of pyridines and related N-heterocycles. The aim of the study described in the present Doctoral Thesis is thus an in deep examination of this transformation, in order to establish the scope of the reaction and its mechanism. In addition, and since nowadays NHCs (NHC stands for N-heterocyclic carbene) represent a class of ligands of great importance,¹² the reactivity of the new complexes was also pursued, and the results are also described herein.

II.1. Reaction of $\text{Tp}^{\text{Me}_2}\text{IrPh}_2(\text{N}_2)$ with Pyridines

II.1.1. Reaction of $\text{Tp}^{\text{Me}_2}\text{IrPh}_2(\text{N}_2)$ with 2-Picoline

II.1.1.1. Synthesis of the N-Heterocyclic Carbene Complex **2**

2-Methylpyridine reacts with $\text{Tp}^{\text{Me}_2}\text{IrPh}_2(\text{N}_2)$ (**1**) at 90 °C in C_6H_6 to afford the yellow complex **2**, as the only reaction product (Eq. 1). The transformation is very clean and no side products are detected. After purification by chromatography, **2** was fully characterized by elemental analysis and by spectroscopy. All data obtained are in accord with the proposed N-heterocyclic carbene structure **2**, as represented in Eq. 1.



Equation 1

¹² a) D. Bourissou, O. Guerret, F. Gabbai, G. Bertrand, *Chem. Rev.* **2000**, *100*, 39. b) W. Herrmann, *Angew. Chem. Int. Ed.* **2002**, *41*, 1290. c) E. Peris, R. H. Crabtree, *Coord. Chem. Rev.* **2004**, *248*, 2239. d) O. Köhl, *Chem. Soc. Rev.* **2007**, *36*, 592. e) F. Hahn, M. Jahnke, *Angew. Chem. Int. Ed.* **2008**, *47*, 3122. f) P. de Fremont, N. Marion, S. P. Nolan, *Coord. Chem. Rev.* **2009**, *253*, 862. g) O. Schuster, L. Yang, H. Raubenheimer, M. Albrecht, *Chem. Rev.* **2009**, *109*, 3445.

The IR spectrum of **2** features an absorption at 3325 cm^{-1} , associated with the NH group. The ^1H NMR spectrum of **2** at room temperature shows some very broad signals (Fig. II – 1). Low temperature NMR studies are in fact in accord with complex **2** existing as a mixture of two interchanging rotamers, **2a** and **2b**, that are in fast

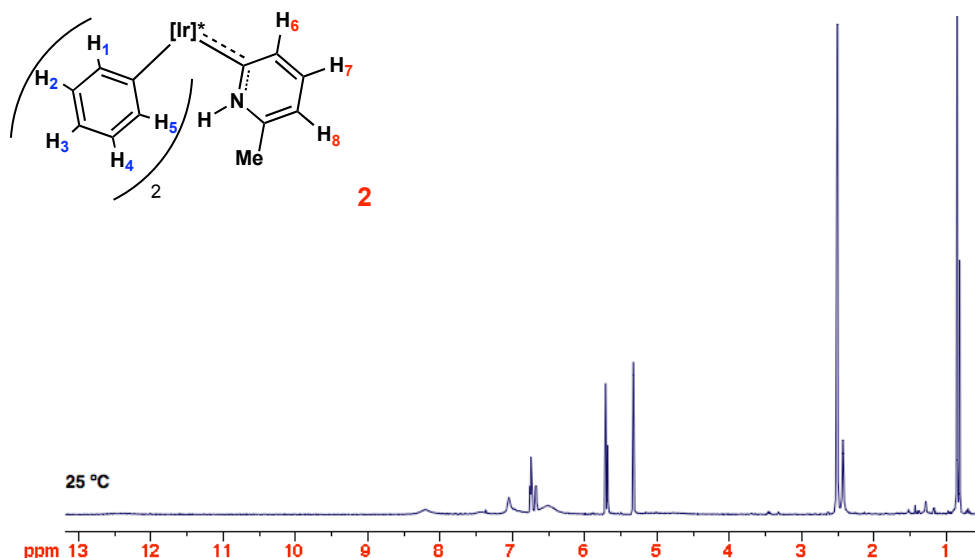


Figure II - 1. ^1H NMR spectrum of complex **2** (25 °C, CD_2Cl_2 , 500 MHz).

equilibrium on the NMR time scale at 25 °C, while they are, in a 5:1 ratio, in the slow exchange regime (CD_2Cl_2 at -60 °C; Fig. II – 2). The ^1H NMR resonances corresponding to the Tp^{Me_2} ligand appear as two collections of signals, one between 0.8 and 2.45 ppm corresponding to six methyl groups, in a 2:1:2:1 ratio, and the other between 5.40 and 5.70, in a 2:1 ratio, as expected for $\text{Tp}^{\text{Me}_2}\text{IrR}_1\text{R}_2\text{L}$ complexes when $\text{R}_1 = \text{R}_2$, and the corresponding C_s symmetry. Relevant spectroscopic ^1H NMR signals at 12.91 (**2a**, major) and 10.14 ppm (**2b**, minor) are attributed to the N-bound proton of the two rotamers and their relationship with respect to the phenyl groups is easily deduced from the 2D NOESY spectrum. In the $^{13}\text{C}\{^1\text{H}\}$ NMR spectrum a carbene signal for the major rotamer **2a** is observed at 175 ppm, comparable to that found in similar complexes.¹³

¹³ E. Mas-Marzá, M. Poyatos, M. Sanaú, E. Peris, *Inorg. Chem.* **2004**, *43*, 2213.

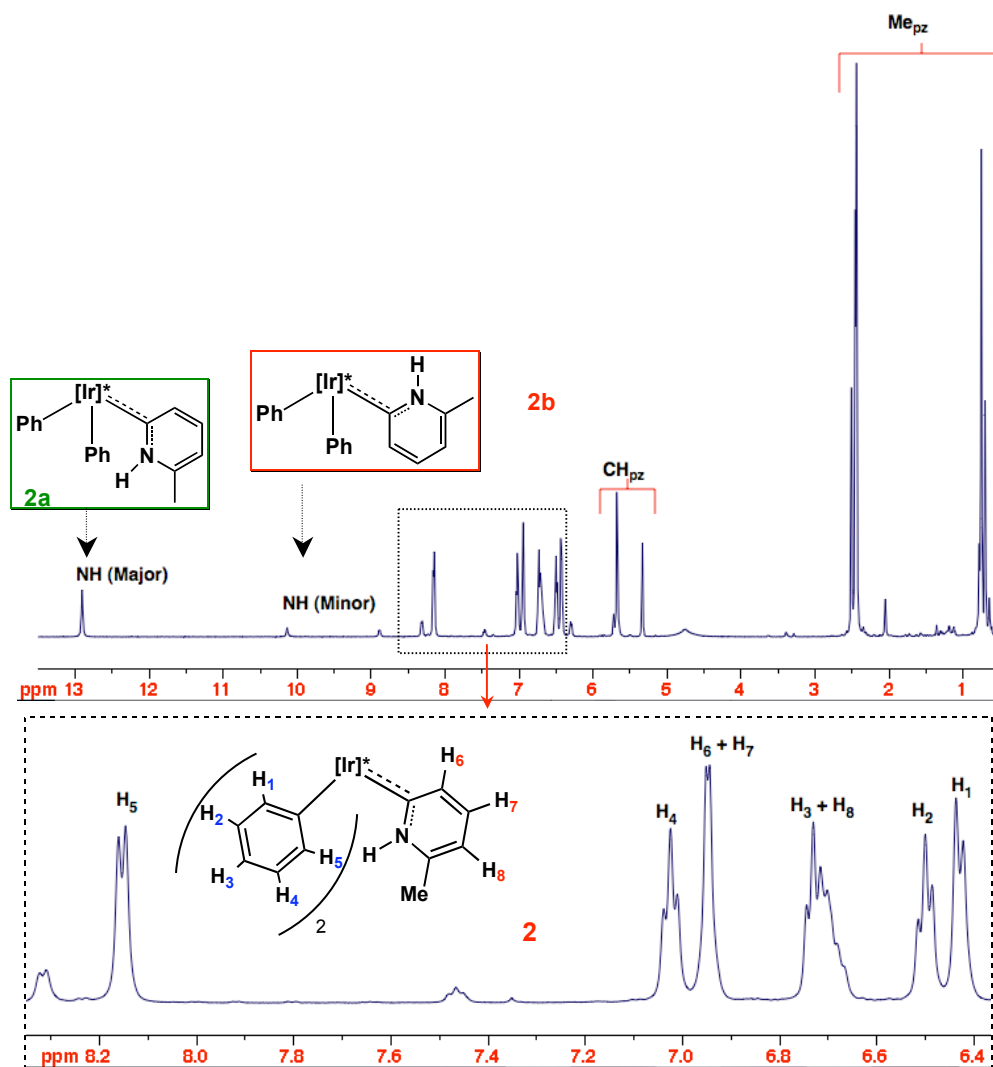


Figure II - 2. ^1H NMR spectrum of complex **2** ($-60\text{ }^\circ\text{C}$, CD_2Cl_2 , 500 MHz).

The molecular structure of **2** in the solid state has been determined by single crystal X-ray crystallography (Fig. II – 3, see Appendix 1- Table A1). As can be observed, the rotamer present in the crystal is **2a**. The Ir–C_{carbene} bond has a normal length of *ca.* 1.98 Å,^{8b,14} somewhat shorter than the corresponding Ir–C distances to the phenyl groups of

¹⁴ L. Appelhans, D. Zuccaccia, A. Kovacevic, A. Chianese, J. Miecznikowski, A. Macchioni, E. Clot, O. Eisenstein, R. Crabtree, *J. Am. Chem. Soc.* **2005**, *127*, 16299.

ca. 2.05 Å, and comparable to corresponding separations found in other NHC iridium compounds.¹⁵

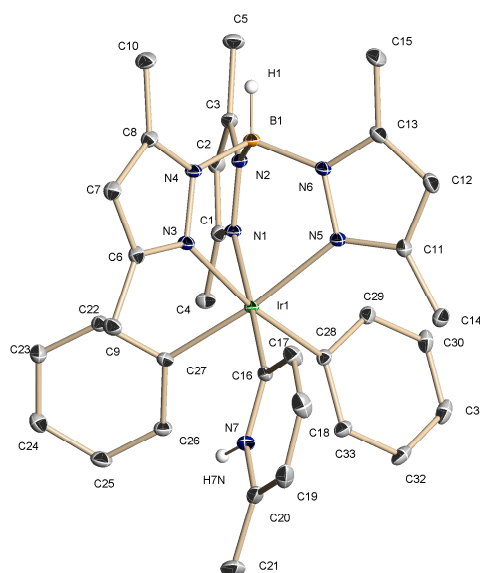


Figure II - 3. ORTEP representation of complex **2a**.

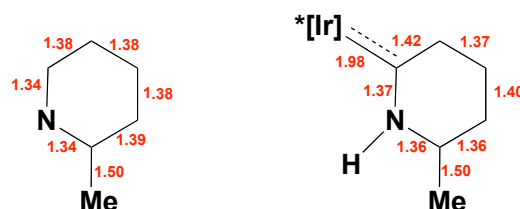


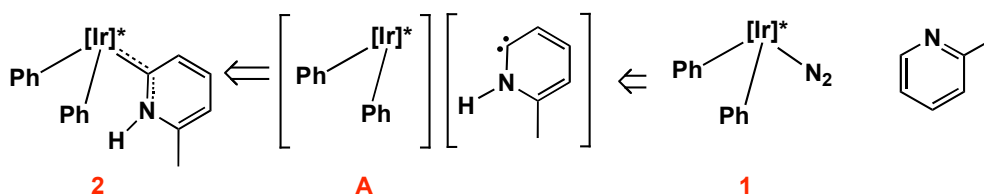
Figure II - 4. Selected bond lengths of 2-picoline and complex **2a**.

A comparison of the bond lengths of free 2-picoline¹⁶ and the carbene ligand of **2** illustrates the distortion of the pyridyl ring when bonded to the metal centre (Fig. II - 4). Thus, whereas the C–C bond lengths in free 2-picoline are identical (1.38 Å), the carbene ligand exhibits two C–C bonds with lengths of around 1.36 Å, which are distinctly shorter than the other two (around 1.41 Å). The coordinated ring therefore exhibits some diene character.

¹⁵ **a)** N. M. Scott, R. Dorta, E. D. Stevens, A. Correa, L. Cavallo, S. P. Nolan, *J. Am. Chem. Soc.* **2005**, *127*, 3516. **b)** S. Leuthäusser, D. Schwarz, H. Plenio, *Chem. Eur. J.* **2007**, *13*, 7195. **c)** Y. Chang, C. Fu, Y. Liu, S. Peng, J. Chen, S. Liu, *Dalton Trans.* **2009**, 861.

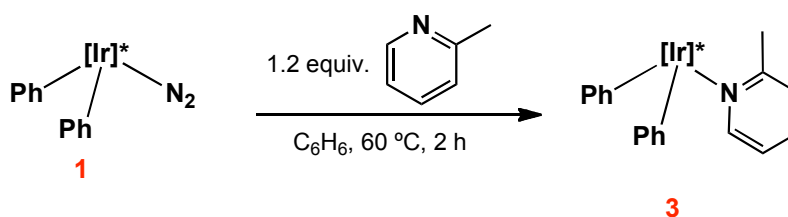
Complex **2** retains the two phenyl groups present in the starting material and results, formally, from a 1,2-hydrogen migration from the C₆ atom of the pyridine to its nitrogen and subsequent carbene binding to the iridium centre (Scheme II – 3). It should be noted in this regard that for free pyridine this 1,2- hydrogen shift needs overcoming a barrier¹⁷ of about 85 kcal·mol⁻¹.

Scheme II - 3



II.1.1.2. Synthesis of the N-Bound Adduct **3**

In order to detect possible intermediates in the reaction leading to **2**, the reaction of complex **1** and 2-picoline was studied at lower temperatures. In fact, 2-picoline reacts with **1** at 60 °C in benzene forming a new complex, the N-bound adduct **3**, in almost quantitative yield (Eq. 2). After chromatographic purification, this new species was fully characterized by spectroscopy.



Equation 2

¹⁶ A. D. Bond, J. E. Davies, *Acta Crystallogr. Sect. E* **2001**, 57, 1089.

¹⁷ D. Lavorato, J. Terlouw, G. McGibbon, T. Dargel, W. Koch, H. Schwarz, *Int. J. Mass Spectrom.* **1998**, 179, 7.

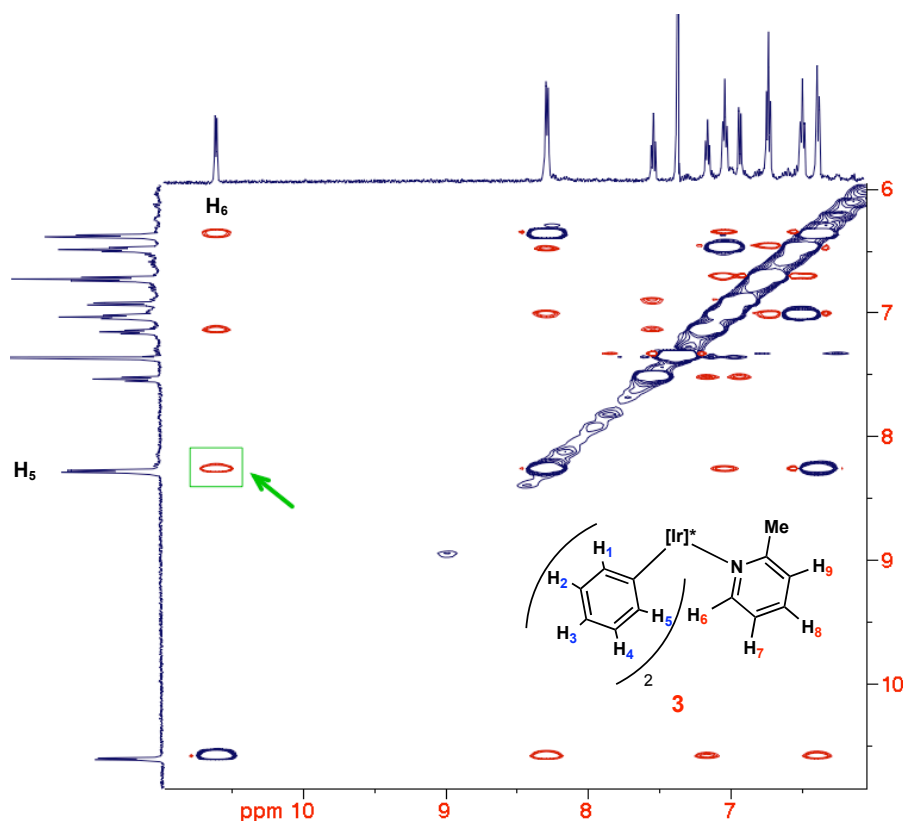


Figure II - 5. NOESY spectrum of complex **3** (0 °C, CDCl₃, 500 MHz).

The room temperature ¹H NMR spectrum shows some broad signals, suggesting hindered rotation around the Ir–C bonds. In CD₂Cl₂, at -60 °C, only one rotamer is observed, and this corresponds to the one that has the methyl group of the pyridine ring pointing away of the phenyl coligands. This is shown by the existence of a strong NOE between H₆ and H₅ as represented in Fig. II - 5. This is also the rotamer present in the solid state as confirmed by X-ray diffraction studies (Fig. II – 6, see Appendix 1- Table A3). The Ir–N(7) bond length is of 2.14 Å, while the average Ir–C_{ph} distance is 2.05 Å. Considering that the covalent radius of nitrogen is somewhat smaller than that of carbon,¹⁸ comparison of the Ir–N and Ir–C distances to the neutral ligand in complexes **3** and **2a** reveals an interesting effect. In carbene **2a** the Ir–C bond length is equal to

¹⁸ B. Cordero, V. Gómez, A. E. Platero-Prats, M. Revés, J. Echeverría, E. Cremades, F. Barragán, S. Álvarez, *Dalton Trans.* **2008**, 2832.

1.98 Å, while the Ir–N separation in **3** is 2.14 Å becomes larger by 0.16 Å. Clearly this is a manifestation of steric hindrance between the sterically demanding Lewis base (as a consequence of its 2-Me substituent) and the also bulky iridium Lewis acid centre. Therefore, it is this strain (called F-strain,¹⁹ see Section 1.4) that destabilizes the N-adduct whereas no such steric hindrance appears to exist in the carbene isomer.

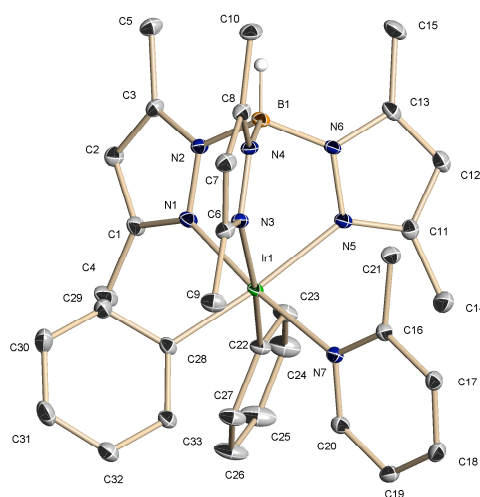
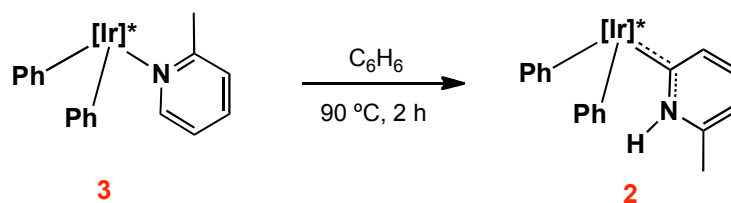


Figure II - 6. ORTEP representation of complex **3**.

In order to determine the role of **3** in the formation of **2**, an isolated sample of the former was heated, in C₆H₆, at 90 °C. As expected, complete conversion of **3** into **2** was observed (Eq. 3). Therefore, we can deduce that **3** is the kinetically controlled product of the reaction whereas **2** is the thermodynamically more stable compound. It cannot be stated, however, that **3** is a true intermediate in the pathway leading to **2**.

¹⁹ a) H. C. Brown, H. Schlesinger, S. Cardon, *J. Am. Chem. Soc.* **1942**, 64, 325. b) H. C. Brown, *Science* **1946**, 103, 385. c) H. C. Brown, *J. Chem. Soc.* **1956**, 1248

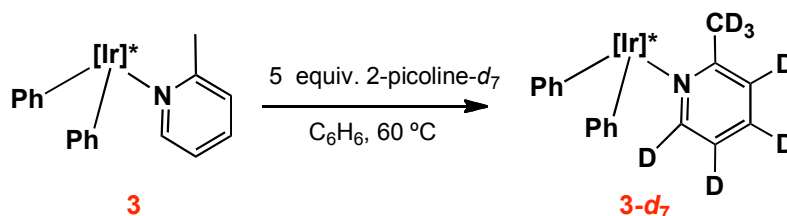


Equation 3

II.1.1.3. Isotopic Studies: Exchange Reactions and Determination of the Kinetic Isotopic Effect

Concerning the question of the real intermediacy of **3** in the mechanistic pathway that produces **2**, it must be recalled that Bergman and Ellman, in a related transformation involving 3-methyl-3,4-dihydro-quinazoline and Rh(I) (Eq. IX, Introduction), have concluded that the N-bound adduct converts intramolecularly into the corresponding N-heterocyclic carbene.²⁰ In an attempt to shed light in this mechanistic step in our system, some isotopic studies were performed.

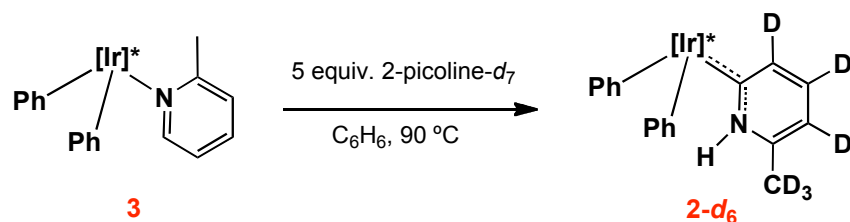
First, it was observed that **3** undergoes exchange when treated with 5 equiv. of 2-picoline-*d*₇ at 60 °C (Eq. 4). Secondly, and according to the observation that carbene



Equation 4

²⁰ S. H. Wiedemann, J. C. Lewis, J. A. Ellman, R. Bergman, *J. Am. Chem. Soc.* **2006**, *128*, 2452.

2 forms when the reaction is performed at 90 °C, if the exchange reaction is executed at 90 °C, carbene **2-*d*₆** is obtained instead (Eq. 5). Most probably, the NH group is not deuterated in **2-*d*₆** due to facile D /H exchange with adventitious water during the manipulation of the reaction mixture.

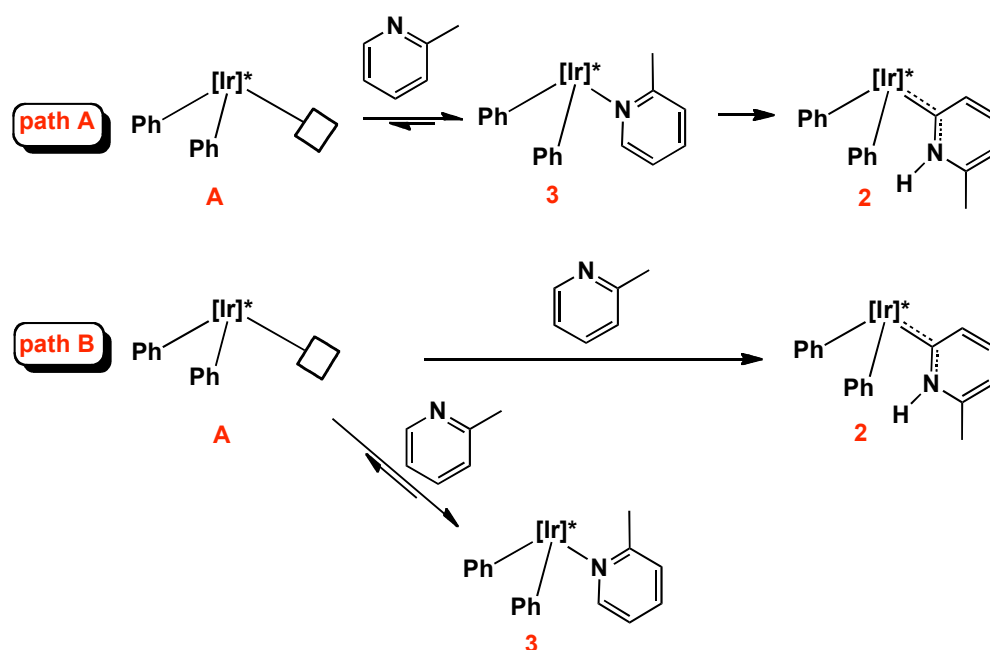


Equation 5

Finally, to determine the kinetic isotope effect, **1** was allowed to react with an excess of a 1:1 mixture of 2-picoline and 2-picoline-*d*₇, to find that **2** and **2-*d*₆** were formed in *ca.* 2:1 ratio, and therefore that $k_{\text{H}}/k_{\text{D}} = 2.0 (\pm 0.2)$.

From these experiments, we can conclude that C–H bond activation is the rate-limiting step in the formation of **2** but we can not determine if this takes place in the adduct **3** (intramolecular activation, Scheme II – 4, path A) or independently of it (intermolecular activation, Scheme II – 4, path B).

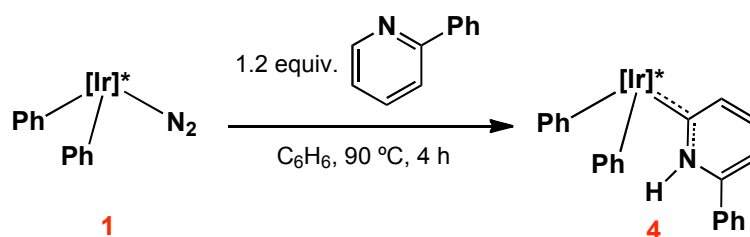
Scheme II - 4



II.1.2. Reactions of $\text{Tp}^{\text{Me}_2}\text{IrPh}_2(\text{N}_2)$ with 2-Phenylpyridine

II.1.2.1. Synthesis of the N-Heterocyclic Carbene Complex **4**

Complex **1** reacts in C_6H_6 , at 90°C , with 1.2 equivalents of 2-phenylpyridine with formation of carbene **4**, in 95% spectroscopic yield (Eq. 6). As previously observed for **2**, complex **4** is characterized by a ^1H NMR spectrum with some very broad resonances at room temperature. Low temperature studies (Fig. II – 7, CD_2Cl_2 , -60°C) identified two rotamers in equilibrium in a 10:1 ratio. The major rotamer **4a** features a singlet at



Equation 6

13.40 ppm for the NH group, while for the minor rotamer **4b**, this functionality resonates at 10.51 ppm. As was the case for complex **2**, the 2D NOESY spectrum indicates that the complex that has the NH group facing the phenyl coligands is the major rotamer. The Ir–C_{carbene} group is responsible for a signal at 178 ppm in the $^{13}\text{C}\{^1\text{H}\}$ NMR spectrum.

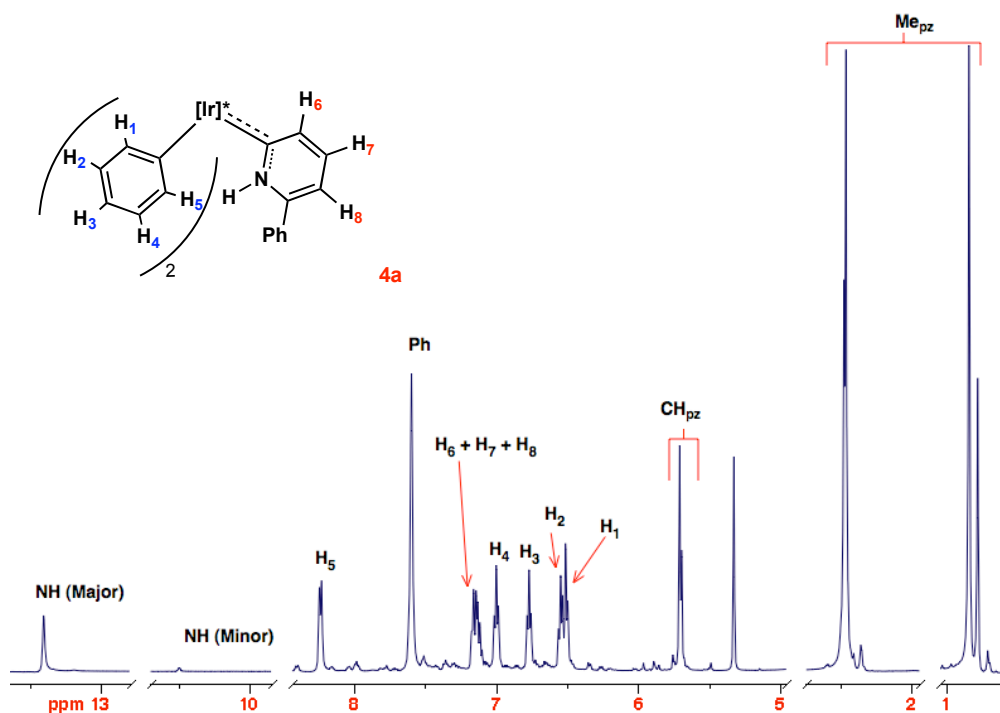


Figure II - 7. ^1H NMR spectrum of **4** (-60°C , CD_2Cl_2 , 500 MHz).

Single crystals of complex **4** were obtained from the slow evaporation of a concentrated solution in hexane:Et₂O. X-ray diffraction studies confirmed the carbene structure (Fig. II – 8, see Appendix 1- Table A5) and showed that the major rotamer present in CD_2Cl_2 solution is the one observed in the crystal. The Ir–C_{carbene} bond distance of 1.98 Å is, once again, slightly shorter than those of Ir–C_{ph} (2.05 Å for both Ir(1)–C(27) and Ir(1)–C(33)).

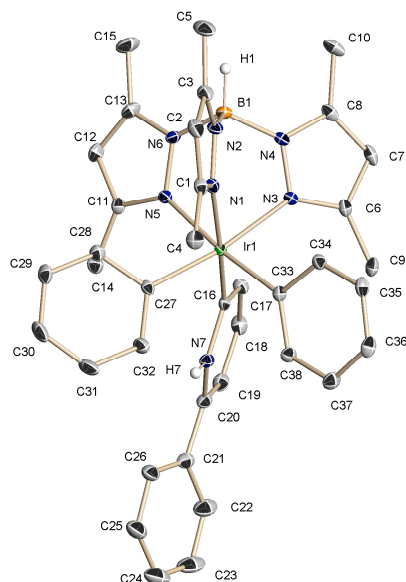
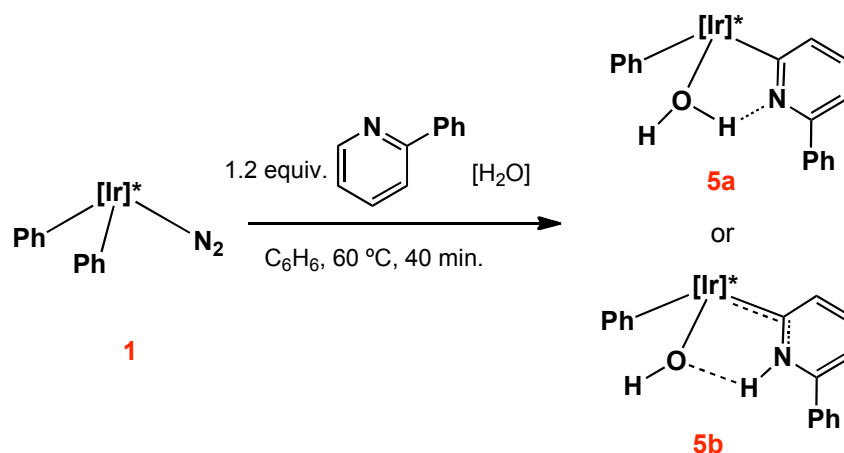


Figure II - 8. ORTEP representation of complex **4a**.

II.1.2.2. Synthesis of Complex 5. Trapping with H₂O a Plausible Intermediate?

Considering the results obtained for 2-picoline, the reaction leading to **4** was followed by ¹H NMR spectroscopy at somewhat lower temperatures (60 °C). After heating in C₆H₆ at 60 °C for 20 minutes a new complex **5** was generated concomitant with the disappearance of **1**, and after 40 minutes **5** was the only reaction product (Eq. 7). At longer reaction times, **4** started to appear, although very slowly, and **5** remained as the major reaction product even after heating the mixture for 2 h.



Equation 7

As shown in Eq. 7, compound **5** may be viewed as a phenyl/pyridyl/water derivative, **5a**, or alternatively as the corresponding phenyl/hydroxide/NHC isomer, **5b**. Even if **5** has been thoroughly studied by NMR spectroscopy and has been further characterized by single crystal X-ray study (Fig. II – 9, see also Appendix 1 - Table A7) distinction between the two structures is difficult.

In CDCl_3 , the pyridyl and phenyl fragments are responsible for ^1H NMR resonances appearing in the range 8.3-6.3 ppm, while the protons of the bound water (or hydroxyl) unit are not detected at room temperature. Registering this spectrum at $-70\text{ }^\circ\text{C}$ allowed the identification of a singlet at 16.9 ppm, integrating approximately for one proton, assigned to the $\text{N}\cdots\text{H}-\text{O}$ hydrogen bridge. This resonance is shifted to downfield by about 3.5 ppm with respect to the NH proton of **4**. It should be added however, that a resonance for the remaining hydroxyl proton could not be positively identified. In the $^{13}\text{C}\{^1\text{H}\}$ NMR spectrum the $\text{Ir}-\text{C}_{\text{pyr}}$ nucleus resonates at 171.9 ppm whereas the $\text{Ir}-\text{C}_{\text{ph}}$ signal is found at 137 ppm.

As already mentioned an X-ray investigation of the molecules of **5** has been carried out. Some relevant bond distances and angles have been collected in Appendix 1. The $\text{Ir}-\text{C}$ bond to the pyridinic ring ($\text{Ir}(1)-\text{C}(16)$) has a length of 1.98 Å, identical to corresponding distance in **2a**, but there is a slight attenuation of the differences among the C–C bonds in comparison with **2a**. For the latter compound C–C bonds span

between 1.36 and 1.42 Å whereas in **5** the range shrinks slightly to 1.37-1.40 Å. Moreover, the Ir(1)–O(1) bond distances found for **5** (2.07 Å) is comparable to those reported for Ir–OH₂²¹ and Ir–OH derivatives.²²

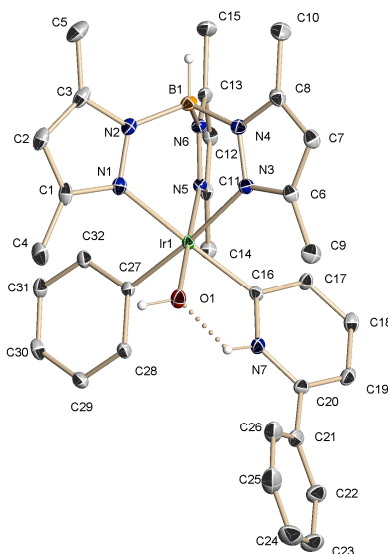


Figure II - 9. ORTEP representation of complex **5**.

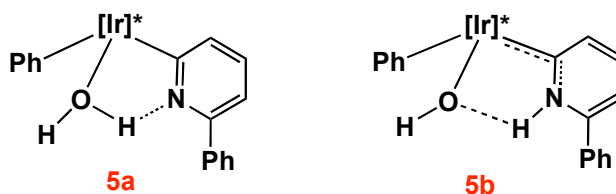


Figure II - 10. Possible isomeric structures for complex **5**.

Although these somewhat contrasting data do not help to clarify this problem, the existence of a hydrogen bond between N(7) and O(1) is self evident, the separation between one H of the water ligand and the nitrogen atom (1.8 Å) being shorter than the

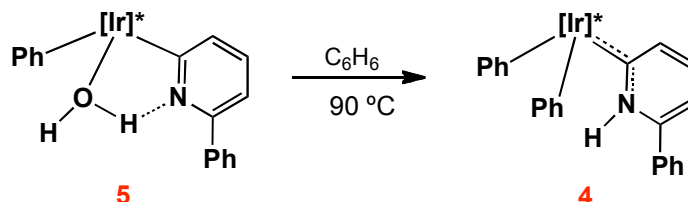
²¹ **a)** X. L. Luo, G. K. Schulte, R. H. Crabtree, *Inorg. Chem.* **1990**, *29*, 682. **b)** L. Dadci, H. Elias, U. Frey, A. Hoernig, U. Koelle, A. Merbach, H. Paulus, J. Schneider, *Inorg. Chem.* **1995**, *34*, 306. **c)** L. C. Porter, S. Bodige, *J. Organomet. Chem.* **1995**, *487*, 1. **d)** H. Amouri, C. Guyard-Duhayon, *Inorg. Chem.* **2002**, *41*, 1397. **e)** M. Paneque, C. M. Posadas, M. L. Poveda, N. Rendón, E. Álvarez, K. Mereiter, *Chem. Eur. J.* **2007**, *13*, 5160.

²² **a)** O. Blum, D. Milstein, *J. Am. Chem. Soc.* **2002**, *124*, 11456. **b)** D. Milstein, J. C. Calabrese, I. D. Williams, *J. Am. Chem. Soc.* **1986**, 6387.

sum of the van der Waals radii of hydrogen (1.20 Å) and nitrogen (1.55 Å).¹⁸ In the IR spectrum, an absorption at 3630 cm⁻¹ is assigned to the OH functionality, while the N...H-O group is found at 3135 cm⁻¹. In summary, the two isomeric structures represented in Fig. II – 10 may be acceptable representations for complex **5**, and it is in fact possible that they may interconvert easily in solution, but in our view, data seem to favour carbene structure **5b** over pyridyl formulation **5a**, but neither spectroscopic nor diffraction data are conclusive.

II.1.2.3. Reactivity of Complex 5

The generation of complex **5** in a previous stage to the formation of **4** is best explained as if **5** is a side product resulting from the trapping of the real intermediate species that ultimately affords carbene **4**. In fact, complex **5** reacts with C₆H₆ at 90 °C with extrusion of water and clean formation of **4** (Eq. 8). It should be noted that as discussed in Section II.1.2.2, this observation is not incompatible with carbene structure **5b**.

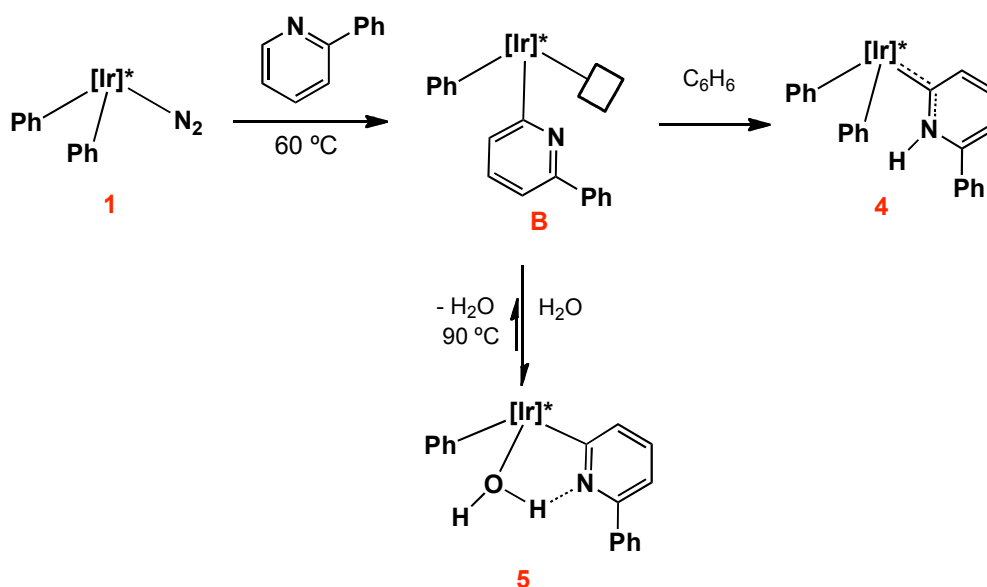


Equation 8

The formation of **5** is indicative that the true intermediate **B** (Scheme II - 5) is very sensitive to the presence of trace amounts of water, and its formation is a competitive reaction that slows down that of **4**. Water coordination to Tp^{Me2}Ir(III) species has been already reported by our group and, for example, it has been found in studies on the coupling of ethylene and alkynes, that water is a very effective trapping agent.^{21c,23}

²³ E. Álvarez, M. Gómez, M. Paneque, C. M. Posadas, M. L. Poveda, N. Rendón, L. L. Santos, S. Rojas-Lima, V. Salazar, K. Mereiter, *J. Am. Chem. Soc.* **2003**, *125*, 1478.

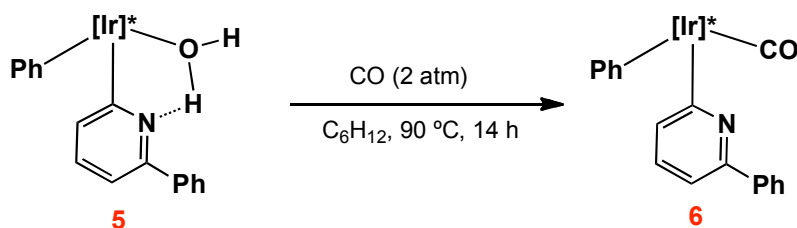
Scheme II - 5



It is also clear from these experiments that the formation of **B**, *i.e.* the C–H activation of the 2-phenylpyridine, already takes place at 60 °C and that its reaction with C₆H₆ “regenerates” the extruded phenyl group in **1** and “protonates” the N of the pyridyl ligand in **B**. Lastly, it is interesting to note the different affinities of diphenyl intermediate **A** and the related phenyl-pyridyl **B** for water. For the former, we have never observed a water adduct even in the presence of added water. It appears reasonable that this is due in a large extent to the hydrogen bond present in **5** that provides sufficient stability to this kind of complexes.

II.1.2.4. Generation of the Carbonyl Derivative **6**

The lability of the water ligand in **5**, generating intermediate **B**, may be useful synthetically.^{21c,23} In fact, when complex **5** was heated in cyclohexane at 90 °C in the presence of carbon monoxide, the adduct **6** was cleanly formed (Eq. 9).



Equation 9

Compound **6** has been fully characterized by microanalytical data and spectroscopy. The ^1H NMR spectrum is similar to that found for **5** while in the $^{13}\text{C}\{^1\text{H}\}$ NMR spectrum the Ir–CO and Ir–C_{pyr} resonances appear at 167.1 ppm and 157.3 ppm respectively, the latter being shifted upfield by about 20 ppm with respect to the carbene resonance found in **4**, and by about 15 ppm with respect to **5**. This observation is more in agreement with carbene structure **5b** than with formulation **5a**. Additionally, complex **6** presents an absorption of 2040 cm^{-1} due to the CO stretching in the IR spectrum. For comparison, $\text{Tp}^{\text{Me}_2}\text{IrPh}_2(\text{CO})$ has a $\nu(\text{CO})$ of 2026 cm^{-1} and this group resonates at 169.7 ppm in the $^{13}\text{C}\{^1\text{H}\}$ NMR spectrum, both values being very close to those found for **6**.⁶ Hence, pyridyl and phenyl groups have very similar electronic properties when coordinated to $\text{Tp}^{\text{Me}_2}\text{Ir(III)}$ centres.

II.1.3. Reactions of $\text{Tp}^{\text{Me}_2}\text{IrPh}_2(\text{N}_2)$ with other Pyridines

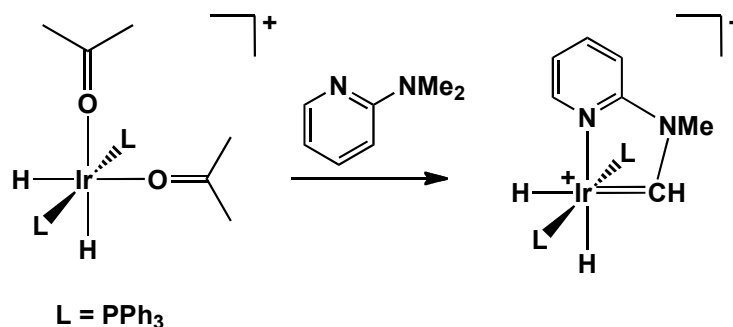
In the above-mentioned reactivity of 2-picoline and 2-phenylpyridine towards **1**, 1,2-hydrogen shifts of the pyridines to yield NHC complexes have been observed. These results prompted us to study other pyridines, in order to ascertain the role of the substituents in this transformation.

II.1.3.1. Reactions with 2-Dimethylaminopyridine and 2-tert-Butylpyridine.

Synthesis of N-Heterocyclic Carbenes **7** and **8**

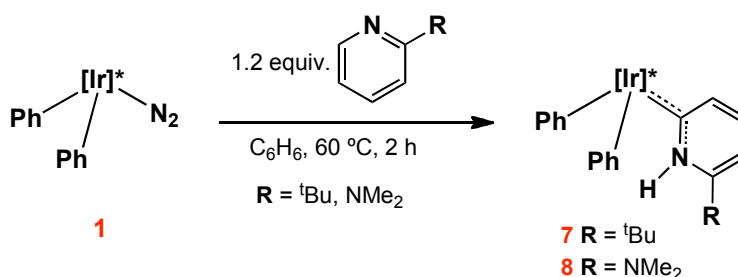
The substituent of 2-tert-butylpyridine is evidently bulkier than that of the 2-dimethylaminopyridine, but 2-dimethylaminopyridine is more basic than

2-tert-butylpyridine due to the more powerful electrodonating group NMe_2 . In addition, 2-dimethylaminopyridine may yield in its reaction with **1** a heteroatom stabilized carbene, as previously reported by Crabtree *et al.* (Eq. 10),²⁴ as the result of a double C–H bond activation of one of the methyl groups of the NMe_2 group.



Equation 10

As a matter of fact, both pyridines react with **1** to afford the corresponding carbene tautomers, **7** and **8** (Eq. 11). Interestingly, tautomerization requires milder reaction conditions for both pyridines as **7** and **8** are generated readily at 60 °C after 2 hours. No intermediates can be observed in either case.



Equation 11

Complexes **7** and **8** feature, like **2** and **4**, some broad signals both in their ^1H and $^{13}\text{C}\{^1\text{H}\}$ NMR spectra at room temperature, due to restricted rotation around Ir–C bonds, but characterization at low temperature (CD_2Cl_2 , $-60\text{ }^\circ\text{C}$) is relatively easy. For **7** a singlet is observed in the ^1H NMR spectrum at 13.10 ppm (major rotamer) and at 10.10 ppm (minor rotamer) for the NH group with their ratio being 3:1. As expected,

²⁴ E. Clot, J. Chen, D. H. Lee, S. Y. Sung, L. N. Appelhans, J. W. Faller, R. H. Crabtree, O. Eisenstein, *J. Am. Chem. Soc.* **2004**, 126, 8795.

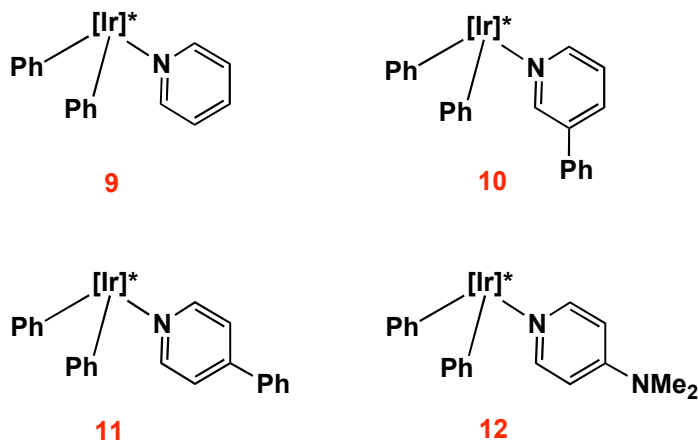
the major rotamer presents the ^tBu group facing the opposite side of the Tp^{Me2} ligand (2D NOESY evidence, see Experimental Part.). This is also the case for **8**, with the rotamers ratio being 5:1 (CD₂Cl₂, -60 °C). Both complexes feature diagnostic ¹³C signals for the Ir–C_{carbene} moiety at 176.0 ppm (**7**) and 169.2 (**8**) ppm.

II.1.3.2. Reactions with Pyridine, 3-Phenylpyridine, 4-Phenylpyridine and 4-Dimethylaminopyridine: Synthesis of complexes **9-12**

Although steric hindrance seems to play a definite role in the tautomerization of 2-substituted pyridines in their reaction with **1**, it was desirable to confirm this assumption by studying the behaviour of pyridines with substituents at other positions of the aromatic ring.

The reactivity of pyridine, 3-phenylpyridine, 4-phenylpyridine and 4-dimethylaminopyridine towards **1** was therefore tested, and in all the cases the N-bound adducts **9-12** were the only observable products, even at temperatures higher than 90 °C. The characterization of these adducts is straightforward and is presented in the Experimental Part. We may only comment that, at room temperature, compounds **9-**

Scheme II - 6



12 show broad signals in their ^1H NMR spectra, due to restricted rotation around Ir–C and Ir–N bonds, but recording the NMR spectra at $-60\text{ }^\circ\text{C}$ allows for their detailed characterization. Interestingly, in the case of **10**, the two possible rotamers are present in a 1:1 ratio.

The molecular structure of complexes **9** and **11** have been determined by single crystal X-ray diffraction measurements and are presented in Fig. II – 11 (**9**) and Fig. II – 12 (**11**) (See Appendix 1, Table A9). In the case of the pyridine N-bound adduct **9**, the crystal structure presents disorder effects, and as a consequence, comparisons of **9** with both **3** and **11** cannot be made with the desired accuracy.

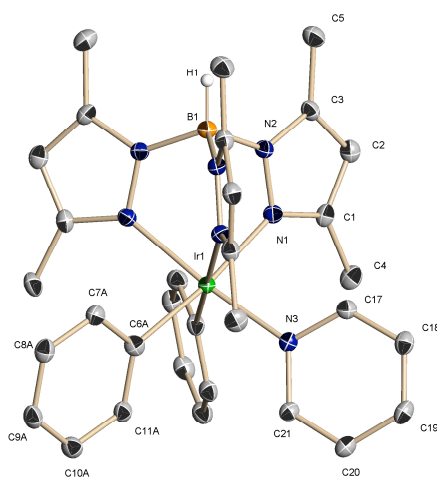


Figure II - 11. ORTEP representation of complex **9**.

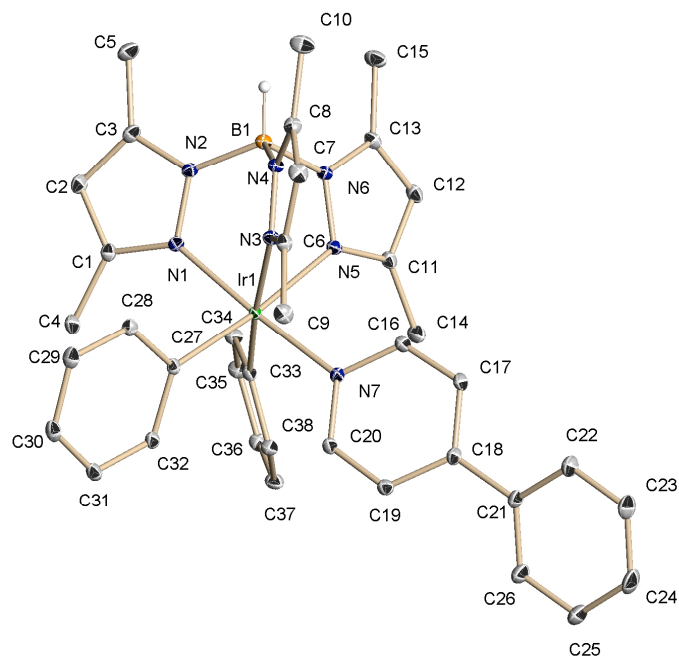


Figure II - 12. ORTEP representation of complex **11**.

In the case of derivative **11**, it is possible to determine an Ir(1)–N(7) bond length of 2.07 Å, that is found to be shorter than that of **3**, by about 0.07 Å. This may be attributed to steric rather than electronic effects (pK_a values for the two pyridines are 6.1 (2-Me) and 5.6 (4-Ph))²⁵ as the presence of the Ph substituent in the 4-position of the ring relieves strain between the Lewis acid and base centres. Once more it is worth remarking that the Ir–N bond is significantly longer than the Ir–C_{carbene} bond found in the Ir–NHC compounds (ca. 1.98 Å). A possible explanation for this is a strong Ir(III)–carbene interaction that seems to be a general phenomenon in all the $Tp^{Me_2}Ir$ compounds of this kind.^{8f}

²⁵ R. Williams, *pKa Compilation* **2001**.

II.1.3.3. Variable Temperature ^1H NMR Studies with Complex **9**

As previously commented the fluxional behaviour of **9** is due to restricted rotation around the Ir–N and Ir–C bonds. The simplicity of its structure prompted us to study these processes in detail.

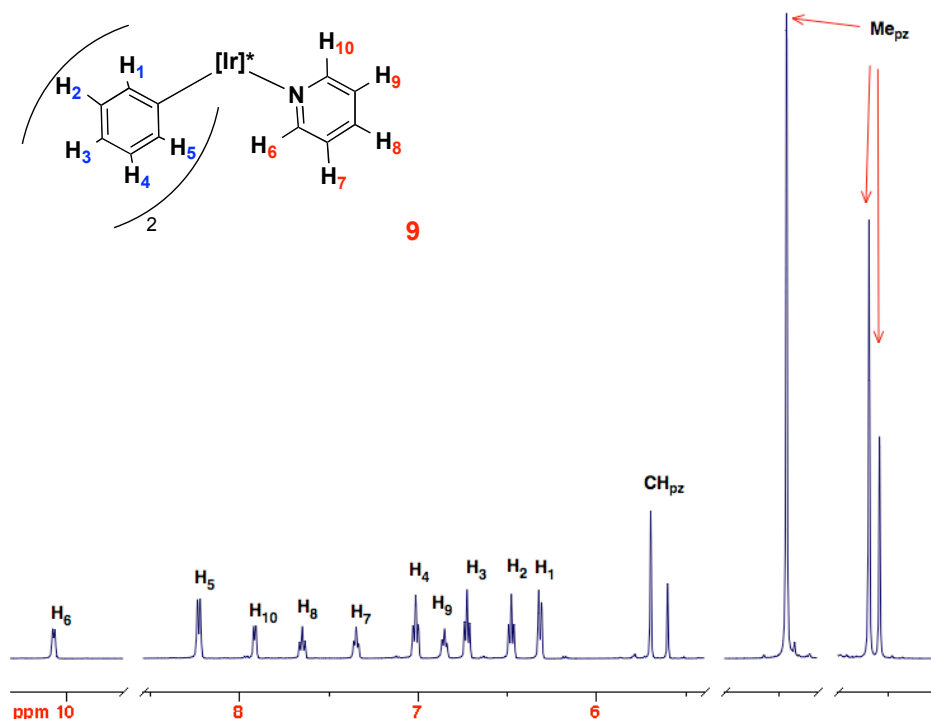


Figure II - 13. ^1H NMR spectrum of complex **9** (-60°C , CD_2Cl_2 , 500 MHz).

In Fig II – 13 the ^1H NMR spectrum of complex **9** at -60°C in CD_2Cl_2 is represented, together with the proton assignments, while Fig. II – 14 shows a series of stacked spectra taken at different temperatures between -60 and 60°C (CD_2Cl_2 , 500 MHz). As expected, in the slow regime all protons of the pyridine and phenyl ligands are distinguishable and can be easily assigned by analysis of the 2D NOESY experiment. On raising the temperature, these signals coalesce pairwise (*i.e.* $\text{H}_1 \leftrightarrow \text{H}_5$,

$H_7 \leftrightarrow H_9$, etc.) with both triplets due to H_3 and H_8 nuclei remaining unaltered through the temperature range investigated. As can be observed, the fast regime, *i.e.* complete free rotation behaviour, was not obtained at the magnetic field used for this study.

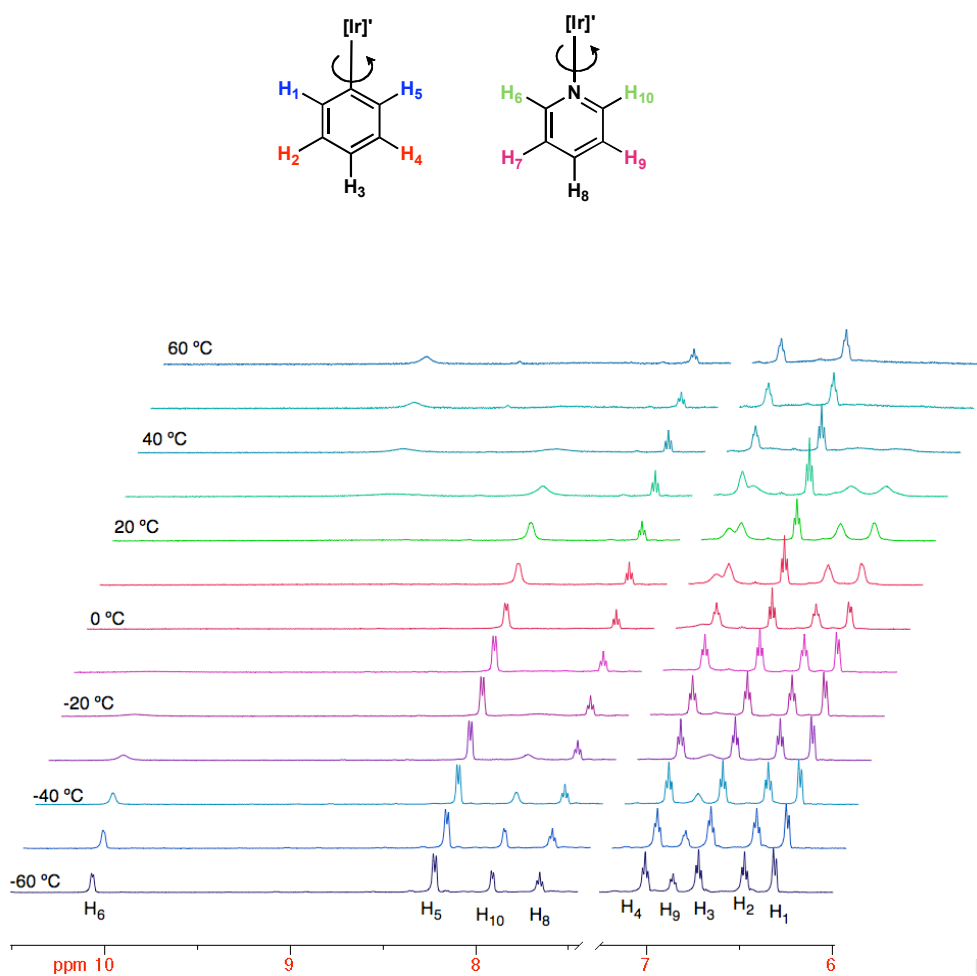


Figure II - 14. ^1H NMR spectra of complex **9** ($-60\text{ }^\circ\text{C}$ to $60\text{ }^\circ\text{C}$, CD_2Cl_2 , 500 MHz).

From these spectra, it can be concluded that the coalescence temperature (T_c) for the H_5 and H_1 nuclei of the phenyl group is 50 °C whereas for the H_{10} and H_6 nuclei of the pyridine is 10 °C. As it is known, the rate constant of the exchange process at the coalescence temperature is given by the equation:

$$k_{\text{exch}} = \frac{\pi}{\sqrt{2}} (\Delta\nu)$$

Where $\Delta\nu$ is the difference between the chemical shifts of the interchanging peaks in Hz. Thus, for complex **9**, the values of $k_{\text{rot}} = 2.40 \times 10^3 \text{ s}^{-1}$ and $k_{\text{rot}} = 4.24 \times 10^3 \text{ s}^{-1}$ can be computed for the pyridine and phenyl rings, respectively. The rate of rotation can also be related with ΔG^\ddagger by the Eyring equation:

$$k_{\text{rot}} = \left(\frac{k_B T}{h} \right) e^{-\frac{\Delta G^\ddagger}{RT}} \quad (\text{s}^{-1})$$

Where:

$k_{\text{rot}} \rightarrow$ Rate constant of the rotation (Hz)

$R \rightarrow 1.987 \times 10^{-3} \text{ kcal}/(\text{mol} \cdot \text{K})$

$k_B \rightarrow$ Boltzmann's constant (erg/K)

$h \rightarrow$ Plank's constant ($\text{erg} \cdot \text{s}^{-1}$)

$T \rightarrow$ Temperature (K)

$\Delta G^\ddagger \rightarrow$ Activation Energy ($\text{kcal} \cdot \text{mol}^{-1}$)

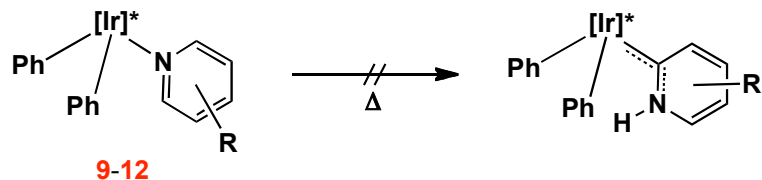
therefore:

$$\Delta G^\ddagger = -RT \ln \left[\left(\frac{k_{\text{rot}}}{T} \right) + \ln \left(\frac{h}{k_B} \right) \right] \quad (\text{kcal} \cdot \text{mol}^{-1})$$

At the T_c , the calculated energies for the rotation of both fragments are very close in value, $\sim 13.6 \text{ kcal} \cdot \text{mol}^{-1}$ (Ph) and $\sim 12.2 \text{ kcal} \cdot \text{mol}^{-1}$ (py), but this $1.4 \text{ kcal} \cdot \text{mol}^{-1}$ difference corresponds to a significant variation in the rates of rotation. For instance, at 30 °C, the rate constant for the pyridine rotation is $1.7 \times 10^4 \text{ s}^{-1}$, whereas for the phenyl groups is $9.8 \times 10^2 \text{ s}^{-1}$. Hence, the pyridine ligand rotates approximately 10 times faster than the phenyl groups, at this temperature.

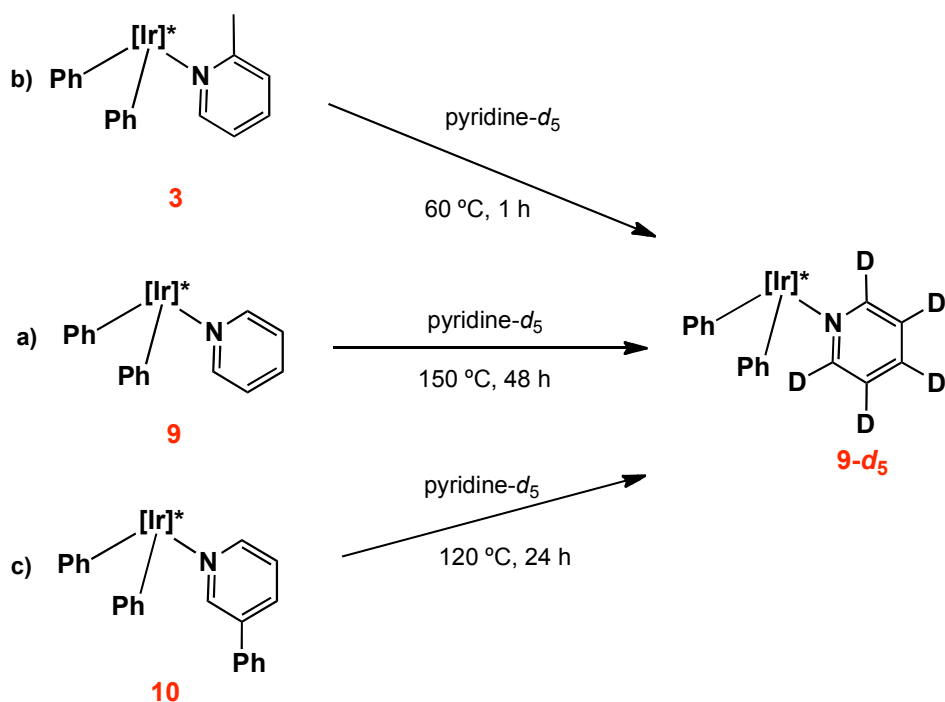
II.1.3.4. Attempts of Synthesis of Carbenes Derived from 9-12

Taking into account the case of 2-picoline, where heating at 90 °C of the N-bound adduct **3** generated the carbene tautomer **2**, complexes **9-12** were heated in benzene at 90-150 °C. No transformation was observed and all the N-bound complexes remain stable, under these conditions (Eq. 12).



Equation 12

Scheme II - 7

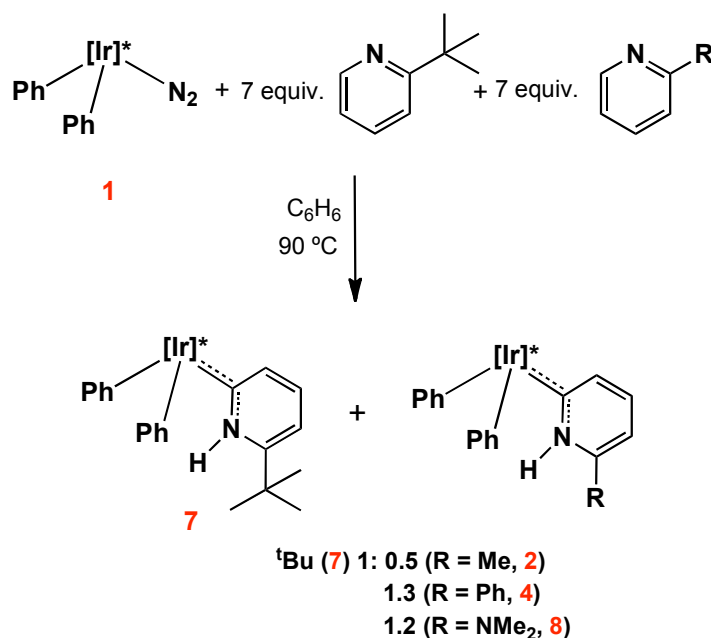


This stability cannot be ascribed to the inertness of the Ir–N bond as these adducts interchange their pyridine ligands with pyridine-*d*₅ (Scheme II – 7, complex **3** has been included as comparison). As expected by simple electronic considerations, **10** reacts

faster than **9** while F-strain (a concept introduced by Brown, see section II.1.2.2 and especially II.1.4) is responsible for the higher reactivity of **3**.

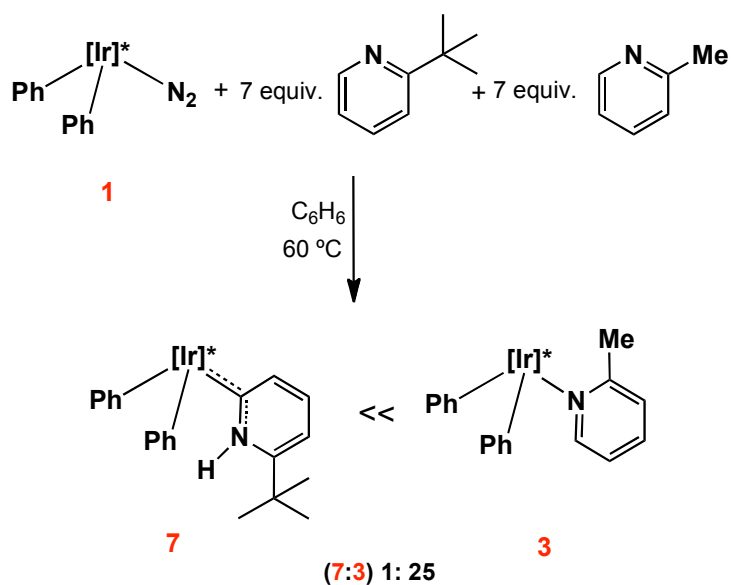
II.1.3.5. Competition Experiments

In order to understand better the factors that influence metal mediated pyridine tautomerization, some competition experiments were undertaken. The reactions were performed using a large excess of substrates to allow for pseudo-first order conditions (Eq. 13). At 90 °C, the results of the reaction of **1** with 7 equiv. of both 2-tert-butylpyridine and different 2-substituted pyridines are as follows:



Equation 13

As it can be observed, carbene formation is quite insensitive to the electronic and steric characteristics of the R group and only the smallest Me substituent leads to a somewhat reduced reactivity. Interestingly, if the competition between 2-tert-butylpyridine and 2-picoline is carried out at 60 °C, adduct formation (complex **3**) is strongly favoured (Eq. 14).

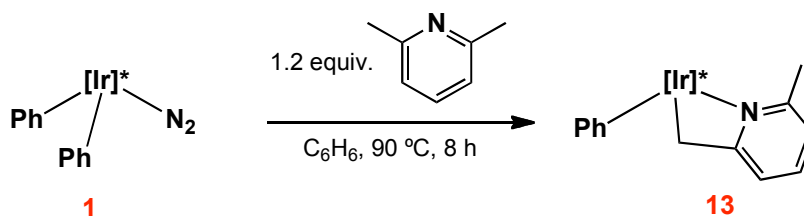


Equation 14

II.1.3.6. Reaction of **1** with 2,6-Lutidine: Activation of a Pyridine Lacking C–H Bonds Adjacent to Nitrogen

The reaction of **1** with 2,6-lutidine (2,6-dimethylpyridine) has also been studied. All pyridines studied so far have at least one C–H bond susceptible of activation contiguous to the nitrogen. In the case of the osmium (II) complex mentioned in the Introduction,²⁶ C–H activation at the 4-position of 2,6-lutidine takes place with formation of a remote carbene (Eq. VIII, Introduction).

²⁶ R. Cordone, H. Taube, *J. Am. Chem. Soc.* **1987**, *109*, 8101.



Equation 15

Treatment of **1** with 2,6-lutidine in C_6H_6 at $90\text{ }^\circ\text{C}$ yields the four membered metallacycle **13**, the result of the C–H activation of one of the methyl groups and the formation of an Ir–N bond (Eq. 15).²⁷ Besides resonances due to the two aromatic rings and the Tp^{Me_2} ligand, the ^1H NMR spectrum of **13** (CDCl_3) displays a signal at 2.06 ppm due to the Ir– CH_2 moiety (there is a casual equivalence of the diastereotopic protons) that in the $^{13}\text{C}\{^1\text{H}\}$ NMR spectrum resonates at -22.0 ppm ($^1J_{\text{CH}} = 135\text{ Hz}$). Interestingly, the two quaternary carbon atoms of the pyridine-derived ligand exhibit disparate chemical shifts. The C–Me has a normal value of 158.6 ppm, while the C– CH_2 resonates at very low fields (185.5 ppm).

Single crystals of complex **13** were obtained and this allowed to perform X-ray diffraction studies that confirmed the proposed structure (Fig. II – 15, see Appendix 1, Table A11). The Ir–N(7) bond has a normal length of *ca.* 2.06 Å, comparable to that found in **11**, but somewhat smaller than that of **3**. The Ir– C_{ph} bond distance is 2.09 Å, whereas for the Ir– CH_2 moiety this value is 2.04 Å. It has to be mentioned that the chelating pyridine ligand is clearly of the $\kappa^2\text{-C},\text{N}$ -type, *i.e.* the central carbon C(17) is not bonded to the Ir centre. The metallacyclic ring is highly tensioned, and this can be observed by comparison of the bond angles $\text{N}(7)\text{--C}(17)\text{--C}(16) = 105.2^\circ$, with $\text{N}(7)\text{--C}(21)\text{--C}(22) = 120.8^\circ$. Nevertheless, it is important to note that four-membered iridacycles are normally quite stable structures,²⁸ and in fact complex **13** survives heating at $120\text{ }^\circ\text{C}$ (C_6H_6 , 14 h).

²⁷ For similar reactivity of 2,6-lutidine see for instance: R. F. Jordan, A. Guram, *Organometallics* **1990**, *9*, 2116.

²⁸ M. Gómez, M. Paneque, M. L. Poveda, E. Álvarez, *J. Am. Chem. Soc.* **2007**, *129*, 6092.

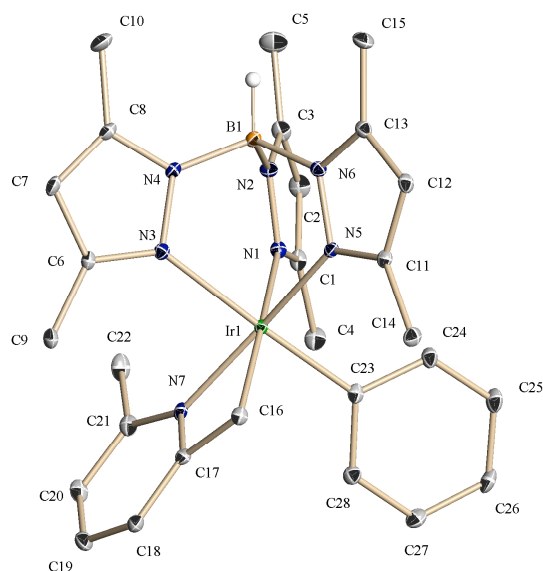
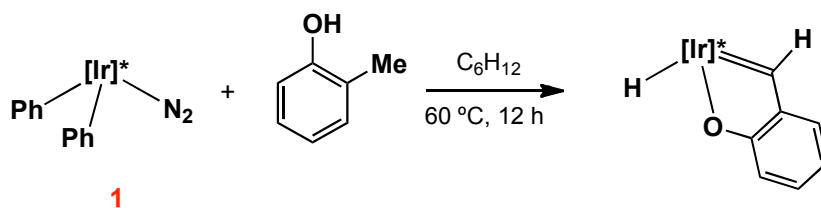


Figure II - 15. ORTEP representation of complex **13**.

Thus, contrarily to the Os(II) system, complex **1** does not induce tautomerization of 2,6-lutidine but prefers the C–H activation of a Me group. The reaction outcome resembles somewhat the behaviour observed for **1** and *o*-methylphenol (Eq. 16) which allows the formation of a hydride-alkylidene by a double C–H activation of the Me group.^{8e}



Equation 16

II.1.4. Some General Comments on the Tautomerization of Pyridines by $[\text{Tp}^{\text{Me}_2}\text{Ir(III)Ph}_2]$ Species

All the observations described so far indicate that only 2-substituted pyridines react with complex **1** to yield pyridine-derived N-heterocyclic carbenes. Clearly steric effects seem to play an important role in carbene formation. This is not an odd observation; actually, in the Introduction of this Thesis where a brief description of the different modes of coordination of pyridines was presented, it was concluded that the coordination mode, among other factors, is strongly dependent on the steric environment around the nitrogen atom. In the case of the $16 e^-$ $[\text{Tp}^{\text{Me}_2}\text{IrPh}_2]$ species, a Lewis acid centre, it is expected that its interaction with pyridines will generate $\kappa^1\text{-N}$ adducts, *i.e.* to form normal Lewis acid-base pairs. However, it is also easy to understand that the behaviour of pyridines as Lewis bases cannot be inferred exclusively from their $\text{p}K_a$ values. Due to steric effects the nitrogen lone electron pair may have a difficult approach to the metal centre, particularly in the case of 2- and 2,6-substituted pyridines. This effect was coined as F-strain.¹⁹ Hence, steric hindrance can induce variations in the observed basic properties of a pyridine toward different Lewis acids. These effects were for the first time studied by Brown, that described them as an *“interference that result in a strain at the “interface” between the two components, a strain which would tend to separate them. This “frontal” strain, in many respects similar to the classical concept of steric hindrance, has been termed F-strain”*.¹⁹ To our purposes, F-strain results in decreased Lewis basicity of 2-substituted pyridines toward the sterically demanding Lewis acid $[\text{Tp}^{\text{Me}_2}\text{IrPh}_2]$ and therefore destabilizing the resulting Ir(III):N acid/base pairs.

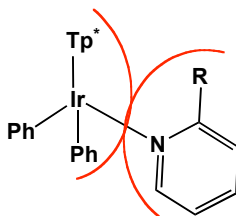


Figure II - 16. F-strain desestabilizing effect in the Lewis acid/base pairs formed by 2-substituted pyridines and $[\text{Tp}^{\text{Me}_2}\text{IrPh}_2]$.

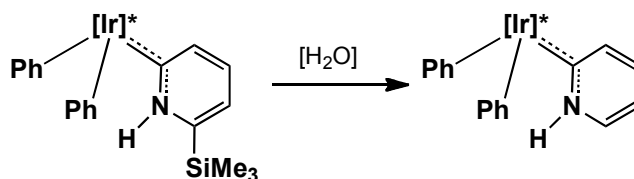
Interestingly it was observed that 2-substituted pyridines react with this Ir(III) centre in a previously unobserved way, to give the thermodynamically more stable carbene derivatives. It seems evident that the increased bulkiness of the 2-substituted pyridines destabilizes the N-adduct by F-strain, while the isomeric carbene structure does not suffer from this kind of steric repulsion. In fact, as already stated, the Ir–C carbene bond lengths in **2** and **4** have normal values (ca. 1.98 Å), whereas the Ir–N distance in the **3** of 2.14 Å is about 0.16 Å longer, despite the somewhat smaller covalent radius of Nsp^2 in comparison with Csp^2 . Clearly, these factors contribute to the comparatively more favourable thermodynamics of the carbene forming reaction. In this regard, it is worth recalling that while 2-tert-butylpyridine is more basic than pyridine against H^+ (pK_a values of 5.8 and 5.3, respectively), the reaction of pyridine with BMe_3 is exothermic by about $15 \text{ kcal}\cdot\text{mol}^{-1}$, whereas that of 2-tert-butylpyridine is endothermic.¹⁹

In the following, the more important experimental observations are presented.

- Only 2-substituted pyridines lead to N-heterocyclic carbenes.
- All 2-substituted pyridines, studied so far, give N-heterocyclic carbenes.
- Picoline, with a small Me 2-substituent, first reacts to give a stable N-adduct, which then rearranges to the carbene tautomer.
- Only pyridines bearing a C–H bond adjacent to nitrogen undergo tautomerization. 2,6-Dimethylpyridine gives rise to a different type of product.
- A kinetic isotope effect of ca. $2.0 (\pm 0.2)$ has been found for the C–H activation step of the reaction.
- Pyridine and the 3- and 4-substituted pyridines tested give stable N-adducts that,

in our hands, do not rearrange to carbenes. This behaviour is not due to the inertness of the Ir–N bond against dissociation.

Although it is quite clear that carbenes derived from 2-substituted pyridines are more stable than the corresponding N-adducts, no conclusion can be inferred from the available experimental data about the relative stabilities of the N-bound adducts of pyridines and 3- and 4-substituted pyridines and their unobserved carbenes. Common sense suggests that the former are more stable species than the latter. However it is important to note in this respect that in related work carried out in our laboratory, the carbene of pyridine has been prepared by the process represented in Eq. 17 and it has been found to be a very stable molecule, incapable so far to isomerize to the N-adduct without undergoing previously thermal decomposition (150 °C).^{29a}



Equation 17

Our group has also described^{29b} the synthesis of both the N-adduct and the carbene tautomer of pyridine in another Tp⁺Ir(III) system, but no interconversion between them could be observed even at the temperature needed for decomposition of both species (*ca.* 90 °C).

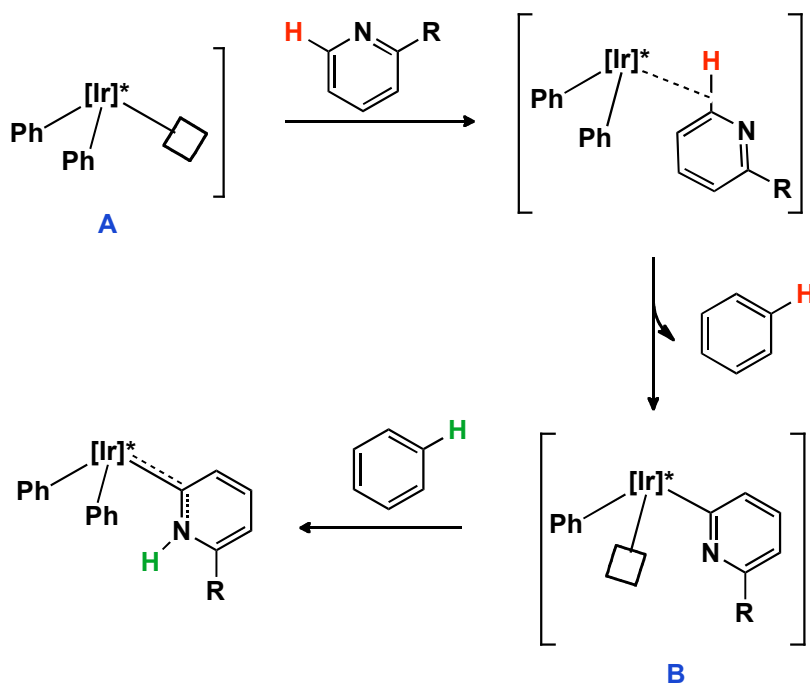
²⁹ **a)** Unpublished results **b)** E. Álvarez, S. Conejero, P. Lara, J. A. López, M. Paneque, A. Petronilho, M. L. Poveda, D. del Río, O. Serrano, E. Carmona, *J. Am. Chem. Soc.* **2007**, *129*, 14130.

II.1.4.1. Mechanism of Carbene Formation with 2-Substituted Pyridines

First of all and to avoid a long discussion it has to be noticed that in another Tp'Ir(III) system we have demonstrated that the N-bound adduct of pyridine is not an active intermediate in the route for carbene, that is, the C–H activation of the heterocycle is intermolecular.

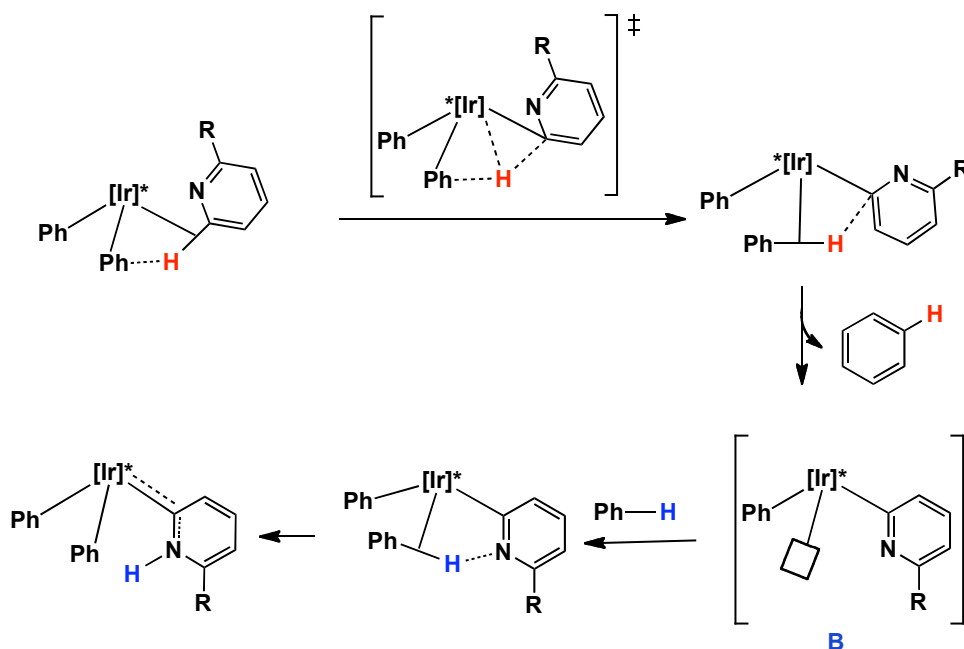
With this in mind and considering all the observations collected so far, as well as the information gathered for related systems,^{29b} the mechanism depicted in Scheme II – 8 can be proposed for the tautomerization process mediated by complex **1**. Although theoretical calculations have not been developed for the system under investigation, related processes as CH bond activation of anisole and other aromatic ethers point to the participation of C_{ar}–H complexes. Thus, following the loss of molecular nitrogen (the rate determining step for all, so far described, carbene-forming processes except for the picoline), the unsaturated intermediate **A** activates the C₆–H bond of the 2-R-pyridine, with elimination of a benzene molecule, to form intermediate **B**.

Scheme II - 8



It seems likely that all pyridine C–H bonds (not only C₆–H) participate in interactions of this kind and this has been demonstrated by deuteration studies in closely related systems.^{29b} However C₆–H is slightly preferred thermodynamically as intermediate **B** may stabilize by weak coordination of the N atom to the Ir(III) centre. The activation of a C–H bond of the solvent would finally place a H atom onto N to yield the N-heterocyclic carbene, regenerating in its matter the two phenyl groups present in the starting material. Thus, C–H activation of the pyridine at C₆ removes the H atom as benzene with the assistance of one of the original phenyl groups. Then, in the final step, a molecule of C₆H₆ (solvent) becomes activated, the H atom binds to N and the C₆H₅ group to iridium producing the N-heterocyclic carbene. Although both on the iridium precursor and the reaction product there are two Ir–C₆H₅ groups they are not innocent but play a crucial role in the tautomerization of the pyridine. A mechanism of this kind is known as σ -complex assisted metathesis or σ -CAM.³⁰ Scheme II – 9 illustrates the σ -CAM mechanism, applied to our case, in a more detailed form.

Scheme II - 9



³⁰ R. N. Perutz, S. Sabo-Etienne, *Angew. Chem. Int. Ed.* **2007**, 46, 2578.

An interesting question that remains to be considered is why 3- and 4-substituted pyridines, particularly those which electronically disfavour N-adduct formation, do not afford NHC complexes. This will be the subject of future studies from our laboratory.

II.1.4.2. Mechanistic Considerations on Somewhat Related Systems

As previously mentioned in the Introduction, during the development of the research work described in this manuscript, similar tautomerization processes of N-heterocycles mediated by transition metal complexes were published in the literature. Therefore a brief discussion of the different mechanisms proposed is appropriate.

Bergman, Ellman and their co-workers described the intermediary role of a NHC complex when studying the catalytic C–C coupling reaction between olefins and N-heterocycles and studied the transformation to identify the active species.^{20,31}

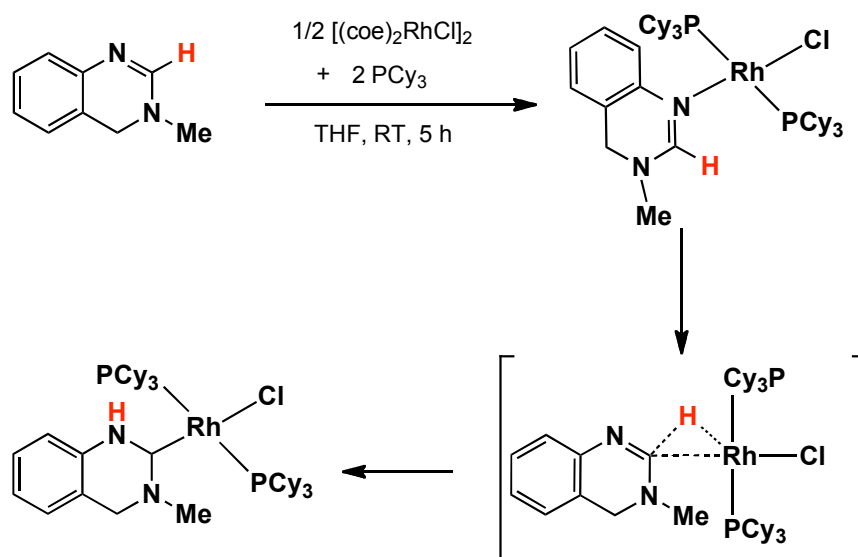
The results of these studies seemed to support an intramolecular mechanism whereby the tautomerization occurs in two steps:

- a) coordination of the N-heterocycle to yield a N-bound adduct.
- b) C–H activation step with 1,2- hydrogen transfer from carbon to nitrogen.

This mechanistic proposal does not find parallel with the $[\text{Tp}^{\text{Me}_2}\text{IrPh}_2]$ system since in our case the N-bound adduct is not a real intermediate of the tautomerization reaction. The authors propose participation of a Rh(III) hydride, and therefore, the 1,2-hydrogen shift is believed to proceed through Rh(I)/Rh(III) oxidative addition/reductive elimination steps, that in our case appear unlikely.

³¹ **a)** J. C. Lewis, R. Bergman, J. A. Ellman, *J. Am. Chem. Soc.* **2007**, *129*, 5332. **b)** A. M. Berman, J. C. Lewis, R. Bergman, J. A. Ellman, *J. Am. Chem. Soc.* **2008**, *130*, 14926.

Scheme II - 10

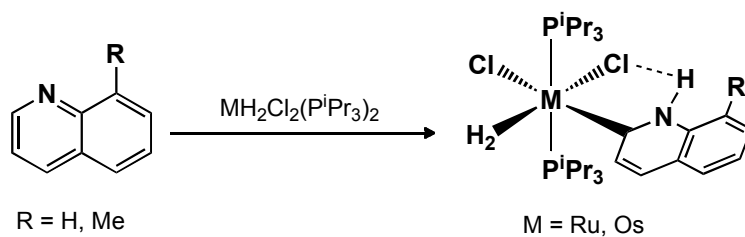


Esteruelas and co-workers reported the stabilization of the NH tautomer of 8-methylquinoline and quinoline by osmium and ruthenium complexes.³²

The authors propose a two-step intermolecular mechanism consisting of:

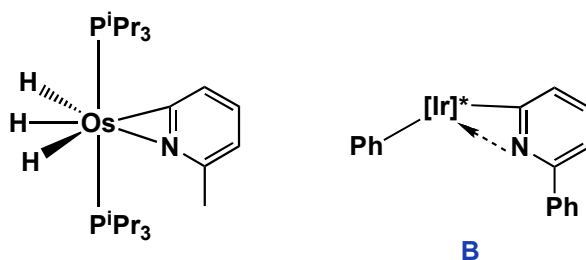
- hydride transfer from the metal complex to nitrogen.
- C–H activation with the H being transferred to the metal and stabilization of the NH group by hydrogen bond interaction.

³² **a)** M. A. Esteruelas, F. Fernández-Álvarez, E. Oñate, *J. Am. Chem. Soc.* **2006**, *128*, 13044. **b)** M. L. Buil, M. A. Esteruelas, K. Garcés, M. Oliván, E. Oñate, *J. Am. Chem. Soc.* **2007**, *129*, 10998. **c)** M. A. Esteruelas, F. Fernández-Álvarez, E. Oñate, *Organometallics* **2007**, *26*, 5239. **d)** M. A. Esteruelas, F. Fernández-Álvarez, E. Oñate, *Organometallics* **2008**, *27*, 6236. **e)** M. Buil, M. A. Esteruelas, K. Garcés, M. Oliván, E. Oñate, *Organometallics* **2008**, *27*, 4680. **f)** M. A. Esteruelas, F. Fernández-Álvarez, M. Oliván, E. Oñate, *Organometallics* **2009**, *28*, 2276.

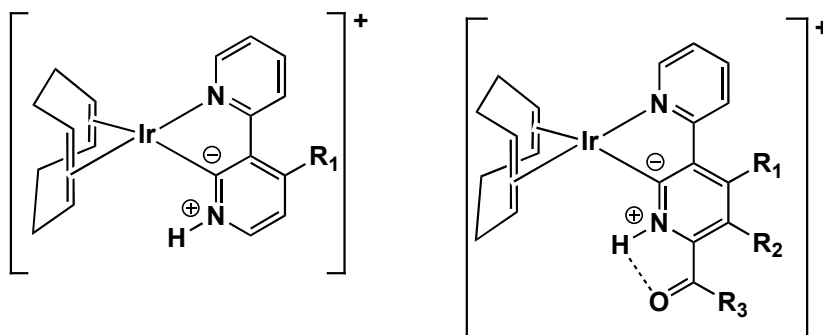


Equation 18

During the course of these studies, a 2-picoline derived $\kappa\text{-}N,C$ bound complex was obtained that holds a close relationship with intermediate **B** proposed as active species in the $[\text{Tp}^{\text{Me}_2}\text{Ir}]$ system. Nonetheless, the $\kappa\text{-}N,C$ osmium complex does not generate the carbene tautomer.



Based on previous work with imidazole tautomerization processes, Li's group studied 2',3'-bipyridines and observed their tautomerization in the presence of $[\text{Ir}(\text{cod})_2]\text{BF}_4$.³³ The process is proposed to be favoured by the chelate effect and stabilization of the NH group by hydrogen bonding, although carbene tautomer can still

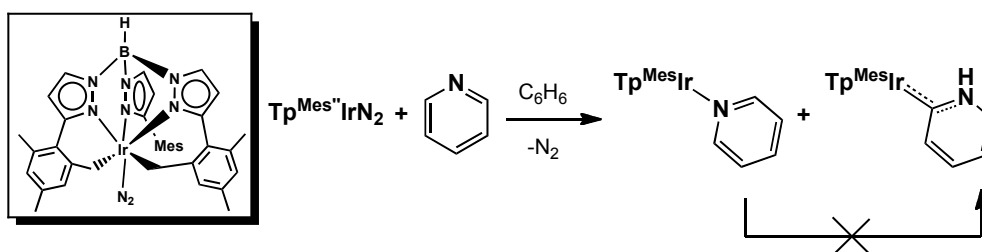


³³ G. Song, Y. Li, S. Chen, X. Li, *Chem. Commun.* **2008**, 3558.

be observed when no suitable group capable of stabilise the NH group is present. Mechanistic details were no further exploited, and only 2-substituted pyridines were studied, but no references are made for the role of steric hindrance.

In work developed by our own group, albeit independently of this Thesis, reaction of the Ir(III) complex $\text{Tp}^{\text{Mes}''}\text{Ir}(\text{N}_2)$ with pyridine was investigated ($\text{Tp}^{\text{Mes}''}$ stands for doubly metallated Tp^{Mes} ligand, as shown in the Scheme II – 11). Once more, Ir– N_2 dissociation is rate determining and the reaction produces an almost 1:1 kinetic mixture of the N-bound adduct and the NHC complex. This result reveals that the C–H activation reaction that generates the NHC has an activation energy nearly identical to that of N-coordination.^{29b}

Scheme II - 11



Isotopic labelling studies with $\text{C}_5\text{D}_5\text{N}$ demonstrated that (i) CH activation of pyridine occurs at all the CH sites; (ii) one of the metallated $[\text{Ir}]-\text{N}_{\text{pz}}-\text{CH}_2$ units mediates the reaction disengaging temporarily from the metal upon accepting the proton of the activated pyridine CH bond (yielding $[\text{Ir}]-\text{N}_{\text{pz}}-\text{CH}_3$) and metallating subsequently (chelate effect) to restore the $[\text{Ir}]-\text{N}_{\text{pz}}-\text{CH}_2$ group and concomitantly, the H atom is placed onto the pyridine N atom, forming in this way the carbene. In other words, one of the Ir– CH_2 bonds acts as a shuttle, transporting the activated pyridine H atom from C_2 to N.^{29b}

Based on the observations reported in this Thesis, and also in other made independently within our group, it may be established that formation of NHCs derived from pyridines becomes possible thanks to:

- Existence of a strong electronic interaction between $\text{Tp}'\text{Ir}(\text{R})(\text{R}')$ fragments and carbene ligands. This is supported by theoretical

calculations by A. Lledós and co-workers for carbene complexes resulting from C–H activations of aromatic ethers.^{8e,f}

- Destabilization of N bound adducts of 2-substituted pyridines due to F-strain. This is an important effect in all cases reported in this Thesis. Strong steric interactions between the bulky Ir(III) environment [Tp^{Me2}IrPh₂] and the pyridine substituent in positions 2 avoids formation of a sufficiently strong Ir–N bond.
- Participation of the solvent (C₆H₆) that readily undergoes C–H activation. Since pyridines are also activated very efficiently by the [Tp^{Me2}IrPh₂] species, phenyl/pyridine exchange is facile and leads ultimately to formation of the Ir–NHCs, the thermodynamic products of the reactions of 2-substituted pyridines.

II.1.4.3. On the Stability of N-Heterocyclic Carbenes Derived from Pyridines: Some Considerations

The generation of carbene complexes exclusively in the C₆ position of the pyridinic ring with the [Tp^{Me2}IrPh₂] system, and the fact that it does not take place in the case where C₆ is blocked, requires some comments.

Studies on the nature of the M–C bonding in this type of carbene complexes show that remote carbenes at C₄ can provide stronger σ -bonds.^{34,35}

Recent DFT studies on the stability of complexes of this type³⁶ show that, as already pointed out by Schwarz³⁷ and more recently by Musavi and coworkers,³⁸ tautomer **I** is the most stable free carbene (about 20 kcal·mol^{–1} in comparison with **I** and **III**; see

³⁴ S. K. Schneider, P. Roembke, G. R. Julius, C. Loschen, H. G. Raubenheimer, G. Frenking, W. A. Herrmann, *Eur. J. Inorg. Chem.* **2005**, 2973.

³⁵ H. Raubenheimer, S. Cronje, *Dalton Trans.* **2008**, 1265.

³⁶ G. Heydenrych, M. Von Hopffgarten, E. Stander, O. Schuster, H. G. Raubenheimer, G. Frenking, *Eur. J. Inorg. Chem.* **2009**, 1892.

³⁷ D. Lavorato, J. Terlouw, T. Dargel, W. Koch, G. McGibbon, H. Schwarz, *J. Am. Chem. Soc.* **1996**, 118, 11898.

³⁸ M. Z. Kassae, F. A. Shakib, M. R. Momeni, M. Ghambarian, S. M. Musavi, *Tetrahedron* **2009**, 65, 10093.

Introduction). However, when coordinated to a metal centre, the stabilization acquired is larger for **III-M**. This result does not necessarily mean that **III-M** would be the most probable carbene to be formed; such result would necessarily depend on the characteristics of the particular system being investigated. If there is an accessible kinetic route leading to **III-M** it would form preferentially, since it attains a larger interaction with the metal centre than **I-M** and **II-M**.

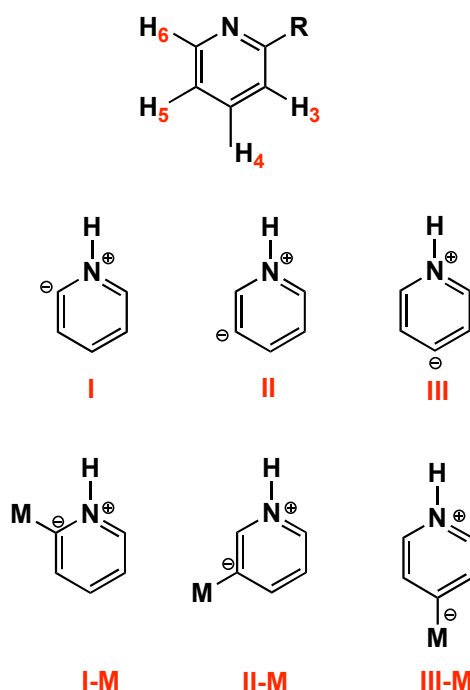


Figure II - 17. Possible NHCs derived from pyridine and corresponding metal derivatives.

Theoretical calculations for the $[\text{Tp}^{\text{Me}_2}\text{IrPh}_2]$ fragment show that in our case **I-M** is indeed more stable than **III-M**, by about $15 \text{ kcal}\cdot\text{mol}^{-1}$. Moreover, as already explained, the mechanistic route leading to our Ir(III)–NHC derivatives supports only structures of the type **I-M**.

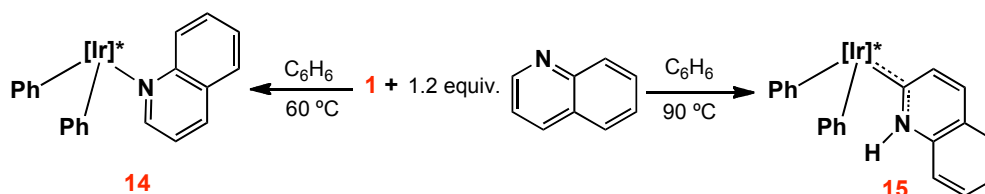
II.1.5. Generalization of the Tautomerization Processes to other N-Heterocycles: Studies with Quinolines and Polypyridines

II.1.5.1. Reaction of $\text{Tp}^{\text{Me}_2}\text{IrPh}_2(\text{N}_2)$ with Quinolines

II.1.5.1.1. Generation of Complexes **14** and **15**

Quinoline is a benzofused pyridine, extensively studied as a substrate in organometallic reactions. For our purposes, it can be considered a pyridine bearing a rigid CH sp^2 substituent at the 2-position (in fact is a 2,3-disubstituted pyridine). Quinoline reacts with complex **1** in C_6H_6 to yield complexes **14** or **15**, depending upon reaction temperature (60 °C or 90 °C, respectively, see Scheme II – 12). In fact, this system presents a behaviour similar to that found for 2-picoline, *i.e.* it leads first to a N-bound adduct (kinetic product) and then to its carbene tautomer (thermodynamic product).

Scheme II - 12



The N-bound adduct **14** features a doublet at 11.07 ppm ($^3J_{\text{HH}} = 5.5$ Hz) corresponding to H_6 , the proton adjacent to the nitrogen of the quinoline ligand. The 2D NOESY spectrum shows that the carbocyclic ring is located between two pyrazolyl rings. This is also the case for the molecular structure adopted in the solid state, as can be observed in the ORTEP plot represented in Fig. II – 18 (see Appendix 1, Table A13). The Ir–N bond has a bond length of 2.13 Å, similar to that found for **3** (2.14 Å), but longer than that of **11** (2.07 Å).

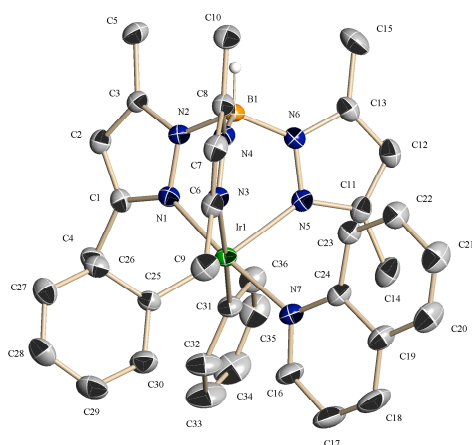


Figure II - 18. ORTEP representation of complex **14**.

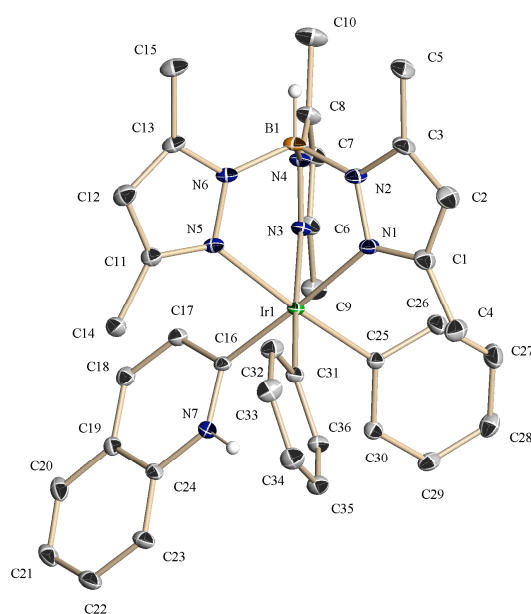
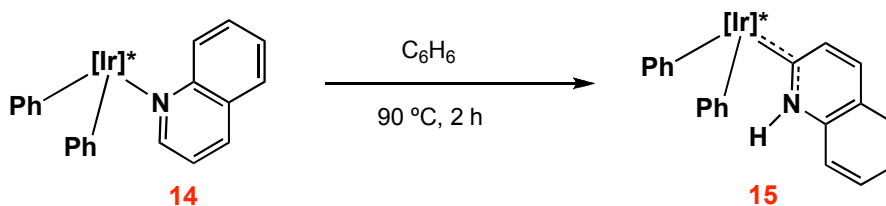


Figure II - 19. ORTEP representation of complex **15**.

For the carbene tautomer **15** only one rotamer is populated under ordinary conditions. Its structure is as shown in Scheme II – 12. The NH group resonates at 13.4 ppm in the ^1H NMR spectrum whereas the carbene carbon can be found at 185 ppm in the $^{13}\text{C}\{^1\text{H}\}$ NMR spectrum. Crystals suitable for X-ray diffraction studies allowed to confirm the structure of this molecule (see Appendix 1, Table A15), that exhibits an Ir–

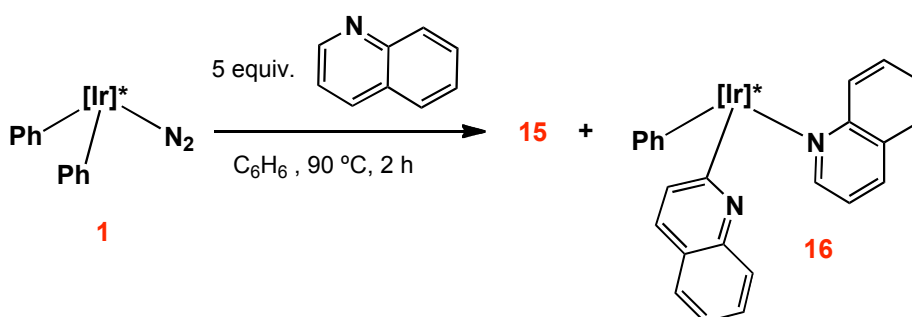
C_{carbene} bond length in 1.99 Å, similar to those found in the carbene complexes previously described. As expected, complex **15** can be obtained from **14** by heating its benzene solutions at 90 °C (Eq. 19).



Equation 19

II.1.5.1.2. Synthesis of Complex 16. Trapping a Plausible Intermediate with Quinoline

A minor product **16** was identified when compound **1** was heated at 90 °C with quinoline, according to the conditions specified in Scheme II – 12 (slight excess of substrate). This new compound is the result of the incorporation of two quinoline rings

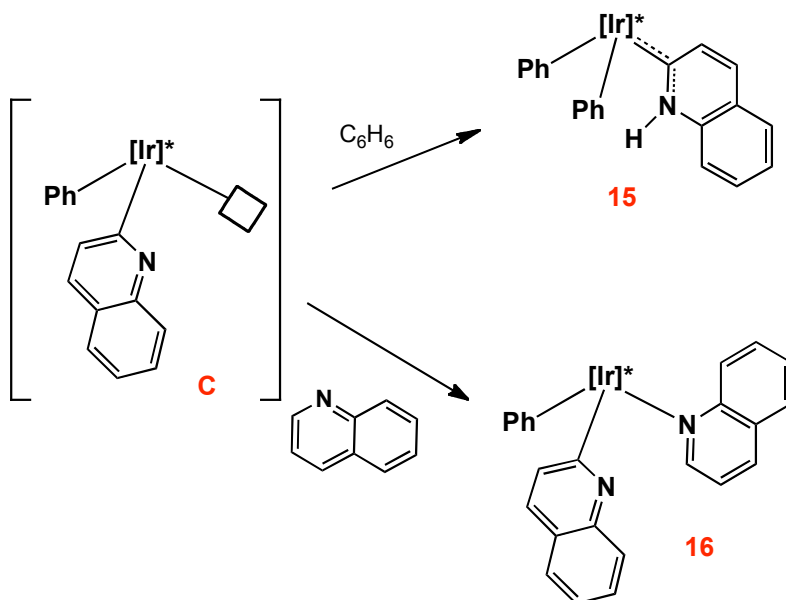


Equation 20

and it becomes the major product if the reagents ratio, quinoline:**1**, is increased to 5:1 (Eq. 20). Compound **16** has a phenyl and a 6-quinolyl group bonded to Ir, while an intact quinoline completes the 18 e⁻ count, acting as a N-bound ligand. The ¹H NMR spectrum of **16** features a doublet at 12.4 ppm assigned to H₆ (adjacent to nitrogen of the quinoline ligand), while in the ¹³C{¹H} NMR spectrum the Ir–C_{quin} resonates at 163.1 ppm.

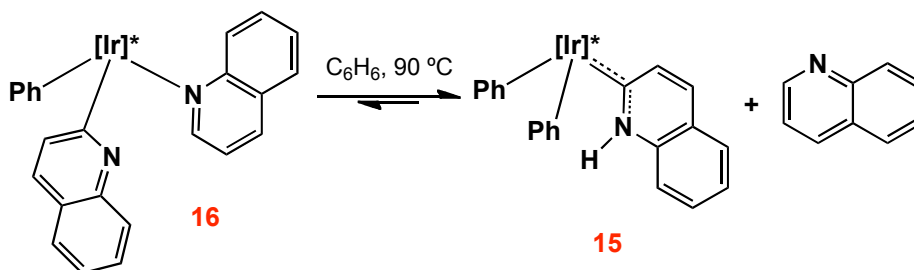
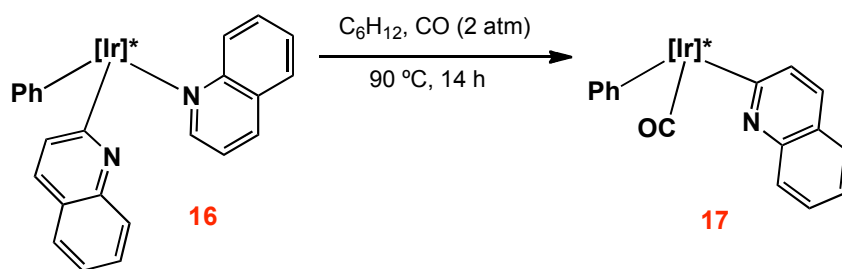
Complex **16** can be regarded as a quinoline-trapped product derived from intermediate **C**, related to **B** in Scheme II – 5, that is responsible for the generation of carbene tautomer **15**. Thus, in the absence of free heterocycle, intermediate **C** funnels to compound **15** by reaction with C_6H_6 (Scheme II – 13).

Scheme II - 13



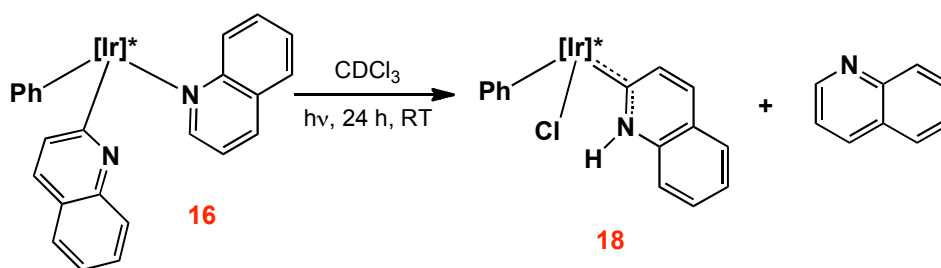
II.1.5.1.3. Reactivity of Complex **16**

Complex **16** can also be viewed as an analogous of the water adduct **5**, with the N-bound quinoline playing the role of H_2O as in the 2-phenylpyridine system. The quinoline ligand in **16** is labile and at 90 °C, in the presence of CO, this adduct cleanly yields the carbon monoxide complex **17** (Eq. 21). In its $^{13}C\{^1H\}$ NMR spectrum a resonance due to the $Ir-C_{quin}$ can be recorded at 159.5 ppm, while the carbonyl ligand resonates at 166.7 ppm. The CO stretching absorption appears at 2020 cm^{-1} in the IR spectrum. On the other hand, heating complex **16** in C_6H_6 at 90 °C gradually gives complex **15**, in accord with the equilibrium shown in Eq. 22.



Interestingly, complex **16** is unstable in CDCl_3 under laboratory light, affording carbene **18** along with free quinoline (Eq. 23). This new complex completes its coordination sphere with a phenyl and a chloride ligand. The proposed formulation is in agreement with the HRMS(FAB) spectrum which shows the M^+ molecular ion with the adequate isotopic composition. Complex **18** presents in its ^1H NMR spectrum a singlet at 13.06 ppm, due to the NH group and in the $^{13}\text{C}\{^1\text{H}\}$ NMR spectrum, the Ir–C_{carbene} resonates at 180.6 ppm. Generation of complex **18** can only be rationalized if small amounts of HCl are being generated from the solvent, and this is in fact the case when CDCl_3 is subjected to irradiation in the presence of adventitious moisture.³⁹

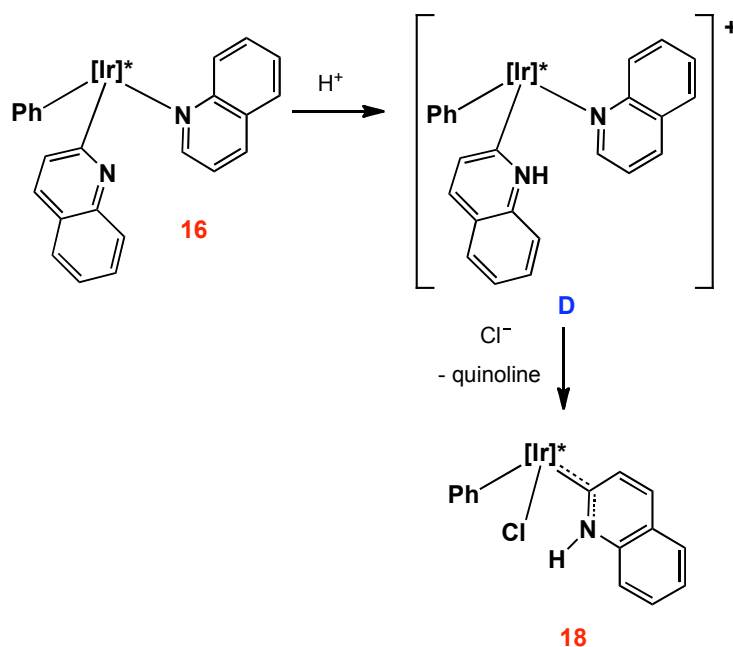
³⁹ P. Hoggard, *Coord. Chem. Rev.* **1997**, 159, 235.



Equation 23

As for the mechanism of formation of **18**, it is proposed that in the first step the quinolyl ligand of **16** is protonated at nitrogen to give a cationic intermediate **D** which then reacts with Cl^- , in a fast second step, with extrusion of quinoline (Scheme II – 14). This is an interesting observation, since it represents an unused process to generate HCl under very mild conditions, that allows to control the amount of HCl generated, since it is dependent of the exposition time to light.

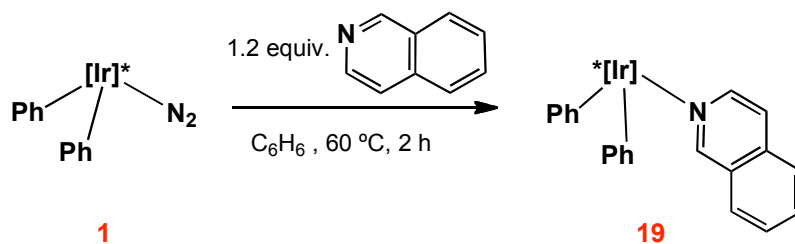
Scheme II - 14



Finally, it should be noticed that complex **16** has a N-quinoline ligand that, in spite of being labile, does not rearrange to a carbene at 90° C, in contrast with the behaviour observed with the $[\text{Tp}^{\text{Me}_2}\text{IrPh}_2]$ fragment (Scheme II – 12). Adduct stability in the case of **16** is also the result of a subtle kinetic effect as carrying out the reaction outlined in Eq. 20 at 120 °C allows the formation of a carbene, with a structure similar to complex **34** commented upon later in this Thesis (Section II.2). As this experiment was performed at the time of the final writings it is not included in the Experimental Part.

II.1.5.1.4. Reaction of **1** with Isoquinoline

Isoquinoline is a benzofused pyridine that bears a rigid CH sp^2 substituent at position 3 with respect to the nitrogen atom, being in fact a 3,4-disubstituted pyridine. In accord with results already presented, isoquinoline reacts with complex **1** at 60 °C to yield the N-bound adduct **19** (Eq. 24) that features, like the previously described N-bound adducts, hindered rotation around both Ir–N and Ir–C bonds (as manifested by variable temperature NMR spectroscopy). The two possible rotamers are present in a 5:3 ratio in CD_2Cl_2 at -60 °C. Complex **19** is very stable thermally and does not rearrange to the carbene tautomer upon heating its C_6H_6 solutions at 120 °C.



Equation 24

II.1.5.2. Study of Polypyridine Reactions

Aromatic nitrogen-containing heterocycles such as 2,2'-bipyridine (bpy), 1,10-phenanthroline (phen), 2,2':6',2-terpyridine (terpy) and related molecules are widely employed as ligands in coordination and organometallic chemistry,⁴⁰ and find widespread applications in homogeneous catalysis by transition metal complexes.⁴¹ Their interesting redox and photoredox chemistry are responsible for the leading role they play in the studies of electron and energy transfer processes.⁴² Moreover, they are commonly utilized as building blocks in supramolecular chemistry.⁴³

The excellent donor properties of these ligands, which are usually viewed as α -diimines, stem from their sp^2 -hybridized N atoms and result almost invariably in N,N'-chelating structures. Monodentate N-coordination has been proposed in several instances,⁴⁴ but has been authenticated by X-ray crystallography in only a few cases.⁴⁵

Following the reactivity trend found for 2-substituted pyridines, it was reasoned that polypyridines could also achieve metal induced tautomerization leading to NHC carbenes. This assumption is based on the obvious fact that bpy, phen and terpy can be viewed as 2-substituted pyridines.

⁴⁰ a) A. P. Smith, C. L. Fraser, *Comprehensive Coordination Chemistry II: from biology to nanotechnology*, Vol. 1, Pergamon, Oxford **2004**. b) E. C. Constable, *Adv. Inorg. Chem. Radiochem.* **1989**, 34, 1.

⁴¹ a) T. M. Boller, J. M. Murphy, M. Hapke, T. Ishiyama, N. Miyauro, J. F. Hartwig, *J. Am. Chem. Soc.* **2005**, 127, 14263. b) I. A. I. Mkhalid, D. N. Coventry, D. Albesa-Jove, A. S. Batsanov, J. A. K. Howard, R. N. Perutz, T. B. Marder, *Angew. Chem. Int. Ed.* **2006**, 45, 489. c) J. McFarland, M. Francis, *J. Am. Chem. Soc.* **2005**, 127, 13490.

⁴² a) O. Maury, H. Le Bozec, *Acc. Chem. Res.* **2005**, 38, 691. b) S. C. Chan, M. C. W. Chan, Y. Wang, C. M. Che, K. Cheung, N. Zhu, *Chem. Eur. J.* **2001**, 7, 4180. c) F. Gao, A. Bard, *J. Am. Chem. Soc.* **2000**, 122, 7426. d) R. J. Watts, *Comments Inorg. Chem.* **1991**, 11, 303. e) M. Al-Anber, S. Vatsadze, R. Holze, H. Lang, W. Thiel, *Dalton Trans.* **2005**, 2005, 3632.

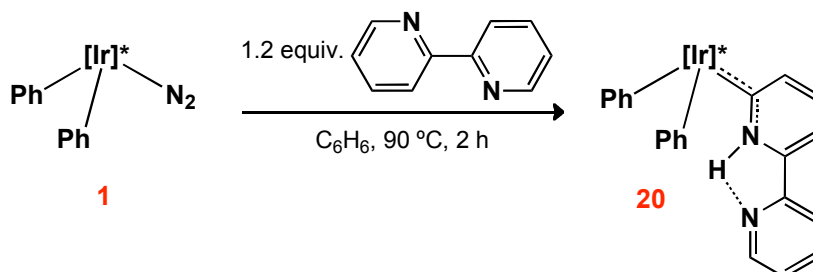
⁴³ a) C. Kaes, A. Katz, M. Hosseini, *Chem. Soc. Rev.* **2000**, 100, 3553. b) V. Balzani, G. Bergamini, F. Marchioni, P. Ceroni, *Coord. Chem. Rev.* **2006**, 250, 1254.

⁴⁴ a) J. Van Houten, R. Watts, *J. Am. Chem. Soc.* **1976**, 98, 4853. b) A. J. Brown, O. W. Howarth, P. Moore, W. J. E. Parr, *J. Chem. Soc., Dalton Trans.* **1978**, 1776. c) S. Dholakia, R. Gillard, F. Wimmer, *Inorg. Chim. Acta* **1983**, 69, 179. d) F. Pruchnik, F. Robert, Y. Jeannin, S. Jeannin, *Inorg. Chem.* **1996**, 35, 4261. e) A. A. Sidorov, G. G. Aleksandrov, E. V. Pakhmutova, A. Y. Chernyad'ev, I. L. Eremenko, I. I. Moiseev, *Russ. Chem. Bull.* **2005**, 54, 588.

⁴⁵ G. W. Bushnell, K. R. Dixon, M. A. Khan, *Can. J. Chem.* **1974**, 52, 1367.

II.1.5.2.1. 2,2'-Bipyridine

The study of the reactivity of complex **1** with bpy have the extra motivation provided by the controversy that has long surrounded one of the $[\text{Ir}(\text{bpy})_3]^{3+}$ cations⁴⁶ (sometimes referred to as Watt's complex), which has two N,N'-bpy ligands and a third N,C-bpy that chelates the metal through the N atom of one ring and the C₃ atom of the other (see below).



Equation 25

2,2'-Bipyridine reacts with **1** at 90 °C in C₆H₆ to afford carbene **20** in very good yield (Eq. 25) with no intermediates being detected at lower temperatures (60 °C). The IR spectrum of compound **20** shows a broad band centred at 3265 cm⁻¹ due to the N–H stretching absorption. In NMR experiments, **20** was characterized at low temperature as in the previous cases, a deshielded resonance at 14.60 ppm can be observed, in the ¹H NMR spectrum, for the NH functionality (major rotamer). Comparison with data obtained for other carbenes previously described suggests the existence of an intramolecular hydrogen bond between the NH unit of the coordinated ring and the N atom of the other. In effect, its chemical shift is downfielded by about 1.2 ppm with respect to the NH resonance of complex **4**. In the ¹³C{¹H} NMR spectrum, the Ir–C_{carbene} resonates at 180.2 ppm.

⁴⁶ a) R. Watts, J. Harrington, J. Van Houten, *J. Am. Chem. Soc.* **1977**, 99, 2179. b) W. A. Wickramasinghe, P. H. Bird, N. Serpone, *J. Chem. Soc., Chem. Commun.* **1981**, 1284. c) G. Nord, A. Hazell, R. Hazell, *Inorg. Chem.* **1983**, 22, 3429. d) N. Serpone, G. Ponterini, M. A. Jamieson, F. Bolletta, M. Maestri, *Coord. Chem. Rev.* **1983**, 50, 209. e) A. Hazell, R. Hazell, *Acta Crystallogr. Sect. C* **1984**, 40, 806. f) N. Serpone, *Comprehensive Coordination Chemistry*, Vol. 4, Pergamon, Oxford, **1987**.

Single crystal X-ray studies were carried out with **20** to demonstrate the presence of the carbene tautomer of bpy (Fig. II – 20, see Appendix 1- Table A17). As can be observed, the rotamer present in the crystal is the major one existing in the CD₂Cl₂ solution. The Ir–C_{carbene} bond, 1.97 Å, in this molecule is similar in length to those previously observed for other carbenes. The two heterocyclic rings are nearly coplanar (dihedral angle of about 6°) in such a way that a N–H···N hydrogen bond is formed. The N(8)···H(7)N(7) distance of *ca.* 2.2 Å is shorter than the sum of the van der Waals radii of H (1.2 Å) and N (1.5 Å)⁴⁷ in agreement with related interactions.⁴⁷

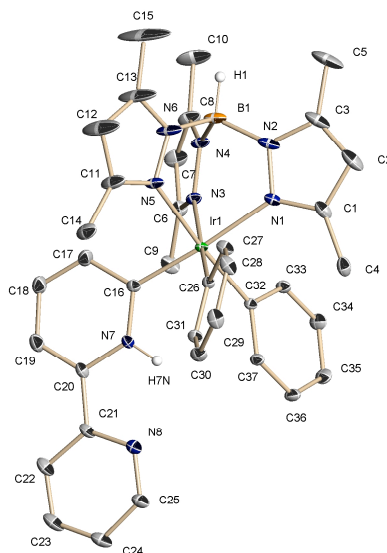


Figure II - 20. ORTEP representation of complex **20**.

⁴⁷ G. R. Desiraju, T. Steiner, *The weak hydrogen bond*, Oxford University Press, Oxford, **1999**.

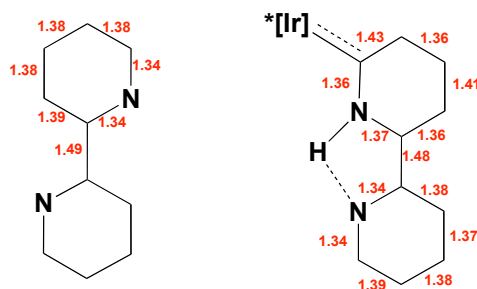


Figure II - 21. Bond distances (Å) in free bpy and complex **20**.

A comparison of the bond lengths of free bpy⁴⁸ and the carbene ligand found in **20** nicely illustrates the distortion of the heterocyclic ring bonded to iridium (Fig. II – 21). Thus, whereas the C–C bond lengths in free bpy are identical (1.38 Å) and in the uncoordinated ring of **20** they cluster in the narrow range 1.38–1.40 Å, the carbene ring exhibits two C–C bonds with lengths of *ca.* 1.36 Å, which are distinctly shorter than the other two (*ca.* 1.42 Å), *i.e.* as expected for the diene contribution to the carbene formulation.

The demonstration of this unprecedented coordination mode of bpy suggests a new way of looking at Watt's complex (Fig. II – 22), for which the represented structure was consolidated after a long and intense controversy. According to our findings, it seems plausible that this structure could be described as containing an ylidic bpy ligand, rather than being “reminiscent of orthometallated compounds”, as originally proposed.⁴⁶

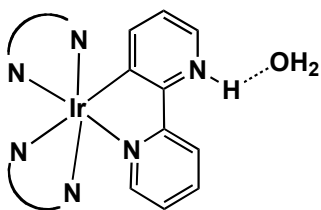


Figure II - 22. Watts complex

⁴⁸ F. Kühn, M. Groarke, E. Bencze, E. Herdtweck, A. Prazeres, A. Santos, M. Calhorda, C. Romão, I. Gonçalves, A. Lopes, *Chem. Eur. J.* **2002**, 8, 2370.

II.1.5.2.2. Phenanthroline

Complex **1** reacts with phen, in C_6H_6 at $100\text{ }^\circ\text{C}$, to provide the NHC compound **21** (Eq. 26). IR and NMR spectroscopic data for **21** are similar to those of **20** and need no further comments (Fig. II – 23). Complex **21** mainly exists in a CD_2Cl_2 solution as the rotamer represented in Eq. 26 (rotamer ratio $\approx 10:1$).

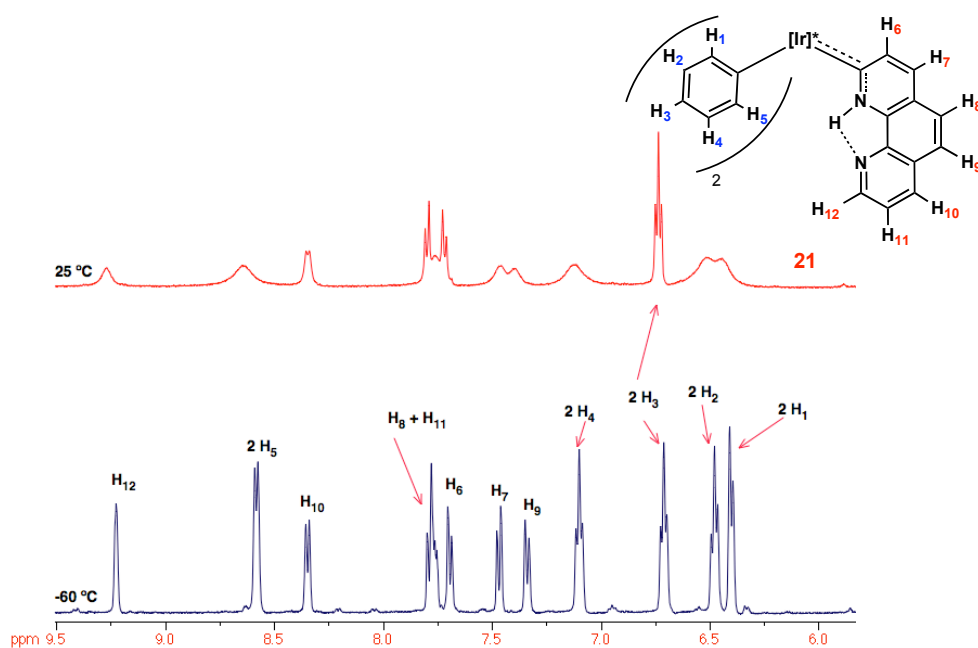
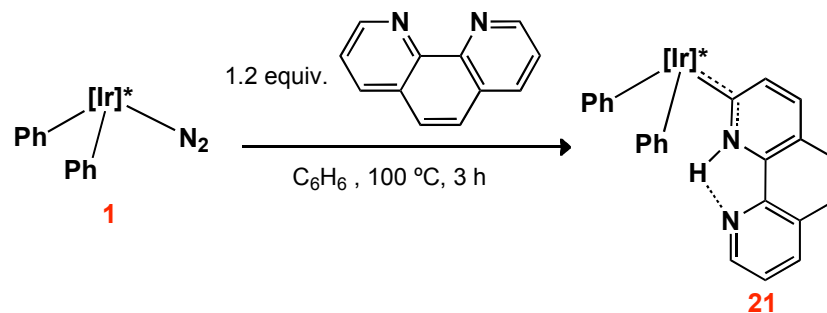


Figure II - 23. ^1H NMR spectra of complex **21** ($25\text{ }^\circ\text{C}$ and $60\text{ }^\circ\text{C}$, CD_2Cl_2 , 500 MHz).

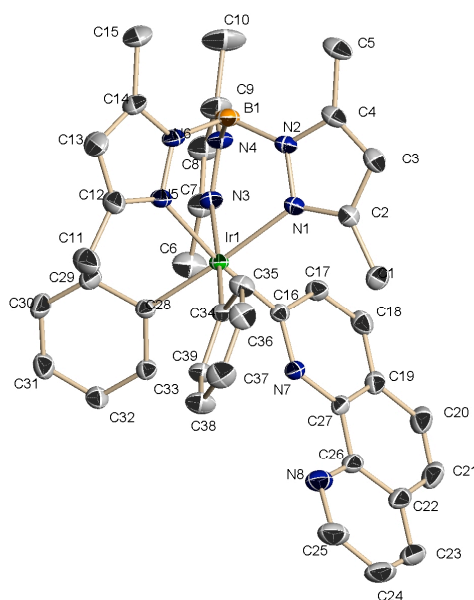
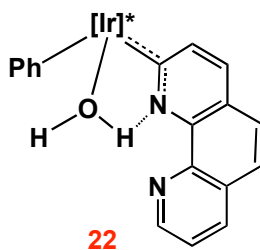


Figure II - 24. ORTEP representation of complex **21**.

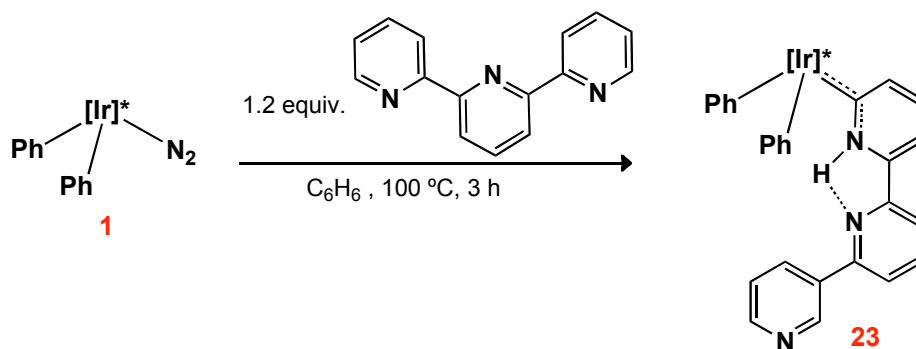
A single-crystal X-ray study was carried out with complex **21** and the results are presented in Fig. II – 24 and collected in Appendix 1 (Table A19). The structure is similar to that found for the 2,2'-bpy carbene and needs no further discussion.

If the reaction represented in Eq. 26 is undertaken at lower temperatures (60 °C), a new complex **22** is detected, as the major reaction product. The spectroscopic data collected in the Experimental Part are fully in agreement with its formulation as an water adduct closely related to the previously described for the case of 2-phenylpyridine. Interestingly, no such species is observed in the **1**:bpy system.



II.1.5.2.3. Terpyridine

Complex **1** reacts with terpyridine, in C₆H₆ at 100 °C, to provide the corresponding NHC compound **23** (Eq. 27).⁴⁹ Fig. II – 25 shows the variable temperature ¹H NMR spectra of this complex, which curiously exists as a 5:1 mixture of rotamers.



A broad IR absorption at around 3270 cm⁻¹ and a ¹H NMR resonance at 14.20 ppm are due to the NH unit, while the carbene carbon atom resonates at δ 179.5 ppm in the ¹³C{¹H} NMR spectrum. As in **20** and **21**, also **23** presents a very deshielded resonance for the NH group, which is in accord with the existence of a hydrogen bond between the NH group and the nitrogen of the other ring.

⁴⁹ For a similar transformation with other Tp^{Me2}IrRR') systems see: M. Paneque, M. Poveda, F. Vattier, E. Álvarez, E. Carmona, *Chem. Comm.* **2009**, 5661.

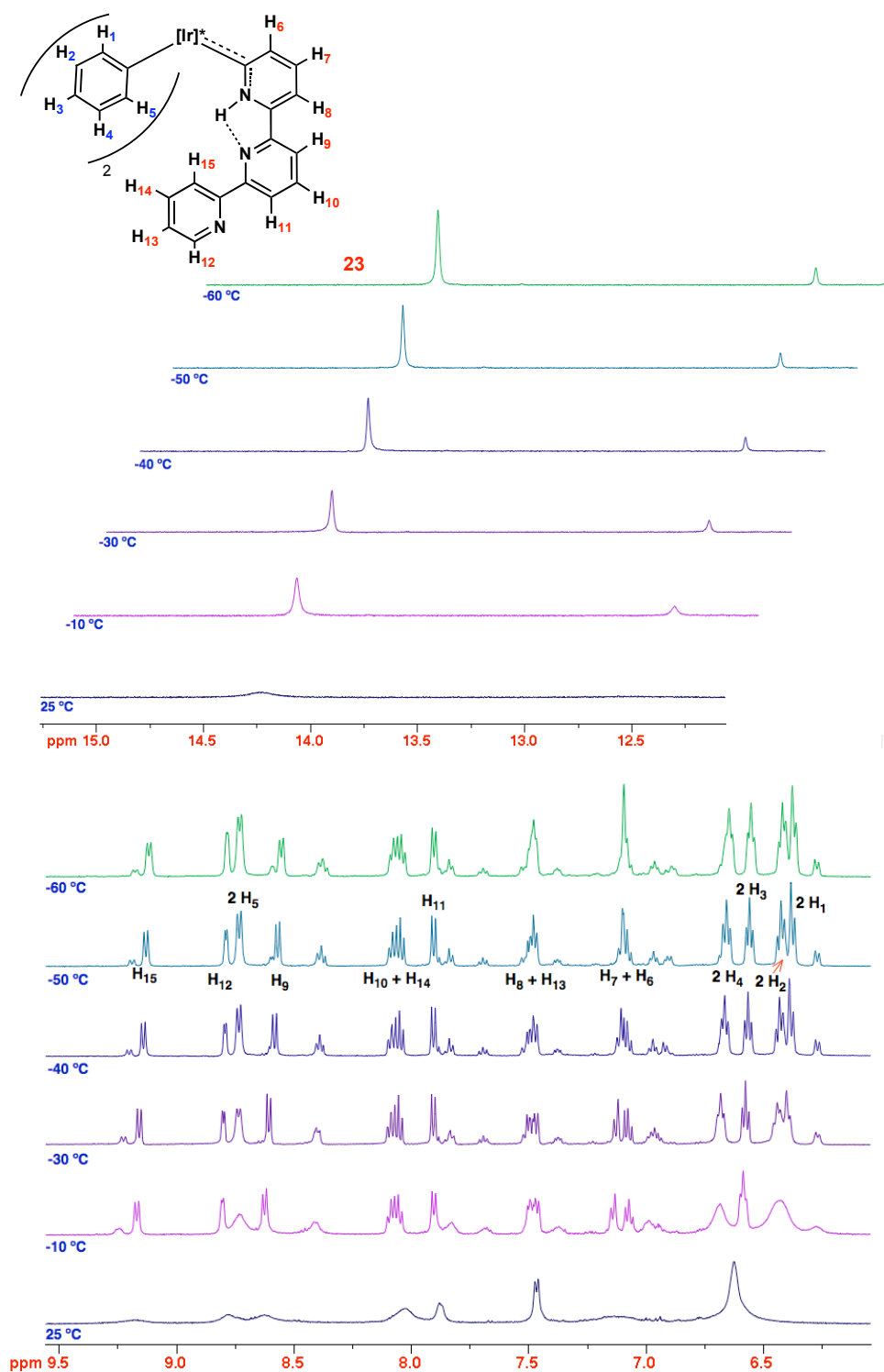


Figure II - 25. ^1H NMR spectra of complex **23** (25 to -70 °C, CD_2Cl_2 , 400 MHz).

II.1.5.2.4. 4,4'-Bypiridine

4,4'-bipyridine reacts with complex **1** to afford a mixture of the N-bound adduct **24** and the related binuclear complex **25**, with their ratio being dependent on the ligand to **1** ratio used in the reaction.

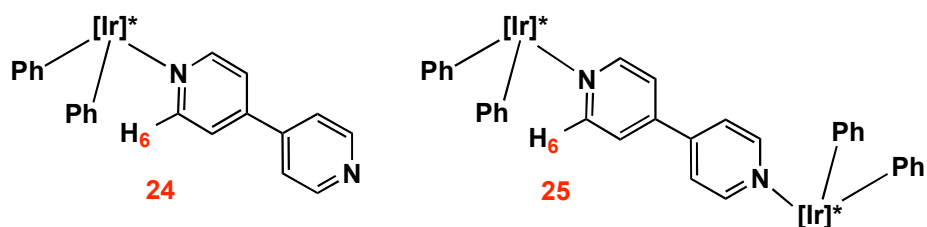


Figure II - 26. Representation of complexes **24** and **25**.

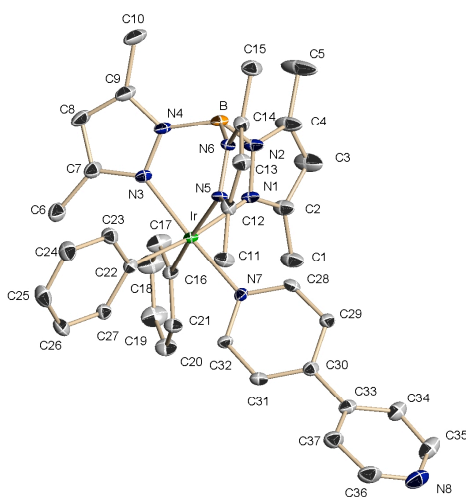


Figure II - 27. ORTEP representation of complex **24**.

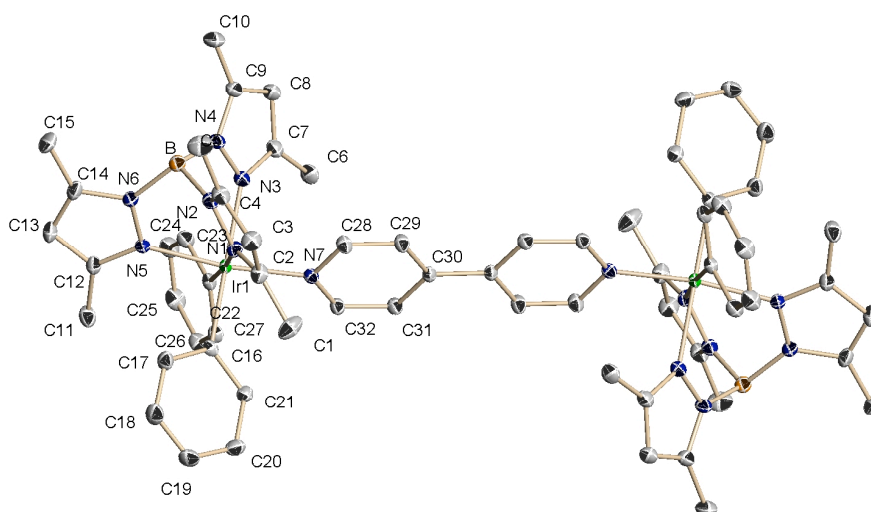


Figure II - 28. ORTEP representation of complex **25**.

Complexes **24** and **25** have been characterized by NMR spectroscopy. In both complexes, the ^1H resonances associated with the H_6 protons are found at low field, at around 10.20 ppm, but can only be detected at low temperatures ($-60\text{ }^\circ\text{C}$, CD_2Cl_2) where rotation around Ir–C and Ir–N bonds becomes slow in the NMR time scale.

X-ray diffraction studies on **24** and **25** have been performed and the results are showed in Fig. II – 27 and Fig. II – 28 (See also Appendix 1, Table A21 and A23). The Ir–N(7) bonds lengths are similar in both complexes, approximately 2.07 \AA , close to that found for complex **11**. As expected, both **24** and **25** are thermally stable and no conversion into the corresponding carbenes have been observed even by heating their C_6H_6 solutions at $120\text{ }^\circ\text{C}$.

II.2. Reactivity of N-Heterocyclic Carbenes Derived from Pyridines

N-heterocyclic carbenes (NHCs) are nowadays extensively used as ligands in organometallic chemistry.¹² Since the isolation of the first stable N-heterocyclic carbene,⁵⁰ these molecules have emerged as a powerful class of carbon-based ligands with broad applications.⁵¹

One of the main reasons of their extended use is the ability of NHCs to provide great stabilization to transition metal complexes, even in high oxidation states, due to their powerful σ -donating properties. In addition, their electronic and steric characteristics can be easily modulated,^{14b} providing NHCs with great versatility as ligands. Until recently, NHCs were also known for their inertness, being considered only as spectator ligands. In the last years, however, several reports have shown that NHCs might be, in fact, far from innocent ligands,⁵² since they can undergo facile C–H,⁵³ C–C^{14,54} and C–N⁵⁵ bond activation processes. The study of this reactivity is of great importance, not only to provide knowledge on their decomposition pathways, but also because it opens further possibilities for their use.

Although not very common, several examples of NHCs featuring a hydrogen bonded to nitrogen are known, and the first part of this chapter describes precisely a recent example. However, studies on the reactivity of this type of N-heterocyclic carbenes are scarce. The work that is described in this section is centred on the reactivity of the NHCs derived from the tautomerization of pyridines.

⁵⁰ A. Arduengo, R. Harlow, M. Kline, *J. Am. Chem. Soc.* **1991**, *113*, 361.

⁵¹ a) W. D. Jones, *J. Am. Chem. Soc.* **2009**, *131*, 15075. b) F. E. Hahn, *Dalton Trans.* **2009**, 6893. c) A. Arduengo, G. Bertrand, *Chem. Rev.* **2009**, *109*, 3209.

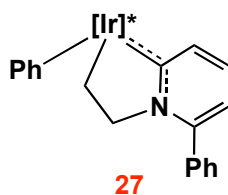
⁵² a) C. Crudden, D. Allen, *Coord. Chem. Rev.* **2004**, *248*, 2247. b) T. Steinke, B. Shaw, H. Jong, B. Patrick, M. Fryzuk, J. Green, *J. Am. Chem. Soc.* **2009**, *131*, 10461.

⁵³ a) T. Trnka, J. Morgan, M. Sanford, T. Wilhelm, M. Scholl, T. Choi, S. Ding, M. Day, R. Grubbs, *J. Am. Chem. Soc.* **2003**, *125*, 2546. b) B. Galan, M. Gembicky, P. Dominiak, J. Keister, S. Diver, *J. Am. Chem. Soc.* **2005**, *127*, 15702. c) C. Cooke, M. Jennings, R. Pomeroy, J. Clyburne, *Organometallics* **2007**, *26*, 6059. d) U. Scheele, S. Dechert, F. Meyer, *Chem. Eur. J.* **2008**, *14*, 5112. e) S. Burling, E. Mas-Marzá, J. E. V. Valpuesta, M. Mahon, M. Whittlesey, *Organometallics* **2009**, *28*, 6676.

⁵⁴ R. Jazzar, S. Macgregor, M. Mahon, S. Richards, M. Whittlesey, *J. Am. Chem. Soc.* **2002**, *124*, 4944.

⁵⁵ S. Burling, M. F. Mahon, R. E. Powell, M. K. Whittlesey, J. Williams, *J. Am. Chem. Soc.* **2006**, *128*, 13702.

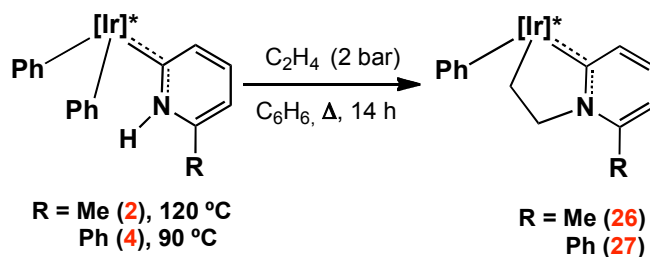
To study the reactivity of these carbene complexes, compounds **2** and **4** were chosen. The choice of complex **2** arises from its simplicity, since it is the easiest carbene tautomer to characterize by NMR spectroscopy. With respect to **4**, different reasons led to its choice: first, in contrast with the Me group, the Ph residue is more electronwithdrawing, and second, it was mentioned previously that intermediate **A** can be generated both from **1** and $\text{Tp}^{\text{Me}_2}\text{Ir}(\text{C}_2\text{H}_4)_2$. Using the latter in the synthesis of **4**, it was observed that **4** is indeed obtained as the major reaction product, but small amounts of another complex were also detected. This minor product was identified as **27**, indicating that a C_2H_4 molecule was incorporated as part of an interesting, unusual iridacycle.



II.2.1. Reactivity of Compounds **2** and **4** towards Alkenes

II.2.1.1. Reaction with Ethylene

When **2** and **4** are heated in benzene under an atmosphere of C_2H_4 , the new complexes, **26** and **27** are generated. The formation of both compounds is quantitative (by spectroscopy) and no intermediates are detected upon NMR monitoring of the reactions. Carbene **2** reacts slower than **4** and this is reflected in the operating temperatures shown in Eq. 28.



Equation 28

As can be observed, a molecule of C_6H_6 is released (by transfer of the NH hydrogen to a phenyl ligand) and the reacting ethylene has ended as a $-CH_2CH_2-$ linkage between the Ir and N centres, forming therefore a metallacycle. The structures proposed for **26** and **27** are supported by elemental analysis and spectroscopic data. For complex **27**, in addition to 1H and $^{13}C\{^1H\}$ NMR resonances due to the phenyl and pyridylidene rings, the incorporated $-CH_2CH_2-$ unit is responsible for 1H multiplets at 2.62 and 2.90 ppm (Ir- CH_2) and at 4.17 and 5.21 ppm (N- CH_2). Corresponding $^{13}C\{^1H\}$ signals are found at -11.7 and 65.8 ppm, respectively, whereas the Ir- C_{carbene} resonates at 190.6 ppm. The latter signal is shifted by about 13 ppm to higher frequency with respect to the parent NHC complex **4**. For **26**, similar values are recorded (see Experimental Section).

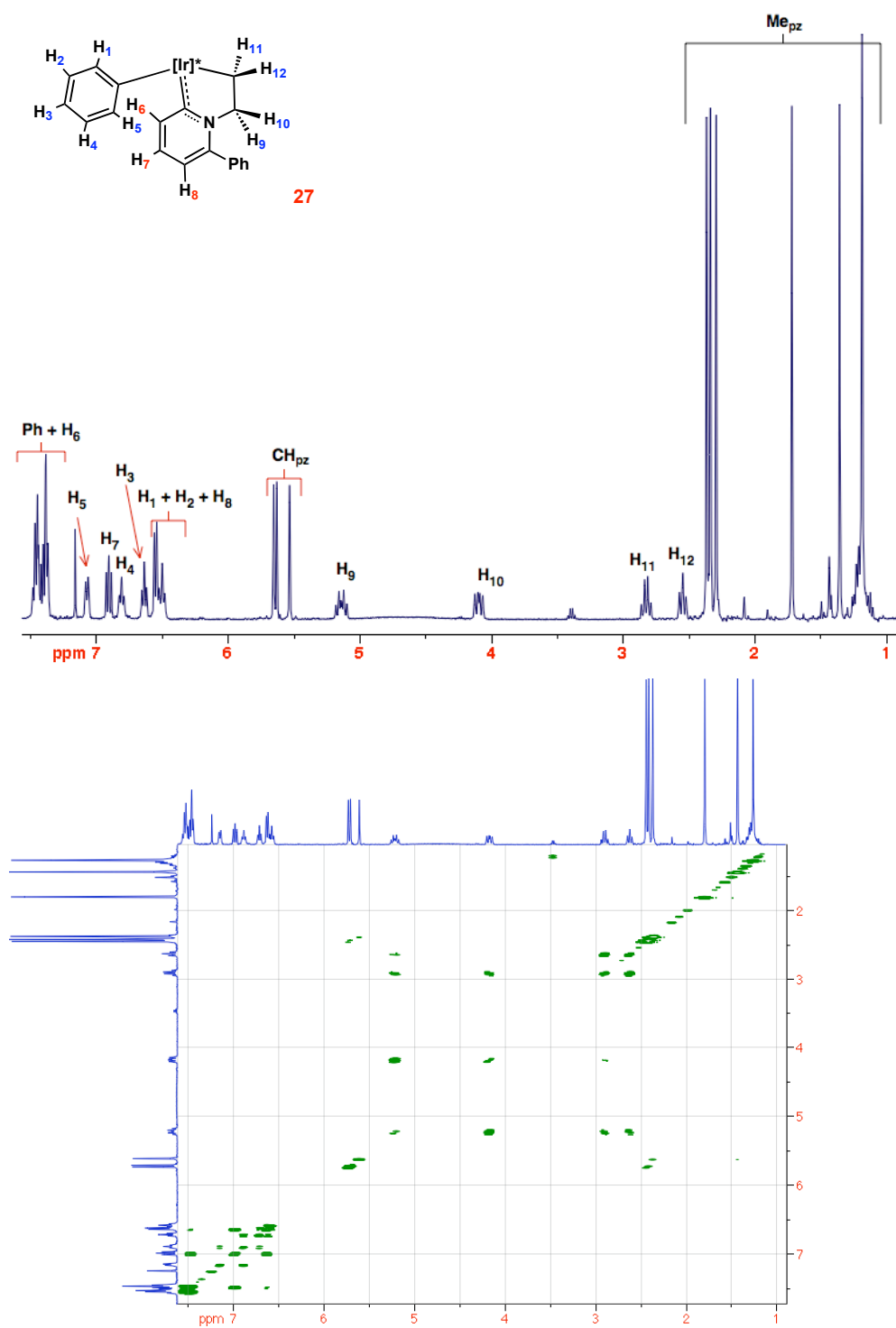


Figure II – 36. ^1H NMR (top) and COSY (bottom) spectra of complex **27** (CDCl_3 , 500 MHz).

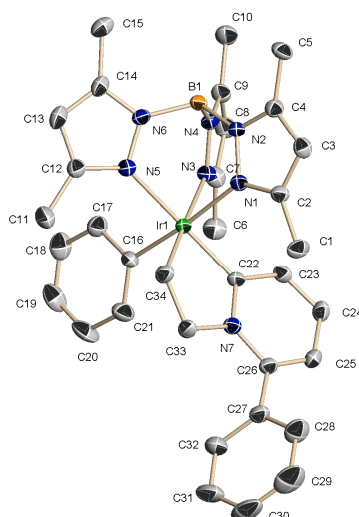
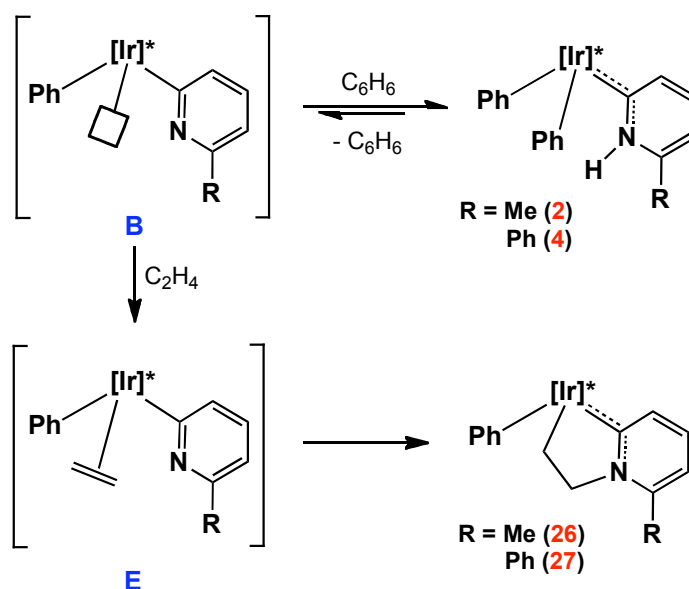


Figure II – 37. ORTEP plot for complex **27**.

For the case of **27**, the molecular structure was confirmed by X-ray diffraction studies (Fig. II – 37, Appendix 1- Table A25). Complex **27** exhibits an Ir–C_{py} bond of 1.95 Å, very similar to that found in related monodentate pyridylidenes, such as **4**. As in these complexes, this distance is somewhat shorter than the two Ir–C_o bonds present in the molecule (Ir–C16 and Ir–C34 at 2.05 and 2.07 Å respectively). The pyridinium N7–C33 bond has a normal length of 1.52 Å, whereas the two originally olefinic carbon atoms, C33 and C34, form in **27** a single C–C bond of regular length (1.53 Å). The structures of **26** and **27** suggest that the C–N bond is formed by a nucleophilic attack of the nitrogen atom to an olefinic carbon and entail the participation of the unsaturated phenyl-pyridyl intermediates of type **B** (Scheme II-15).

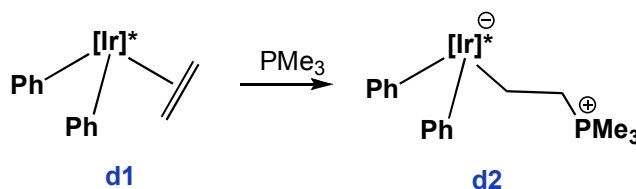
Scheme II - 15



Several groups have described the increased nucleophilic character of the nitrogen atom in 2-pyridyl complexes, with respect to the parent free pyridines⁵⁶ and their use as organometallic nucleophiles has been documented.^{56d,57} In addition, unsaturated intermediates **B**, can be stabilized by the basic nitrogen, but may also allow the coordination of molecules such as olefins (intermediate **E**), capable of stabilizing the electrophilic centre more effectively, since F-strain in 2-pyridyls is expected to restrict N-coordination. The coordination of ethylene to the Ir(III) Lewis centre permits subsequent intramolecular nucleophilic attack of the basic nitrogen to one of the olefinic carbons, to generate both **26** and **27**. Supporting this proposal is the reported reactivity of complex **d1** (Eq. 29) towards PMe_3 .⁶ The phosphine adds to one of the olefinic carbons of the coordinated ethylene, generating zwitterionic complex **d2**, as one of the main products of the reaction.

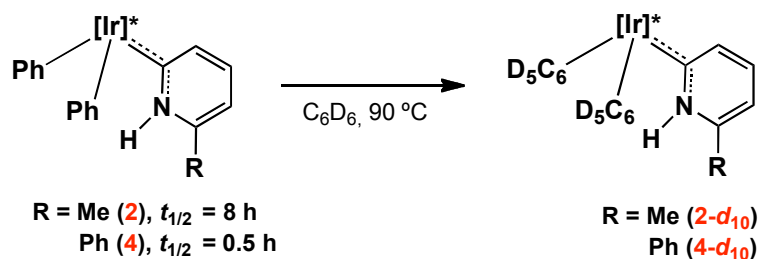
⁵⁶ **a)** K. Nakatsu, K. Kinoshita, H. Kanda, K. Isobe, *Chem. Lett.* **1980**, 913. **b)** K. Isobe, E. Kai, Y. Nakamura, K. Nishimoto, T. Miwa, S. Kawaguchi, K. Kinoshita, K. Nakatsu, *J. Am. Chem. Soc.* **1980**, 102, 2475. **c)** K. Isobe, Y. Nakamura, T. Miwa, S. Kawaguchi, *Bull. Chem. Soc. Jpn.* **1987**, 60, 149. **d)** B. Crociani, F. Di Bianca, A. Giovenco, A. Berton, R. Bertani, *J. Organomet. Chem.* **1989**, 361, 255.

⁵⁷ **a)** B. Crociani, F. Di Bianca, A. Giovenco, A. Scrivanti, *J. Organomet. Chem.* **1983**, 251, 393. **b)** F. Di Bianca, A. Fontana, R. Bertani, B. Crociani, *J. Organomet. Chem.* **1992**, 425, 155.



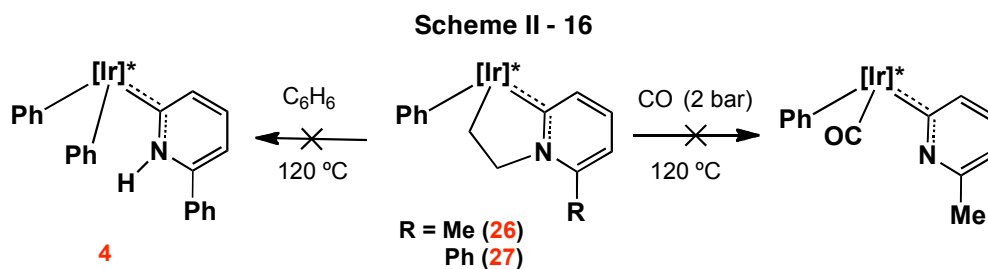
Equation 29

In accord with the intermediacy of **B** in the formation of **26** and **27**, it has been observed that **2** and **4** interchange their phenyl ligands with C_6D_6 at 90°C to give **2-*d*₁₀** and **4-*d*₁₀**, with $t_{1/2}$ of *ca.* 8 and 0.5 h respectively. If the formation of intermediate **B**, derived from **2** or **4**, is the rate determining step in the reaction with a particular substrate, this difference in the deuteration rate will be reflected in the relative reactivity of these two complexes. Indeed we qualitatively observe this behaviour in the facility of C_2H_4 incorporation shown by the reaction temperatures needed for the reactions of Eq. 28.



Equation 30

Both **26** and **27** are quite stable thermally and ethylene incorporation seems not to be reversible; this conclusion arises from the observation that **26** does not react with CO upon heating at 120°C for several hours. Additionally **27** remains unchanged after 24 hours, at 120°C , in benzene under nitrogen (Scheme II – 16).



II.2.1.2. Light Effects on the NMR Spectra of Complex 26

During the development of spectroscopic studies aimed to the characterization of complex **26**, we observed interesting variations in the ^1H NMR spectrum, when its solutions in CDCl_3 were exposed to light (fluorescent or solar). Thus, some of the aromatic C–H signals of the coligands as well as those of the Ir–bound methylene moiety of the $-\text{CH}_2\text{CH}_2-$ fragment, first broaden and then disappear gradually from the spectra depending on the exposition time to light. The effect is better explained when only the Ir– $\text{CH}_2\text{CH}_2\text{N}$ protons are taken into consideration. As it is shown in Fig. II – 41, both Ir– CH_2 protons broaden at the same rate until they disappear from the baseline. At the same time, the NCH_2 protons are becoming “decoupled” from the Ir– CH_2 protons to finally give two doublets due to their mutual coupling $^2J_{\text{HH}}$ constant. All these variations take place without appreciably changing the chemical shifts of the nuclei involved. In parallel, some of the ^{13}C resonances in the $^{13}\text{C}\{^1\text{H}\}$ NMR spectrum broaden and in particular the three Ir–C resonances almost disappear from the baseline.

These NMR–light effects are observed under O_2 or under N_2 and they also occur in CD_2Cl_2 although they are slower than in CDCl_3 . However, no such behaviour is observed in C_6D_6 or CD_3COCD_3 .

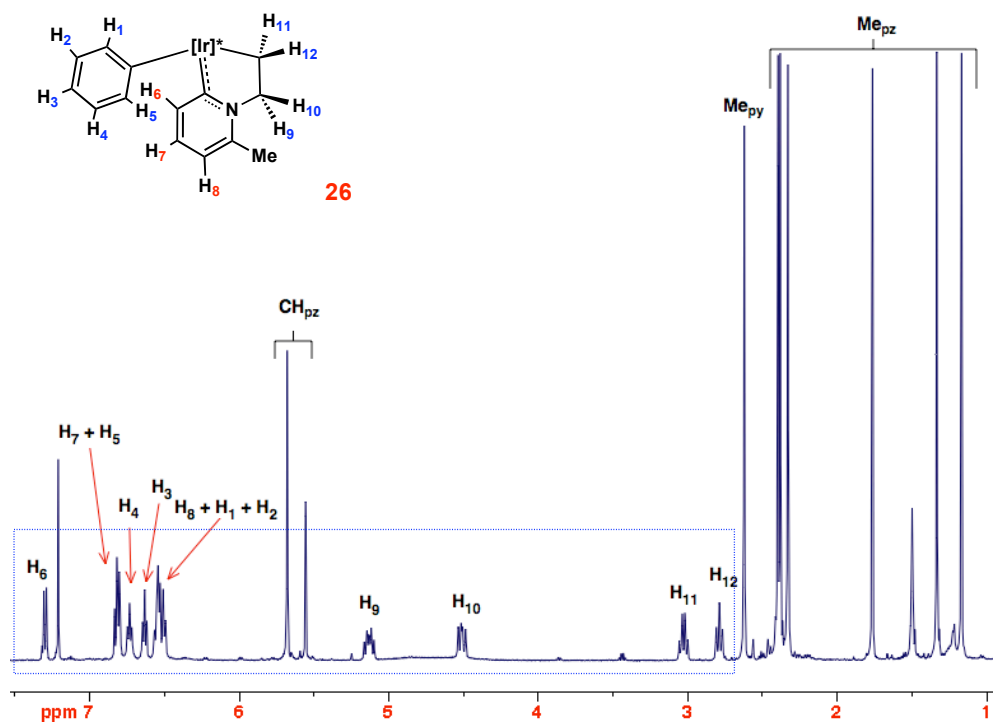


Figure II – 38. ^1H NMR spectrum of **26** in CDCl_3 (500 MHz, 25 $^\circ\text{C}$).

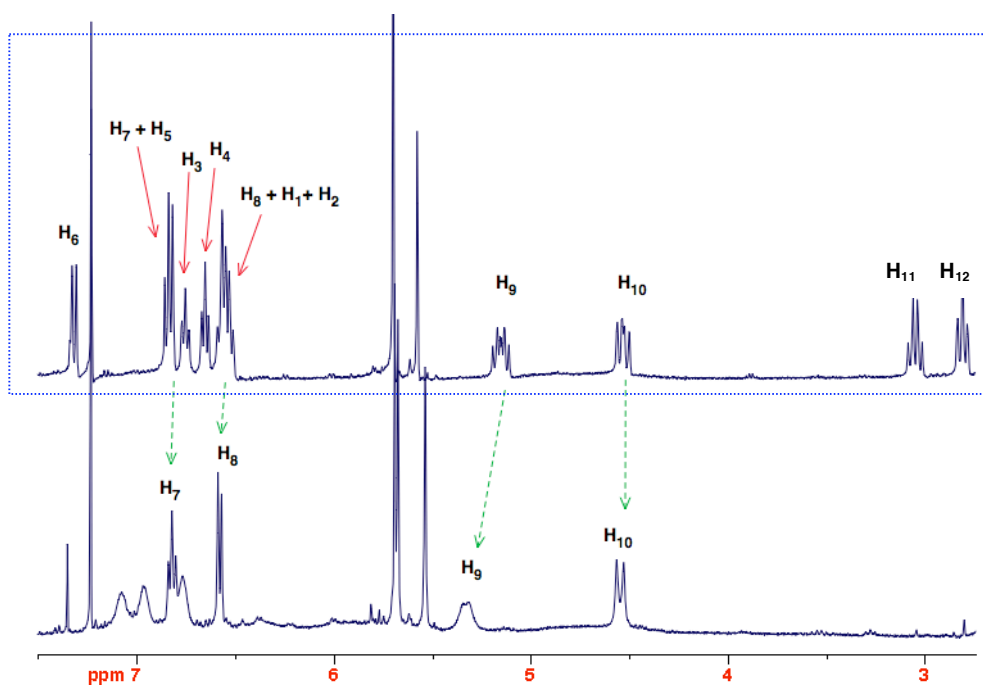


Figure II – 39. ^1H NMR spectrum of **26** before (top) and after (bottom) exposition to light. (25 $^\circ\text{C}$, CDCl_3 , 500 MHz).

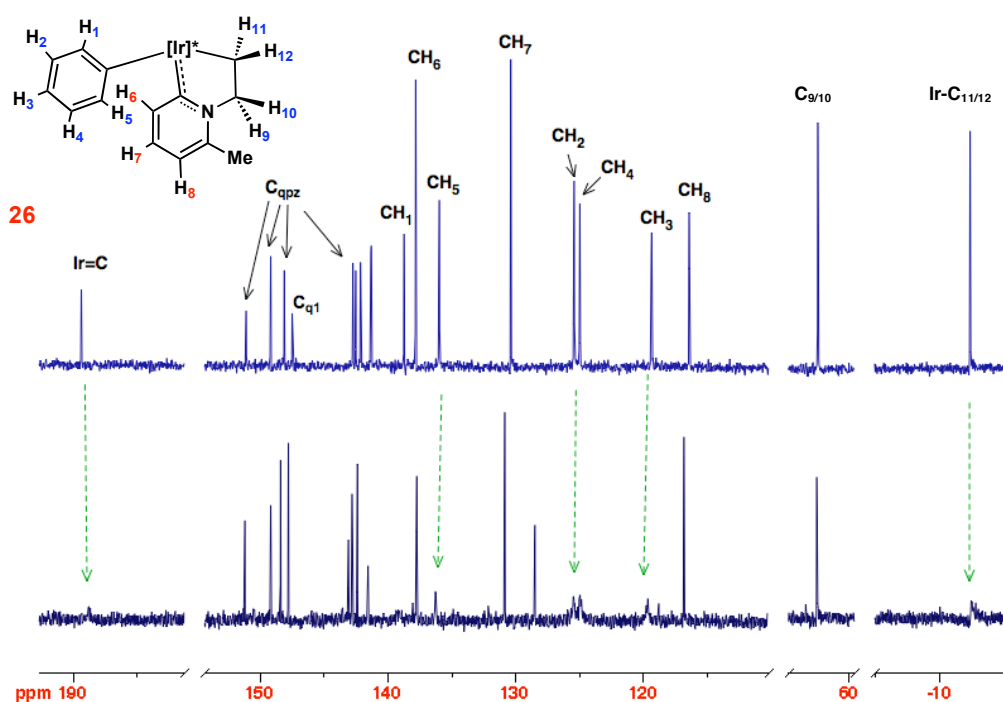
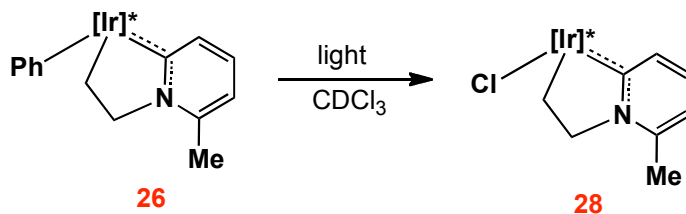


Figure II – 40. $^{13}\text{C}\{^1\text{H}\}$ NMR spectrum of **26** at 25 °C before (above) and after (below) exposition to light.

The commented NMR variations are slowly reversible and, in the absence of light, the solution gradually restores the original spectrum at 25 °C, but faster as the temperature is raised. If the sample is exposed to light for several hours, a new complex **28** gradually forms at the expense of **26**, and this is the result of the substitution of the phenyl group for a chloride (Eq. 31). In the absence of light, the sample remains stable for several months, in CDCl_3 or CD_2Cl_2 . Curiously, **28** does not experience the NMR effects described for **26**.



Equation 31

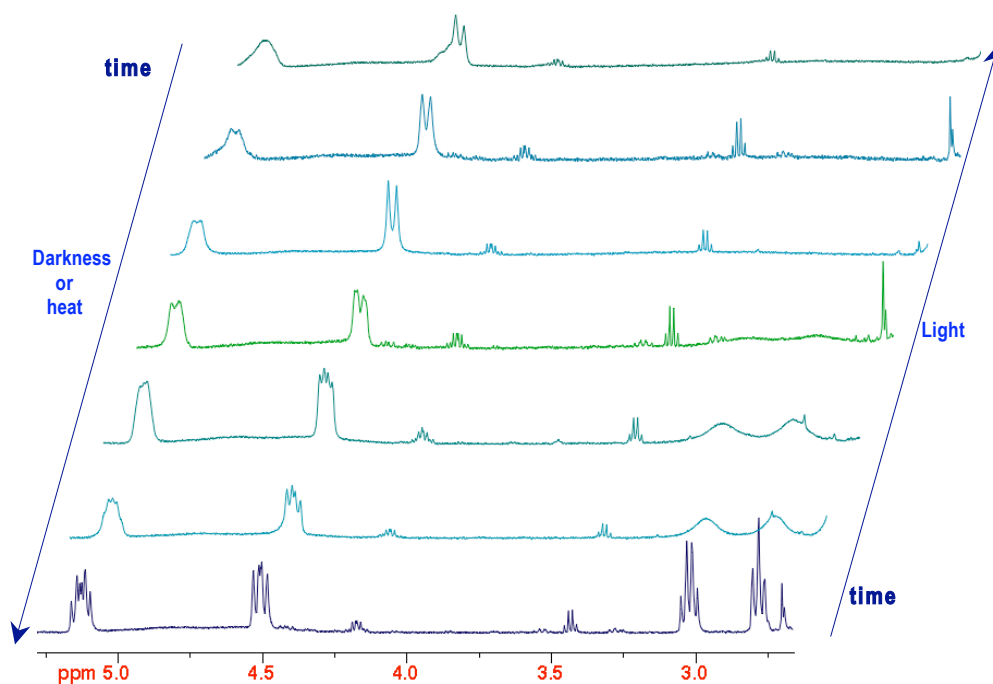
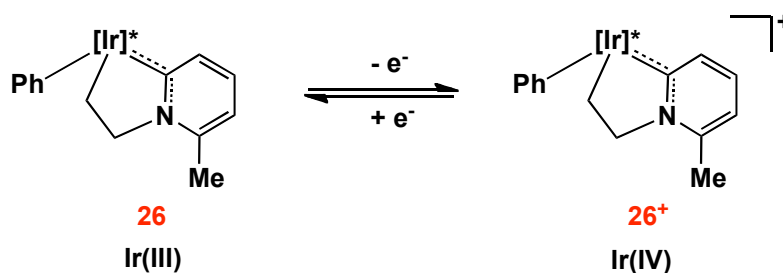


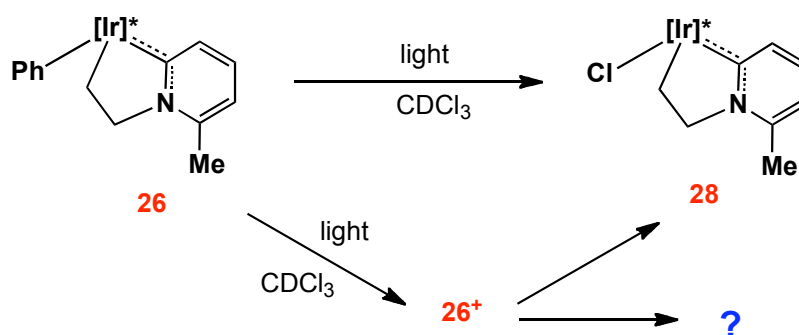
Figure II – 41. Stacked spectra of complex **26** under different conditions (500 MHz, CDCl₃).

These observations can be tentatively explained by the generation of very small amounts of a paramagnetic cationic 17 e⁻ Ir(IV) complex, with the same structure of complex **26**. The resulting Ir(III)/Ir(IV) couple will be in fast exchange on the NMR time scale at 25 °C⁵⁸ and the nuclei “apparently” more affected by this process will be those nearest to the Ir centre, where the electron density of the unpaired electron is expected to be highest.

⁵⁸ A. Wu, J. Mayer, *J. Am. Chem. Soc.* **2008**, 130, 14745.

**Equation 32**

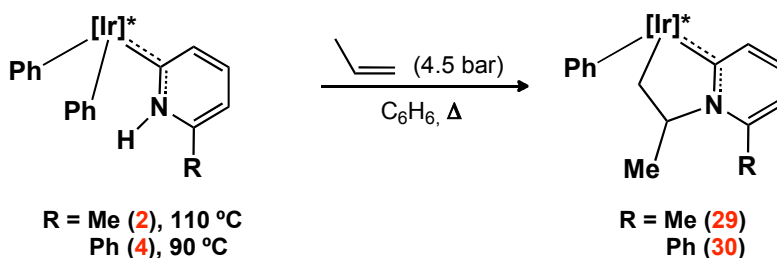
The oxidant involved may be a chloride radical generated from CDCl_3 or CD_2Cl_2 , under the influence of light.^{39,59} The presumed cationic Ir(IV) needs to slowly decay in the absence of light in order to explain the experimental observations. It is not known however, if **26⁺** is an active intermediate (or initiator) in the formation of chloride **28** (probably a radical reaction), or if it decays by a different pathway(s) (Scheme II-17). Further studies are clearly needed to clarify these points.

Scheme II – 17

II.2.1.3. Reaction with Propene

To gain further insight into the reactivity towards olefins, studies with propene and tert-butylethylene were undertaken. Compounds **2** and **4** react similarly with propene, to generate **29** and **30**, respectively. Probably for steric or electronic reasons, C–N bond formation is regioselective and occurs at the substituted olefin carbon atom, giving a

thermodynamic mixture of two diastereoisomers, **a** and **b** (3:1 and 1:5 ratio for **29** and **30** respectively). As expected, the formation of **29** is slower than that of **30** and its synthesis is better performed at 110 °C.



Equation 33

In the case of **29**, purification of the crude product by chromatography allowed the clean separation of both **29a** and **29b**, and these species have been fully characterized as the isomers shown in Fig. II – 42 by NMR spectroscopy. In the ^1H NMR spectrum, the $\text{CH}(\text{Me})$ proton of **29a** can be found at 5.90 ppm, whereas the diastereotopic nuclei of the $\text{Ir}-\text{CH}_2$ group resonate at 3.71 and 3.01 ppm. In the $^{13}\text{C}\{^1\text{H}\}$ NMR spectrum, the corresponding carbons are responsible for signals at -2.0 ($\text{Ir}-\text{CH}_2$) and 71.0 ($\text{CH}(\text{Me})$), whereas the $\text{Ir}-\text{C}_{\text{carbene}}$ resonates at 191.0 ppm. 2D NOESY experiment allowed to perform the correct assignment of the stereochemistry of **29a** and **29b**, since **29b** shows a strong signal between the Me group of the propene linkage and a Me from the Tp^{Me_2} ligands (see Experimental Part).

⁵⁹ **a)** M. Abadie, *Rad. Phys. Chem.* **1982**, *19*, 68. **b)** A. L. Le, P. E. Hoggard, *Photochem. Photobiol.* **2008**, *84*, 86.

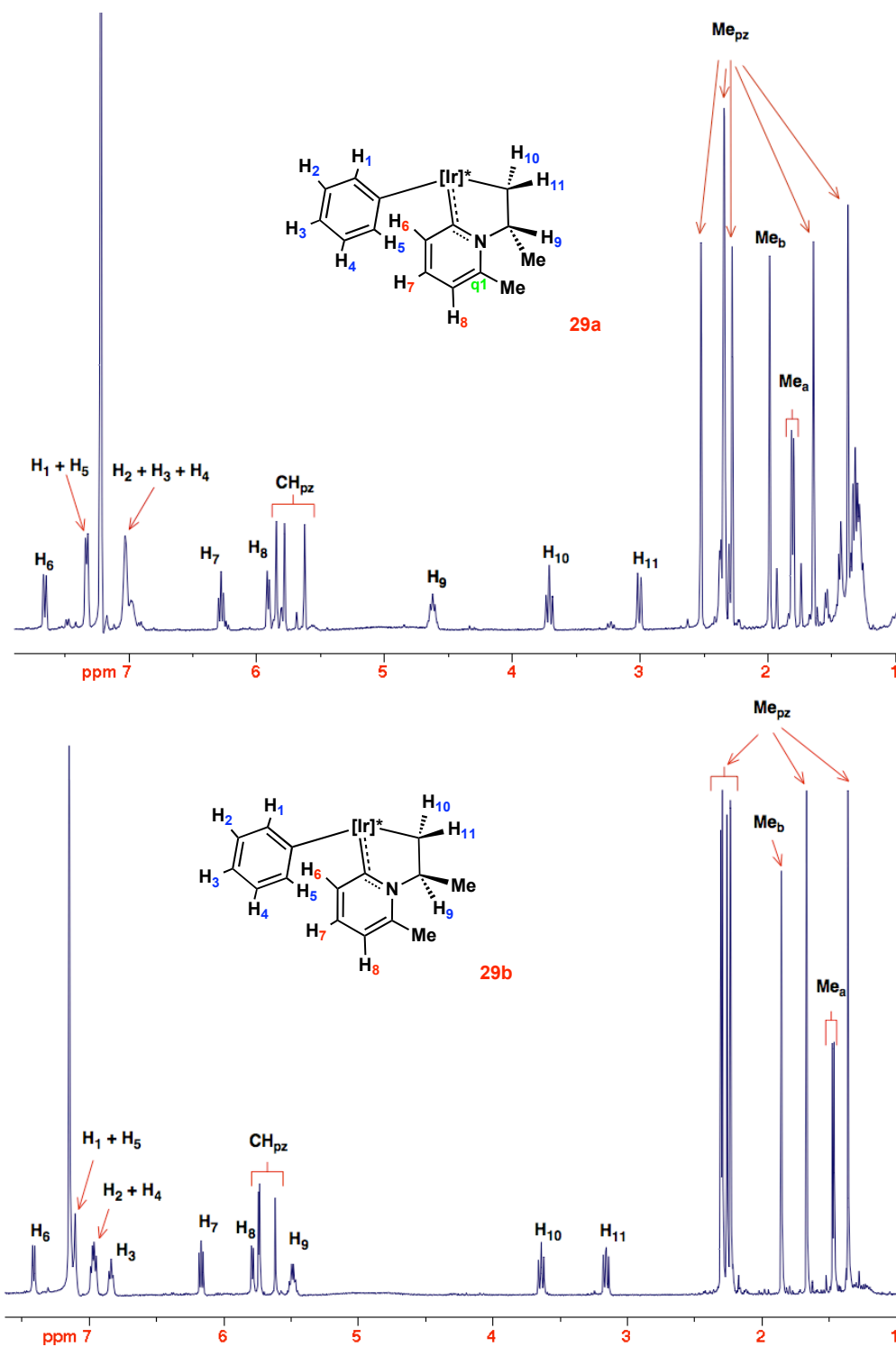


Figure II - 42. ^1H NMR spectra of **29a** (top) and **29b** (bottom) (C_6D_6 , 500 MHz).

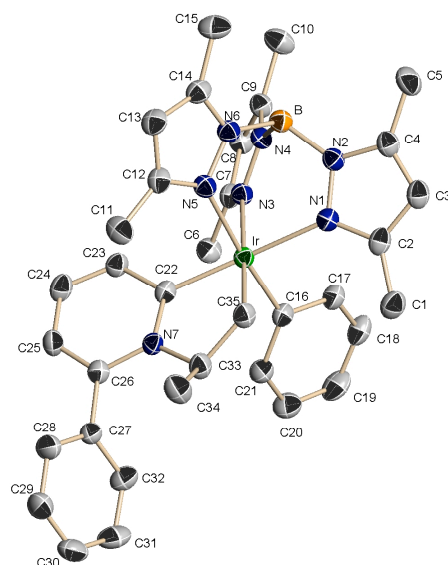


Figure II - 43. ORTEP representation of complex **30**.

In the case of **30** purification of the crude product by chromatography did not allow in our hands the separation of the two diastereoisomers. Both species, **30a** and **30b**, could be characterized by NMR spectroscopy in their mixtures. The major diastereomer **30b** presents diagnostic ^1H NMR resonances at 3.04 and 2.75 ppm (both multiplets, Ir-CH₂) and $^{13}\text{C}\{^1\text{H}\}$ NMR signals at 2.7 (Ir-CH₂) and 194.2 ppm (Ir-C_{carbene}).

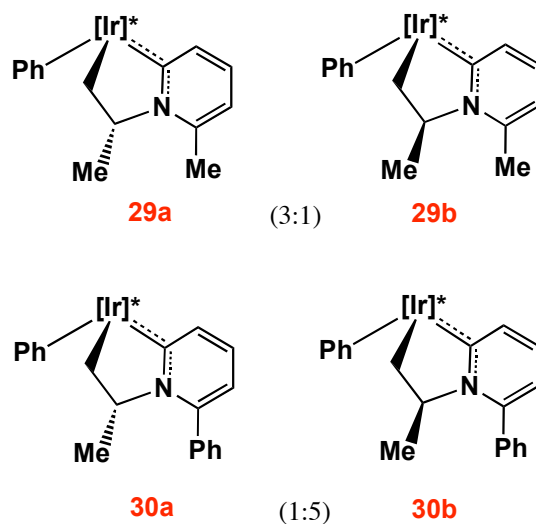
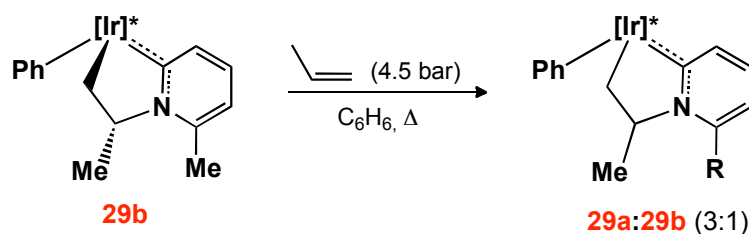


Figure II – 44. Representation of the diastereoisomers of complexes **29** and **30**.

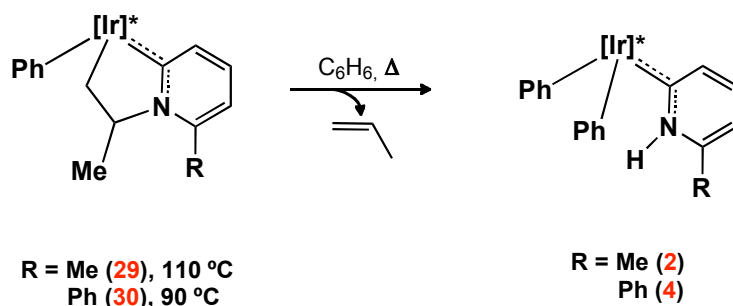
Complex **30** has also been characterized by single crystal X-ray diffraction analysis (Appendix 1-Table A27). Only the diastereoisomer shown in Fig. II – 43 was observed in the selected crystal (the one having the Me group of the NCH(Me)CH₂Ir chain pointing towards the Tp^{Me2} ligand, i.e. **30b**). It exhibits an Ir–C carbene bond of 1.95 Å, very similar to that found for **27**. The N7–C33 bond has a normal length of 1.51 Å, whereas the two originally olefinic carbon atoms, C33 and C34, form in **30b** a single C–C bond of normal length (1.53 Å).



Equation 34

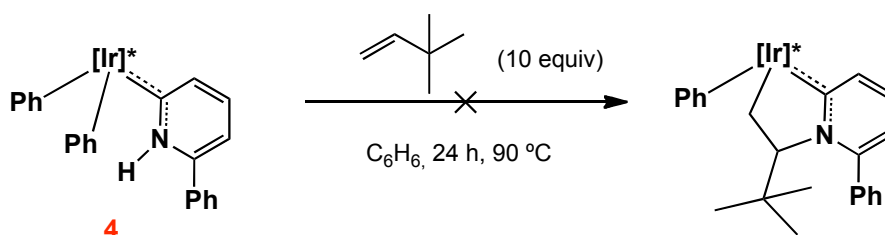
As already mentioned, the ratio of the **a** and **b** diastereoisomers is under thermodynamic control. For the case of **29** this is easily demonstrated by heating an isolated sample of **29b** under propene, in C₆H₆ at 110 °C (Eq. 34), to generate a mixture of **29a** and **29b** in a 3:1 ratio. This observation also outlines that, by contrast with the C₂H₄ case, propene incorporation is reversible and, in fact, heating solutions of **29** or **30** in C₆H₆, under an atmosphere of dinitrogen, eliminates the olefin and regenerate cleanly complexes **2** or **4** (Eq. 35). This distinct behaviour is probably a reflection of the weaker N–C(Me)H bond of **29/30**, in comparison with the N–CH₂ bond in **26/27**.⁶⁰

⁶⁰ For comparative purposes bond dissociation energies for the C–N bonds in CH₃NH₂, CH₃CH₂NH₂ and C₆H₅CH₂NH₂ are respectively *ca.* 85, 82 and 71 kcal·mol^{–1}. See D. F. McMillen, D. M. Golden, *Ann. Rev. Phys. Chem.* **1982**, 33, 493.



Equation 35

In agreement with this stability trend it has been found that the bulkier olefin *tert*-butylethylene does not react with **4** at 90 °C for 24 hours (Eq. 36), not even by using the substrate itself as the solvent.

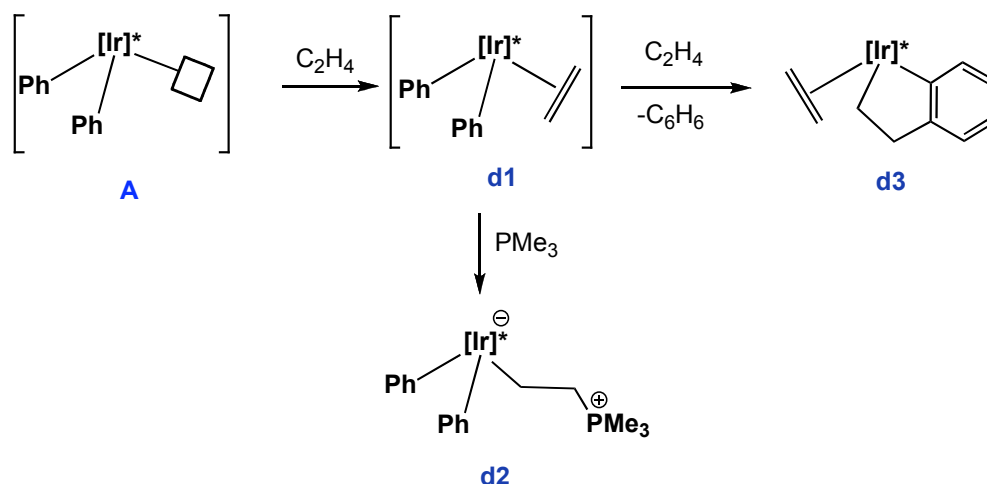


Equation 36

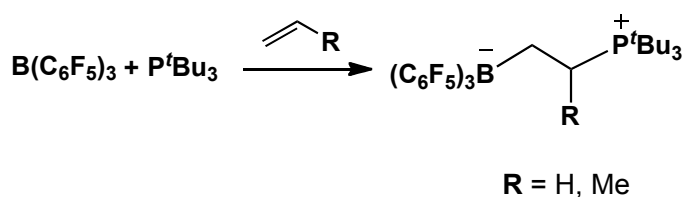
It is interesting to compare the reactivity of intermediates **B** ($[\text{Ir}]^*/\text{phenyl/pyridyl}$ ligand) and **A** ($[\text{Ir}]^*\text{Ph}_2$) against C_2H_4 . For **A**, generated from the N_2 adduct **1** at 60 °C, an unobserved C_2H_4 complex **d1** is proposed to form in the first place (it can be trapped by PMe_3) but the reaction product is **d3**, *i.e.* the result of the insertion of C_2H_4 into a Ir-Ph bond and subsequent cyclometallation⁶ (Scheme II – 18). Therefore it can be concluded that for the intermediate **B**, C–N bond formation is a preferred outcome over insertion into the Ir-Ph ,⁶ or the Ir-pyridyl ⁶¹ bonds.

⁶¹ a) R. F. Jordan, D. Taylor, *J. Am. Chem. Soc.* **1989**, *111*, 778. b) R. Jordan, D. Taylor, N. Baenziger, *Organometallics* **1990**, *9*, 1546. c) A. Guram, R. F. Jordan, *Organometallics* **1991**, *10*, 3470.

Scheme II – 18



The reactivity found for intermediates **B** with alkenes bears a close relationship to very recent work, developed by Stephan and Erker's groups, on the reactivity of the so called frustrated Lewis pairs (FLP).⁶² These FLP systems stem from Lewis acids and Lewis bases that are sterically precluded from adduct formation, as a consequence of F-strain. This unquenched Lewis acidity (electrophilic centre) and Lewis basicity (lone pair) was exploited for the activation of small molecules, among others ethylene and propene. Interestingly, for the case of propene, regioselectivity is also observed and the outcome (Eq. 37) is the same to those observed for **29** and **30**.⁶³ Thus, intermediate **B** can be viewed also as unsaturated species featuring an internal FLP.



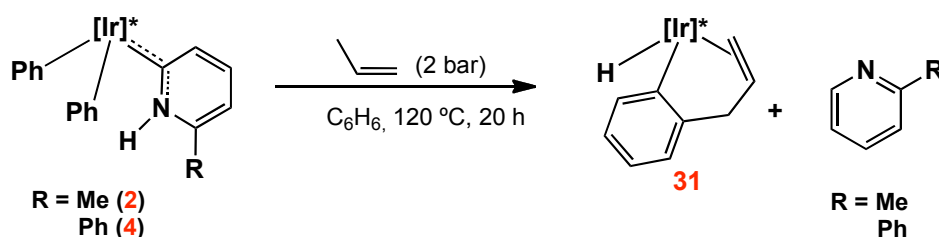
Equation 37

⁶² a) S. Geier, A. Gille, T. Gilbert, D. Stephan, *Inorg. Chem.* **2009**, 48, 10466. b) D. Stephan, *Org. Biomol. Chem.* **2008**, 6, 1535. c) D. W. Stephan, G. Erker, *Angew. Chem. Int. Ed.* **2010**, 49, 46.

⁶³ J. S. J. McCahill, G. C. Welch, D. W. Stephan, *Angew. Chem. Int. Ed.* **2007**, 46, 4968.

II.2.1.4. Selective C-H Bond Activation and C-C Bond Formation: Activation of the Methyl Group of Propene

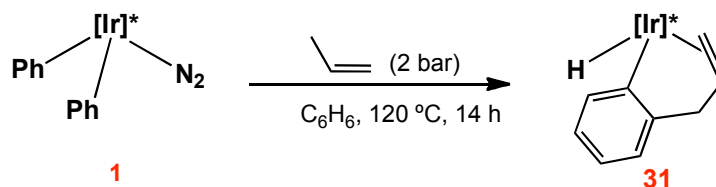
We have already described that **2** and **4** react with propene to give iridacycles **29** and **30**. However, if the reaction is carried out at higher temperatures, or for prolonged periods of time, the corresponding pyridine is extruded and a new hydride species, **31**, is formed. Only one stereoisomer is observed and features the configuration shown in Eq. 38. As can be observed, the Me group of propene has undergone C-H activation with subsequent formation of a C_{ar}-CH₂ bond. A molecule of C₆H₆ needs to be formed to satisfy the stoichiometry.



Equation 38

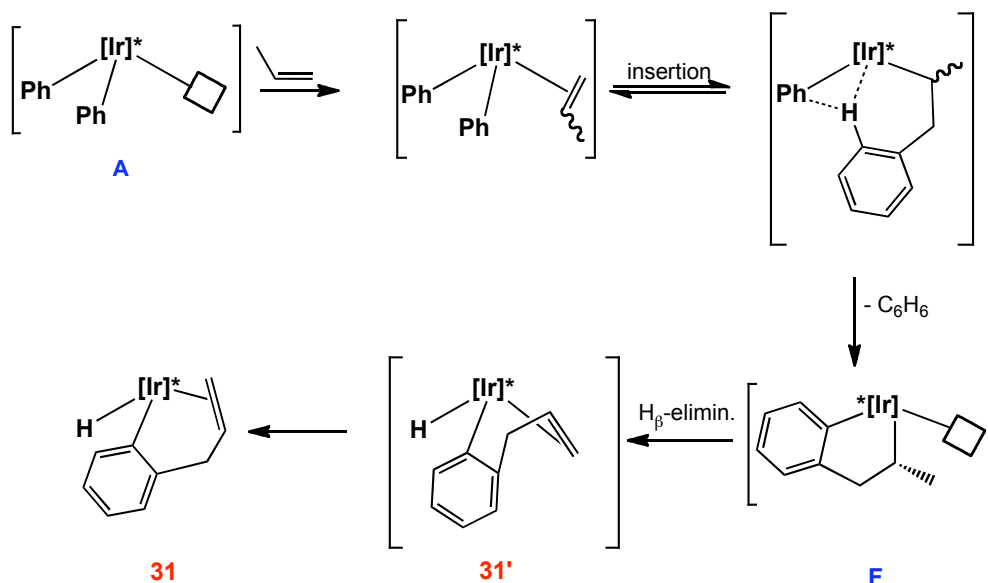
Complex **31** shows in the ¹H NMR spectrum multiplets at 2.71, 3.23 and 5.37 ppm assigned to the olefinic moiety; the benzylic protons resonate at 3.62 and 3.73 ppm, while the hydride ligand is responsible for the resonance found at -16.67 ppm. ¹³C{¹H} NMR signals are found at 69.5 (CH₂CH=CH₂), 41.7 (CH₂CH=CH₂) and 40.3 (CH₂CH=CH₂) ppm, whereas the Ir-C_{ph} carbon nucleus resonates at 136.9 ppm.

Considering the structure of **31** it was reasoned that this complex may also be obtained from complex **1**. In fact, **31** is generated from **1** and propene, as the only reaction product (120 °C, Eq 39).



Equation 39

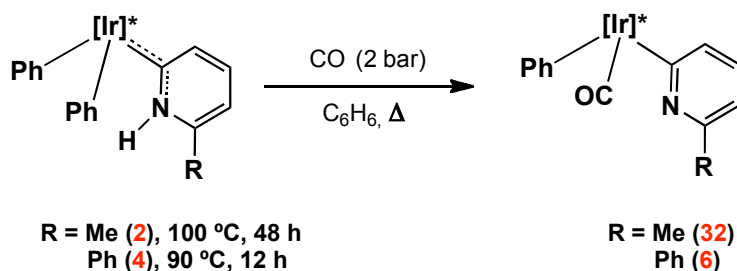
Scheme II – 19



Taking into account the already described reaction of **1** with ethylene, a plausible mechanism for this transformation is shown in Scheme II – 19. Propene can insert regioselectively into one of the Ir–C_{Ph} bonds to give a Ir–CH(Me)CH₂Ph ligand that experiences cyclometallation^{8b} to give intermediate **F**. This species then undergoes β -H elimination to give **31'**, the diastereoisomer of **31**, which then transforms into the more stable, observed compound, by a change of the face of the coordinated, prochiral olefin.

II.2.2. Reactivity of Carbenes **2** and **4** Towards CO

In light of the reactivity described so far for complexes **2** and **4** it was not surprising to find that they react also with carbon monoxide with formation of the corresponding carbonyl derivatives **32** and **6** (Eq. 40). The spectroscopic data obtained for **32** (Experimental Section) are very similar to those discussed for **6** and need no further comments.



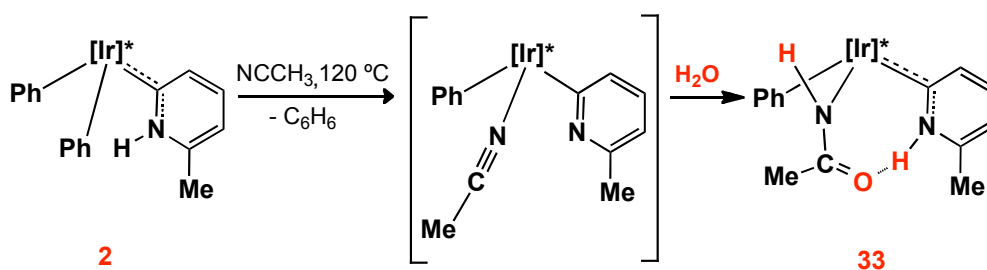
Equation 40

It is important to remark that **32** and **6** have been unambiguously characterized as Ir(III)-carbonyls, i.e. the CO ligand is not sufficiently electrophilic to be attacked by the N atom of the pyridyl with formation of a β -lactam ring.

II.2.3. Reactivity of Carbene **2** towards NCCH_3

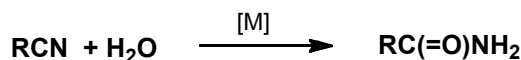
Previous studies carried out in our group have shown that acetonitrile is a very effective trapping reagent of $16\text{ e}^- \text{Tp}^{\text{Me}_2}\text{Ir}(\text{R}_1)(\text{R}_2)$ unsaturated species, although at variance with CO, its coordination is reversible in most cases. Interestingly, when complex **2** is heated with NCCH_3 at $120\text{ }^\circ\text{C}$, instead of the expected adduct, the formation of a new complex **33**, formulated as containing an acetamide-derived ligand, is observed. Obviously this is the result of the addition of adventitious water to coordinated NCCH_3 (Scheme II – 20).

Scheme II – 20



The ^1H NMR spectrum of complex **33** shows two singlets at 18.0 ppm and 4.5 ppm, assigned respectively to the NH groups of the carbene and acetamide moieties respectively, while in the $^{13}\text{C}\{^1\text{H}\}$ NMR spectrum the carbonyl group resonates at 177.4 ppm and the Ir–C_{carbene} at 169.9 ppm. The chemical shift of the NH group (18.03 ppm) of the carbene moiety indicates the existence of a hydrogen bonding with the oxygen of the acetyl group. The NOESY spectrum is in accord with a cisoid disposition of the NH and CMe groups of the acetamide ligand.

At this point it should be mentioned that addition of water to a NCCH_3 ligand in $\text{Tp}^{\text{Me}_2}\text{Ir(III)}$ complexes has not been observed previously, although it is a rather common feature of other transition metal systems.⁶⁴ In fact, some of them can be used as catalysts in the hydration of nitriles (Eq. 41), and therefore observation of -NHC(O)R complexes provides mechanistic insights on the mechanism of metal-mediated or metal-catalyzed conversion of organonitriles into carboxamides. In our case no free acetamide is generated under the reaction conditions and therefore the process is only stoichiometric.



Equation 41

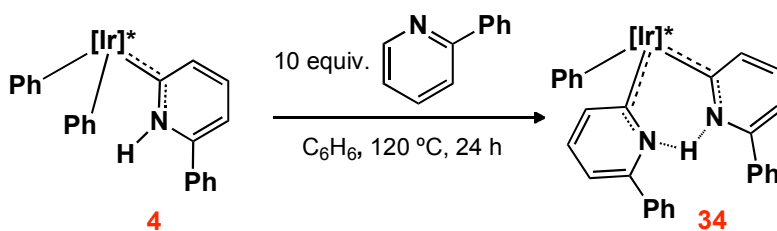
Finally it must be pointed out that in the formation of **33**, the pyridyl ligand in the presumed NCMe adduct intermediate, plays a definite role in the observed hydration as the hydrogen bond present in **33** is clearly stabilizing the structure.

II.2.4. Reactivity of **4** towards 2-Phenylpyridine

Intermediate **B** is also responsible for the generation of complex **34**, formed when compound **4** is allowed to react with an excess of 2-phenylpyridine in C_6H_6 at 120 °C

⁶⁴ a) C. Leung, W. Zheng, Z. Zhou, Z. Lin, C. Lau, *Organometallics* **2008**, 27, 4957. b) E. S. Kim, H. S. Kim, J. N. Kim, *Tetrahedron Lett.* **2009**, 50, 2973. c) W. Zheng, C. W. Leung, Z. Zhou, C. P. Lau, Z. Lin, *J. Theor. Comput. Chem.* **2009**, 8, 417. d) R. S. Ramón, N. Marion, S. P. Nolan, *Chem. Eur. J.* **2009**, 15, 8695. e) M. G. Crestani, A. Steffen, A. M. Kenwright, A. S. Batsanov, J. A. K. Howard, T. B. Marder, *Organometallics* **2009**, 28, 2904.

(Eq. 42). This pyridyl-carbene compound results from the C–H activation of the C–H₆ bond of 2-phenylpyridine, with concomitant elimination of a benzene molecule.



Complex **34** has an effective plane of symmetry, as shown by its ^1H and $^{13}\text{C}\{^1\text{H}\}$ NMR spectra, and this is due to the presence of a N–H \cdots N bridging hydrogen bond. This proton appears in the ^1H NMR spectrum at 17.4 ppm, *i.e.* 4 ppm downfield with respect to the parent compound **4**. Additionally, in the $^{13}\text{C}\{^1\text{H}\}$ NMR spectrum, the Ir–C_{carbene} nuclei resonate at 172.3 ppm.

With the data on hand it is not possible to distinguish between the two situations that are commonly discussed when dealing with these kind of structures. Thus the ground state could be (a) a symmetric N \cdots H \cdots N bridge or (b) a degenerate N–H \cdots N double minima⁶⁵ separated by a small energy barrier:

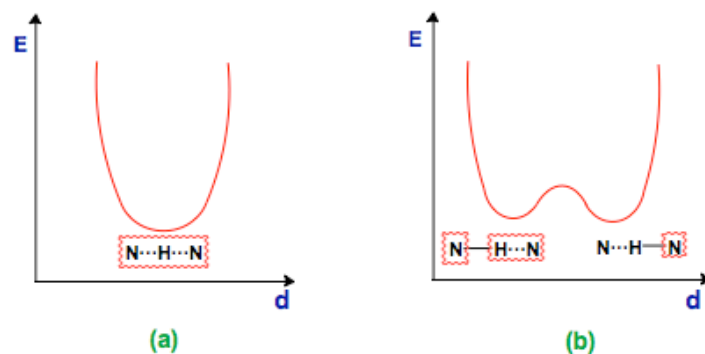
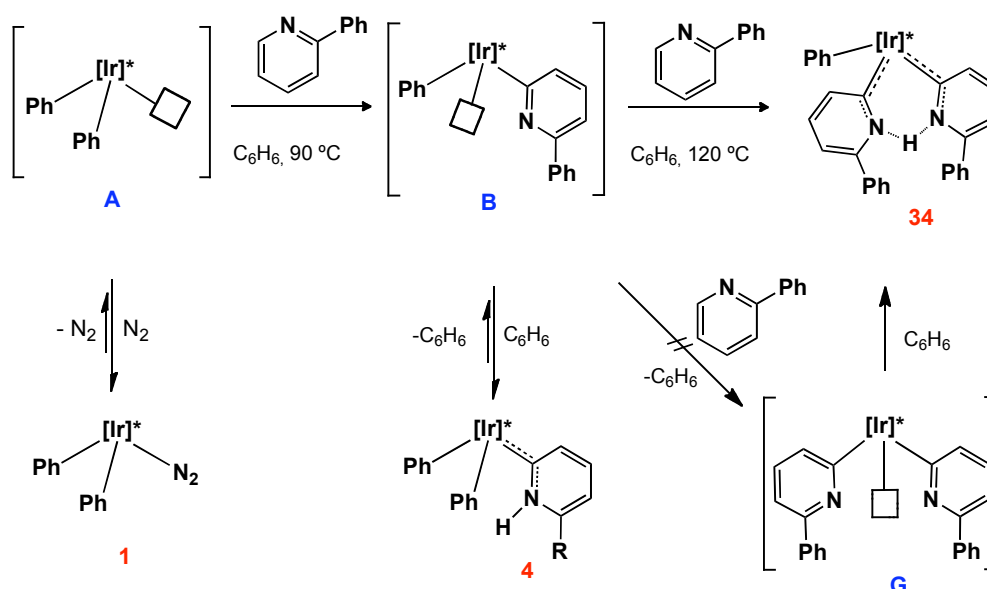


Figure II – 45. Representation of the possible ground states for N \cdots H \cdots N hydrogen bonds.

⁶⁵ C. L. Perrin, *Science* **1994**, 266, 1665.

With respect to the formation of **34** from **4**, the proposed mechanism is shown in Scheme II – 21, which include also the steps needed when the reaction starts with complex **1**. It is proposed that the incorporation of the second molecule of the pyridine takes place by activation of its C₆–H bond by intermediate **B**, a phenyl pyridyl species and concomitant H transfer from C₆ of the incoming pyridine molecule to the N atom of **B**. Complex **34** is however represented in Scheme II – 21 in the form of the symmetric structure.

Scheme II – 21



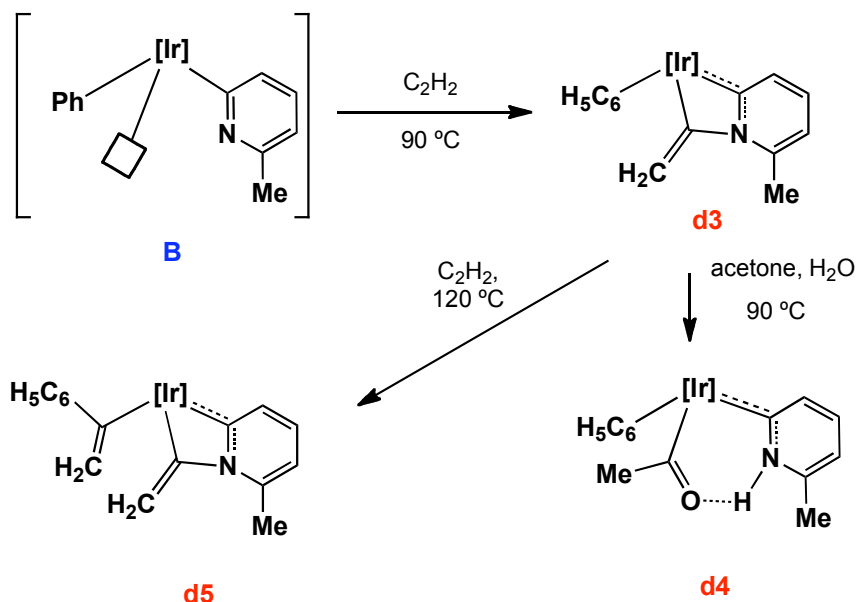
II.2.5. Reactivity of **4** towards Alkynes

II.2.5.1. Reactivity of **4** towards Acetylene

In a parallel study carried out in our laboratory on the reaction of complex **2** with acetylene, it has been shown that two HC≡CH molecules can be sequentially incorporated to give the unusual four-membered metallacycles **d3** and **d5** (Scheme II – 22). Complexes **d3** and **d5** appear to be formed by nucleophilic attack of the N atom of a pyridyl ligand onto the carbene carbon of an Ir=C=CH₂ moiety that results from the

rearrangement of the alkyne ligand.⁶⁶ Theoretical studies (Dr. Joaquín Lopez, this laboratory) show that this rearrangement is facilitated by the pyridyl ligand that acts as a shuttle for the proton transfer reaction (Scheme II – 23). In the presence of water, compound **d4**, the result of the hydration of the vinylidene ligand, is also observed.

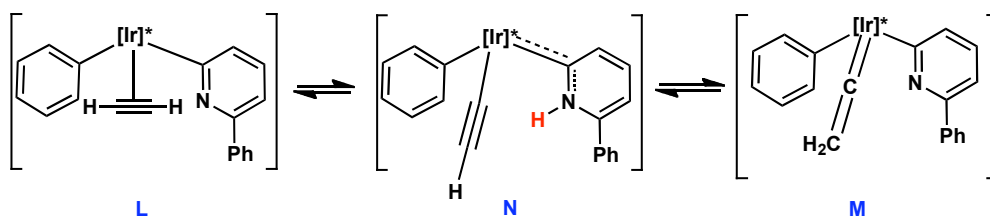
Scheme II - 22



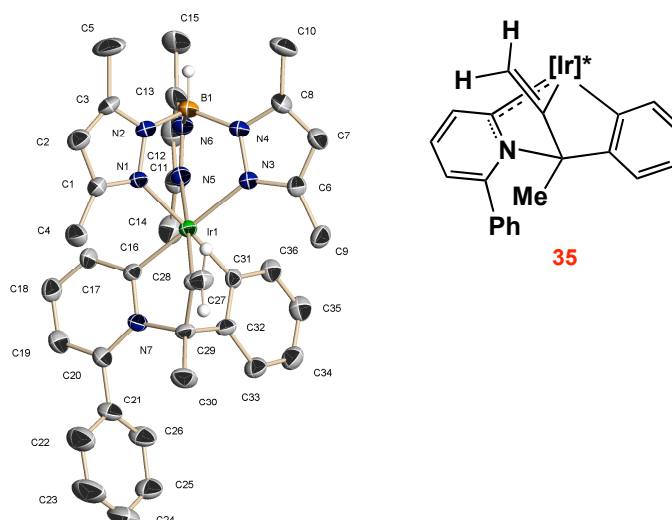
It seems surprising that the alkyne ligands in the proposed intermediates are not able to form five-membered ring species akin to the C_2H_4 -derived complexes **26** and **27**. In fact, theoretical studies (Dr. Joaquín López, this laboratory) predict that these species should be thermodynamically more stable than the observed iridacycles, but they also show that kinetic reasons may be responsible for the observed reaction outcome.

⁶⁶ a) D. Grotjahn, D. Lev, *J. Am. Chem. Soc.* **2004**, *126*, 12232. b) D. Grotjahn, J. Hoerter, J. Hubbard, *J. Am. Chem. Soc.* **2004**, *126*, 8866. c) D. Grotjahn, X. Zeng, A. Cooksy, *J. Am. Chem. Soc.* **2006**, *128*, 2798. d) D. Grotjahn, Y. Gong, A. DiPasquale, *Organometallics* **2006**, *25*, 5693. e) D. Grotjahn, V. Miranda-Soto, E. Kragulj, D. Lev, G. Erdogan, X. Zeng, A. Cooksy, *J. Am. Chem. Soc.* **2008**, *130*, 20. f) D. Grotjahn, E. Kragulj, C. Zeinalipour-Yazdi, V. Miranda-Soto, D. Lev, A. Cooksy, *J. Am. Chem. Soc.* **2008**, *130*, 10860. g) V. Miranda-Soto, D. Grotjahn, A. DiPasquale, A. Rheingold, *J. Am. Chem. Soc.* **2008**, *130*, 13200.

Scheme II - 23

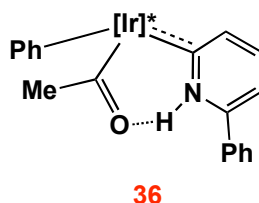


When a similar reaction is carried out with complex **4**, ^1H NMR monitoring reveals that a much more complicated reaction, as a mixture of at least four species, none of them predominant, is formed even under the mildest conditions needed for the rearrangement to proceed. A complex related to **d5** was easily detected in this mixture due to the appearance of the characteristic signals of the $=\text{CH}_2$ moiety. However, upon chromatography in silica gel, only complexes **35** and **36** could be isolated in a pure state. The unusual complex **35** was characterized by single crystal X-ray studies as having the metalla-bicyclic structure shown below.

Figure II - 46. ORTEP representation of complex **35**.

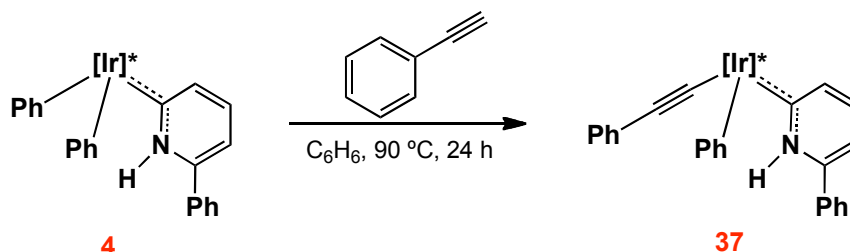
Once the structure of this molecule become known to us thanks to the X-ray study (Fig. II – 46, see also Appendix 1- Table A29), its NMR spectra could be completely analyzed. The ^1H NMR spectrum shows two singlets at 5.22 and 3.82 ppm respectively, due to the $\text{Ir}-\text{C}(=\text{CH}_2)$ group, whereas in the $^{13}\text{C}\{^1\text{H}\}$ NMR spectrum the $\text{Ir}-\text{C}_{\text{carbene}}$ resonates at 190.7 ppm, a value close to those found for both **27** and **30**. At present we are not able to give a rational, experimentally supported explanation for the formation of **35**. As implied by its molecular structure, C–C coupling between two molecules of acetylene is needed along with the formation of a C–C bond with one of the original phenyl groups, and of a C–N bond with the pyridine derived ligand.

On the contrary, complex **36** is analogous to **d4** in Scheme II – 22. Formulation of **36** as an acetyl-pyridylidene, rather than an hydroxycarbene-pyridyl tautomer, is supported by $^{13}\text{C}\{^1\text{H}\}$ NMR data, since the acetyl carbonyl resonance is recorded at 240 ppm and the carbene at 175 ppm, the latter chemical shift being very close to the carbene resonance of parent complex **4**. As for the ^1H NMR spectrum, a singlet at 16.38 ppm due to the NH group was found, which is shifted downfield by about 3 ppm with respect to **4**, as a consequence of hydrogen bonding. An IR absorption at *ca.* 1595 cm^{-1} can also be taken as diagnostic for the acetyl moiety of **36**, whereas the NH group is responsible for an absorption at *ca.* 3190 cm^{-1} . The latter value is lower in frequency than that found for **4**, in agreement with the proposed N–H \cdots O bonding.



II.2.5.2. Reactivity of **4** towards Phenylacetylene

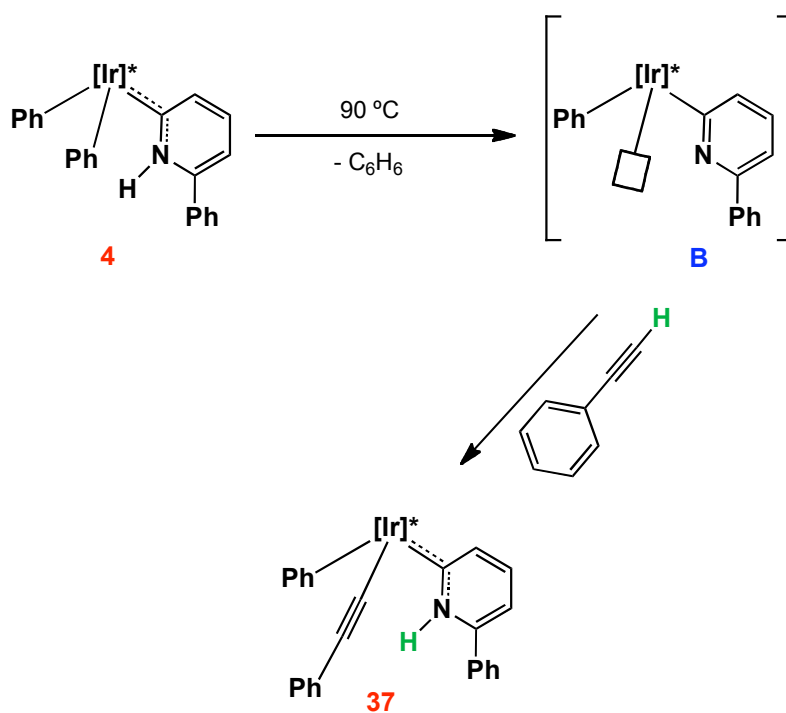
Carbene **4** reacts with this terminal acetylene, in C_6H_6 at $90\text{ }^\circ\text{C}$, to yield cleanly complex **37** (Eq. 43). As can be observed, a $PhC\equiv C-$ group has replaced a phenyl ligand in the coordination sphere of the Ir centre, *i.e.* the alkyne has acted formally as a Brönsted acid to extrude a molecule of C_6H_6 .



Equation 43

In agreement with the proposed structure, complex **37** shows in the 1H NMR spectrum a broad singlet at 13.8 ppm, corresponding to the NH functionality, whereas in the $^{13}C\{^1H\}$ NMR spectrum, the carbene resonates at 175.3 ppm and the acetylide moiety gives rise to two signals at 100.7 (Ir– $C\equiv C$) and 95.6 ppm (Ir– $C\equiv C$). With respect to the mechanism of its formation, we believe that phenylacetylene reacts with intermediate **B** to give an Ir– $C\equiv C$ –Ph species as in the case of acetylene (see Scheme II – 24), with the relatively acidic $\equiv C$ –H proton being transferred to the basic nitrogen of the pyridyl group.

Scheme II - 24



Why this system does not afford a $\text{Ir}=\text{C}=\text{CH}(\text{Ph})$ group as in the case of $\text{HC}\equiv\text{CH}$ is presently not known, but it can be said that this transformation is also common with other transition metal complexes.⁶⁷

⁶⁷ Y. Wakatsuki, N. Koga, H. Werner, K. Morokuma, *J. Am. Chem. Soc.* **1997**, *119*, 360.

II.3. Bibliography

1. T. Meyer, *Pure Appl. Chem.* **1986**, *58*, 1193.
2. **a)** C. Kütal, A. Corbin, G. Ferraudi, *Organometallics* **1987**, *6*, 553. **b)** J. Van Diemen, R. Hage, J. Haasnoot, H. Lempers, J. Reedijk, J. Vos, L. De Cola, F. Barigelletti, V. Balzani, *Inorg. Chem.* **1992**, *31*, 3518. **c)** F. Johnson, M. George, F. Hartl, J. Turner, *Organometallics* **1996**, *15*, 3374. **d)** Y. Hayashi, S. Kita, B. Brunschwig, E. Fujita, *J. Am. Chem. Soc.* **2003**, *125*, 11976.
3. **a)** E. Holder, B. Langeveld, U. Schubert, *Adv. Mat.* **2005**, *17*, 1109. **b)** H. Yersin, *Highly efficient OLEDs with phosphorescent materials*, Wiley-VCH, Weinheim, **2007**.
4. **a)** N. McDaniel, F. Coughlin, L. Tinker, S. Bernhard, *J. Am. Chem. Soc.* **2008**, *130*, 210. **b)** J. Hull, D. Balcells, J. Blakemore, C. Incarvito, O. Eisenstein, G. Brudvig, R. H. Crabtree, *J. Am. Chem. Soc.* **2009**, *131*, 8730.
5. **a)** S. Lamansky, P. Djurovich, D. Murphy, F. Abdel-Razzaq, H. E. Lee, C. Adachi, P. E. Burrows, S. R. Forrest, M. E. Thompson, *J. Am. Chem. Soc.* **2001**, *123*, 4304. **b)** K. Lo, D. Ng, C. Chung, *Organometallics* **2001**, *20*, 4999. **c)** A. B. Tamayo, B. D. Alleyne, P. I. Djurovich, S. Lamansky, I. Tsyba, N. N. Ho, R. Bau, M. E. Thompson, *J. Am. Chem. Soc.* **2003**, *125*, 7377. **d)** J. D. Slinker, A. A. Gorodetsky, M. S. Lowry, J. Wang, S. Parker, R. Rohl, S. Bernhard, G. G. Malliaras, *J. Am. Chem. Soc.* **2004**, *126*, 2763. **e)** K. Lo, J. Chan, L. Lui, C. Chung, *Organometallics* **2004**, *23*, 3108. **f)** T. Sajoto, P. Djurovich, A. Tamayo, M. Yousufuddin, R. Bau, M. Thompson, R. Holmes, S. Forrest, *Inorg. Chem.* **2005**, *44*, 7992. **g)** M. Lowry, S. Bernhard, *Chem. Eur. J.* **2006**, *12*, 7971. **h)** T. Sajoto, P. Djurovich, A. Tamayo, J. Oxgaard, W. Goddard, M. Thompson, *J. Am. Chem. Soc.* **2009**, *131*, 9813.
6. E. Gutiérrez-Puebla, A. Monge, M. C. Nicasio, P. J. Pérez, M. L. Poveda, E. Carmona, *Chem. Eur. J.* **1998**, *4*, 2225.
7. E. Gutiérrez-Puebla, A. Monge, M. Paneque, M. L. Poveda, V. Salazar, E. Carmona, *J. Am. Chem. Soc.* **1999**, *121*, 248.

8. a) L. Santos, K. Mereiter, M. Paneque, C. Slugovc, E. Carmona, *New J. Chem.* **2003**, 27, 107. b) M. Paneque, M. L. Poveda, L. L. Santos, E. Carmona, A. Lledós, G. Ujaque, K. Mereiter, *Angew. Chem. Int. Ed.* **2004**, 43, 3708. c) P. Lara, M. Paneque, M. L. Poveda, V. Salazar, L. L. Santos, E. Carmona, *J. Am. Chem. Soc.* **2006**, 128, 3512. d) E. Álvarez, M. Paneque, A. Petronilho, M. L. Poveda, L. L. Santos, E. Carmona, K. Mereiter, *Organometallics* **2007**, 26, 1231. e) P. Lara, M. Paneque, M. L. Poveda, L. L. Santos, J. E. V. Valpuesta, V. Salazar, E. Carmona, S. Moncho, G. Ujaque, A. Lledós, C. Maya, K. Mereiter, *Chem. Eur. J.* **2009**, 15, 9046. f) P. Lara, M. Paneque, M. L. Poveda, L. L. Santos, J. E. V. Valpuesta, E. Carmona, S. Moncho, G. Ujaque, A. Lledós, E. Álvarez, K. Mereiter, *Chem. Eur. J.* **2009**, 15, 9034. g) S. Conejero, M. Paneque, M. L. Poveda, L. L. Santos, E. Carmona, *Acc. Chem. Res.* **2010**, 43, 572.
9. M. Albrecht, *Chem. Rev.* **2009**, 110, 576.
10. a) S. Sprouse, K. King, P. Spellane, R. Watts, *J. Am. Chem. Soc.* **1984**, 106, 6647. b) K. King, P. Spellane, R. Watts, *J. Am. Chem. Soc.* **1985**, 107, 1431. c) K. King, R. Watts, *J. Am. Chem. Soc.* **1987**, 109, 1589. d) K. Garcés, K. King, R. Watts, *Inorg. Chem.* **1988**, 27, 3464. e) S. Lamansky, P. Djurovich, D. Murphy, F. Abdel-Razzaq, R. Kwong, I. Tsyba, M. Bortz, B. Mui, R. Bau, M. Thompson, *Inorg. Chem.* **2001**, 40, 1704.
11. a) L. Li, W. Brennessel, W. Jones, *Organometallics* **2009**, 28, 3492. b) L. S. Park-Gehrke, J. Freudenthal, W. Kaminsky, A. G. Dipasquale, J. M. Mayer, *Dalton Trans.* **2009**, 1972.
12. a) D. Bourissou, O. Guerret, F. Gabbai, G. Bertrand, *Chem. Rev.* **2000**, 100, 39. b) W. Herrmann, *Angew. Chem. Int. Ed.* **2002**, 41, 1290. c) E. Peris, R. H. Crabtree, *Coord. Chem. Rev.* **2004**, 248, 2239. d) O. Köhl, *Chem. Soc. Rev.* **2007**, 36, 592. e) F. Hahn, M. Jahnke, *Angew. Chem. Int. Ed.* **2008**, 47, 3122. f) P. de Fremont, N. Marion, S. P. Nolan, *Coord. Chem. Rev.* **2009**, 253, 862. g) O. Schuster, L. Yang, H. Raubenheimer, M. Albrecht, *Chem. Rev.* **2009**, 109, 3445.
13. E. Mas-Marzá, M. Poyatos, M. Sanaú, E. Peris, *Inorg. Chem.* **2004**, 43, 2213.

14. L. Appelhans, D. Zuccaccia, A. Kovacevic, A. Chianese, J. Miecznikowski, A. Macchioni, E. Clot, O. Eisenstein, R. Crabtree, *J. Am. Chem. Soc.* **2005**, *127*, 16299.
15. a) N. M. Scott, R. Dorta, E. D. Stevens, A. Correa, L. Cavallo, S. P. Nolan, *J. Am. Chem. Soc.* **2005**, *127*, 3516. b) S. Leuthäusser, D. Schwarz, H. Plenio, *Chem. Eur. J.* **2007**, *13*, 7195. c) Y. Chang, C. Fu, Y. Liu, S. Peng, J. Chen, S. Liu, *Dalton Trans.* **2009**, 861.
16. A. D. Bond, J. E. Davies, *Acta Crystallogr. Sect. E* **2001**, *57*, 1089.
17. D. Lavorato, J. Terlouw, G. McGibbon, T. Dargel, W. Koch, H. Schwarz, *Int. J. Mass Spectrom.* **1998**, *179*, 7.
18. B. Cordero, V. Gómez, A. E. Platero-Prats, M. Revés, J. Echeverría, E. Cremades, F. Barragán, S. Álvarez, *Dalton Trans.* **2008**, 2832.
19. a) H. C. Brown, H. Schlesinger, S. Cardon, *J. Am. Chem. Soc.* **1942**, *64*, 325. b) H. C. Brown, *Science* **1946**, *103*, 385. c) H. C. Brown, *J. Chem. Soc.* **1956**, 1248.
20. S. H. Wiedemann, J. C. Lewis, J. A. Ellman, R. Bergman, *J. Am. Chem. Soc.* **2006**, *128*, 2452.
21. a) X. L. Luo, G. K. Schulte, R. H. Crabtree, *Inorg. Chem.* **1990**, *29*, 682. b) L. Dadci, H. Elias, U. Frey, A. Hoernig, U. Koelle, A. Merbach, H. Paulus, J. Schneider, *Inorg. Chem.* **1995**, *34*, 306. c) L. C. Porter, S. Bodige, *J. Organomet. Chem.* **1995**, *487*, 1. d) H. Amouri, C. Guyard-Duhayon, *Inorg. Chem.* **2002**, *41*, 1397. e) M. Paneque, C. M. Posadas, M. L. Poveda, N. Rendón, E. Álvarez, K. Mereiter, *Chem. Eur. J.* **2007**, *13*, 5160.
22. a) O. Blum, D. Milstein, *J. Am. Chem. Soc.* **2002**, *124*, 11456. b) D. Milstein, J. C. Calabrese, I. D. Williams, *J. Am. Chem. Soc.* **1986**, 6387.
23. E. Álvarez, M. Gómez, M. Paneque, C. M. Posadas, M. L. Poveda, N. Rendón, L. L. Santos, S. Rojas-Lima, V. Salazar, K. Mereiter, *J. Am. Chem. Soc.* **2003**, *125*, 1478.
24. E. Clot, J. Chen, D. H. Lee, S. Y. Sung, L. N. Appelhans, J. W. Faller, R. H. Crabtree, O. Eisenstein, *J. Am. Chem. Soc.* **2004**, *126*, 8795.
25. R. Williams, *pKa Compilation* **2001**.

26. R. Cordone, H. Taube, *J. Am. Chem. Soc.* **1987**, *109*, 8101.
27. For similar reactivity of 2,6-lutidine see for instance: R. F. Jordan, A. Guram, *Organometallics* **1990**, *9*, 2116.
28. M. Gómez, M. Paneque, M. L. Poveda, E. Álvarez, *J. Am. Chem. Soc.* **2007**, *129*, 6092.
29. E. Álvarez, S. Conejero, P. Lara, J. A. López, M. Paneque, A. Petronilho, M. L. Poveda, D. del Rio, O. Serrano, E. Carmona, *J. Am. Chem. Soc.* **2007**, *129*, 14130.
30. R. N. Perutz, S. Sabo-Etienne, *Angew. Chem. Int. Ed.* **2007**, *46*, 2578.
31. a) J. C. Lewis, R. Bergman, J. A. Ellman, *J. Am. Chem. Soc.* **2007**, *129*, 5332. b) A. M. Berman, J. C. Lewis, R. Bergman, J. A. Ellman, *J. Am. Chem. Soc.* **2008**, *130*, 14926.
32. a) M. A. Esteruelas, F. Fernandez-Álvarez, E. Oñate, *J. Am. Chem. Soc.* **2006**, *128*, 13044. b) M. L. Buil, M. A. Esteruelas, K. Garcés, M. Oliván, E. Oñate, *J. Am. Chem. Soc.* **2007**, *129*, 10998. c) M. A. Esteruelas, F. Fernández-Álvarez, E. Oñate, *Organometallics* **2007**, *26*, 5239. d) M. A. Esteruelas, F. Fernández-Alvarez, E. Oñate, *Organometallics* **2008**, *27*, 6236. e) M. Buil, M. A. Esteruelas, K. Garcés, M. Oliván, E. Oñate, *Organometallics* **2008**, *27*, 4680. f) M. A. Esteruelas, F. Fernández-Alvarez, M. Oliván, E. Oñate, *Organometallics* **2009**, *28*, 2276.
33. G. Song, Y. Li, S. Chen, X. Li, *Chem. Commun.* **2008**, 3558.
34. S. K. Schneider, P. Roembke, G. R. Julius, C. Loschen, H. G. Raubenheimer, G. Frenking, W. A. Herrmann, *Eur. J. Inorg. Chem.* **2005**, 2973.
35. H. Raubenheimer, S. Cronje, *Dalton Trans.* **2008**, 1265.
36. G. Heydenrych, M. Von Hopffgarten, E. Stander, O. Schuster, H. G. Raubenheimer, G. Frenking, *Eur. J. Inorg. Chem.* **2009**, 1892.
37. D. Lavorato, J. Terlouw, T. Dargel, W. Koch, G. McGibbon, H. Schwarz, *J. Am. Chem. Soc.* **1996**, *118*, 11898.
38. M. Z. Kassae, F. A. Shakib, M. R. Momeni, M. Ghambarian, S. M. Musavi, *Tetrahedron* **2009**, *65*, 10093.
39. P. Hoggard, *Coord. Chem. Rev.* **1997**, *159*, 235.

- 40. a)** A. P. Smith, C. L. Fraser, *Comprehensive Coordination Chemistry II: from biology to nanotechnology, Vol. 1*, Pergamon, Oxford **2004**. **b)** E. C. Constable, *Adv. Inorg. Chem. Radiochem.* **1989**, 34, 1.
- 41. a)** T. M. Boller, J. M. Murphy, M. Hapke, T. Ishiyama, N. Miyaura, J. F. Hartwig, *J. Am. Chem. Soc.* **2005**, 127, 14263. **b)** I. A. I. Mkhaliid, D. N. Coventry, D. Albesa-Jove, A. S. Batsanov, J. A. K. Howard, R. N. Perutz, T. B. Marder, *Angew. Chem. Int. Ed.* **2006**, 45, 489. **c)** J. McFarland, M. Francis, *J. Am. Chem. Soc.* **2005**, 127, 13490.
- 42. a)** O. Maury, H. Le Bozec, *Acc. Chem. Res.* **2005**, 38, 691. **b)** S. C. Chan, M. C. W. Chan, Y. Wang, C. M. Che, K. Cheung, N. Zhu, *Chem. Eur. J.* **2001**, 7, 4180. **c)** F. Gao, A. Bard, *J. Am. Chem. Soc.* **2000**, 122, 7426. **d)** R. J. Watts, *Comments Inorg. Chem.* **1991**, 11, 303. **e)** M. Al-Anber, S. Vatsadze, R. Holze, H. Lang, W. Thiel, *Dalton Trans.* **2005**, 2005, 3632.
- 43. a)** C. Kaes, A. Katz, M. Hosseini, *Chem. Soc. Rev.* **2000**, 100, 3553. **b)** V. Balzani, G. Bergamini, F. Marchioni, P. Ceroni, *Coord. Chem. Rev.* **2006**, 250, 1254.
- 44. a)** J. Van Houten, R. Watts, *J. Am. Chem. Soc.* **1976**, 98, 4853. **b)** A. J. Brown, O. W. Howarth, P. Moore, W. J. E. Parr, *J. Chem. Soc., Dalton Trans.* **1978**, 1776. **c)** S. Dholakia, R. Gillard, F. Wimmer, *Inorg. Chim. Acta* **1983**, 69, 179. **d)** F. Pruchnik, F. Robert, Y. Jeannin, S. Jeannin, *Inorg. Chem.* **1996**, 35, 4261. **e)** A. A. Sidorov, G. G. Aleksandrov, E. V. Pakhmutova, A. Y. Chernyad'ev, I. L. Eremenko, I. I. Moiseev, *Russ. Chem. Bull.* **2005**, 54, 588.
- 45.** G. W. Bushnell, K. R. Dixon, M. A. Khan, *Can. J. Chem.* **1974**, 52, 1367.
- 46. a)** R. Watts, J. Harrington, J. Van Houten, *J. Am. Chem. Soc.* **1977**, 99, 2179. **b)** W. A. Wickramasinghe, P. H. Bird, N. Serpone, *J. Chem. Soc., Chem. Commun.* **1981**, 1284. **c)** G. Nord, A. Hazell, R. Hazell, *Inorg. Chem.* **1983**, 22, 3429. **d)** N. Serpone, G. Ponterini, M. A. Jamieson, F. Bolletta, M. Maestri, *Coord. Chem. Rev.* **1983**, 50, 209. **e)** A. Hazell, R. Hazell, *Acta Crystallogr. Sect. C* **1984**, 40, 806. **f)** N. Serpone, *Comprehensive Coordination Chemistry, Vol. 4*, Pergamon, Oxford, **1987**.

47. G. R. Desiraju, T. Steiner, *The weak hydrogen bond*, Oxford University Press, Oxford, **1999**.
48. F. Kühn, M. Groarke, E. Bencze, E. Herdtweck, A. Prazeres, A. Santos, M. Calhorda, C. Romão, I. Gonçalves, A. Lopes, *Chem. Eur. J.* **2002**, *8*, 2370.
49. M. Paneque, M. Poveda, F. Vattier, E. Álvarez, E. Carmona, *Chem. Comm.* **2009**, 5661.
50. A. Arduengo, R. Harlow, M. Kline, *J. Am. Chem. Soc.* **1991**, *113*, 361.
51. a) W. D. Jones, *J. Am. Chem. Soc.* **2009**, *131*, 15075. b) F. E. Hahn, *Dalton Trans.* **2009**, 6893. c) A. Arduengo, G. Bertrand, *Chem. Rev.* **2009**, *109*, 3209.
52. a) C. Crudden, D. Allen, *Coord. Chem. Rev.* **2004**, *248*, 2247. b) T. Steinke, B. Shaw, H. Jong, B. Patrick, M. Fryzuk, J. Green, *J. Am. Chem. Soc.* **2009**, *131*, 10461.
53. a) T. Trnka, J. Morgan, M. Sanford, T. Wilhelm, M. Scholl, T. Choi, S. Ding, M. Day, R. Grubbs, *J. Am. Chem. Soc.* **2003**, *125*, 2546. b) B. Galan, M. Gembicky, P. Dominiak, J. Keister, S. Diver, *J. Am. Chem. Soc.* **2005**, *127*, 15702. c) C. Cooke, M. Jennings, R. Pomeroy, J. Clyburne, *Organometallics* **2007**, *26*, 6059. d) U. Scheele, S. Dechert, F. Meyer, *Chem. Eur. J.* **2008**, *14*, 5112. e) S. Burling, E. Mas-Marzá, J. E. V. Valpuesta, M. Mahon, M. Whittlesey, *Organometallics* **2009**, *28*, 6676.
54. R. Jazzar, S. Macgregor, M. Mahon, S. Richards, M. Whittlesey, *J. Am. Chem. Soc.* **2002**, *124*, 4944.
55. S. Burling, M. F. Mahon, R. E. Powell, M. K. Whittlesey, J. Williams, *J. Am. Chem. Soc.* **2006**, *128*, 13702.
56. a) K. Nakatsu, K. Kinoshita, H. Kanda, K. Isobe, *Chem. Lett.* **1980**, 913. b) K. Isobe, E. Kai, Y. Nakamura, K. Nishimoto, T. Miwa, S. Kawaguchi, K. Kinoshita, K. Nakatsu, *J. Am. Chem. Soc.* **1980**, *102*, 2475. c) K. Isobe, Y. Nakamura, T. Miwa, S. Kawaguchi, *Bull. Chem. Soc. Jpn.* **1987**, *60*, 149. d) B. Crociani, F. Di Bianca, A. Giovenco, A. Berton, R. Bertani, *J. Organomet. Chem.* **1989**, *361*, 255.

57. a) B. Crociani, F. Di Bianca, A. Giovenco, A. Scrivanti, *J. Organomet. Chem.* **1983**, 251, 393. b) F. Di Bianca, A. Fontana, R. Bertani, B. Crociani, *J. Organomet. Chem.* **1992**, 425, 155.
58. A. Wu, J. Mayer, *J. Am. Chem. Soc.* **2008**, 130, 14745.
59. a) M. Abadie, *Rad. Phy. Chem.* **1982**, 19, 68. b) A. L. Le, P. E. Hoggard, *Photochem. Photobiol.* **2008**, 84, 86.
60. D. F. McMillen, D. M. Golden, *Ann. Rev. Phys. Chem.* **1982**, 33, 493.
61. a) R. F. Jordan, D. Taylor, *J. Am. Chem. Soc.* **1989**, 111, 778. b) R. Jordan, D. Taylor, N. Baenziger, *Organometallics* **1990**, 9, 1546. c) A. Guram, R. F. Jordan, *Organometallics* **1991**, 10, 3470.
62. a) S. Geier, A. Gille, T. Gilbert, D. Stephan, *Inorg. Chem.* **2009**, 48, 10466. b) D. Stephan *Org. Biomol. Chem.* **2008**, 6, 1535. c) D. W. Stephan, G. Erker, *Angew. Chem. Int. Ed.* **2010**, 49, 46.
63. J. S. J. McCahill, G. C. Welch, D. W. Stephan, *Angew. Chem. Int. Ed.* **2007**, 46, 4968.
64. a) C. Leung, W. Zheng, Z. Zhou, Z. Lin, C. Lau, *Organometallics* **2008**, 27, 4957. b) E. S. Kim, H. S. Kim, J. N. Kim, *Tetrahedron Lett.* **2009**, 50, 2973. c) W. Zheng, C. W. Leung, Z. Zhou, C. P. Lau, Z. Lin, *J. Theor. Comput. Chem.* **2009**, 8, 417. d) R. S. Ramón, N. Marion, S. P. Nolan, *Chem. Eur. J.* **2009**, 15, 8695. e) M. G. Crestani, A. Steffen, A. M. Kenwright, A. S. Batsanov, J. A. K. Howard, T. B. Marder, *Organometallics* **2009**, 28, 2904.
65. C. L. Perrin, *Science* **1994**, 266, 1665.
66. a) D. Grotjahn, D. Lev, *J. Am. Chem. Soc.* **2004**, 126, 12232. b) D. Grotjahn, J. Hoerter, J. Hubbard, *J. Am. Chem. Soc.* **2004**, 126, 8866. c) D. Grotjahn, X. Zeng, A. Cooksy, *J. Am. Chem. Soc.* **2006**, 128, 2798. d) D. Grotjahn, Y. Gong, A. DiPasquale, *Organometallics* **2006**, 25, 5693. e) D. Grotjahn, V. Miranda-Soto, E. Kragulj, D. Lev, G. Erdogan, X. Zeng, A. Cooksy, *J. Am. Chem. Soc.* **2008**, 130, 20. f) D. Grotjahn, E. Kragulj, C. Zeinalipour-Yazdi, V. Miranda-Soto, D. Lev, A. Cooksy, *J. Am. Chem. Soc.* **2008**, 130, 10860. g) V. Miranda-Soto, D. Grotjahn, A. DiPasquale, A. Rheingold, *J. Am. Chem. Soc.* **2008**, 130, 13200.

- 67.** Y. Wakatsuki, N. Koga, H. Werner, K. Morokuma, *J. Am. Chem. Soc.* **1997**, *119*, 360.

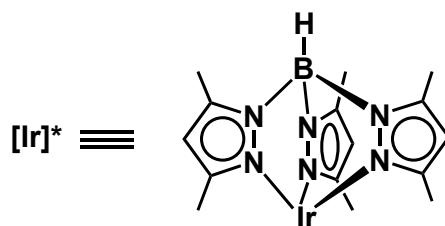
III. Parte experimental

Parte Experimental

Consideraciones Generales

Los análisis de los nuevos compuestos incluidos en el presente trabajo se han llevado a cabo en el Servicio de Microanálisis del Instituto de Investigaciones Químicas de Sevilla, en los laboratorios Mikroanalytisches Labor Pascher (Alemania) y en los servicios de análisis de la Universidad de Sevilla. Los espectros de masas se han realizado en el Servicio de Masas de la Universidad de Sevilla (FAB/alta resolución). Los espectros de IR se han registrado en un espectrómetro Bruker Vector 22 y los de Resonancia Magnética Nuclear en espectrómetros Bruker, modelos DPX-300, DRX-400 y DRX-500. Los desplazamientos químicos en los espectros de RMN de ^1H y de ^{13}C están referenciados con respecto al tetrametilsilano, utilizando las señales residuales de resonancia de ^1H y las de ^{13}C del disolvente empleado en cada caso como referencia interna. La mayoría de las asignaciones de ^1H y de ^{13}C realizadas se basan en el análisis de experimentos mono y bidimensionales (^1H , $^{13}\text{C}\{^1\text{H}\}$, $^{13}\text{C}\{^1\text{H}\}$ -gated, COSY, NOESY, HMQC y HMBC ^1H - ^{13}C normal y largo alcance, etc.). Los espectros de IR de todos los complejos incluidos muestran una absorción intensa en las proximidades de 2530 cm^{-1} que se

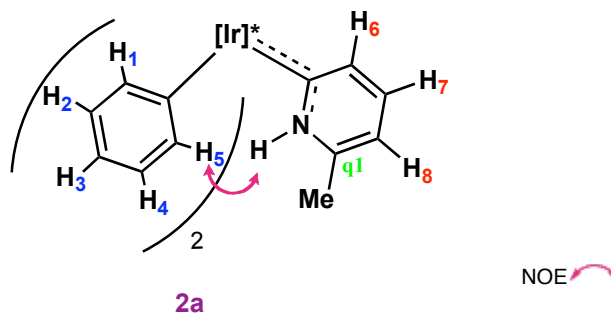
atribuye a la vibración de tensión BH del ligando Tp^{Me_2} coordinado en su forma tridentada $k^3\text{-N,N',N''}$.



Todos los experimentos se han realizado bajo atmósfera inerte utilizando las técnicas convencionales de Schlenk. El compuesto $\text{Tp}^{\text{Me}_2}\text{Ir}(\text{C}_6\text{H}_5)_2(\text{N}_2)$ se ha sintetizado mediante el método descrito en la bibliografía.¹

¹ E. Gutiérrez-Puebla, A. Monge, M. C. Nicasio, P. J. Pérez, M. L. Poveda, E. Carmona, *Chem. Eur. J.* **1998**, *4*, 2225.

Compuesto 2



Rotámero mayoritario en CD_2Cl_2

Se disuelve el compuesto $\text{Tp}^{\text{Me}_2}\text{Ir}(\text{C}_6\text{H}_5)_2(\text{N}_2)$ (200 mg, 0.3 mmol) en benceno (8 mL) y se añade 2-picolina (1.2 equiv., 35 μL). La disolución resultante se agita durante 2 horas a 90 °C y posteriormente se evapora el disolvente bajo presión reducida. El análisis mediante RMN de ^1H del residuo indica que la conversión del producto de partida en el compuesto **2** es prácticamente cuantitativa. La muestra se purifica mediante cromatografía en columna de gel de sílice (10:1, hexano: Et_2O), obteniéndose el complejo deseado con un rendimiento del 45%. Se pueden obtener cristales amarillos mediante cristalización, a -23 °C, desde una disolución saturada de **2** en CH_2Cl_2 /hexano.

Datos analíticos y espectroscópicos:

Sólido Amarillo

Masa molecular: 737.3 g/mol.

IR (KBr): $\nu(\text{N-H})$ 3325, $\nu(\text{B-H})$ 2530 cm^{-1} .

Rotámero mayoritario (2a):

^1H RMN (CD_2Cl_2 , 500 MHz, -60 °C): δ 12.91 (sa, 1 H, NH), 8.15 (d, 2 H, $^3J_{\text{HH}} = 7.3$ Hz, 2 H_5), 7.02 (t, 2 H, $^3J_{\text{HH}} = 6.9$ Hz, 2 H_4), 6.95 (m, 2 H, H_6 , H_7), 6.72 (m, 3 H, 2 H_3 , H_8), 6.50 (t, 2 H, $^3J_{\text{HH}} = 7.3$ Hz, 2 H_2), 6.43 (d, 2 H, $^3J_{\text{HH}} = 7.4$ Hz, 2 H_1), 5.68,

5.67 (s, 1:2, 3 H, 3 CH_{pz}), 2.51 (s, 3 H, Me_{py}), 2.46, 2.44, 0.75, 0.70 (s, 1:2:2:1, 18 H, 6 Me_{pz}).

¹³C{¹H} RMN (CD₂Cl₂, 125 MHz, -60 °C): δ 176.6 (Ir=C), 151.0, 149.9 (1:2, C_{qpz}), 148.2 (C_{q1}), 143.4 (3 C_{qpz}), 141.7 (2 CH₁), 140.2 (2 Ir-C_{ph}), 135.2 (CH₈), 134.5 (2 CH₅), 126.3 (2 CH₂), 126.2 (2 CH₄), 125.0 (CH₆), 120.8 (2 CH₃), 116.0 (CH₇), 107.2, 107.0 (1:2, CH_{pz}), 20.0 (Me_{py}), 14.1, 13.6, 13.5 (1:2:3, Me_{pz}).

Rotámero minoritario (2b):

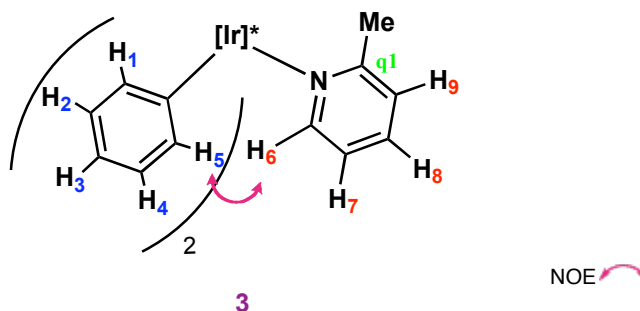
¹H RMN (CD₂Cl₂, 500 MHz, -60 °C): δ 10.14 (sa, 1 H, NH), 8.89 (d, 1 H, ³J_{HH} = 8.1 Hz, H_{py}), 8.32 (d, 2 H, ³J_{HH} = 7.0 Hz, 2 H₅), 7.47 (m, 1 H, H_{py}), 6.30 (d, 2 H, ³J_{HH} = 7.6 Hz, 2 H₁), 2.05 (s, 3 H, Me_{py}).

Proporción de rotámeros (CD₂Cl₂, -60 °C): 5:1.

HRMS (FAB) *m/z* calcd. (expt.) C₃₃H₃₉BIrN₇: 737.2989 (737.3039).

Anal. Calcd. C₃₃H₃₉BIrN₇·1/2 C₆H₁₄: C, 55.5; H, 6.0; N, 12.6. **Exp.:** C, 55.2; H, 5.9; N, 12.6.

Compuesto 3



Se disuelve el compuesto $\text{Tp}^{\text{Me}_2}\text{Ir}(\text{C}_6\text{H}_5)_2(\text{N}_2)$ (200 mg, 0.3 mmol) en benceno (8 mL) y se añade 2-picolina (1.2 equiv., 35 μL). La disolución resultante se agita durante 2 horas a 60 $^\circ\text{C}$ y, transcurrido este tiempo, se evapora el disolvente bajo presión reducida. El análisis mediante RMN de ^1H del residuo indica que la conversión del producto de partida en el compuesto **3** es prácticamente cuantitativa. El residuo se lava con pentano frío y se seca bajo vacío.

Datos analíticos y espectroscópicos:

Sólido blanco

Masa molecular: 737.3 g/mol.

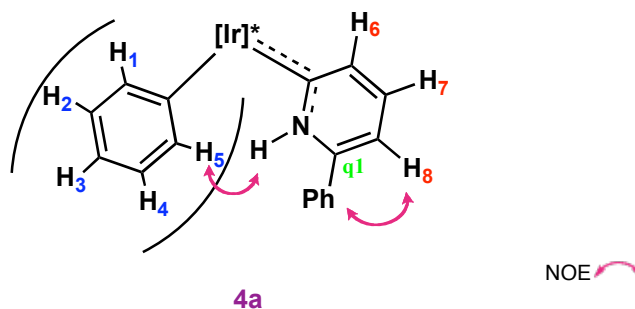
IR (nujol): $\nu(\text{B-H})$ 2535 cm^{-1} .

^1H RMN (CD_2Cl_2 , 500 MHz, $-60\text{ }^\circ\text{C}$): δ 10.54 (d, 1 H, $^3J_{\text{HH}} = 5.8$ Hz, H₆), 8.24 (d, 2 H, $^3J_{\text{HH}} = 7.6$ Hz, 2 H₅), 7.53 (t, 1 H, $^3J_{\text{HH}} = 6.4$ Hz, H₈), 7.14 (t, 1 H, $^3J_{\text{HH}} = 7.3$ Hz, H₇), 7.02 (t, 2 H, $^3J_{\text{HH}} = 5.8$ Hz, 2 H₄), 6.92 (d, 1 H, $^3J_{\text{HH}} = 7.4$ Hz, H₉), 6.73 (t, 2 H, $^3J_{\text{HH}} = 6.9$ Hz, 2 H₃), 6.48 (t, 2 H, $^3J_{\text{HH}} = 7.3$ Hz, 2 H₂), 6.39 (d, 2 H, $^3J_{\text{HH}} = 7.4$ Hz, 2 H₁), 5.71, 5.54 (s, 1:2, 3 H, 3 CH_{pz}), 2.44 (s, 3 H, Me_{py}), 2.49, 1.04, 0.73, 0.46 (s, 2:1:2:1, 18 H, 6 Me_{pz}).

$^{13}\text{C}\{^1\text{H}\}$ RMN (CD_2Cl_2 , 125 MHz, $-60\text{ }^\circ\text{C}$): δ 165.1 (C_{q1}), 156.2 (CH_6), 152.2, 150.6, 144.0, 143.5 (1:2:2:1, C_{qpz}), 142.6 (2 CH_1), 137.2 (2 Ir-C_{ph}), 137.0 (CH_8), 136.1 (2 CH_5), 128.1 (CH_9), 125.5 (2 CH_2), 124.9 (2 CH_4), 122.1 (CH_7), 121.0 (2 CH_3), 107.7, 107.0 (1:2, CH_{pz}), 22.6 (Me_{py}), 14.3, 13.8, 13.2, 12.8 (1:1:2:2, Me_{pz}).

HRMS (FAB) m/z calcd. (expt.) $\text{C}_{33}\text{H}_{39}\text{BIrN}_7$: 737.2989 (737.2957).

Anal. Calcd. $\text{C}_{33}\text{H}_{39}\text{BIrN}_7$: C, 53.8; H, 5.4; N, 13.3. **Expt.:** C, 53.8; H, 5.4; N, 12.3.

Compuesto 4**Rotámero mayoritario en CD₂Cl₂**

Se disuelve el compuesto $\text{Tp}^{\text{Me}_2}\text{Ir}(\text{C}_6\text{H}_5)_2(\text{N}_2)$ (200 mg, 0.3 mmol) en benceno (8 mL) y se añade 2-fenilpiridina (1.2 equiv., 52 μL). La disolución resultante se agita durante 4 horas a 90 °C y transcurrido este tiempo, se evapora el disolvente bajo presión reducida. El análisis mediante RMN de ^1H del residuo indica que la conversión del producto de partida en el compuesto **4** es prácticamente cuantitativa. La muestra se purifica mediante cromatografía en columna de gel de sílice (40:1 \rightarrow 10:1, hexano:Et₂O), obteniéndose el complejo deseado con un rendimiento del 65%. Se pueden obtener cristales de color naranja de pureza analítica mediante la evaporación lenta de sus disoluciones en hexano:Et₂O a la temperatura ambiente.

Datos analíticos y espectroscópicos:

Sólido naranja

Masa Molecular: 799.3 g/mol.

IR (nujol): $\nu(\text{N-H})$ 3325, $\nu(\text{B-H})$ 2525 cm^{-1} .

Rotámero maioritario (4a):

^1H RMN (CD₂Cl₂, 500 MHz, -60 °C): δ 13.40 (sa, 1 H, NH), 8.25 (d, 2 H, $^3J_{\text{HH}} = 7.3$ Hz, 2 H₅), 7.60 (sa, 5 H, 5 CH_{phpy}), 7.14 (m, 3 H, H₆, H₇, H₈), 7.00 (t, 2 H, $^3J_{\text{HH}} = 7.5$ Hz, 2 H₄), 6.77 (t, 2 H, $^3J_{\text{HH}} = 7.4$ Hz, 2 H₃), 6.55 (t, 2 H, $^3J_{\text{HH}} = 7.2$ Hz, 2 H₂),

6.51 (d, 2 H, $^3J_{\text{HH}} = 7.9$ Hz, 2 H₁), 5.71, 5.70 (s, 2:1, 3 H, 3 CH_{pz}), 2.48, 2.47, 0.84, 0.78 (s, 1:2:2:1, 18 H, 6 Me_{pz}).

$^{13}\text{C}\{^1\text{H}\}$ RMN (CD₂Cl₂, 125 MHz, -60 °C): δ 177.5 (Ir=C), 151.1, 150.0 (1:2, C_{qpz}), 148.8 (C_{q1}), 143.5 (3 C_{qpz}), 141.6 (2 CH₁), 140.7 (CH₆), 140.0 (2 Ir-C_{ph}), 135.2 (2 CH₅), 135.1 (CH₇), 133.3 (C_{qphpy}), 131.1, 130.2, 126.9 (1:2:2, CH_{phpy}), 126.4 (2 CH₂), 126.3 (2 CH₄), 121.0 (2 CH₃), 114.8 (CH₈), 107.3, 107.2 (1:2, CH_{pz}), 14.2, 13.5 (1:5, Me_{pz}).

Rotámero minoritario (4b):

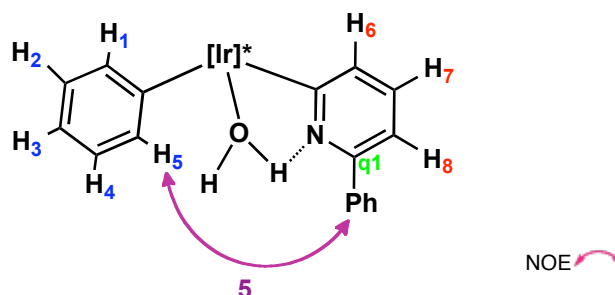
^1H RMN (CD₂Cl₂, 500 MHz, -60 °C): δ 10.50 (sa, NH).

Proporción de rotámeros (CD₂Cl₂, -60 °C): 10:1.

HRMS (FAB) m/z calcd. (expt.) C₃₈H₄₁BIrN₇: 799.3144 (799.3146).

Anal. Calcd. C₃₈H₄₁BIrN₇: C, 57.1; H, 5.2; N, 12.3. **Expt.:** C, 57.2; H, 5.2; N, 12.2.

Compuesto 5



Se disuelve el compuesto $\text{Tp}^{\text{Me}_2}\text{Ir}(\text{C}_6\text{H}_5)_2(\text{N}_2)$ (200 mg, 0.3 mmol) en benceno (10 mL) y se añade 2-fenilpiridina (1.2 equiv., 52 μL). La disolución resultante se agita durante 2 horas a 60 °C y transcurrido este tiempo se evapora el disolvente bajo presión reducida. El análisis mediante RMN de ^1H del residuo indica que la conversión del producto de partida en el compuesto **5** es prácticamente cuantitativa. La muestra se purifica mediante cromatografía en columna de gel de sílice (10:1, hexano: Et_2O), obteniéndose el complejo **5** con un rendimiento del 55%. Se pueden obtener cristales amarillos de pureza analítica por evaporación lenta de sus disoluciones en hexano/ Et_2O a la temperatura ambiente.

Datos analíticos y espectroscópicos:

Sólido amarillo

Masa molecular: 739.7 g/mol.

IR (KBr): $\nu(\text{O-H})$ 3630, $\nu(\text{B-H})$ 2520 cm^{-1} .

^1H RMN (CD_2Cl_2 , 500 MHz, -10 °C): δ 8.03, 7.63, 7.57 (d, t, t, 2:2:1, 5 H, $^3J_{\text{HH}} \approx 7.0$ Hz, 5 CH_{phpy}), 7.51 (t, 1 H, $^3J_{\text{HH}} = 7.4$ Hz, H_5), 7.20 (sa, 3 H, H_6 , H_7 , H_8), 6.99 (t, 1 H, $^3J_{\text{HH}} = 7.2$ Hz, H_4), 6.78 (t, 1 H, $^3J_{\text{HH}} = 7.1$ Hz, H_3), 6.66 (t, 1 H, $^3J_{\text{HH}} = 7.5$ Hz,

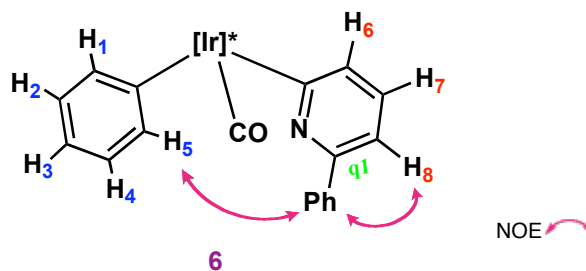
H₂), 6.38 (d, 1 H, $^3J_{\text{HH}} = 7.8$ Hz, H₁), 5.79, 5.69, 5.61 (s, 1 H cada, 3 CH_{pz}), 2.49, 2.42, 2.39, 1.52, 1.49, 1.30 (s, 3 H cada, 6 Me_{pz}).

El núcleo del hidrógeno puente se observa a 16.90 ppm a más baja temperatura (-70 °C) mientras que no se ha podido asignar el OH restante.

$^{13}\text{C}\{^1\text{H}\}$ RMN (CD₂Cl₂, 100 MHz, -10 °C): δ 171.9 (Ir-C_{py}), 150.7, 150.6, 150.2 (C_{qpz}), 147.3 (C_{q1}), 143.4, 142.9, 142.8 (C_{qpz}), 140.9 (CH₁), 137.1 (CH₆), 136.7 (Ir-C_{ph}), 134.9 (CH₇), 133.9 (C_{qphpy}), 130.7, 129.9, 126.3 (1:2:2, CH_{phpy}), 130.6 (CH₅), 126.2 (CH₂), 125.0 (CH₄), 121.3 (CH₃), 114.1 (CH₈), 107.3, 107.1, 107.0 (CH_{pz}), 16.3, 13.4, 13.2, 13.0, 12.8, 12.0.

HRMS (FAB) m/z calcd. (expt.) C₃₂H₃₈BIrN₇+Na: 762.2680 (762.2665).

Anal. Calcd. C₃₂H₃₈BIrN₇: C, 52.0; H, 5.2; N, 13.3. **Expt.:** C, 52.5; H, 5.1; N, 13.4.

Compuesto 6**MÉTODO A:**

Se disuelve el compuesto **5** (50 mg, 0.07 mmol) en ciclohexano (5 mL) y se calienta la disolución resultante a 120 °C, bajo 2 atm. de CO, durante 12 horas. Transcurrido este tiempo se evapora el disolvente bajo presión reducida. El análisis mediante RMN de ^1H del residuo indica que la conversión del producto de partida en el compuesto **6** es cuantitativa. Se lava el residuo con 4 mL de pentano y se seca bajo vacío. Se obtiene un sólido amarillo, con un rendimiento del 82%.

MÉTODO B:

Se disuelve el compuesto **4** (40 mg, 0.05 mmol) en benceno (2 mL) y la disolución resultante se calienta a 90 °C, bajo 2 atm. de CO, durante 12 horas. Transcurrido este tiempo, se evapora el disolvente bajo presión reducida. El análisis mediante RMN de ^1H del residuo indica que la conversión del producto de partida en el compuesto **6** es cuantitativa. Se lava el producto resultante con 2 mL de pentano y se seca bajo vacío.

Datos analíticos y espectroscópicos:

Sólido amarillo pálido

Masa molecular: 748.8 g/mol.

IR (KBr): $\nu(\text{CO})$ 2040, $\nu(\text{B-H})$ 2520 cm^{-1} .

^1H RMN (CDCl_3 , 500 MHz, 25 °C): δ 8.90 (d, 1 H, $^3J_{\text{HH}} = 7.7$ Hz, H_5), 8.35, 7.44, 7.33 (d, t, t, 2:2:1, 5 H, $^3J_{\text{HH}} \approx 7.5$ Hz, 5 CH_{phpy}), 7.30 (d, 1 H, $^3J_{\text{HH}} = 7.2$ Hz, H_8),

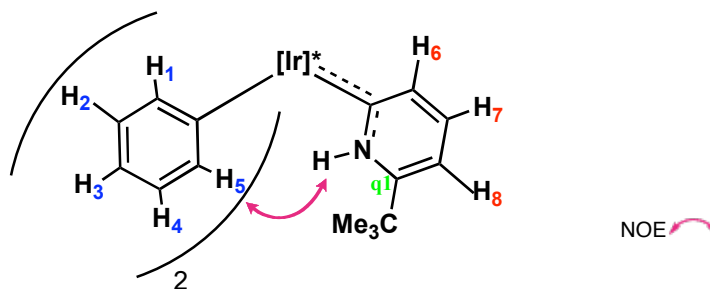
7.01 (t, 1 H, $^3J_{\text{HH}} = 7.1$ Hz, H₄), 6.89 (t, 1 H, $^3J_{\text{HH}} = 7.5$ Hz, H₇), 6.84 (t, 1 H, $^3J_{\text{HH}} = 7.1$ Hz, H₃), 6.68 (t, 1 H, $^3J_{\text{HH}} = 7.3$ Hz, H₂), 6.38 (m, 2 H, H₁, H₆), 5.78, 5.77, 5.73 (s, 1 H cada, 3 CH_{pz}), 2.49, 2.45, 2.44, 1.66, 1.50, 1.49, 0.86 (s, 3 H cada, 6 Me_{pz}).

$^{13}\text{C}\{^1\text{H}\}$ RMN (CDCl₃, 100 MHz, 25°C): δ 167.1 (Ir–CO), 157.3 (Ir–C_{py}), 153.8 (C_{q1}), 152.1, 151.2, 143.7, 143.8 (1:2:2:1, C_{qpz}), 140.9 (C_{qph}), 138.3 (CH₆), 137.7 (CH₁), 132.7 (CH₇), 131.7 (CH₅), 129.2 (Ir–C_{phpy}), 128.5, 128.0, 126.7 (1:2:2, 5 CH_{phpy}), 126.6 (CH₄), 126.1 (CH₂), 122.6 (CH₃), 113.5 (CH₈), 108.1, 107.0, 106.9 (CH_{pz}), 15.3, 13.9, 13.4, 13.0, 12.6, 12.0 (Me_{pz}).

HRMS (FAB) m/z calcd. (expt.) C₃₃H₃₅BIrN₇O + H: 750.2740 (750.2704).

Anal. Calcd. C₃₃H₃₅BIrN₇O: C 52.9; H 4.7; N, 13.1. **Expt.:** C, 53.7; H, 5.2; N, 12.2.

Compuesto 7



7a

Rotámero mayoritario en CD_2Cl_2

Se disuelve el compuesto $\text{Tp}^{\text{Me}_2}\text{Ir}(\text{C}_6\text{H}_5)_2(\text{N}_2)$ (200 mg, 0.3 mmol) en benceno (8 mL) y se añade 2-terc-butilpiridina (1.2 equiv., 49 mg). La disolución se agita durante 2 horas a 60 °C tras lo cual se evapora el disolvente bajo presión reducida. El análisis mediante RMN de ^1H del residuo indica que la conversión del producto de partida en el compuesto **7** es prácticamente cuantitativa. El residuo sólido se purifica mediante cromatografía en columna de gel de sílice (10:1, hexano:Et₂O), obteniéndose el complejo **7** con un rendimiento del 70%.

Datos analíticos y espectroscópicos:

Sólido amarillo

Masa Molecular: 779.3 g/mol.

IR (KBr): $\nu(\text{N-H})$ 3345, $\nu(\text{B-H})$ 2525 cm^{-1} .

Rotámero mayoritario (7a):

^1H RMN (CD_2Cl_2 , 500 MHz, -60 °C): δ 13.08 (sa, 1 H, NH), 8.18 (d, 2 H, $^3J_{\text{HH}} = 7.0$ Hz, 2 H₅), 7.03 (t, 2 H, $^3J_{\text{HH}} = 6.7$ Hz, 2 H₄), 6.96 (m, 2 H, H₆, H₇), 6.74 (m, 3 H, 2 H₃, H₈), 6.52 (t, 2 H, $^3J_{\text{HH}} = 7.1$ Hz, 2 H₂), 6.48 (d, 2 H, $^3J_{\text{HH}} = 7.2$ Hz, 2 H₁), 5.71,

5.68 (s, 1:2, 3 H, 3 CH_{pz}), 2.45, 2.44, 0.76 (s, 2:1:3, 18 H, 6 Me_{pz}), 1.29 (s, 9 H, CMe₃).

¹³C{¹H} RMN (CD₂Cl₂, 125 MHz, -60 °C): δ 176.0 (Ir=C), 158.9 (C_{q1}), 151.1, 149.9, 143.4, 143.4 (1:2:1:2, C_{qpz}), 141.5 (2 CH₁), 140.1 (2 Ir-C_{ph}), 135.7 (2 CH₅), 135.1 (CH₆), 126.4 (2 CH₂), 126.3 (2 CH₄), 125.1 (CH₇), 120.9 (2 CH₃), 112.0 (CH₈), 107.3, 107.1 (1:2, CH_{pz}), 35.9 (CMe₃), 29.2 (CMe₃), 14.2, 13.7, 13.5, 13.3 (1:1:2:2, Me_{pz}).

Rotámero minoritario (7b):

¹H RMN (CD₂Cl₂, 500 MHz, -60 °C): 10.10 (sa, 1 H, NH), 8.78 (d, 1 H, H_{py}), 8.38 (d, 2 H, 2 H₅), 7.50 (t, 1 H, H_{py}), 6.67 (t, 2 H, 2 H₃), 6.43 (t, 2 H, 2 H₂), 6.36 (d, 2 H, 2 H₁).

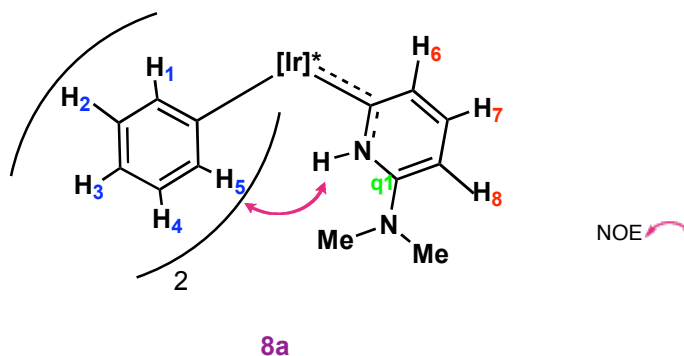
¹³C{¹H} RMN (CD₂Cl₂, 500 MHz, -60 °C): 177.8 (Ir=C), 141.3 (2 CH₅), 139.2 (2 Ir-C_{ph}), 135.9 (CH_{py}), 34.6 (CMe₃), 28.3 (CMe₃).

Proporción de rotámeros (CD₂Cl₂, -60 °C): 3:1.

HRMS (FAB) *m/z* calcd. (expt.) C₃₆H₄₅BIrN₇ + Na: 802.3357 (802.3403).

Anal. Calcd. C₃₆H₄₅BIrN₇: C, 55.5; H, 5.8; N, 12.6. **Expt.:** C, 56.2; H, 6.2; N, 11.6.

Compuesto 8



Rotámero mayoritario en CD_2Cl_2

Se disuelve el compuesto $\text{Tp}^{\text{Me}_2}\text{Ir}(\text{C}_6\text{H}_5)_2(\text{N}_2)$ (200 mg, 0.3 mmol) en benceno (8 mL) y se añade 2-dimetilaminopiridina (1.2 equiv., 44 μL) y la disolución resultante se agita durante 2 horas a 60 $^\circ\text{C}$. Transcurrido este tiempo, se evapora el disolvente bajo presión reducida, indicando el análisis mediante RMN de ^1H del residuo que la conversión del producto de partida en el compuesto **8** es prácticamente cuantitativa. La muestra se purifica mediante cromatografía en columna de gel de sílice (40:1 \rightarrow 10:1, hexano: Et_2O), obteniéndose el complejo **8** con un rendimiento del 60%.

Datos analíticos y espectroscópicos:

Sólido amarillo verdoso

Masa Molecular: 776.4 g/mol.

IR (KBr): $\nu(\text{N-H})$ 3365, $\nu(\text{B-H})$ 2520 cm^{-1} .

Rotámero mayoritario (8a):

^1H RMN (CD_2Cl_2 , 500 MHz, -60 $^\circ\text{C}$): δ 11.91 (sa, 1 H, NH), 8.41 (d, 2 H, $^3J_{\text{HH}} = 7.6$ Hz, 2 H₅), 6.99 (t, 2 H, $^3J_{\text{HH}} = 7.1$ Hz, 2 H₄), 6.84 (t, 1 H, $^3J_{\text{HH}} = 8.0$ Hz, H₇), 6.73 (t, 2 H, $^3J_{\text{HH}} = 6.7$ Hz, 2 H₃), 6.50 (m, 4 H, 2 H₂, 2 H₁), 6.26 (d, 1 H, $^3J_{\text{HH}} = 7.4$

Hz, H₆), 5.99 (d, 1 H, $^3J_{\text{HH}} = 7.4$ Hz, H₈), 5.70, 5.66 (s, 1:2, 3 H, 3 CH_{pz}), 3.11 (s, 6 H, NMe₂), 2.45, 0.87, 0.72 (s, 3:2:1, 18 H, 6 Me_{pz}).

$^{13}\text{C}\{^1\text{H}\}$ RMN (CD₂Cl₂, 125 MHz, -60 °C): δ 169.2 (Ir=C), 152.2 (C_{q1}), 150.9, 150.0, 143.3, 143.2 (1:2:2:1, C_{qpz}), 141.7 (2 CH_I), 140.7 (2 Ir-C_{ph}), 136.7 (CH₇), 136.2 (2 CH₅), 127.1 (CH₆), 126.1 (2 CH₂, 2 CH₄), 120.6 (2 CH₃), 107.2, 107.0 (1:2, CH_{pz}), 98.5 (CH₈), 40.2 (NMe₂), 14.1, 13.7, 13.6, 13.5 (1:2:1:2, Me_{pz}).

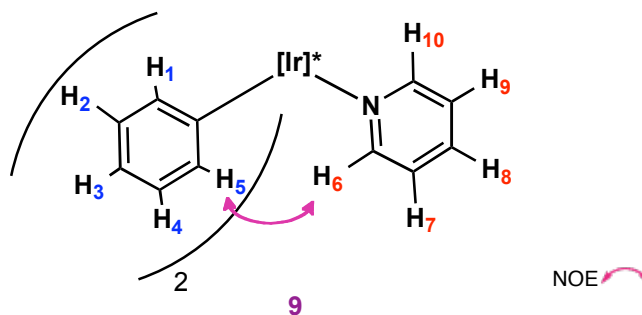
Rotámero minoritario (8b):

^1H RMN (CD₂Cl₂, 500 MHz, -60 °C): δ 9.12 (sa, 1 H, NH), 8.40 (d, 2 H, 2 H₅), 8.00 (d, 1 H, H_{py}), 7.35 (t, H, H_{py}), 6.96 (t, 2 H, 2 H₄), 6.66 (t, 2 H, 2 H₃), 6.42 (t, 2 H, 2 H₂), 6.39 (d, 2 H, 2 H₁).

Proporción de rotámeros (CD₂Cl₂, -60 °C): 5:1.

HRMS (FAB) m/z calcd. (expt.) C₃₄H₄₂BlrN₈: 766.3255 (766.3264).

Anal. Calcd. C₃₄H₄₂BlrN₈·1/2 CH₂Cl₂: C, 51.3; H, 5.4. N, 13.9. **Expt.:** C, 51.6; H, 5.5; N, 14.7.

Compuesto 9

Se disuelve el compuesto $\text{Tp}^{\text{Me}_2}\text{Ir}(\text{C}_6\text{H}_5)_2(\text{N}_2)$ (200 mg, 0.3 mmol) en benceno (8 mL) y se añade piridina (1.2 equiv., 29 μL). La disolución resultante se agita durante 2 horas a 60 $^\circ\text{C}$ y transcurrido este tiempo se evapora el disolvente bajo presión reducida. El análisis mediante RMN de ^1H del residuo indica que la conversión del producto de partida en el compuesto **9** es prácticamente cuantitativa. La muestra resultante se purifica mediante cromatografía en columna de gel de sílice (20:1 \rightarrow 10:1, hexano: Et_2O), obteniéndose el complejo **9** con un rendimiento del 56%.

Datos analíticos y espectroscópicos:

Sólido amarillo

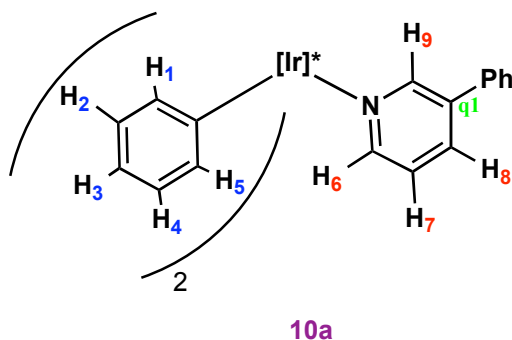
Masa molecular: 723.4 g/mol.

IR (nujol): $\nu(\text{B-H})$ 2535 cm^{-1} .

^1H RMN (CD_2Cl_2 , 500 MHz, -60°C): δ 10.07 (d, 1 H, $^3J_{\text{HH}} = 5.7$ Hz, H_6), 8.23 (d, 2 H, $^3J_{\text{HH}} = 7.7$ Hz, 2 H_5), 7.92 (d, 1 H, $^3J_{\text{HH}} = 5.9$ Hz, H_{10}), 7.65 (t, 1 H, $^3J_{\text{HH}} = 7.5$ Hz, H_7), 7.36, (t, 1 H, $^3J_{\text{HH}} = 6.2$ Hz, H_8), 7.01 (t, 2 H, $^3J_{\text{HH}} = 7.3$ Hz, 2 H_4), 6.86 (t, 1 H, $^3J_{\text{HH}} = 6.6$ Hz, H_9), 6.73 (t, 2 H, $^3J_{\text{HH}} = 7.0$ Hz, 2 H_3), 6.48 (t, 2 H, $^3J_{\text{HH}} = 7.3$ Hz, 2 H_2), 6.32 (d, 2 H, $^3J_{\text{HH}} = 7.9$ Hz, 2 H_1), 5.69, 5.60 (s, 2:1, 3 H, 3 CH_{pz}), 2.46, 0.60, 0.55 (s, 3:2:1, 18 H, 6 Me_{pz}).

$^{13}\text{C}\{^1\text{H}\}$ RMN (CD_2Cl_2 , 125 MHz, -60°C): δ 155.9 (CH_6), 153.2 (CH_{10}), 151.8, 149.8, 143.7, (1:2:3, C_{qpz}), 143.7 (2 CH_1), 141.8 (2 CH_5), 136.8 (CH_8), 136.7 (Ir- C_{ph}), 125.7 (2 CH_2), 125.0 (CH_7), 123.9 (2 CH_4 , CH_9), 121.0 (2 CH_3), 107.7, 107.2 (1:2, CH_{pz}) 14.4, 13.8, 13.2, 12.5 (1:1:2:2, Me_{pz}).

Anal. Calcd. $\text{C}_{32}\text{H}_{37}\text{BIrN}_7$: C, 53.6; H, 4.5; N, 13.7. **Expt.**: C, 53.9; H, 5.5; N, 12.5.

Compuesto 10

Se disuelve el compuesto $\text{Tp}^{\text{Me}_2}\text{Ir}(\text{C}_6\text{H}_5)_2(\text{N}_2)$ (200 mg, 0.3 mmol) en benceno (8 mL) y se añade 3-fenilpiridina (1.2 equiv., 55 μL). La disolución resultante se agita durante 2 horas a 60 °C y transcurrido este tiempo, se evapora el disolvente bajo presión reducida. El análisis mediante RMN de ^1H del residuo indica que la conversión del producto de partida en el compuesto **10** es prácticamente cuantitativa. La muestra se purifica mediante cromatografía en columna de gel de sílice (30:1 \rightarrow 10:1, hexano:Et₂O), obteniéndose el complejo **10** con un rendimiento del 65%.

Datos analíticos y espectroscópicos:

Sólido amarillo

Masa molecular: 799.3 g/mol.

IR (nujol): $\nu(\text{B-H})$ 2520 cm^{-1} .

A continuación se presentan conjuntamente los desplazamientos químicos para ambos rotámeros (los protones del **10b** se representan con un apóstrofe):

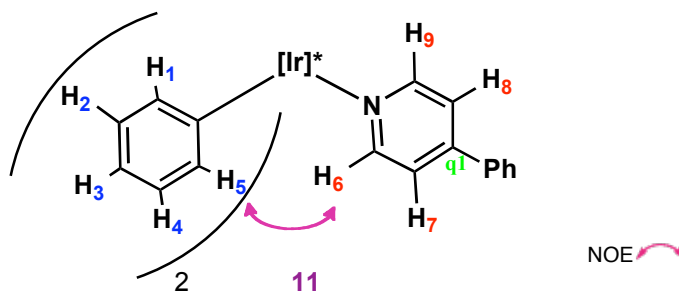
^1H RMN (CD_2Cl_2 , 500 MHz, -60°C): δ 10.46 (s, 1 H, H_9'), 8.41 (t, 1 H, $^3J_{\text{HH}} = 7.2$ Hz, H_6), 8.01 (m, 4 H, 2 H_5 , 2 H_5'), 8.08 (s, 1 H, H_9), 7.95 (d, 1 H, $^3J_{\text{HH}} = 5.8$ Hz, H_6'), 7.85 (d, 1 H, $^3J_{\text{HH}} = 7.6$ Hz, H_8), 7.83 (d, 1 H, $^3J_{\text{HH}} = 7.9$ Hz, H_8'), 7.63, 7.55, 7.48 (d, t, t, 2:2:1, 5 H, $^3J_{\text{HH}} \approx 7.4$ Hz, 5 CH_{ph}), 7.41 (t, 1 H, $^3J_{\text{HH}} = 7.2$ Hz, H_7'), 7.32,

7.09 (sa, 3:2, 5 H, 5 CH_{ph}'), 7.01 (m, 4 H, 2 H₄, 2 H₄'), 6.91 (t, 1 H, $^3J_{\text{HH}} = 6.6$ Hz, H₇), 6.73 (m, 4 H, 2 H₃, 2 H₃'), 6.49 (m, 4 H, 2 H₂, 2 H₂'), 6.32 (d, 4 H, $^3J_{\text{HH}} = 7.8$ Hz, 2 H₁, 2 H₁'), 5.73, 5.70, 5.62, 5.61 (s, 2:2:1:1, 6 H, 6 CH_{pz}), 2.46, 2.45, 2.43, 0.71, 0.65, 0.59, 0.57 (s, 3:1:2:2:2:1:1, 36 H, 12 Me_{pz}).

Proporción de rotámeros (CD₂Cl₂, -60 °C): 1:1.

HRMS (FAB) m/z calcd. (expt.) C₃₈H₄₁BIrN₇: 799.3178 (799.3146).

Anal. Calcd. C₃₈H₄₁BIrN₇ · 1/2 CH₂Cl₂: C, 54.9; H, 5.3; N, 11.6. **Expt.:** C, 55.5; H, 5.5; N, 11.3.

Compuesto 11

Se disuelve el compuesto $\text{Tp}^{\text{Me}_2}\text{Ir}(\text{C}_6\text{H}_5)_2(\text{N}_2)$ (200 mg, 0.3 mmol) en benceno (8 mL) y se añade 4-fenilpiridina (1.2 equiv., 56 mg). La disolución resultante se agita durante 2 horas a 60 °C y transcurrido este tiempo, se evapora el disolvente bajo presión reducida. El análisis mediante RMN de ^1H del residuo indica que la conversión del producto de partida en el compuesto **11** es prácticamente cuantitativa. El residuo sólido se purifica mediante cromatografía en columna de gel de sílice (10:1, hexano: Et_2O), obteniéndose el complejo **11** con un rendimiento del 57%.

Datos analíticos y espectroscópicos:

Sólido amarillo

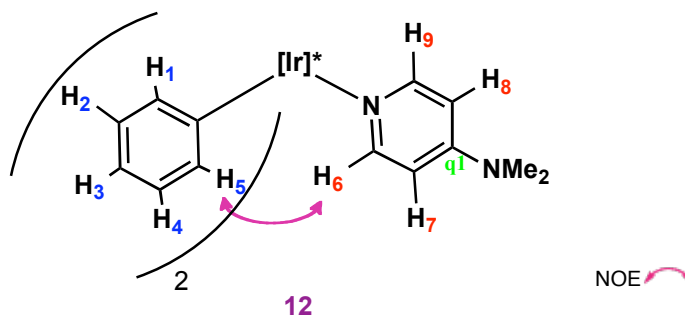
Masa molecular: 799.3 g/mol.

IR (nujol): ν (B–H) 2525 cm^{-1} .

^1H RMN (CD_2Cl_2 , 500 MHz, –60 °C): δ 10.08 (d, 1 H, $^3J_{\text{HH}} = 4.2$ Hz, H_6), 8.27 (d, 2 H, $^3J_{\text{HH}} = 6.9$ Hz, 2 H_5), 7.95 (d, 1 H, $^3J_{\text{HH}} = 4.9$ Hz, H_9), 7.64, 7.46 (d, m, 2:3, 5 H, 5 CH_{phpy}), 7.58 (d, 1 H, $^3J_{\text{HH}} = 4.7$ Hz, H_7), 7.09 (d, 1 H, $^3J_{\text{HH}} = 5.1$ Hz, H_8), 7.03 (t, 2 H, $^3J_{\text{HH}} = 7.7$ Hz, 2 H_4), 6.73 (t, 2 H, $^3J_{\text{HH}} = 7.0$ Hz, 2 H_3), 6.48 (t, 2 H, $^3J_{\text{HH}} = 7.3$ Hz, 2 H_2), 6.33 (d, 2 H, $^3J_{\text{HH}} = 6.7$ Hz, 2 H_1), 5.70, 5.61 (s, 2:1, 3 H, 3 CH_{pz}), 2.46, 0.67, 0.56 (s, 3:2:1, 18 H, 6 Me_{pz}).

$^{13}\text{C}\{^1\text{H}\}$ RMN (CD_2Cl_2 , 125 MHz, $-60\text{ }^\circ\text{C}$): δ 155.8 (CH_9), 153.0 (CH_6), 151.5, 149.6 (1:2, C_{qpz}), 147.6 (C_{q1}), 143.5, 143.4 (1:2, C_{qpz}), 141.4 (2 CH_1), 136.5 (2 Ir- C_{phpy}), 136.0 (C_{qph}), 135.2 (2 CH_5), 130.1, 129.5, 127.0 (1:2:2, CH_{phpy}), 125.5 (2 CH_2), 124.8 (2 CH_4), 122.3 (CH_7), 122.1 (CH_8), 120.7 (2 CH_3), 107.4, 106.9 (2:1, CH_{pz}), 14.5, 14.1, 13.0, 12.4 (1:1:2:2, Me_{pz}).

HRMS (FAB) m/z calcd. (expt.) $\text{C}_{38}\text{H}_{41}\text{BIrN}_7$: 799.3146 (799.3158).

Compuesto 12

Se disuelve el compuesto $\text{Tp}^{\text{Me}_2}\text{Ir}(\text{C}_6\text{H}_5)_2(\text{N}_2)$ (200 mg, 0.3 mmol) en benceno (8 mL) y se añade 4-dimetilaminopiridina (1.2 equiv., 43 mg). La disolución resultante se agita durante 2 horas a 60 °C, tras lo cual se evapora el disolvente bajo presión reducida. El análisis mediante RMN de ^1H del residuo indica que la conversión del producto de partida en el compuesto **12** es prácticamente cuantitativa. A continuación el residuo sólido se lava con pentano frío, obteniéndose el complejo **12** en forma de un sólido blanco.

Datos analíticos y espectroscópicos:

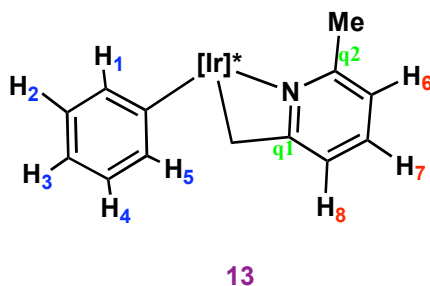
Sólido blanco

Masa Molecular: 776.4 g/mol.

IR (nujol): $\nu(\text{B-H})$ 2535 cm^{-1} .

^1H RMN (CD_2Cl_2 , 400 MHz, -60 °C): δ 9.40 (d, 1 H, $^3J_{\text{HH}} = 6.6$ Hz, H_6), 8.18 (d, 2 H, $^3J_{\text{HH}} = 7.3$ Hz, 2 H_5), 7.26 (d, 1 H, $^3J_{\text{HH}} = 6.8$ Hz, H_8), 6.97 (t, 2 H, $^3J_{\text{HH}} = 7.1$ Hz, 2 H_4), 6.69 (t, 2 H, $^3J_{\text{HH}} = 6.7$ Hz, 2 H_3), 6.45 (m, 3 H, 2 H_2 , H_7), 6.32 (d, 2 H, $^3J_{\text{HH}} = 7.5$ Hz, 2 H_1), 5.97 (d, 1 H, $^3J_{\text{HH}} = 4.2$ Hz, H_9), 5.65, 5.56 (s, 2:1, 3 H, 3 CH_{pz}), 2.93 (s, 6 H, NMe_2), 2.44, 0.72, 0.54 (s, 3:2:1, 18 H, 6 Me_{pz}).

HRMS (FAB) m/z calcd. (expt.) $\text{C}_{34}\text{H}_{42}\text{BIrN}_8 + \text{Na}$: 789.3131 (789.3153).

Compuesto 13

Se disuelve el compuesto $\text{Tp}^{\text{Me}_2}\text{Ir}(\text{C}_6\text{H}_5)_2(\text{N}_2)$ (100 mg, 0.15 mmol) en benceno (8 mL) y se añade 2,6-lutidina (1.2 equiv., 16 mL). La disolución resultante se agita durante 2 horas a 140 °C, tras lo cual se evapora el disolvente bajo presión reducida. El análisis mediante RMN de ^1H del residuo indica que la conversión del producto de partida en el compuesto **13** es prácticamente cuantitativa. El residuo sólido se lava con pentano, obteniéndose un sólido marrón.

Datos analíticos y espectroscópicos:

Sólido marrón.

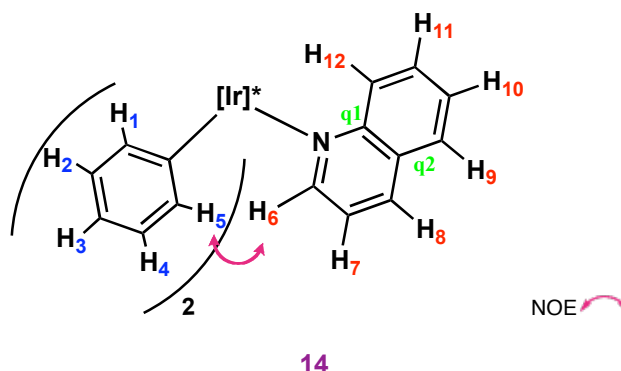
Masa Molecular: 673.3 g/mol.

IR (nujol): $\nu(\text{B-H})$ 2520 cm^{-1} .

^1H RMN (CD_2Cl_2 , 400 MHz, 25 °C): δ 7.53 (t, 1 H, $^3J_{\text{HH}} = 7.7$ Hz, H_7), 6.89 (m, 2 H, H_8 , H_4), 6.74 (t, 1 H, $^3J_{\text{HH}} = 7.0$ Hz, H_3), 6.70 (d, 1 H, $^3J_{\text{HH}} = 7.6$ Hz, H_6), 6.62 (t, 1 H, $^3J_{\text{HH}} = 7.5$ Hz, H_2), 6.47 (t, 1 H, $^3J_{\text{HH}} = 7.5$ Hz, H_5), 6.32 (d, 1 H, $^3J_{\text{HH}} = 7.0$ Hz, H_1), 5.77, 5.67 (s, 1:2, 3 H, 3 CH_{pz}), 2.48, 2.45, 2.43, 1.56, 1.41, 1.28 (s, 3 H cada, 6 Me_{pz}), 2.06 (m, 2 H, Ir-CH_2), 2.05 (s, 3 H, Me_{py}).

$^{13}\text{C}\{^1\text{H}\}$ RMN (CD_2Cl_2 , 100 MHz, 25 °C): δ 185.5 (C_{q1}), 158.3 (C_{q2}), 152.3, 152.7, 150.4, 143.1, 142.6, 142.5 (C_{qpz}), 143.1 (CH_1), 136.5 (Ir-C_{ph}), 134.5 (CH_7), 131.4

(CH₅), 125.5 (CH₂), 124.7 (CH₄), 123.0 (CH₆), 120.4 (CH₃), 120.1 (CH₈), 107.6,
 107.1, 106.1 (2:1, CH_{pz}), 21.2 (Me_{py}) 15.5, 14.3, 13.0, 12.9, 12.7, 10.8 (Me_{pz}), -22.0
 (¹J_{CH} = 135 Hz, Ir-CH₂).

Compuesto 14

Se disuelve el compuesto $\text{Tp}^{\text{Me}_2}\text{Ir}(\text{C}_6\text{H}_5)_2(\text{N}_2)$ (200 mg, 0.3 mmol) en benceno (8 mL) y se añade quinolina (1.2 equiv., 42 μL). La disolución resultante se agita durante 2 horas a 60 °C y transcurrido este tiempo, se evapora el disolvente bajo presión reducida. El análisis mediante RMN de ^1H del residuo indica que la conversión del producto de partida en el compuesto **14** es prácticamente cuantitativa. El residuo sólido se cromatografía en columna de gel de sílice (100:1 \rightarrow 30:1, hexano:Et₂O), para obtener un sólido amarillo que cristaliza desde CH₂Cl₂:pentano (1:3) con un rendimiento del 60%.

Datos analíticos y espectroscópicos:

Sólido amarillo

Masa Molecular: 772.9 g/mol.

IR (KBr): $\nu(\text{B-H})$ 2525 cm^{-1} .

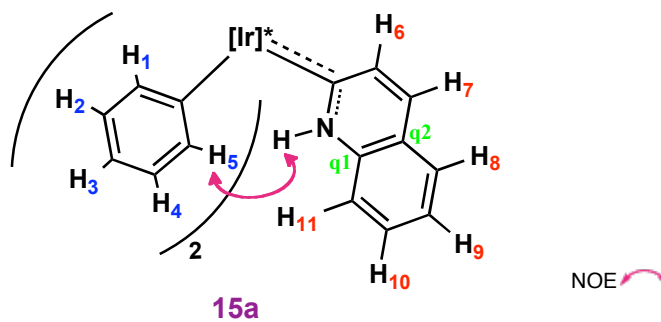
^1H RMN (CD₂Cl₂, 500 MHz, -60 °C): δ 11.10 (d, 1 H, $^3J_{\text{HH}} = 5.5$ Hz, H₆), 8.33 (d, 2 H, $^3J_{\text{HH}} = 7.4$ Hz, 2 H₅), 8.11 (d, 1 H, $^3J_{\text{HH}} = 8.1$ Hz, H₇), 7.59 (d, 1 H, $^3J_{\text{HH}} = 6.7$ Hz, H₉), 7.40 (d, 1 H, $^3J_{\text{HH}} = 5.7$ Hz, H₈), 7.22 (t, 1 H, $^3J_{\text{HH}} = 7.3$ Hz, H₁₀), 7.09 (t, 2 H, $^3J_{\text{HH}} = 7.3$ Hz, 2 H₄), 6.77 (m, 3 H, 2 H₃, H₁₁), 6.54 (t, 2 H, $^3J_{\text{HH}} = 7.1$ Hz, 2 H₂), 6.50

(d, 2 H, $^3J_{\text{HH}} = 7.3$ Hz, 2 H₁), 6.23 (d, 1 H, $^3J_{\text{HHh}} = 9.3$ Hz, H₁₂), 5.54, 5.52 (s, 1:2, 3 H, 3 CH_{pz}), 2.58, 2.50, 0.64, 0.39 (s, 2:1:1:2, 18 H, 6 Me_{pz}).

$^{13}\text{C}\{^1\text{H}\}$ RMN (CD₂Cl₂, 125 MHz, -60 °C): δ 158.5 (CH₆), 152.9, 151.2 (1:2, C_{qpz}), 149.2 (C_{q1}), 143.3, 142.9 (2:1, C_{qpz}), 142.8 (2 CH₁), 138.4 (CH₈), 135.9 (2 Ir-C_{ph}), 134.8 (CH₅), 129.2 (C_{q2}), 128.2 (CH₁₂), 128.1 (CH₁₁), 126.5 (CH₁₀), 126.4 (CH₉), 125.5 (2 CH₂), 124.9 (2 CH₄), 120.9 (CH₇), 120.7 (2 CH₃), 107.9, 107.0 (1:2, CH_{pz}) 14.4, 13.6, 12.9, 12.6 (1:2:1:2, Me_{pz}).

HRMS (FAB) m/z calcd. (expt.) C₃₆H₃₉BIrN₇: 773.3035 (773.2989).

Anal. Calcd. C₃₆H₃₉BIrN₇: C, 56.0; H, 5.4; N, 12.7. **Expt.**: C, 55.3; H, 5.4; N, 12.3.

Compuesto 15**Rotámero mayoritario en CD₂Cl₂**

Se disuelve el compuesto $\text{Tp}^{\text{Me}_2}\text{Ir}(\text{C}_6\text{H}_5)_2(\text{N}_2)$ (200 mg, 0.3 mmol) en benceno (6 mL) y se añade quinolina (1.2 equiv. 42 μL). La disolución se agita durante 2 horas a 90 °C y transcurrido este tiempo, se evapora el disolvente bajo presión reducida. El residuo sólido se purifica mediante cromatografía en columna de gel de sílice (100:1 \rightarrow 30:1, hexano:Et₂O). Mediante evaporación lenta de sus disoluciones en hexano:Et₂O se obtiene el complejo **15**, un sólido cristalino de color rojo oscuro, con un rendimiento del 60%.

Datos analíticos y espectroscópicos:

Sólido rojo oscuro

Masa Molecular: 772.9 g/mol.

IR (KBr): ν (N–H) 3325, ν (B–H) 2525 cm^{-1} .

Rotámero mayoritario (15a):

¹H RMN (CD₂Cl₂, 500 MHz, –60 °C): δ 13.19 (sa, 1 H, NH), 8.34 (d, 2 H, $^3J_{\text{HH}} = 7.6$ Hz, 2 H₅), 7.60 (m, 3 H, H₈, H₁₀, H₁₁), 7.48 (t, 1 H, $^3J_{\text{HH}} = 7.1$ Hz, H₉), 7.40 (d, 1 H, $^3J_{\text{HH}} = 9.1$ Hz, H₆), 7.18 (d, 1 H, $^3J_{\text{HH}} = 9.1$ Hz, H₇), 7.07 (t, 2 H, $^3J_{\text{HH}} = 7.0$ Hz, 2 H₄), 6.75 (t, 2 H, $^3J_{\text{HH}} = 7.1$ Hz, 2 H₃), 6.49 (t, 2 H, $^3J_{\text{HH}} = 7.1$ Hz, 2 H₂), 6.35 (d, 2

H, $^3J_{\text{HH}} = 7.7$ Hz, 2 H₁), 5.72, 5.71 (s, 1:2, 3 H, 3 CH_{pz}), 2.52, 2.51, 0.83, 0.82 (s, 1:2:1:2, 18 H, 6 Me_{pz}).

$^{13}\text{C}\{^1\text{H}\}$ RMN (CD₂Cl₂, 125 MHz, -60 °C): δ 185.7 (Ir=C), 150.9, 149.8, 143.3 (1:2:3, C_{qpz}), 141.2 (2 CH₁), 139.5 (C_{q1}), 139.3 (CH₇), 139.0 (2 Ir-C_{ph}), 134.3 (2 CH₅), 131.6 (CH₆), 130.5 (CH₈), 128.2 (CH₁₀), 126.1 (2 CH₄), 126.0 (2 CH₂), 125.6 (CH₉), 124.20 (C_{q2}), 120.8 (2 CH₃), 117.1 (CH₁₁), 107.1, 106.8 (1:2, CH_{pz}), 13.8, 13.3, 13.2 (1:2:3, Me_{pz}).

Rotámero minoritario (15b):

^1H RMN (CD₂Cl₂, 500 MHz, -60 °C): δ 10.71 (sa, 1 H, NH), 8.95 (d, 1 H, $^3J_{\text{HH}} = 8.6$ Hz, H_{py}), 8.37 (d, 2 H, $^3J_{\text{HH}} = 7.6$ Hz, 2 H₅), 7.96 (d, 1 H, $^3J_{\text{HH}} = 8.4$ Hz, H_{py}), 6.97 (t, 2 H, $^3J_{\text{HH}} = 7.4$ Hz, 2 H₄), 6.72 (t, 2 H, $^3J_{\text{HH}} = 7.4$ Hz, 2 H₃), 6.47 (t, 2 H, $^3J_{\text{HH}} = 7.1$ Hz, 2 H₂), 6.34 (d, 2 H, $^3J_{\text{HH}} = 7.8$ Hz, 2 H₁).

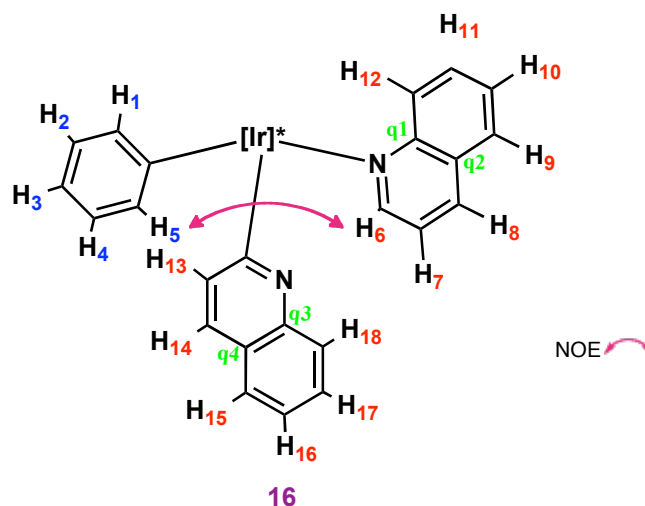
$^{13}\text{C}\{^1\text{H}\}$ RMN (CD₂Cl₂, 125 MHz, -60 °C): δ 187.6 (Ir=C).

Proporción de rotámeros (CD₂Cl₂, -60 °C): 5:1.

HRMS (FAB) m/z calcd. (expt.) C₃₆H₃₉BIrN₇: 773.3030 (773.2989).

Anal. Calcd. C₃₆H₃₉BIrN₇: C, 56.0; H, 5.4; N, 12.7. **Expt.:** C, 55.9; H, 5.4; N, 12.6.

Compuesto 16



Se disuelve el compuesto $\text{Tp}^{\text{Me}_2}\text{Ir}(\text{C}_6\text{H}_5)_2(\text{N}_2)$ (200 mg, 0.3 mmol) en benceno (8 mL) y se añade quinolina (5 equiv., 175 μL). La disolución resultante se agita durante 2 horas a 90 °C y con posterioridad se evapora el disolvente bajo presión reducida. Mediante condensación sobre un dedo frío (-78 °C) a 120 °C, bajo vacío, se retira el exceso de quinolina. El residuo sólido se purifica mediante cromatografía en columna de gel de sílice (10:1, hexano: Et_2O), para obtener el compuesto **16** como un sólido amarillo. Se pueden obtener microagujas cristalinas por evaporación de una disolución de **16** en $\text{MeOH}/\text{CH}_2\text{Cl}_2$ (2:3), con un rendimiento del 40%.

Datos analíticos y espectroscópicos:

Sólido amarillo

Masa Molecular: 824.3 g/mol.

IR (nujol): $\nu(\text{B-H})$ 2525 cm^{-1} .

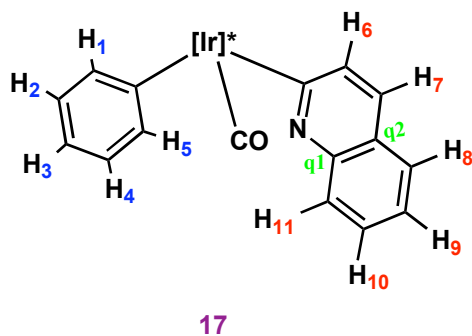
^1H RMN (CDCl_3 , 400 MHz, 25 °C): δ 12.38 (d, 1 H, $^3J_{\text{HH}} = 4.8$ Hz, H₆), 9.21 (d, 1 H, $^3J_{\text{HH}} = 7.9$ Hz, H₅), 8.30 (d, 1 H, $^3J_{\text{HH}} = 8.0$ Hz, H₁₂), 8.02 (d, 1 H, $^3J_{\text{HH}} = 7.5$ Hz,

H₈), 7.60 (t, 1 H, $^3J_{\text{HH}} = 7.5$ Hz, H₁₁), 7.53 (m, 3 H, H₇, H₉, H₁₅), 7.27 (t, 1 H, $^3J_{\text{HH}} = 7.3$ Hz, H₁₀), 7.17 (t, 1 H, $^3J_{\text{HH}} = 7.3$ Hz, H₁₆), 7.13 (t, 1 H, $^3J_{\text{HH}} = 7.9$ Hz, H₄), 7.00 (d, 1 H, $^3J_{\text{HH}} = 8.7$ Hz, H₁₄), 6.77 (t, 1 H, H₁₇), 6.72 (t, 1 H, H₃), 6.48 (m, 3 H, H₁, H₂, H₁₃), 6.21 (d, 1 H, $^3J_{\text{HH}} = 9.2$ Hz, H₁₈), 5.57, 5.55, 5.53 (s, 1 H cada, 3 CH_{pz}), 2.63, 2.62, 2.54, 0.47, 0.45, 0.20 (s, 3 H cada, 6 Me_{pz}).

$^{13}\text{C}\{^1\text{H}\}$ RMN (CDCl₃, 100 MHz, 25 °C): δ 163.1 (Ir–C_{quino}), 161.6 (CH₆), 152.8, 151.2, 150.3 (3 C_{qpz}), 148.5 (C_{q1}), 145.8 (C_{q3}), 143.5, 143.4, 143.1 (C_{qpz}), 142.2 (CH₁), 137.7 (CH₈), 136.0 (Ir–C_{ph}), 135.3 (CH₁₃), 134.7 (CH₅), 128.8 (C_{q2}), 128.3 (CH₁₂), 128.1 (CH₁₅), 127.9 (CH₁₄), 127.6 (CH₁₇), 127.0 (CH₉), 126.6 (CH₁₁), 126.0 (CH₁₈), 125.4 (CH₂), 125.2 (C_{q4}), 124.8 (CH₄), 124.2 (CH₁₆), 122.5 (CH₁₀), 120.8 (CH₃), 120.6 (CH₇), 107.5, 106.7, 106.6 (CH_{pz}), 13.7, 13.2, 13.1, 12.6, 11.9 (1:1:1:2:1, Me_{pz}).

HRMS (FAB) m/z calcd. (expt.) C₃₉H₄₁BIrN₈ + H: 825.3177 (825.3177).

Anal. Calcd. C₃₉H₄₀BIrN₈: C, 56.9; H, 5.4; N, 12.7. **Expt.:** C, 55.9; H, 5.4; N, 12.6.

Compuesto 17**MÉTODO A:**

Se disuelve el compuesto **15** (50 mg, 0.06 mmol) en ciclohexano (5 mL) y se calienta la disolución resultante a 120 °C, bajo 2 atm. de CO, durante 12 horas. Transcurrido este tiempo, se evapora el disolvente bajo presión reducida. El análisis de RMN de ^1H del residuo indica que la conversión del producto de partida en el compuesto **17** es cuantitativa. Se lava el residuo con 4 mL de pentano frío y se seca bajo vacío, obteniéndose un sólido amarillo con un rendimiento del 80%.

MÉTODO B:

Se disuelve el compuesto **16** (40 mg, 0.05 mmol) en benceno (2 mL) y se calienta la disolución resultante a 90 °C, bajo 2 atm. de CO, durante 12 horas. Transcurrido este tiempo, se evapora el disolvente bajo presión reducida. El análisis de RMN de ^1H del residuo indica que la conversión del producto de partida en el compuesto **17** es cuantitativa. Se lava con 3 mL de pentano frío y se seca bajo vacío obteniéndose un sólido amarillo con un rendimiento de 82%.

Datos analíticos y espectroscópicos:

Sólido amarillo

Masa molecular: 724.3 g/mol.

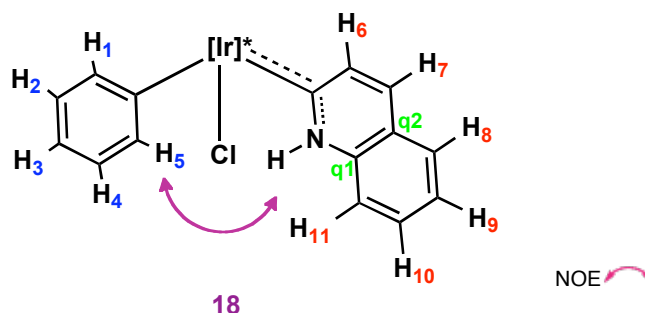
IR (KBr): $\nu(\text{CO})$ 2030, $\nu(\text{B-H})$ 2520 cm^{-1} .

^1H RMN (CDCl_3 , 400 MHz, 25 °C): δ 9.07 (d, 2 H, $^3J_{\text{HH}} = 8.4$ Hz, H_5), 8.19 (d, 1 H, $^3J_{\text{HH}} = 8.4$ Hz, H_{11}), 7.61 (t, 1 H, $^3J_{\text{HH}} = 7.0$ Hz, H_{10}), 7.57 (d, 1 H, $^3J_{\text{HH}} = 8.4$ Hz, H_8), 7.31 (d, 1 H, $^3J_{\text{HH}} = 8.4$ Hz, H_9), 7.22 (d, 1 H, H_6), 7.09 (t, 1 H, $^3J_{\text{HH}} = 7.3$ Hz, H_4), 6.85 (t, 1 H, $^3J_{\text{HH}} = 7.2$ Hz, H_3), 6.67 (t, 1 H, $^3J_{\text{HH}} = 7.8$ Hz, H_2), 6.53 (d, 1 H, $^3J_{\text{HH}} = 8.7$ Hz, H_7), 6.35 (d, 1 H, $^3J_{\text{HH}} = 7.9$ Hz, H_1), 5.78, 5.77, 5.73 (s, 1:2, 3 H, 3 CH_{pz}), 2.49, 2.44, 2.43, 1.67, 1.42, 0.86 (s, 3 H cada, 6 Me_{pz}).

$^{13}\text{C}\{^1\text{H}\}$ RMN (CDCl_3 , 100 MHz, 25 °C): δ 166.7 (Ir–CO), 159.5 (Ir– C_{quin}), 152.0, 151.2, 151.1 (C_{qpz}), 148.4 (C_{q1}), 143.8, 143.7, 143.6 (3 C_{qpz}), 138.1 (CH_1), 137.6 (CH_5), 131.4 (CH_6), 130.0 (CH_7), 129.1 (CH_{11}), 129.0 (Ir– C_{Ph}), 127.4 (CH_{10}), 126.9 (CH_8), 126.3 (CH_2), 125.4 (CH_4), 125.0 (C_{q2}), 123.7 (CH_9), 122.5 (CH_3), 107.9, 106.8, 106.7 (CH_{pz}), 14.7, 13.8, 13.4, 12.9, 12.5, 12.4 (Me_{pz}).

HRMS (FAB) m/z calcd. (expt.) $\text{C}_{31}\text{H}_{34}\text{BIrN}_7 + \text{H}$: 724.2547 (724.2540).

Compuesto 18



Se disuelve el compuesto **16** (20 mg, 0.024 mmol) en CDCl_3 (1 mL) y se irradia bajo un tubo fluorescente durante 5 días. Cuando la transformación en el compuesto **18** es completa (^1H RMN), se evapora a sequedad y el residuo sólido se cromatografía en columna de gel de sílice (10:1 \rightarrow 5:1, hexano:Et₂O), obteniéndose un sólido amarillo. Rendimiento: 65%.

Datos analíticos y espectroscópicos:

Sólido amarillo

Masa molecular: 731.3 g mol^{-1} .

IR (KBr): ν (N–H) 3330, (B–H) 2520 cm^{-1} .

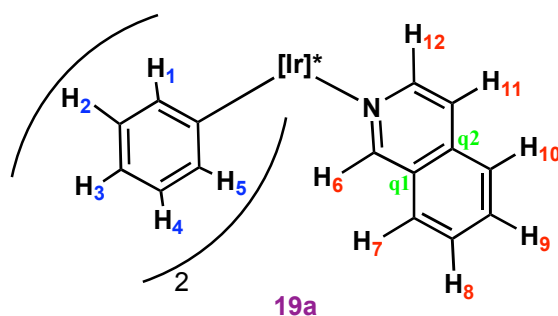
^1H RMN (CDCl_3 , 500 MHz, 25 °C): δ 13.06 (sa, 1 H, NH), 7.97 (d, 1 H, $^3J_{\text{HH}} = 7.7$ Hz, H₅), 7.90 (d, 1 H, $^3J_{\text{HH}} = 8.3$ Hz, H₁₁), 7.74 (m, 2 H, H₁₀, H₈), 7.51 (t, 1 H, $^3J_{\text{HH}} = 7.6$ Hz, H₉), 7.44 (d, 1 H, $^3J_{\text{HH}} = 8.9$ Hz, H₇), 7.11 (t, 1 H, $^3J_{\text{HH}} = 7.0$ Hz, H₄), 7.06 (d, 1 H, $^2J_{\text{HH}} = 8.9$ Hz, H₆), 6.79 (t, 1 H, $^3J_{\text{HH}} = 7.2$ Hz, H₃), 6.62 (t, 1 H, $^3J_{\text{HH}} = 7.0$ Hz, H₂), 6.18 (d, 1 H, $^3J_{\text{HH}} = 7.7$ Hz, H₁), 5.77, 5.70, 5.67 (s, 1 H cada, 3 CH_{pz}), 2.51, 2.44, 2.42, 1.64, 1.54, 0.88 (s, 3 H cada, 6 Me_{pz}).

$^{13}\text{C}\{^1\text{H}\}$ RMN (CDCl_3 , 125 MHz, 25 °C): δ 180.6 (Ir=C), 153.2, 151.3, 150.4, 143.7, 143.1, 142.9 (C_{qpz}), 140.3 (CH₁), 139.9 (C_{q1}), 137.7 (CH₆), 133.8 (CH₅),

132.2 (Ir-C_{ph}), 131.9 (CH₇) 130.8 (CH₈), 127.8 (CH₁₀), 125.8 (CH₉, CH₂), 125.2 (CH₄), 124.4 (C_{q2}), 121.6 (CH₃), 117.7 (CH₁₁), 107.8, 107.6, 107.2 (CH_{pz}) 15.6, 13.4, 13.1, 12.8, 12.6, 12.4 (6 Me_{pz}).

HRMS (FAB) *m/z* calcd. (expt.) C₃₀H₃₄BClIrN₇: 731.2299(731.2287).

Anal. Calcd. C₃₀H₃₄BClIrN₇: C, 49.3; H, 4.7; N, 13.4. **Expt.:** C, 49.5; H, 4.9; N, 13.5.

Compuesto 19**Rotámero mayoritario en CD₂Cl₂**

Se disuelve el compuesto $\text{Tp}^{\text{Me}_2}\text{Ir}(\text{C}_6\text{H}_5)_2(\text{N}_2)$ (200 mg, 0.3 mmol) en benceno (8 mL) y se añade isoquinolina (1.2 equiv., 42 μL). La disolución resultante se agita durante 3 horas a 60 °C y transcurrido este tiempo, se evapora el disolvente bajo presión reducida. El análisis de RMN de ^1H del residuo indica que la conversión del producto de partida en el compuesto **19** es cuantitativa. El residuo sólido se cromatografía en columna de gel de sílice (30:1, hexano:Et₂O), obteniéndose un sólido amarillo, el compuesto **19**, con un rendimiento del 60%.

Datos analíticos y espectroscópicos:

Sólido amarillo

Masa Molecular: 772.9 g/mol.

IR (nujol): $\nu(\text{B-H})$ 2530 cm^{-1} .

Rotámero mayoritario (19a):

^1H RMN (CD₂Cl₂, 500 MHz, -60 °C): δ 10.73 (s, 1 H, $^3J_{\text{HH}} = 6.5$ Hz, H₆), 8.34 (m, 3 H, 2 H₅, H₁₂), 8.18 (d, 1 H, $^3J_{\text{HH}} = 8.0$ Hz, H₁₀), 7.72 (m, 2 H, H₈, H₉), 7.21 (d, 1 H, $^3J_{\text{HH}} = 6.5$ Hz, H₇), 7.07 (t, 2 H, $^3J_{\text{HH}} = 7.3$ Hz, 2 H₄), 7.00 (d, 1 H, $^3J_{\text{HH}} = 7.0$ Hz,

H₁₁), 6.74 (t, 2 H, $^3J_{\text{HH}} = 7.0$ Hz, 2 H₃), 6.48 (t, 2 H, $^3J_{\text{HH}} = 7.2$ Hz, 2 H₂), 6.36 (d, 2 H, $^3J_{\text{HH}} = 7.8$ Hz, 2 H₁), 5.69, 5.62 (s, 2:1, 3 H, 3 CH_{pz}), 2.48, 0.56, 0.52 (s, 3:2:1, 18 H, 6 Me_{pz}).

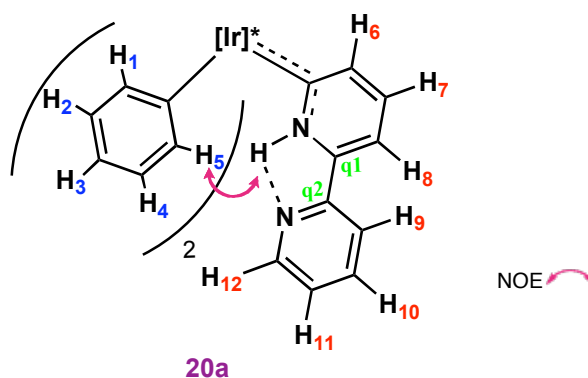
Rotámero minoritario (19b):

^1H RMN (CD₂Cl₂, 500 MHz, -60 °C): δ 9.96 (d, 1 H, $^3J_{\text{HH}} = 5.7$ Hz, H₁₂), 8.72 (s, 1 H, H₆), 8.34 (d, 2 H, $^3J_{\text{HH}} = 7.5$ Hz, 2 H₅), 7.86 (t, 1 H, $^3J_{\text{HH}} = 8.1$ Hz, H₁₀), 7.76 (d, 1 H, $^3J_{\text{HH}} = 7.5$ Hz, H₈), 7.54 (d, 1 H, $^3J_{\text{HH}} = 7.9$ Hz, H₇), 7.49 (t, 1 H, $^3J_{\text{HH}} = 6.9$ Hz, H₉).

Proporción de rotámeros (CD₂Cl₂, -60 °C): 5:2.

HRMS (FAB) m/z calcd. (expt.) C₃₇H₃₉BIrN₇: 773.298942 (773.304645).

Anal. Calcd. C₃₇H₃₉BIrN₇: C, 55.9; H, 5.4; N, 12.7. **Expt.:** C, 56.3; H, 5.6; N, 12.3.

Compuesto 20**Rotámero mayoritario en CD₂Cl₂**

Se disuelve el compuesto $\text{Tp}^{\text{Me}_2}\text{Ir}(\text{C}_6\text{H}_5)_2(\text{N}_2)$ (200 mg, 0.3 mmol) y 2,2'-bipiridina (1.2 equiv., 56 mg) en benceno (5 mL). La disolución resultante se agita durante 4 horas a 90 °C y, transcurrido este tiempo, se evapora el disolvente bajo presión reducida. El análisis de RMN de ^1H del residuo indica que la conversión del producto de partida en el compuesto **20** es prácticamente cuantitativa. La muestra se purifica mediante cromatografía en columna de gel de sílice (40:1 \rightarrow 10:1, hexano:Et₂O), obteniéndose un sólido de color naranja que se recrystaliza desde una mezcla Et₂O:hexano, con un rendimiento del 40%.

Datos analíticos y espectroscópicos:

Sólido naranja

Masa Molecular: 800.3 g/mol.

IR (KBr): $\nu(\text{N-H})$ 3265, $\nu(\text{B-H})$ 2520 cm^{-1} .

Rotámero mayoritario (20a):

^1H RMN (CD_2Cl_2 , 500 MHz, -60 °C): δ 14.60 (s, 1 H, NH), 8.93 (d, 1 H, $^3J_{\text{HH}} = 4.5$ Hz, H₁₂), 8.46 (d, 2 H, $^3J_{\text{HH}} = 7.5$ Hz, 2 H₅), 7.93 (sa, 2 H, H₉, H₁₀), 7.54 (ta, 1 H, H₁₁), 7.46 (d, 1 H, $^3J_{\text{HH}} = 7.1$ Hz, H₈), 7.13 (d, 1 H, $^3J_{\text{HH}} = 8.4$ Hz, H₆), 7.09 (t, 1 H,

$^3J_{\text{HH}} = 7.0$ Hz, H_7), 7.07 (t, 2 H, $^3J_{\text{HH}} = 7.1$ Hz, 2 H_4), 6.70 (t, 2 H, $^3J_{\text{HH}} = 7.5$ Hz, 2 H_3), 6.47 (t, 2 H, $^3J_{\text{HH}} = 7.5$ Hz, 2 H_2), 6.40 (d, 2 H, $^3J_{\text{HH}} = 7.5$ Hz, 2 H_1), 5.68, 5.67 (s, 2:1, 3 H, 3 CH_{pz}), 2.45, 2.44, 0.82, 0.73 (s, 1:2:2:1, 18 H, 6 Me_{pz}).

$^{13}\text{C}\{^1\text{H}\}$ RMN (CD_2Cl_2 , 125 MHz, -60 °C): δ 180.2 (Ir=C), 152.9, 151.5 (1:2, 3 C_{qpz}), 151.6 (CH_{12}), 150.1 (C_{q2}), 144.9 (C_{q1}) 145.9 (CH_6), 145.0 (3 C_{qpz}), 143.3 (2 CH_1), 140.2 (2 Ir- C_{ph}), 139.9 (CH_{10}), 137.3 (2 CH_5), 135.6 (CH_7), 127.4 (CH_{11} , 2 CH_2), 127.2 (2 CH_4), 122.7 (2 CH_3), 121.8 (CH_9), 114.0 (CH_8), 108.9, 108.6 (1:2, CH_{pz}) 15.6, 15.4, 15.0, 14.9 (1:2:1:2, 6 Me_{pz}).

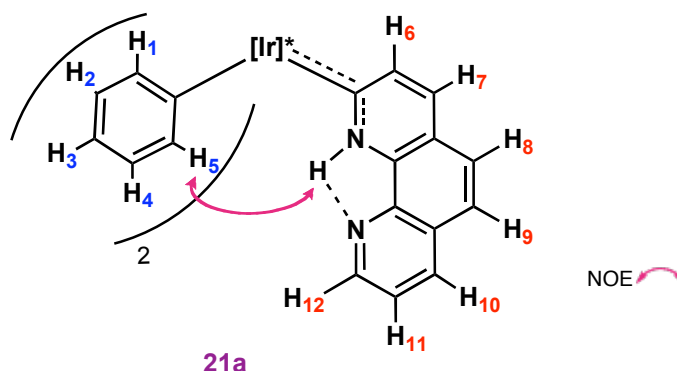
Rotámero minoritario (20b):

^1H RMN (CD_2Cl_2 , 500 MHz, -60 °C): δ 12.40 (s, NH),

Proporción de rotámeros (CD_2Cl_2 , -60 °C): 20:1.

HRMS (FAB) m/z calcd. (expt.) $\text{C}_{37}\text{H}_{40}\text{BIrN}_8$: 800.3098 (800.3134).

Anal. Calcd. $\text{C}_{37}\text{H}_{40}\text{BIrN}_8$: C, 55.6; H, 5.0; N, 14.0. **Expt.:** C, 55.1; H, 5.3; N, 13.6.

Compuesto 21**Rotámero mayoritario en CD₂Cl₂**

Se disuelven el compuesto $\text{Tp}^{\text{Me}_2}\text{Ir}(\text{C}_6\text{H}_5)_2(\text{N}_2)$ (200 mg, 0.3 mmol) y fenantrolina (1.2 equiv., 54 mg) en benceno (8 mL) y la disolución que resulta se agita durante 3 horas a 100 °C. Transcurrido este periodo de tiempo, se evapora el disolvente bajo presión reducida y el análisis mediante RMN de ^1H del residuo indica que la conversión del producto de partida en el compuesto **21** es cuantitativa. El residuo sólido se purifica mediante cromatografía en columna de gel de sílice (20:1 \rightarrow 5:1, hexano:Et₂O) aislandose el complejo **21**, sólido rojo, con un rendimiento del 45%, que se recristaliza desde una mezcla MeOH:CH₂Cl₂ (1:1).

Datos analíticos y espectroscópicos:

Sólido rojo

Masa Molecular: 824.3 g/mol.

IR (nujol): $\nu(\text{N-H})$ 3235, $\nu(\text{B-H})$ 2520 cm^{-1} .

Rotámero mayoritario (21a):

^1H RMN (CD₂Cl₂, 500 MHz, -60 °C): δ 14.92 (s, 1 H, NH), 9.22 (da, 1 H, $^3J_{\text{HH}} = 5.0$ Hz, H₁₂), 8.59 (d, 2 H, $^3J_{\text{HH}} = 7.5$ Hz, 2 H₅), 8.35 (d, 1 H, $^3J_{\text{HH}} = 8.2$ Hz, H₁₀), 7.78 (m, 2 H, H₈, H₁₁), 7.69 (d, 1 H, $^3J_{\text{HH}} = 8.9$ Hz, H₆), 7.47 (d, 1 H, $^3J_{\text{HH}} = 8.9$ Hz, H₇), 7.34 (d, 1 H, $^3J_{\text{HH}} = 8.8$ Hz, H₉), 7.10 (t, 2 H, $^3J_{\text{HH}} = 7.3$ Hz, 2 H₄), 6.71 (t, 2 H,

$^3J_{\text{HH}} = 7.0$ Hz, 2 H₃), 6.48 (t, 2 H, $^3J_{\text{HH}} = 7.2$ Hz, 2 H₂), 6.40 (d, 2 H, $^3J_{\text{HH}} = 7.7$ Hz, 2 H₁), 5.69 (sa, 3 H, 3 CH_{pz}), 2.49, 2.48, 0.79, 0.76 (s, 1:2:1:2, 18 H, 6 Me_{pz}).

$^{13}\text{C}\{^1\text{H}\}$ RMN (CD₂Cl₂, 125 MHz, -60 °C): δ 178.5 (Ir=C), 151.1, 149.7 (1:2, C_{qpz}), 150.0 (CH₁₂), 143.2 (3 C_{qpz}), 142.0 (CH₆), 141.0 (2 CH₁), 138.2 (2 Ir-C_{ph}, 2 C_{qphen}), 136.8 (C_{qphen}), 136.5 (CH₁₀), 135.0 (2 CH₅), 131.2 (CH₇), 127.9 (C_{qphen}), 125.7 (2 CH₄), 125.6 (2 CH₂), 124.4 (CH₈), 124.3 (CH₉), 124.2 (CH₁₁), 120.4 (CH₃), 107.1, 106.7 (1:2, CH_{pz}), 14.2, 13.5 (1:5, Me_{pz}).

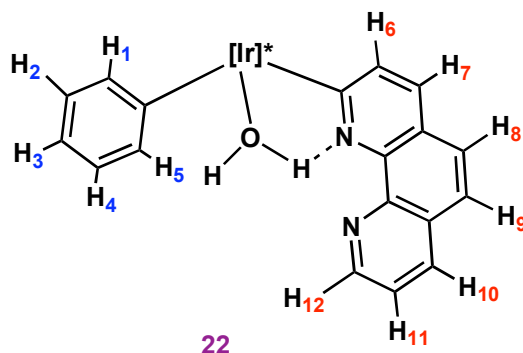
Rotámero minoritario (21b):

^1H RMN (CD₂Cl₂, 500 MHz, -60 °C): δ 12.67 (sa, NH).

Proporción de rotámeros (CD₂Cl₂, -60 °C): 20:1.

HRMS (FAB) m/z calcd. (expt.) C₃₉H₄₀BIrN₈: 824.3098 (824.3126).

Anal. Calcd. C₃₉H₄₀BIrN₈·CH₂Cl₂: C, 52.9; H, 4.7; N, 12.3. **Expt.:** C, 52.9; H 5.0; N, 12.7.

Compuesto 22

Se disuelve el compuesto $\text{Tp}^{\text{Me}_2}\text{Ir}(\text{C}_6\text{H}_5)_2(\text{N}_2)$ (200 mg, 0.3 mmol) y fenantrolina (1.2 equiv. 54 mg) en benceno (7 mL), y la disolución resultante se agita durante 2 horas a 60 °C, evaporándose posteriormente el disolvente bajo presión reducida. El análisis de RMN de ^1H del residuo indica que la conversión del producto de partida en el compuesto **22** es cuantitativa. El residuo sólido se purifica mediante cromatografía en columna de gel de sílice (5:1 \rightarrow 1:5, hexano:Et₂O), obteniéndose el complejo **22** con un rendimiento del 45%.

Datos analíticos y espectroscópicos:

Sólido naranja

Masa Molecular: 764.7 g/mol.

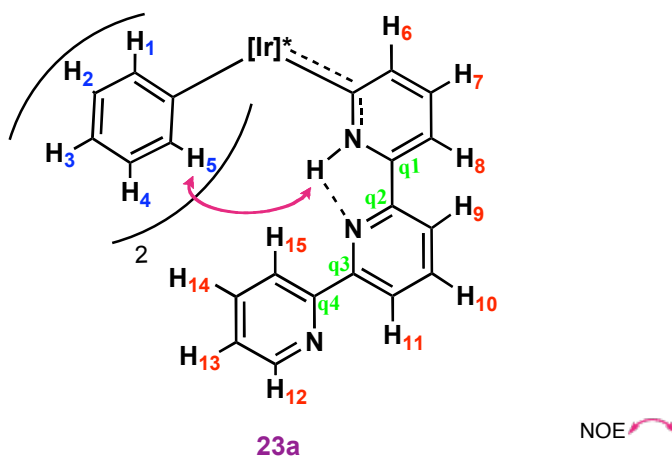
IR (nujol): $\nu(\text{O-H})$ 3605, $\nu(\text{B-H})$ 2515 cm^{-1} .

^1H RMN (CDCl_3 , 400 MHz, 25 °C): δ 9.27 (da, 1 H, $^3J_{\text{HH}} = 5.0$ Hz, H₁₂), 8.28 (d, 1 H, $^3J_{\text{HH}} = 8.1$ Hz, H₁₀), 7.98 (d, 1 H, $^3J_{\text{HH}} = 7.3$ Hz, H₅), 7.70 (m, 3 H, H₈, H₉, H₁₁), 7.57 (d, 1 H, $^3J_{\text{HH}} = 8.7$ Hz, H₇), 7.43 (d, 1 H, $^3J_{\text{HH}} = 8.6$ Hz, H₆), 7.04 (t, 1 H, $^3J_{\text{HH}} = 7.3$ Hz, H₄), 6.76 (t, 1 H, $^3J_{\text{HH}} = 7.3$ Hz, H₃), 6.65 (t, 1 H, $^3J_{\text{HH}} = 7.0$ Hz, H₂), 6.39 (d, 1 H, $^3J_{\text{HH}} = 7.2$ Hz, H₁) 5.81, 5.69, 5.59 (s, 1 H cada, 3 CH_{pz}), 2.39, 2.47, 0.84, 0.78 (s, 1:2:2:1, 18 H, 6 Me_{pz}).

El núcleo del hidrógeno puente se observa a 16.60 ppm a más baja temperatura (-70 °C) mientras que no se ha podido asignar el OH restante.

$^{13}\text{C}\{^1\text{H}\}$ RMN (CDCl_3 , 100 MHz, 25 °C): δ 180.6 (Ir-C_{phen}), 151.2, 150.4 (C_{qpz}) 150.4 (CH₁₂), 150.2, 143.2, 143.1, 142.6 (C_{qpz}), 140.5 (CH₁), 139.3 (CH₆), 138.9, 138.2, 136.3 (C_{qphen}), 138.8 (Ir-C_{ph}), 135.8 (CH₁₀), 131.0 (CH₇), 130.1 (CH₅), 128.2 (C_{qphen}), 125.7 (CH₂), 125.1 (CH₄), 124.4 (CH₈), 123.8 (CH₉), 123.6 (CH₁₁), 121.2 (CH₃), 107.5, 107.3, 107.0 (CH_{pz}), 16.3, 13.7, 13.2, 13.1, 13.0, 11.9 (Me_{pz}).

HRMS (FAB) m/z calc. (expt.) C₃₃H₃₅BIrN₈ - H₂O: 747.2698 (747.2707).

Compuesto 23**Rotámero mayoritario en CD₂Cl₂**

Se disuelven el compuesto $\text{Tp}^{\text{Me}_2}\text{Ir}(\text{C}_6\text{H}_5)_2(\text{N}_2)$ (200 mg, 0.3 mmol) y terpiridina (1.2 equiv., 83 mg) en 8 mL de benceno y la disolución resultante se agita durante 3 horas a 100 °C. Transcurrido este tiempo, se evapora el disolvente bajo presión reducida y el análisis mediante RMN de ^1H del residuo indica que la conversión del producto de partida en el compuesto **23** es cuantitativa. Este compuesto se purifica mediante cromatografía en columna de gel de sílice (20:1 \rightarrow 1:1, hexano:Et₂O), obteniéndose el complejo con un rendimiento del 25%.

Datos analíticos y espectroscópicos:

Sólido naranja

Masa Molecular: 877.3 g/mol.

IR (nujol): $\nu(\text{N-H})$ 3272, $\nu(\text{B-H})$ 2530 cm^{-1} .

Rotámero mayoritario (23a):

^1H RMN (CD_2Cl_2 , 400 MHz, -50 °C): δ 14.20 (s, 1 H, NH), 9.15 (d, 1 H, $^3J_{\text{HH}} = 8.2$ Hz, H₁₅), 8.79 (d, 1 H, $^3J_{\text{HH}} = 4.1$ Hz, H₁₂), 8.74 (d, 2 H, $^3J_{\text{HH}} = 7.9$ Hz, 2 H₅), 8.60 (d, 1 H, $^3J_{\text{HH}} = 7.9$ Hz, H₉), 8.08 (m, 2 H, H₁₀, H₁₄), 7.90 (d, 1 H, $^3J_{\text{HH}} = 7.9$ Hz,

H₁₁), 7.49 (m, 2 H, H₁₃, H₈), 7.10 (m, 2 H, H₇, H₆), 6.68 (t, 2 H, $^3J_{\text{HH}} = 7.3$ Hz, 2 H₄), 6.58 (t, 2 H, $^3J_{\text{HH}} = 7.3$ Hz, 2 H₃), 6.44 (t, 2 H, $^3J_{\text{HH}} = 7.3$ Hz, 2 H₂), 6.40 (d, 2 H, $^3J_{\text{HH}} = 7.9$ Hz, 2 H₁), 5.70, 5.66 (s, 2:1, 3 H, 3 CH_{pz}), 2.47, 0.78, 0.73 (s, 3:2:1, 18 H, 6 Me_{pz}).

¹³C{¹H} RMN (CD₂Cl₂, 100 MHz, -50 °C): δ 179.5 (Ir=C), 156.5 (C_{q4}), 154.9 (C_{q3}), 151.1 (C_{qpz}), 149.6 (CH₁₅), 149.4 (2 C_{qpz}), 148.2 (C_{q1}), 144.2 (C_{q2}), 143.2 (CH₆), 143.0 (3 C_{qpz}), 141.1 (2 CH₁), 139.1 (2 Ir-C_{ph}), 139.0 (CH₁₃), 137.8 (CH₁₀), 134.8 (2 CH₅), 133.7 (CH₇), 125.5 (2 CH₂), 125.2 (2 CH₄), 124.8 (CH₁₄), 122.7 (CH₉), 121.4 (CH₁₂), 120.2 (CH₁₁), 120.1 (2 CH₃), 113.3 (CH₈), 106.7, 106.5 (1:2, CH_{pz}), 13.7, 13.2, 13.3, 13. (1:2:1:2, Me_{pz}).

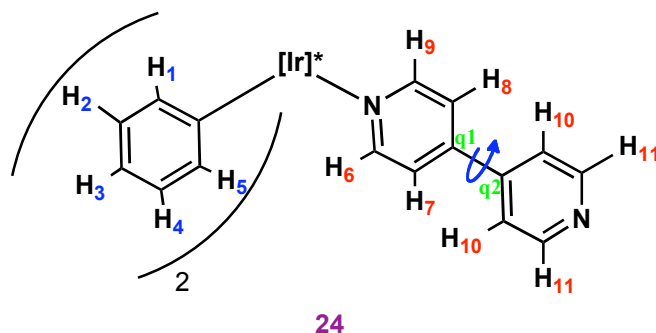
Rotámero minoritario (23b):

¹H RMN (CD₂Cl₂, 400 MHz, -50 °C): δ 12.45 (sa, 1 H, NH), 9.21 (d, 1 H, $^3J_{\text{HH}} = 8.6$ Hz, H₁₅), 7.69 (d, 1 H, $^3J_{\text{HH}} = 7.9$ Hz, H₁₁), 6.27 (d, 2 H, $^3J_{\text{HH}} = 7.8$ Hz, 2 H₁), 5.64, 5.55 (s, 2:1, 3 H, 3 CH_{pz}).

Proporción de rotámeros (CD₂Cl₂, -50 °C): 5:1.

HRMS (FAB) *m/z* calcd. (expt.) C₄₂H₄₃BIrN₉: 877.3364 (877.3363).

Anal. Calcd. C₄₂H₄₃BIrN₉ · 1/2 CH₂Cl₂: C, 55.9; H, 4.7; N, 13.6. **Expt.:** C, 55.8; H, 5.0; N, 13.7.

Compuesto 24

Se disuelve el compuesto $\text{Tp}^{\text{Me}_2}\text{Ir}(\text{C}_6\text{H}_5)_2(\text{N}_2)$ (200 mg, 0.3 mmol) y la 4,4'-bipiridina (1.2 equiv., 56 mg) en benceno (5 mL) y la disolución se agita durante 2 horas a 60 °C. Transcurrido este período de tiempo, se evapora el disolvente bajo presión reducida y el análisis de RMN de ^1H del residuo indica que la conversión del producto de partida en **24** es aproximadamente del 70%. El residuo sólido se cromatografía, utilizando una mezcla 80:1 hexano: Et_2O como eluyente, aislándose el compuesto **24** con un rendimiento del 30%.

Datos analíticos y espectroscópicos:

Sólido rojo burdeos

Masa molecular: 800.3 g/mol.

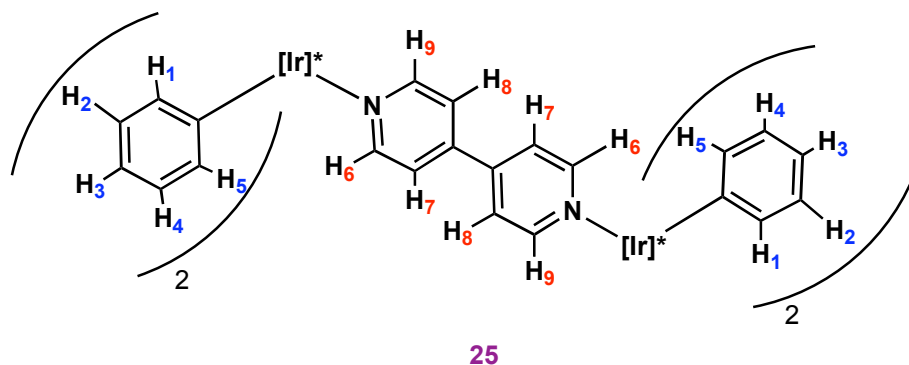
IR (KBr): $\nu(\text{B-H})$ 2520 cm^{-1} .

^1H RMN (CDCl_3 , 500 MHz, -10 °C): 10.20 (d, 1 H, $^3J_{\text{HH}} = 4.8$ Hz, H_6), 8.68 (d, 2 H, $^3J_{\text{HH}} = 4.8$ Hz, 2 H_{11}), 8.25 (da, 2 H, $^3J_{\text{HH}} = 7.5$ Hz, 2 H_5), 8.07 (d, 1 H, $^3J_{\text{HH}} = 5.0$ Hz, H_9), 7.62 (d, 1 H, $^3J_{\text{HH}} = 4.5$ Hz, H_7), 7.54 (d, 2 H, $^3J_{\text{HH}} = 5.2$ Hz, 2 H_{10}), 7.14 (da, 1 H, $^3J_{\text{HH}} = 5.0$ Hz, H_8), 7.03 (t, 2 H, $^3J_{\text{HH}} = 6.5$ Hz, 2 H_4), 6.73 (t, 2 H, $^3J_{\text{HH}} = 6.9$ Hz, 2 H_3), 6.50 (t, 2 H, $^3J_{\text{HH}} = 7.0$ Hz, 2 H_2), 6.33 (d, 2 H, $^3J_{\text{HH}} = 7.2$ Hz, 2 H_1), 5.71, 5.62 (s, 2:1, 3 H, 3 CH_{pz}), 2.46, 0.66, 0.57 (s, 3:2:1, 18 H, 6 Me_{pz}).

$^{13}\text{C}\{^1\text{H}\}$ RMN (CDCl_3 , 125 MHz, $-10\text{ }^\circ\text{C}$): δ 156.5 (CH_9), 153.6 (CH_8), 151.6, 149.5 (1:2, C_{qpz}), 150.9 (CH_{11} , CH_{12}), 144.8 (C_{q1}) 143.5, 143.4 (1:2, C_{qpz}), 141.4 (2 CH_1), 136.2 (2 Ir- C_{ph}), 135.1 (2 CH_5), 125.5 (2 CH_4), 124.8 (2 CH_3), 122.3 (CH_7 , CH_8 , C_{q2}), 121.3 (CH_{10} , CH_{13}), 120.8 (2 CH_3), 107.3, 107.1 (1:2, 3 CH_{pz}), 14.5, 14.1, 13.0, 12.4 (2:2:1:1, Me_{pz}).

HRMS (FAB) m/z calcd. (expt.) $\text{C}_{37}\text{H}_{40}\text{BIrN}_8$: 800.3098 (800.3085).

Anal. Calcd. $\text{C}_{37}\text{H}_{40}\text{BIrN}_8$: C, 55.6; H, 5.0; N, 14.0. **Expt.:** C, 56.1; H, 5.3; N, 13.9.

Compuesto 25

Se disuelven el compuesto $\text{Tp}^{\text{Me}_2}\text{Ir}(\text{C}_6\text{H}_5)_2(\text{N}_2)$ (200 mg, 0.3 mmol) y 4,4'-bipiridina (0.5 equiv., 28 mg) en benceno (5 mL) y la disolución se agita durante 2 horas a 60 °C. Transcurrido este tiempo, se evapora el disolvente bajo presión reducida y se analiza mediante RMN de ^1H el residuo resultante, observándose que la conversión del producto de partida en **25** es aproximadamente del 70%. Este compuesto se purifica mediante cromatografía en columna de gel de sílice, utilizando una mezcla 80:1 hexano: Et_2O como eluyente, con un rendimiento del 45%.

Datos analíticos y espectroscópicos:

Sólido rojo burdeos

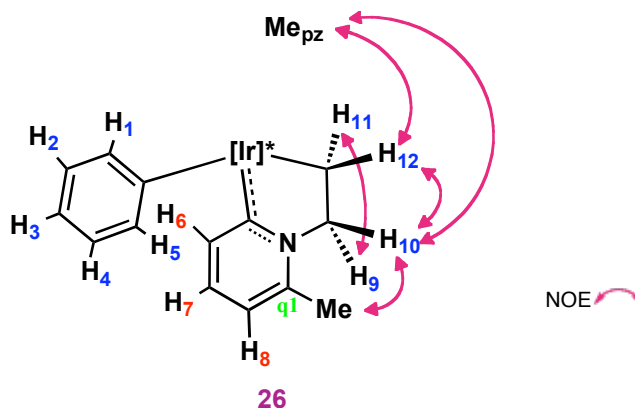
Masa molecular: 1443.4 g/mol.

IR (KBr): $\nu(\text{B-H}) = 2525 \text{ cm}^{-1}$.

^1H RMN (CD_2Cl_2 , 500 MHz, -60°C): δ 10.16 (d, 2 H, $^3J_{\text{HH}} = 4.8 \text{ Hz}$, 2 H_6), 8.18 (d, 4 H, $^3J_{\text{HH}} = 7.7 \text{ Hz}$, 4 H_5), 8.03 (d, 2 H, $^3J_{\text{HH}} = 5.0 \text{ Hz}$, 2 H_8), 7.56 (d, 2 H, $^3J_{\text{HH}} = 4.3 \text{ Hz}$, 2 H_7), 7.06 (d, 2 H, $^3J_{\text{HH}} = 4.6 \text{ Hz}$, 2 H_9), 6.99 (t, 4 H, $^3J_{\text{HH}} = 7.3 \text{ Hz}$, 4 H_4), 6.70 (t, 4 H, $^3J_{\text{HH}} = 6.9 \text{ Hz}$, 4 H_3), 6.45 (t, 4 H, $^3J_{\text{HH}} = 7.0 \text{ Hz}$, 4 H_2), 6.30 (d, 4 H, $^3J_{\text{HH}} = 7.8 \text{ Hz}$, 4 H_1), 5.67, 5.58 (s, 2:1, 6 CH_{pz}), 2.42, 0.59, 0.53 (s, 3:2:1, 12 Me_{pz}).

HRMS (FAB) m/z calcd.(expt.) $C_{64}H_{72}B_2Ir_2N_{14}$: 1444.5490 (1444.5509).

Compuesto 26



Se disuelve el compuesto **2** (50 mg, 0.07 mmol) en benceno (3 mL) y se transfiere la disolución a un tubo de presión, que se carga con 2 atm. de etileno. Se agita durante 12 horas a 120 °C y, transcurrido este tiempo, se evapora el disolvente bajo presión reducida. El análisis mediante RMN de ^1H del residuo indica que la conversión del producto de partida en el compuesto **26** es cuantitativa. La muestra se purifica mediante cromatografía en columna de gel de sílice (15:1 \rightarrow 5:1, hexano:Et₂O), obteniéndose el complejo con un rendimiento de 65%. Se pueden obtener cristales amarillos por evaporación lenta de sus disoluciones en hexano:Et₂O a temperatura ambiente.

Datos analíticos y espectroscópicos:

Sólido amarillo

Masa Molecular: 686.7 g/mol.

IR (nujol): $\nu(\text{B-H})$ 2530 cm^{-1} .

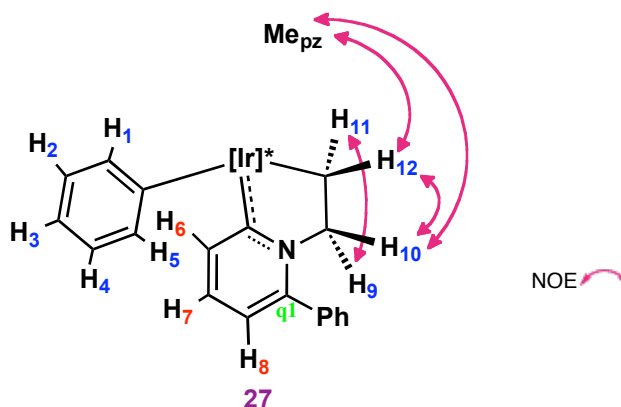
^1H NMR (CDCl₃, 500 MHz, 25 °C): δ 7.32 (d, 1 H, $^3J_{\text{HH}} = 7.3$ Hz, H₆), 6.84 (m, 2 H, H₇, H₅), 6.76 (t, 1 H, $^3J_{\text{HH}} = 7.3$ Hz, H₄), 6.66 (t, 1 H, $^3J_{\text{HH}} = 7.3$ Hz, H₃), 6.54 (m, 3 H, H₈, H₂, H₁), 5.73, 5.71, 5.61 (s, 1 H cada, 3 CH_{pz}), 5.15, 4.54 (dt, ddd, 1 H cada,

$^2J_{\text{HH}} = 14.5$, $^3J_{\text{HH}} = 9.6$; $^3J_{\text{HH}} = 9.9$, 1.5 Hz, H₉, H₁₀), 3.05, 2.81 (dt, td, 1 H cada, $^2J_{\text{HH}} = 10.2$, $^3J_{\text{HH}} = 9.0$; $^3J_{\text{HH}} = 10.2$, 1.4 Hz, H₁₂, H₁₁), 2.65 (s, 3 H, Me_{py}), 2.42, 2.40, 2.36, 1.78, 1.51, 1.18 (s, 3 H cada, 6 Me_{pz}).

$^{13}\text{C}\{^1\text{H}\}$ NMR (CDCl₃, 125 MHz, 25 °C): δ 189.4 (Ir=C), 151.1, 149.2, 148.0 (C_{qpz}), 147.5 (C_{q1}), 142.7, 142.5, 142.1 (C_{qpz}), 141.3 (CH₁), 138.7 (Ir-C_{ph}), 137.8 (CH₆), 136.2 (CH₅), 130.4 (CH₇), 125.4 (CH₂), 125.0 (CH₄), 119.4 (CH₃), 116.4 (CH₈), 107.1, 106.6 (2:1, CH_{pz}), 62.4 (NCH₂, $^1J_{\text{CH}} = 138$ Hz), 23.0 (Me_{py}), 14.0, 13.9, 12.8, 11.7 (1:1:3:1, Me_{pz}), -12.4 (Ir-CH₂, $^1J_{\text{CH}} = 128$ Hz).

HRMS (FAB) m/z calcd. (expt.) C₂₉H₃₇BIrN₇: 687.2833 (687.2845).

Anal. Calcd. C₂₉H₃₇BIrN₇: C, 50.7.; H, 5.4; N, 14.3. **Expt.:** C, 50.9; H, 5.7; N, 13.8.

Compuesto 27

Se disuelve el compuesto **4** (50 mg, 0.06 mmol) en benceno (3 mL) y la disolución se transfiere a un tubo de presión que se carga con 2 atmósferas de etileno y se agita durante 12 horas a 90 °C. Transcurrido este tiempo, se evapora el disolvente bajo presión reducida y el análisis mediante RMN de ^1H del residuo indica que la conversión del producto de partida en el compuesto **27** es cuantitativa. La muestra se purifica mediante cromatografía en columna de gel de sílice (20:1 \rightarrow 5:1, hexano:Et₂O), obteniéndose el complejo **27** con un rendimiento del 60%.

Datos analíticos y espectroscópicos:

Sólido naranja

Masa Molecular: 749.3 g/mol.

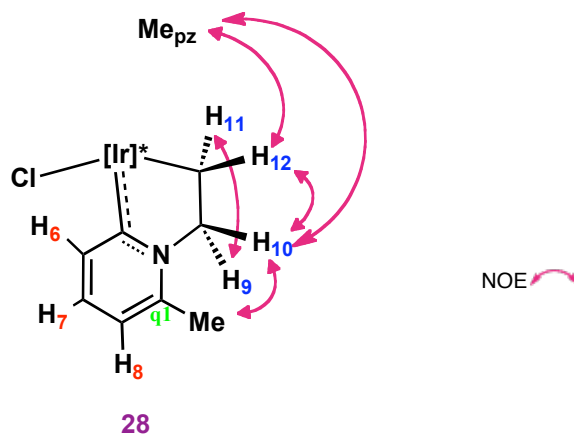
IR (nujol): $\nu(\text{B-H})$ 2520 cm^{-1} .

^1H NMR (CDCl_3 , 500 MHz, 25 °C): δ 7.47 (m, 6 H, H₆, 5 CH_{phpy}), 7.15 (d, 1 H, $^3J_{\text{HH}} = 7.3$ Hz, H₅), 6.97 (t, 1 H, $^3J_{\text{HH}} = 7.3$ Hz, H₇), 6.89 (t, 1 H, $^3J_{\text{HH}} = 7.3$ Hz, H₄), 6.71 (t, 1 H, $^3J_{\text{HH}} = 7.3$ Hz, H₃), 6.60 (m, 3 H, H₁, H₂, H₈), 5.73, 5.71, 5.61 (s, 1 H cada, 3 CH_{pz}), 5.21, 4.17 (dt, ddd, 1 H cada, $^2J_{\text{HH}} = 14.5$, $^3J_{\text{HH}} = 9.6$; $^3J_{\text{HH}} = 9.9$, 1.5 Hz, H₉, H₁₀), 2.90, 2.62 (dt, td, 1 H cada, $^2J_{\text{HH}} = 10.5$, $^3J_{\text{HH}} = 9.0$; $^3J_{\text{HH}} = 10.5$, 1.4 Hz, H₁₂, H₁₁), 2.44, 2.41, 2.37, 1.79, 1.42, 1.26 (s, 3 H cada, 6 Me_{pz}).

$^{13}\text{C}\{^1\text{H}\}$ NMR (CDCl_3 , 125 MHz, 25 °C): δ 190.6 (Ir=C), 151.2 (C_{q1}), 151.1, 149.2, 148.1, 142.8, 142.6, 142.2 (C_{qpz}), 141.9 (CH_1), 139.3 (CH_6), 138.3 (C_{qphpy}), 137.1 (Ir- C_{ph}), 136.2 (CH_5), 129.9 (CH_7), 128.8, 128.8, 127.7 (1:2:2 ratio, CH_{phpy}), 125.6 (CH_2), 125.0 (CH_4), 119.6 (CH_3), 117.0 (CH_8), 107.3, 107.0, 106.6 (CH_{pz}), 65.8 (NCH_2 , $^1J_{\text{CH}} = 139$ Hz), 14.8, 13.8, 12.8, 11.7 (1:1:3:1, Me_{pz}), -11.7 (Ir- CH_2 , $^1J_{\text{CH}} = 130$ Hz).

HRMS (FAB) m/z calcd. (expt.) $\text{C}_{34}\text{H}_{40}\text{BIrN}_7$: 749.2974 (749.2989).

Anal. Calcd. $\text{C}_{34}\text{H}_{40}\text{BIrN}_7$: C, 54.5; H, 5.3; N, 13.10. **Expt.:** C, 54.5; H, 5.3; N, 12.5.

Compuesto 28

El compuesto **26** (30 mg, 0.044 mmol) se disuelve en CDCl_3 , en un tubo de RMN, y se somete a la acción de la luz (tubo fluorescente del laboratorio). La reacción se sigue mediante RMN de ^1H . Al cabo de ~ 24 h se lleva a sequedad, se cromatografía en columna de gel de sílice ($5:1 \rightarrow 1:1$, hexano: Et_2O) y se obtiene el compuesto **28** con un rendimiento del 45%.

Datos analíticos y espectroscópicos:

Sólido verde claro

Masa Molecular: 645.0 g/mol.

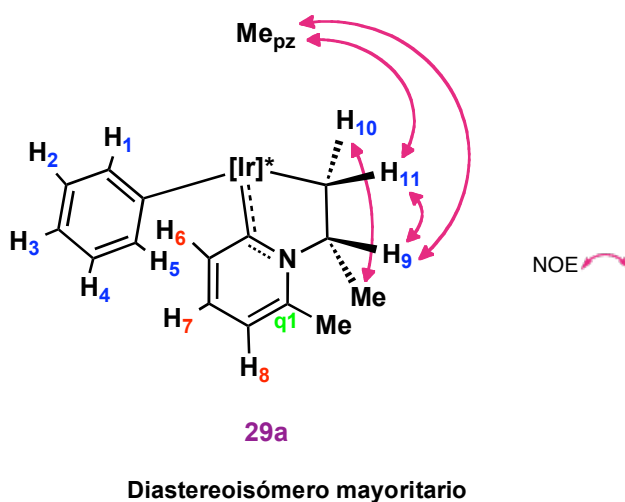
^1H RMN (CDCl_3 , 500 MHz, 25 °C): δ 7.41 (d, 1 H, $^3J_{\text{HH}} = 8.0$ Hz, H_6), 7.24 (t, 1 H, $^3J_{\text{HH}} = 7.7$ Hz, H_7), 6.72 (d, 1 H, $^3J_{\text{HH}} = 7.2$ Hz, H_8), 5.80, 5.75, 5.52 (s, 1 H cada, 3 CH_{pz}), 5.15, 4.44 (dt, ddd, 1 H cada, $^2J_{\text{HH}} = 12.5$, $^3J_{\text{HH}} = 9.5$; $^3J_{\text{HH}} = 8.0$, 1.5 Hz, H_9 , H_{10}), 3.55, 3.30 (dt, td, 1 H cada, $^2J_{\text{HH}} = 9.3$, $^3J_{\text{HH}} = 9.2$; $^3J_{\text{HH}} = 9.4$, 1.2 Hz, H_{12} , H_{11}), 2.72, 2.37, 2.35, 2.33, 2.23, 1.23 (s, 3 H cada, 6 Me_{pz}), 2.61 (s, 3 H, Me_{py}).

$^{13}\text{C}\{^1\text{H}\}$ RMN (CDCl_3 , 125 MHz, 25 °C): δ 181.7 (Ir=C), 150.5, 149.5, 148.3, 143.2, 142.6, 142.4 (C_{qpz}), 147.3 (C_{q1}), 138.1 (CH_6), 130.4 (CH_7), 118.5 (CH_8), 108.4, 107.9, 107.0 (CH_{pz}), 63.5 (NCH_2), 22.8 (Me_{py}), 14.8, 14.5, 13.2, 12.9, 12.6, 12.51 (Me_{pz}), -10.1 (Ir- CH_2).

HRMS (FAB) m/z calcd. (expt.) $\text{C}_{23}\text{H}_{32}\text{BIrClN}_7 + \text{Na}$: 668.2028 (668.2010).

Compuestos 29a y 29b

Se disuelve el compuesto **2** (50 mg, 0.06 mmol) en benceno (3 mL) y la disolución resultante se calienta durante 12 horas a 110 °C bajo 4 atm. de propeno. Transcurrido este tiempo se evapora el disolvente bajo presión reducida y el análisis de RMN de ^1H del residuo indica que la conversión del producto de partida en el compuesto **29** (mezcla de los diastereoisómeros **29a** y **29b** en proporción 3:1) es cuantitativa. La muestra se purifica mediante cromatografía en columna de gel de sílice (40:1 \rightarrow 10:1, hexano:Et₂O), obteniéndose el isómero **29b** (rendimiento: 23%) y sucesivamente el isómero **29a** (rendimiento: 40%)



Datos analíticos y espectroscópicos:

Sólido amarillo

Masa Molecular: 700.7 g/mol.

IR (nujol): ν (B–H) 2525 cm^{-1} .

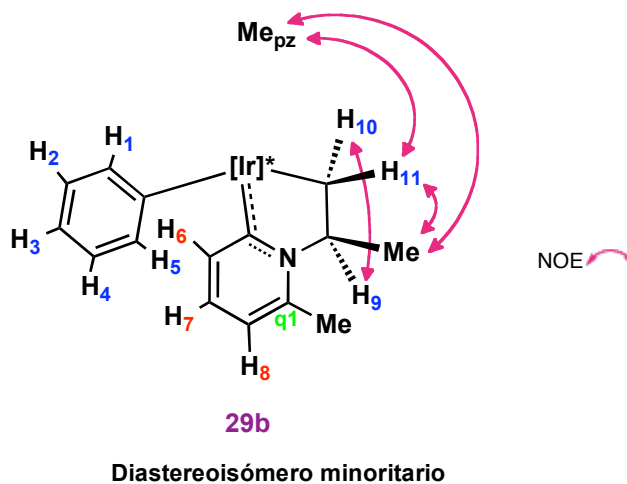
^1H RMN (C₆D₆, 500 MHz, 25 °C): δ 7.66 (d, 1 H, $^3J_{\text{HH}}$ = 8.5 Hz, H₆), 7.33 (m, 2 H, H₄, H₅), 7.00 (m, 3 H, H₂, H₃, H₁), 6.27 (t, 1 H, $^3J_{\text{HH}}$ = 7.7 Hz, H₇), 5.90 (d, 1 H, $^3J_{\text{HH}}$ = 7.2 Hz, H₈), 5.85, 5.78, 5.63 (s, 1 H cada, 3 CH_{pz}), 4.62 (m, 1 H, H₉), 3.71, 3.01 (t,

d, 1 H cada, $^2J_{\text{HH}} = ^3J_{\text{HH}} = 9.9$ Hz; H₁₁, H₁₀), 2.52, 2.35, 2.34, 2.27, 1.64, 1.37 (s, 3 H cada, 6 Me_{pz}), 1.98 (s, 3 H, Me_{py}), 1.80 (d, 3 H, $^3J_{\text{HH}} = 6.0$ Hz, NCH(Me)).

$^{13}\text{C}\{^1\text{H}\}$ RMN (C₆D₆, 125 MHz, 25 °C): δ 191.0 (Ir=C), 151.4 (C_{q1}), 150.6, 148.7, 148.0, 143.0, 142.9, 142.6 (C_{qpz}), 141.8 (CH₁, CH₅), 138.6 (CH₆), 135.4 (Ir-C_{ph}), 130.7 (CH₇), 126.5 (CH₂), 124.6 (CH₄), 120.9 (CH₃), 117.8 (CH₈), 108.1, 108.0, 107.9 (CH_{pz}), 71.0 (NCH(Me)), $^1J_{\text{CH}} = 135$ Hz), 25.7 (NCH(Me)), 21.4 (Me_{py}) 16.4, 14.4, 13.2, 13.0, 11.9 (1:1:1:2:1, 6 Me_{pz}), -2.0 (Ir-CH₂, $^1J_{\text{CH}} = 129$ Hz).

HRMS (FAB) m/z calc. (expt.) C₃₀H₃₉BIrN₇(Na): 724.2887 (724.2836)

Anal. Calc. C₃₀H₃₉BIrN₇·1/2 C₆H₁₄: C, 53.3; H, 6.2; N, 13.2. **Expt.:** C, 52.7; H, 6.0; N, 12.9.



Datos analíticos y espectroscópicos:

Sólido amarillo

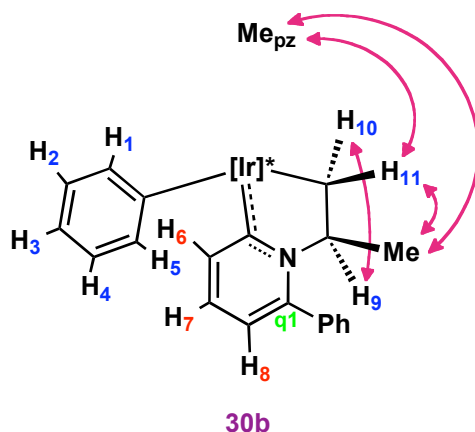
Masa Molecular: 700.7 g/mol.

IR (nujol): ν (B–H) 2520 cm^{-1} .

^1H RMN (C_6D_6 , 500 MHz, 25 °C): δ 7.41 (d, 1 H, $^3J_{\text{HH}} = 7.7$ Hz, H_6), 7.10 (m, 2 H, H_4, H_5), 6.97 (m, 2 H, H_3, H_1), 6.84 (t, 1 H, $^3J_{\text{HH}} = 6.7$ Hz, H_2), 6.17 (t, 1 H, $^3J_{\text{HH}} = 7.7$ Hz, H_7), 5.79 (d, 1 H, $^3J_{\text{HH}} = 6.8$ Hz, H_8), 5.71, 5.66, 5.63 (s, 1 H cada, 3 CH_{pz}), 5.49 (m, 1 H, H_9), 3.64, 3.16 (dd, dd, 1 H cada, $^2J_{\text{HH}} = 10.9$, $^3J_{\text{HH}} = 9.2$; $^3J_{\text{HH}} = 9.0$ Hz, $\text{H}_{11}, \text{H}_{10}$) 2.31, 2.30, 2.26, 2.24, 1.67, 1.36 (s, 3 H cada, 6 Me_{pz}), 1.86 (Me_{py}) 1.47 (d, 3 H, $^3J_{\text{HH}} = 6.0$ Hz, $\text{NCH}(\text{Me})$).

$^{13}\text{C}\{^1\text{H}\}$ RMN (C_6D_6 , 125 MHz, 25 °C): δ 193.8 (Ir=C), 151.4, 149.6, 148.7, 142.7, 142.4, 142.0 (C_{qpz}), 149.0 (C_{q1}), 141.9 (CH_1), 138.5 (CH_6), 136.9 (Ir– C_{ph}), 135.7 (CH_5), 129.3 (CH_7), 126.0 (CH_2), 125.4 (CH_4), 120.3 (CH_3), 117.9 (CH_8), 107.8, 107.2, 107.1 (CH_{pz}), 69.2 ($\text{NCH}(\text{Me})$, $^1J_{\text{CH}} = 141$ Hz), 25.7 ($\text{NCH}(\text{Me})$), 21.4 (Me_{py}) 15.4, 14.5, 14.0, 12.8, 12.7, 12.6 (Me_{pz}), 3.3 (Ir– CH_2 , $^1J_{\text{CH}} = 129$ Hz).

HRMS (FAB) m/z calcd. (expt.) $\text{C}_{30}\text{H}_{39}\text{BIrN}_7(\text{Na})$: 724.2887 (724.2924).

Compuesto 30a y 30b**Diastereoisómero mayoritario**

Se disuelve el compuesto **3** (50 mg, 0.06 mmol) en benceno (8 mL) y la disolución se calienta durante 12 horas a 90 °C bajo 4 atm. de propeno. Transcurrido este tiempo se evapora el disolvente bajo presión reducida y el análisis mediante RMN de ^1H del residuo indica que la conversión del producto de partida en el compuesto **30** (mezcla de diastereoisómeros **30a** y **30b** en proporción 1:5). La muestra se purifica mediante cromatografía en columna de gel de sílice (40:1 → 10:1, hexano:Et₂O), obteniéndose la mezcla **30a** y **30b** con un rendimiento del 50%.

Datos analíticos y espectroscópicos:

Sólido naranja

Masa Molecular 764.3 g/mol.

IR (nujol): ν (B–H) 2520 cm^{-1} .

Isómero mayoritario (30b):

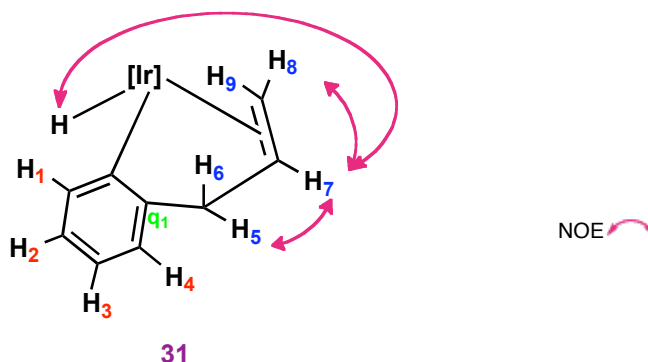
^1H NMR (CDCl_3 , 500 MHz, 5 °C): δ 7.52 (m, 5 H, 5 CH_{ppy}), 7.45 (d, 1 H, $^3J_{\text{HH}} = 7.3$ Hz, H₆), 7.38 (d, 1 H, $^3J_{\text{HH}} = 7.3$ Hz, H₅), 6.94 (m, 2 H, H₇, H₄), 6.71 (t, 1 H, $^3J_{\text{HH}} = 7.3$ Hz, H₃), 6.67 (d, 1 H, $^3J_{\text{HH}} = 7.3$ Hz, H₈), 6.60 (t, 1 H, $^3J_{\text{HH}} = 7.3$ Hz, H₂),

6.53 (d, 1 H, $^3J_{\text{HH}} = 7.3$ Hz, H₁), 5.81 (m, 1 H, H₉), 5.71, 5.66, 5.63 (s, 1 H cada, 3 CH_{pz}), 3.04, 2.75 (t, t, 1 H cada, $^2J_{\text{HH}} = 10.1$, $^3J_{\text{HH}} = 10.1$ Hz, H₁₁, H₁₀), 2.43, 2.42, 2.37, 1.95, 1.53, 1.08 (s, 3 H cada, 6 Me_{pz}), 1.02 (d, 3 H, $^3J_{\text{HH}} = 6.0$ Hz, NCH(Me)).

$^{13}\text{C}\{^1\text{H}\}$ NMR (CDCl₃, 125 MHz, 5 °C): δ 194.2 (Ir=C), 153.0 (C_{q1}), 151.3, 149.2, 148.7, 143.1, 143.0, 142.1 (C_{qpz}), 141.5 (CH₁), 139.7 (CH₆), 137.6 (Ir-C_{ph}), 137.1 (C_{qphpy}), 135.8 (CH₅), 130.2 (CH₇), 129.2, 129.1, 129.0 (2:2:1, CH_{phpy}), 125.8 (CH₂), 125.6 (CH₄), 119.7 (CH₃), 119.6 (CH₈), 107.4, 107.2, 106.4 (CH_{pz}), 70.6 (NCH(Me), $^1J_{\text{CH}} = 143$ Hz), 24.5 (NCH(Me)), 15.4, 14.2, 13.9, 13.4, 13.1, 13.0 (Me_{pz}), 2.7 (Ir-CH₂, $^1J_{\text{CH}} = 126$ Hz).

HRMS (FAB) m/z calcd. (expt.) C₃₅H₄₁BIrN₇: 763.3146 (763.3185).

Anal. Calcd. C₃₅H₄₁BIrN₇·C₆H₁₄: C, 58.0; H, 6.5; N, 11.6. **Expt.:** C, 57.4; H, 5.9; N, 12.4.

Compuesto 31**MÉTODO A:**

Se disuelve el compuesto **4** (50 mg, 0.06 mmol) en benceno (2 mL) y se transfiere la disolución a un tubo de presión que se carga con 2 atm. de propeno. Se agita la disolución durante 12 horas a 120 °C y se evapora después el disolvente bajo presión reducida. El residuo que resulta se disuelve en pentano (3×10 mL), se filtra y se concentra a un cuarto de su volumen y se deja cristalizar a - 23 °C. Los cristales obtenidos se filtran y se secan a vacío. El rendimiento del producto aislado es del 60%.

MÉTODO B:

Se disuelve el compuesto $\text{Tp}^{\text{Me}_2}\text{Ir}(\text{C}_6\text{H}_5)_2(\text{N}_2)$ (200 mg, 0.3 mmol) en benceno (8 mL) y se calienta durante 12 horas a 90 °C bajo 4 atm. de propeno. Transcurrido este tiempo se evapora el disolvente bajo presión reducida, observándose mediante RMN de ^1H del residuo que la conversión del producto de partida en el compuesto **31** es cuantitativa. El residuo se disuelve en una mezcla pentano/ Et_2O , se filtra, se concentra y la disolución se enfría a -20 °C. El sólido que se obtiene se lava con pentano frío y se seca a vacío. Rendimiento: 70%.

Datos analíticos y espectroscópicos:

Sólido marrón claro

Masa Molecular: 607.6 g/mol.

IR (nujol): $\nu(\text{B-H})$ 2530; $\nu(\text{Ir-H})$ 2030 cm^{-1} .

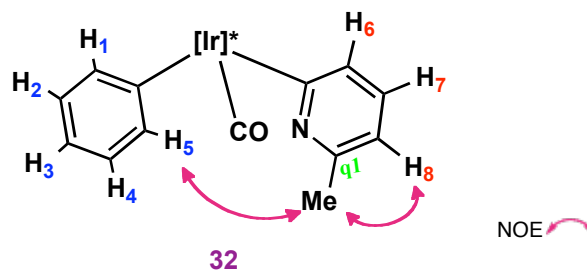
^1H RMN (C_6D_6 , 400 MHz, 25 $^\circ\text{C}$): δ 7.12 (d, 1 H, $^3J_{\text{HH}} = 7.2$ Hz, H_4), 6.92 (t, 1 H, $^3J_{\text{HH}} = 7.2$ Hz, H_3), 6.71 (t, 1 H, $^3J_{\text{HH}} = 7.2$ Hz, H_2), 6.66 (d, 1 H, $^3J_{\text{HH}} = 7.5$ Hz, H_1), 5.37 (dd, 1 H, $^3J_{\text{HH}} = 16.6$, 9.1 Hz, H_7), 5.63, 5.59, 5.47 (s, 3 H cada, 3 CH_{pz}) 3.73 (dd, 1 H, $^2J_{\text{HH}} = 16.2$, $^3J_{\text{HH}} = 6.2$ Hz, H_5) 3.63 (d, 1 H, $^2J_{\text{HH}} = 16.4$ Hz, H_6), 3.23 (d, 1 H, $^3J_{\text{HH}} = 11.2$ Hz, H_9), 2.71 (d, 1 H, $^1J_{\text{HH}} = 8.4$ Hz, H_8), 2.20, 2.16, 2.11, 2.02, 1.77, 1.50 (s, 3 H cada, 6 Me_{pz}), -16.67 (s, 1 H, Ir-H).

$^{13}\text{C}\{^1\text{H}\}$ RMN (C_6D_6 , 100 MHz, 25 $^\circ\text{C}$): δ 152.6 (C_{q1}), 151.9, 150.5, 149.9, 143.0, 142.0 (1:1:1:1:2, C_{qpz}), 136.9 (Ir- C_{ph}), 136.4 (CH_4), 123.9 (CH_3), 122.7 (CH_1), 122.1 (CH_2), 108.2, 106.7, 106.6 (CH_{pz}), 69.5 (CH_7), 41.7 (CH_5H_6), 40.3 (CH_8H_9) 16.2, 14.0, 13.6, 12.4, 12.3, 12.2 (Me_{pz}).

HRMS (FAB) m/z calcd. (expt.) $\text{C}_{24}\text{H}_{32}\text{BIrN}_6\text{-H}$: 607.2333 (607.2330).

Anal. Calcd. $\text{C}_{24}\text{H}_{33}\text{BIrN}_6$: C, 47.4; H, 5.5; N, 13.8. **Expt.:** C, 48.3; H, 5.8; N, 12.7.

Compuesto 32



Se disuelve el compuesto **2** (70 mg, 0.10 mmol) en benceno (10 mL) y se calienta la disolución resultante a 100 °C, bajo 2 atm. de CO, durante 12 horas. Transcurrido este tiempo se evapora el disolvente bajo presión reducida y el análisis mediante RMN de ^1H del residuo indica que la conversión del producto de partida en el compuesto **32** es cuantitativa. Se lava el residuo con 4 mL de pentano y se seca bajo vacío. Se obtiene un sólido amarillo pálido, con un rendimiento del 80%.

Datos analíticos y espectroscópicos:

Sólido amarillo pálido

Masa Molecular: 686.6 g/mol.

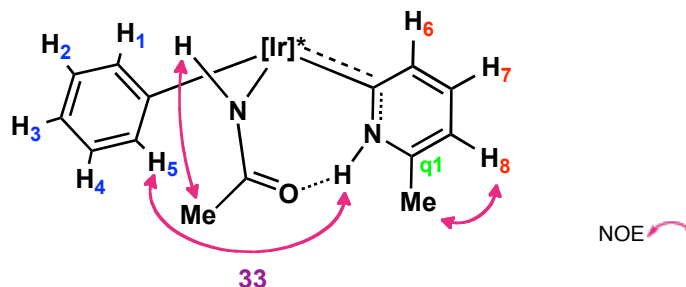
IR (KBr): $\nu(\text{B-H})$ 2520; $\nu(\text{CO})$ 2040 cm^{-1} .

^1H NMR (CDCl_3 , 400 MHz, 25 °C): δ 8.89 (d, 1 H, $^3J_{\text{HH}} = 7.3$ Hz, H₅), 7.08 (t, 1 H, $^3J_{\text{HH}} = 7.3$ Hz, H₄), 6.97 (t, 1 H, $^3J_{\text{HH}} = 7.3$ Hz, H₃), 6.69 (m, 2 H, H₂, H₇), 6.57 (d, 1 H, $^3J_{\text{HH}} = 7.3$ Hz, H₈), 6.37 (d, 1 H, $^3J_{\text{HH}} = 7.3$ Hz, H₁), 6.20 (d, 1 H, $^3J_{\text{HH}} = 7.3$ Hz, H₆), 5.76, 5.75 (s, 2:1, 3 CH_{pz}), 2.59 (s, 3 H, Me_{py}), 2.48, 2.44, 2.43, 1.64, 1.51, 0.97 (s, 3 H cada, 6 Me_{pz}).

$^{13}\text{C}\{^1\text{H}\}$ NMR (CDCl_3 , 100 MHz, 25 °C): δ 167.0 (Ir–CO), 156.3 (Ir–C_{py}), 155.4 (C_{q1}), 151.9, 150.9, 143.6, 143.5, 143.4 (1:2:1:1:1, C_{qpz}), 138.2 (CH₁), 137.8 (Ir–C_{ph}), 137.6 (CH₅), 132.0 (CH₇), 129.5 (CH₆), 126.3 (CH₂), 125.8 (CH₄), 122.3 (CH₃), 115.9 (CH₈), 107.8, 106.7, 106.6 (CH_{pz}), 24.6 (Me_{py}), 15.0, 13.7, 13.3, 12.8, 12.5, 12.4 (Me_{pz}).

HRMS (FAB) m/z calcd. (expt.): C₂₈H₃₃BIrN₇O (expt.): 687.2469 (687.2496).

Anal. Calcd.: C₂₈H₃₃BIrN₇O: C, 49.0; H, 4.8; N, 14.3. **Expt.:** C, 48.5; H, 5.3; N, 13.9.

Compuesto 33

Se disuelve el compuesto **2** (60 mg, 0.08 mmol) en una mezcla de NCCH_3 y benceno (1:1; 6 mL) y se calienta durante 12 horas a 120 °C. Transcurrido este tiempo se evapora el disolvente y, mediante el análisis de RMN de ^1H del residuo, se observa que la conversión del producto de partida en el compuesto **33** es cuantitativa. El producto se disuelve en una mezcla de CH_2Cl_2 :MeOH (1:2), se filtra y mediante evaporación lenta se obtiene un precipitado cristalino, que se aísla y se seca a vacío. Rendimiento: 70%.

Datos analíticos y espectroscópicos:

Sólido amarillo pálido

Masa Molecular: 717.7 g/mol.

IR (KBr): $\nu(\text{B-H})$ 2520 cm^{-1} .

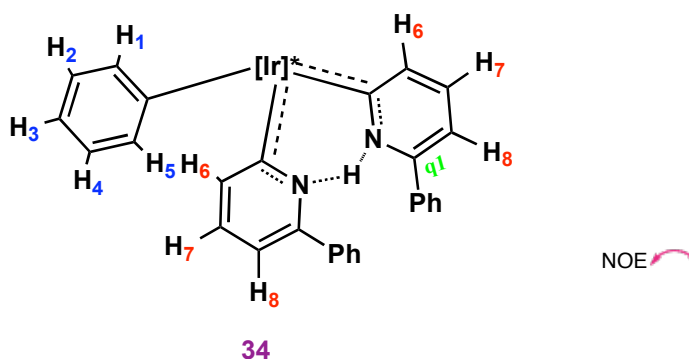
^1H RMN (CDCl_3 , 400 MHz, 25 °C): δ 18.03 (s, 1 H, NH), 8.51 (d, 1 H, $^3J_{\text{HH}} = 7.7$ Hz, H₅), 7.05 (t, 1 H, $^3J_{\text{HH}} = 6.8$ Hz, H₄), 6.86 (t, 1 H, $^3J_{\text{HH}} = 7.8$ Hz, H₇), 6.74 (t, 1 H, $^3J_{\text{HH}} = 7.0$ Hz, H₃), 6.62 (d, 1 H, $^3J_{\text{HH}} = 7.1$ Hz, H₈), 6.52 (m, 2 H, H₂, H₆), 6.11 (d, 1 H, $^3J_{\text{HH}} = 7.9$ Hz, H₁), 5.71, 5.70, 5.69 (s, 3 H cada, 3 CH_{pz}), 4.87 (s, 1 H, $\text{NH}(\text{C}(=\text{O})\text{Me})$), 2.73 (s, 3 H, Me_{py}), 2.47, 2.42, 2.41, 1.47, 1.42, 0.83 (s, 3 H cada, 6 Me_{pz}), 1.95 (s, 3 H, $\text{C}(=\text{O})\text{Me}$).

$^{13}\text{C}\{^1\text{H}\}$ RMN (CDCl_3 , 100 MHz, 25 °C): δ 177.4 (NH(C=O)Me), 169.9 (Ir=C), 150.4, 150.3, 150.2, 143.3, 143.1, 142.9 (C_{qpz}), 148.6 (C_{ql}), 140.7 (CH_1), 138.6 (CH_5), 137.6 (CH_6), 135.0 (Ir- C_{ph}), 134.0 (CH_7), 125.3 (CH_2), 125.2 (CH_4), 120.4 (CH_3), 115.8 (CH_8), 107.4, 107.2, 106.4 (CH_{pz}), 27.4 (NH(CO)Me), 19.6 (Me_{py}) 15.4, 13.1, 12.7, 12.6, 12.4, 12.3 (Me_{pz}).

HRMS (FAB) m/z calcd. (expt.): $\text{C}_{29}\text{H}_{38}\text{BIrN}_8\text{O}$: 718.2333 (718.2330)

Anal. Calcd.: $\text{C}_{29}\text{H}_{38}\text{BIrN}_8\text{O}$: C, 48.5; H, 5.3; N, 15.6. **Expt.:** C, 48.7; H 5.3; N, 15.5.

Compuesto 34



Se disuelve el compuesto **4** (20 mg, 0.025 mmol) en benceno (2 mL) y se añade 2-fenilpiridina (20 equiv., ~ 8 μ L). La disolución se agita durante 24 horas a 120 °C y, transcurrido este tiempo, se evapora el disolvente bajo presión reducida. Se cromatografía en columna de gel de sílice (30:1, hexano:Et₂O), obteniéndose el compuesto **34**.

Datos analíticos y espectroscópicos:

Sólido naranja

Masa Molecular: 799.3 g/mol.

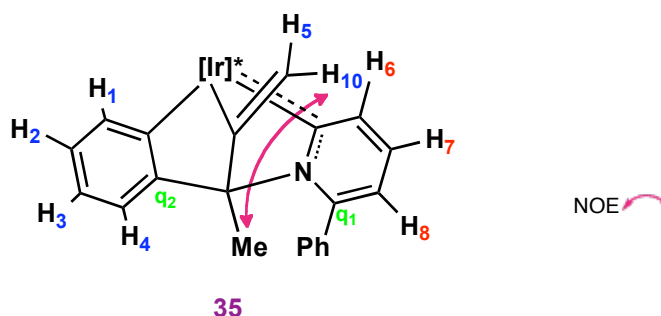
¹H RMN (CD₂Cl₂, 400 MHz, 25°C): δ 17.30 (s, 1 H, NH), 8.84 (d, 1 H, ³J_{HH} = 7.3 Hz, H₅), 7.75, 7.23, 7.10 (d, t, m, 4:2:5, ³J_{HH} = 7.2 Hz, 10 CH_{phpy}, H₄), 6.90 (d, 2 H, ³J_{HH} = 7.2 Hz, 2 H₈), 6.81 (m, 4 H, 2 H₆, 2 H₇), 6.63 (ta, 1 H, ³J_{HH} = 7.2 Hz, H₃), 6.45 (ta, 1 H, ³J_{HH} = 7.2 Hz, H₂), 6.30 (d, 1 H, ³J_{HH} = 7.1 Hz, H₁), 5.71, 5.70 (s, 2:1, 3 CH_{pz}), 2.48, 2.47, 0.84, 0.78 (s, 1:2:1:2, 6 Me_{pz}).

¹³C{¹H} RMN (CD₂Cl₂, 100 MHz, 25°C): δ 172.3 (2 Ir=C), 151.5 (2 C_{q1}), 150.5, 149.4, 143.7 (2:1:3, C_{qpz}), 141.3 (CH₁), 138.1 (2 CH₆), 137.8 (2 C_{qphpy}), 137.1 (Ir-C_{ph}), 134.5 (CH₅), 132.1 (2 CH₇), 128.5, 128.3, 127.2 (1:2:2, 10 CH_{phpy}), 125.3

(CH₂), 123.4 (CH₄), 119.4.0 (CH₃), 114.4 (2 CH₈), 106.5, 107.2 (1:2, CH_{pz}), 14.3, 12.9, 12.8, 12.7 (2:2:1:1, Me_{pz}).

HRMS (FAB) *m/z* calcd. (expt.) C₄₃H₄₄BIrN₈: 877.3490 (877.3500).

Compuesto 35



Se disuelve el compuesto **4** (100 mg, 0.125 mmol) en benceno (4 mL) y la disolución se transfiere a un tubo de presión que se carga con 2 atm. de acetileno. La mezcla se agita durante 14 horas a 90 °C y, transcurrido este tiempo, se evapora el disolvente bajo presión reducida. El residuo sólido se cromatografía en columna de gel de sílice (40:1 → 10:1, hexano:Et₂O), obteniéndose el complejo **35** en la primera fracción, con un rendimiento del 20%.

Datos analíticos y espectroscópicos:

Sólido amarillo

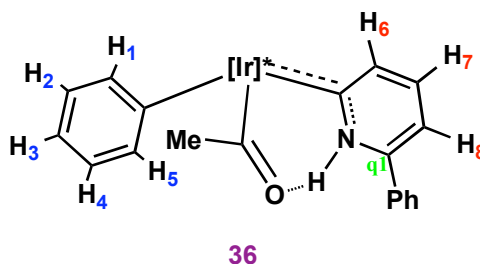
Masa Molecular: 772.8 g/mol.

IR (nujol): $\nu(\text{B-H})$ 2525 cm^{-1} .

¹H RMN (CDCl₃:C₆D₆ (7:3), 500 MHz, 25 °C): δ 7.28 (d, 1 H, $^3J_{\text{HH}} = 7.6$ Hz, H₆), 7.25 - 7.10 (m, 5 H, 5 CH_{phpy}), 7.03 (d, 1 H, $^3J_{\text{HH}} = 6.8$ Hz, H₁), 6.91 (d, 1 H, $^3J_{\text{HH}} = 6.8$ Hz, H₄), 6.86 (t, 1 H, $^3J_{\text{HH}} = 6.8$ Hz, H₃), 6.70 (t, 1 H, $^3J_{\text{HH}} = 6.8$ Hz, H₂), 6.56 (t, 1 H, $^3J_{\text{HH}} = 7.6$ Hz, H₇), 6.23 (d, 1 H, $^3J_{\text{HH}} = 7.6$ Hz, H₈), 5.66, 5.57, 5.47 (s, 1 H cada, 3 CH_{pz}), 5.22 (s, 1 H, H₁₀) 3.82 (s, 1 H, H₅) 2.30, 2.26, 2.22, 1.49, 1.46, 1.23 (s, 3 H cada, 6 Me_{pz}) 1.46 (s, 3 H, Me).

$^{13}\text{C}\{^1\text{H}\}$ RMN ($\text{CDCl}_3:\text{C}_6\text{D}_6$ (7:3), 125 MHz, 25 °C): δ 190.7 (Ir=C), 163.5 (Ir–C(=CH₂)), 152.0, 150.2, 149.4, 142.9, 142.8, 142.7 (C_{qpz}), 151.6 (Ir–CH_{ph}) 151.1 (C_{q1}), 150.7 (C_{q2}), 138.8 (CH₆), 138.2 (C_{qphpy}), 137.8 (CH₁), 130.0 (CH₇), 129.2, 128.7, 127.2 (1:2:2, CH_{phpy}), 129.6 (CH₇), 125.0 (CH₂), 120.9 (CH₈) 120.8 (CH₃), 119.1 (CH₄), 107.1 (CH₅H₁₀, $^1J_{\text{CH}}$ = 157, 150 Hz), 107.1, 106.7, 106.1 (CH_{pz}), 98.3 (C(Me)N), 20.0 (C(Me)N), 15.2, 14.4, 13.3, 13.0, 12.8, 12.7 (Me_{pz}).

HRMS (FAB) m/z calcd. (expt.) C₃₆H₃₉BIrN₇: 773.2965 (773.2961).

Compuesto 36

Al desarrollar el procedimiento descrito para el complejo **35**, se obtiene también el compuesto **36**, en la segunda fracción de la columna cromatográfica, con un rendimiento del 30% .

Datos analíticos y espectroscópicos:

Sólido amarillo

Masa Molecular: 764.7 g/mol.

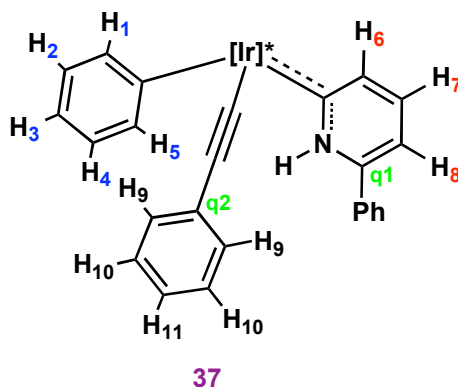
IR (nujol): $\nu(\text{N-H})$ 3137, $\nu(\text{B-H})$ 2525, $\nu(\text{CO})$ 1595 cm^{-1} .

^1H RMN (CDCl_3 , 400 MHz, 25 °C): δ 16.38 (s, 1 H, NH), 8.26, 7.67, 7.57 (d, t, t, 2:2:1, 5 H, $^3J_{\text{HH}} \approx 7.5$ Hz, 5 CH_{phpy}), 8.12 (d, 1 H, $^3J_{\text{HH}} = 7.5$ Hz, H_5), 7.17 (d, 1 H, $^3J_{\text{HH}} = 7.0$ Hz, H_8), 7.03 (m, 2 H, H_6 , H_7), 6.97 (t, 1 H, $^3J_{\text{HH}} = 7.2$ Hz, H_4), 6.67 (t, 1 H, $^3J_{\text{HH}} = 7.2$ Hz, H_3), 6.49 (t, 1 H, $^3J_{\text{HH}} = 7.3$ Hz, H_2), 6.25 (d, 1 H, $^3J_{\text{HH}} = 7.9$ Hz, H_1), 5.74, 5.73, 5.69 (s, 1 H cada, 3 CH_{pz}), 2.50, 2.49, 2.47, 1.21, 1.10, 1.04 (s, 3 H cada, 6 Me_{pz}), 1.76 (s, 3 H, COMe).

$^{13}\text{C}\{^1\text{H}\}$ RMN(CDCl_3 , 100 MHz, 25 °C): δ 240.8 (Ir-C(=O)Me), 174.9 (Ir=C), 151.0, 150.6, 149.5, 143.3 (1:1:1:3, C_{qpy}), 148.4 (C_{q1}), 140.8 (CH_1), 139.5 (CH_6 ó 7), 134.5 (Ir- C_{ph}), 134.1 (CH_7 ó 6), 133.5 (CH_5), 130.4, 129.7, 126.4 (1:2:2, CH_{phpy}),

126.2 (C_{qphpy}) 125.5 (CH_2), 124.5 (CH_4), 120.5 (CH_3), 113.7 (CH_8), 106.8, 106.6, 106.4 (CH_{pz}), 42.4 (C(=O)Me), 15.2, 14.4, 13.3, 13.0, 12.8, 12.7 (Me_{pz}).

HRMS (FAB) m/z calcd. (expt.) $\text{C}_{34}\text{H}_{39}\text{BIrN}_7\text{O} + \text{Na}$: 788.2885 (788.2836).

Compuesto 37

Se disuelve el compuesto **4** (100 mg, 0.13 mmol) en benceno (4 mL), se añade fenilacetileno (0.13 mmol, 13 μ L) y la disolución resultante se agita durante 24 horas a 90 $^{\circ}$ C. Transcurrido este tiempo se evapora el disolvente bajo presión reducida y el residuo se cromatografía en columna de gel de sílice utilizando una mezcla hexano:éter (20:1) como eluyente. Se obtiene el complejo **37** con un rendimiento del 65%.

Datos analíticos y espectroscópicos:

Sólido amarillo

Masa Molecular: 824.3 g/mol.

^1H RMN (CD_2Cl_2 , 500 MHz, 25 $^{\circ}$ C): δ 13.80 (s, 1 H, NH), 8.04 (d, 1 H, $^3J_{\text{HH}} = 7.2$ Hz, H₅), 7.93, 7.49, 7.36, (d, t, t, 2:1:2, 5 H, $^3J_{\text{HH}} \approx 7.5$ Hz, 5 CH_{phpy}), 7.20 (m, 3 H, H₆, 2 H₁₀), 7.14 (m, 4 H, H₈, 2 H₉, H₁₁), 7.05 (t, 1 H, $^3J_{\text{HH}} = 7.2$ Hz, H₇), 6.97 (t, 1 H, $^3J_{\text{HH}} = 7.2$ Hz, H₄), 6.75 (t, 1 H, $^3J_{\text{HH}} = 7.2$ Hz, H₃), 6.61 (t, 1 H, $^3J_{\text{HH}} = 7.0$ Hz, H₂), 6.43 (d, 1 H, $^3J_{\text{HH}} = 7.9$ Hz, H₁), 5.80, 5.66 (s, 1:2, 3 CH_{pz}) 2.50, 2.49, 2.47, 1.21, 1.10, 1.04 (s, 3 H cada, 6 Me_{pz}).

$^{13}\text{C}\{^1\text{H}\}$ RMN (CD_2Cl_2 , 125 MHz, 25 °C): δ 175.3 (Ir=C), 152.8, 150.8, 149.7, 143.0, 142.9, 142.8 (C_{qpz}), 148.5 (C_{q1}), 140.2 (CH_1), 139.4 (CH_6), 135.4 (CH_5), 134.3 (CH_{11}), 134.2 (Ir- C_{ph}), 132.9 (C_{qphpy}), 131.6 (2 CH_{10}), 130.6, 129.7, 126.1 (1:2:2, CH_{phpy}), 129.7 (C_{q2}), 127.6 (2 CH_9), 125.8 (CH_2), 125.0 (CH_4), 123.4 (CH_7), 120.5 (CH_3), 113.7 (CH_8), 107.2, 106.6, 105.8 (CH_{pz}), 100.7, 95.6 (Ir- $\text{C}\equiv\text{C}$), 15.6, 14.0, 12.9, 12.8, 12.6, 12.0 (Me_{pz}).

HRMS (FAB) m/z calc. $\text{C}_{40}\text{H}_{41}\text{BIrN}_7$ (expt.): 824.3212 (824.3224).

Apéndice I

Complejo 2

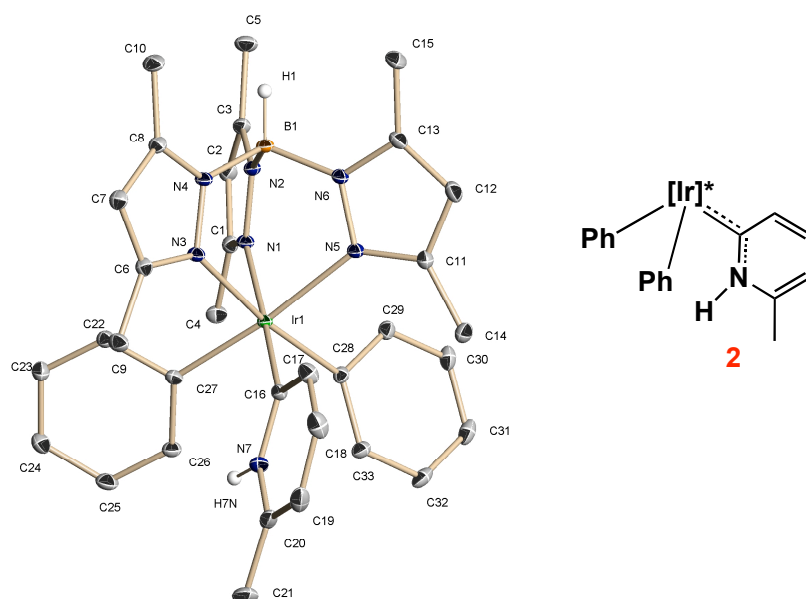


Tabla A1. Distancias (Å) y ángulos de enlace (°) seleccionados para **2**.

Longitudes de enlace (Å)			
Ir(1)—N(1)	2.1174(4)	Ir(1)—C(16)	1.982 (3)
Ir(1)—N(3)	2.1570(5)	Ir(1)—C(28)	2.0463(6)
Ir(1)—N(5)	2.1873(5)	Ir(1)—C(27)	2.0567(6)
C(16)—C(17)	1.422(2)	C(17)—C(18)	1.373(3)
C(18)—C(19)	1.402(3)	C(19)—C(20)	1.358(3)
Ángulos de enlace (°)			
C(28)—Ir(1)—N(1)	90.80(6)	N(3)—Ir(1)—N(5)	85.13(5)
N(3)—Ir(1)—C(16)	89.46(6)	C(16)—Ir(1)—C(28)	92.84(7)
N(5)—Ir(1)—C(28)	87.30(6)	C(16)—Ir(1)—C(27)	92.94(6)
N(1)—Ir(1)—N(5)	86.86(5)	C(16)—Ir(1)—N(5)	92.67(6)
N(1)—Ir(1)—N(3)	86.91(5)	N(7)—C(16)—Ir(1)	121.84(1)

Tabla A2. Datos cristalográficos para el complejo **2**.

Fórmula	$C_{71}H_{90}B_2Ir_2N_{14} [2(C_{33}H_{39}BirN_7), C_5H_{12}]$		
Peso molecular	1545.59		
Temperatura	100(2) K		
Longitud de onda	0.71073 Å		
Sistema cristalino	Monoclínico		
Grupo espacial	P2(1)/n		
Dimensiones de la celda unidad	$a = 10.3293(2)$ Å	$\alpha = 90^\circ$	
	$b = 25.2058(5)$ Å	$\beta = 99.9410(10)^\circ$	
	$c = 13.1798(3)$ Å	$\gamma = 90^\circ$	
Volumen	$3379.95(12)$ Å ³		
Z	2		
Densidad (calculada)	1.519 Mg/m ³		
Coefficiente de absorción	3.986 mm ⁻¹		
F(000)	1556		
Dimensiones del cristal	0.29 x 0.26 x 0.20 mm ³		
Intervalo de toma de datos	2.86 a 30.51°		
Reflexiones medidas	60903		
Reflexiones independientes	10242 [R(int) = 0.0255]		
Índices R finales [$I > 2\sigma(I)$]	R1 = 0.0177, wR2 = 0.0404		
Índices R (todos los datos)	R1 = 0.0219, wR2 = 0.0417		

Complejo 3

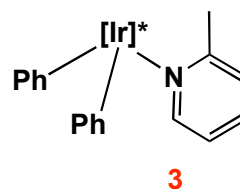
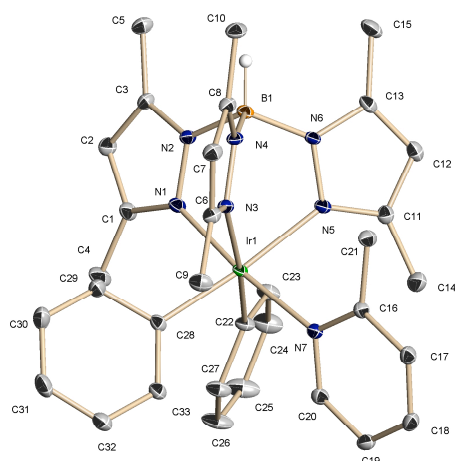


Tabla A3. Distancias (Å) y ángulos de enlace (°) seleccionados para **3**.

Longitudes de enlace (Å)			
Ir(1)—N(1)	2.051(3)	N(7)—C(20)	1.355(4)
Ir(1)—N(3)	2.155(3)	N(7)—C(16)	1.366(4)
Ir(1)—N(5)	2.155(3)	C(16)—C(17)	1.396(4)
Ir(1)—N(7)	2.135(3)	C(17)—C(18)	1.378(4)
Ir(1)—C(22)	2.057(3)	C(18)—C(19)	1.382(4)
Ir(1)—C(28)	2.062(3)	C(19)—C(20)	1.377(5)
Ángulos de enlace (°)			
N(1)—Ir(1)—C(28)	90.98(11)	C(28)—Ir(1)—C(22)	94.52(12)
N(1)—Ir(1)—C(22)	86.07(1)	C(22)—Ir(1)—N(7)	93.74(11)
N(7)—Ir(1)—N(5)	86.78(6)	C(28)—Ir(1)—N(5)	173.87(12)
N(7)—C(16)—C(17)	121.0(3)	C(22)—Ir(1)—N(5)	91.11(11)
C(20)—N(7)—Ir(1)	117.0(2)	C(22)—N(7)—C(16)	116.1(3)

Tabla A4. Datos cristalográficos para el complejo 3.

Fórmula	$C_{67}H_{80}B_2Cl_2Ir_2N_{14}$	
Peso molecular	1558.37	
Temperatura	100(2) K	
Longitud de onda	0.71073 Å	
Sistema cristalino	Monoclínico	
Grupo espacial	$P2_1/n$	
Dimensiones de la celda unidad	$a = 11.7247(8)$ Å	$\alpha = 90^\circ$
	$b = 18.4378(11)$ Å	$\beta = 101.610(2)^\circ$
	$c = 15.7524(10)$ Å	$\gamma = 90^\circ$
Volumen	$3335.6(4)$ Å ³	
Z	2	
Densidad (calculada)	1.552 Mg/m ³	
Coefficiente de absorción	4.117 mm ⁻¹	
F(000)	1556	
Dimensiones del cristal	0.24 x 0.20 x 0.11 mm ³	
Intervalo de toma de datos	2.86 a 30.61°	
Reflexiones medidas	74114	
Reflexiones independientes	10224 [R(int) = 0.0406]	
Índices R finales [$I > 2\sigma(I)$]	R1 = 0.0271, wR2 = 0.0683	
Índices R (todos los datos)	R1 = 0.0381, wR2 = 0.0756	

Complejo 4

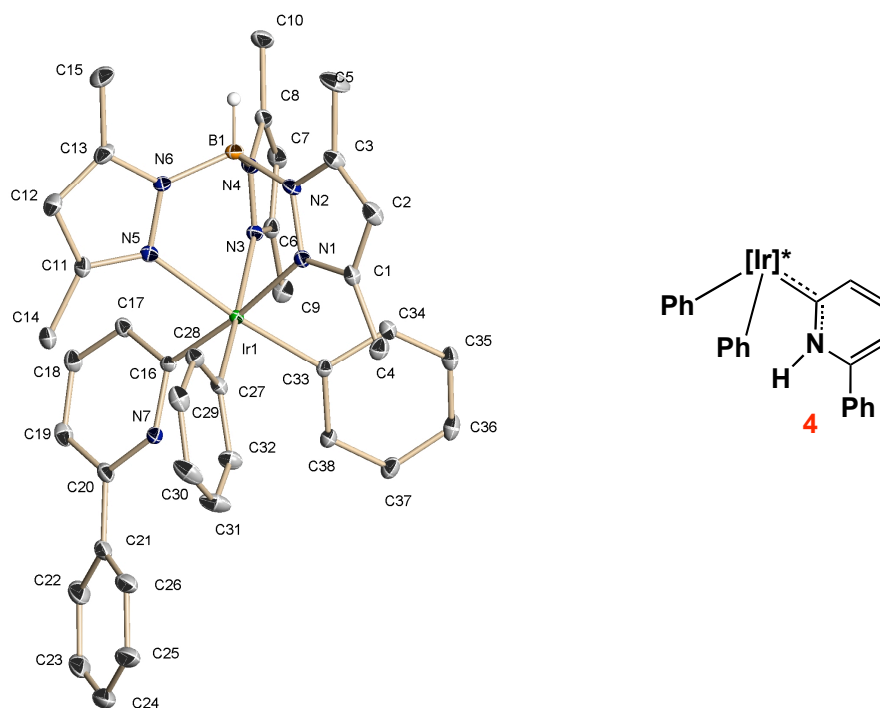


Tabla A5. Distancias (Å) y ángulos de enlace (°) seleccionados para **4**.

Longitudes de enlace (Å)			
Ir(1)—N(1)	2.132(3)	N(7)—C(20)	1.369(4)
Ir(1)—N(3)	2.147(3)	C(20)—C(19)	1.366(5)
Ir(1)—N(5)	2.149(2)	C(19)—C(18)	1.397(5)
Ir(1)—C(16)	1.978 (1)	C(16)—C(17)	1.403(3)
Ir(1)—C(27)	2.052(3)	C(16)—N(7)	1.369(4)
Ir(1)—C(33)	2.057(3)	C(18)—C(17)	1.379(4)
Ángulos de enlace (°)			
N(1)-Ir(1)-N(3)	86.55(10)	C(16)-Ir(1)-C(33)	95.38(12)
C(16)-Ir(1)-N(7)	93.98(12)	C(27)-Ir(1)-N(5)	89.38(11)
C(27)-Ir(1)-N(3)	171.95(11)	C(16)-Ir(1)-N(5)	86.81(11)
C(33)-Ir(1)-N(3)	89.04(11)	C(27)-Ir(1)-C(33)	95.69(12)
Ángulo de torsión(°)			
N(7)-C(20)-C(21)-C(26)		25.3(5)	

Tabla A6. Datos cristalográficos para el complejo 4.

Fórmula	$C_{39}H_{43}BCl_2IrN_7$ [$C_{38}H_{41}BIrN_7$, CH_2Cl_2]	
Peso molecular	883.71	
Temperatura	100(2) K	
Longitud de onda	0.71073 Å	
Sistema cristalino	Monoclínico	
Grupo espacial	C2/c	
Dimensiones de la celda unidad	$a = 40.2432(8)$ Å	$\alpha = 90^\circ$
	$b = 10.1628(2)$ Å	$\beta = 101.4560(10)^\circ$
	$c = 18.6214(4)$ Å	$\gamma = 90^\circ$
Volumen	$7464.1(3)$ Å ³	
Z	8	
Densidad (calculada)	1.573 Mg/m ³	
Coefficiente de absorción	3.759 mm ⁻¹	
F(000)	3536	
Dimensiones del cristal	$0.27 \times 0.20 \times 0.18$ mm ³	
Intervalo de toma de datos	2.89 a 30.57°	
Reflexiones medidas	69220	
Reflexiones independientes	11433 [$R(\text{int}) = 0.0417$]	
Índices [$I > 2\sigma(I)$]	$R1 = 0.0296$, $wR2 = 0.0601$	
Índices R (todos los datos)	$R1 = 0.0437$, $wR2 = 0.0649$	

Complejo 5

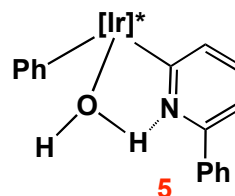
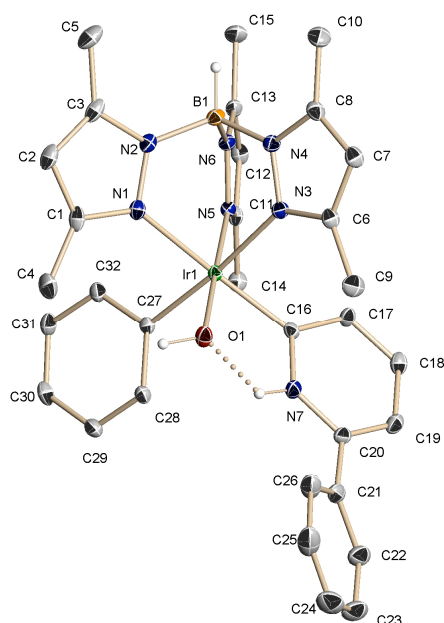


Tabla A7. Distancias (Å) y ángulos de enlace (°) seleccionados para 5.

Longitudes de enlace (Å)			
Ir(1)—N(1)	2.123(3)	C(16)—C(17)	1.404(4)
Ir(1)—N(3)	2.155(3)	C(17)—C(18)	1.400(4)
Ir(1)—N(5)	2.050(2)	C(18)—C(19)	1.394(5)
Ir(1)—C(16)	1.982(1)	C(19)—C(20)	1.368(5)
Ir(1)—C(27)	2.033(3)	C(20)—N(7)	1.356(3)
Ir(1)—O(1)	2.069(2)	C(16)—N(7)	1.361(4)
Ángulos de enlace (°)			
O(1)-Ir(1)-N(3)	90.69(10)	C(16)-Ir(1)-C(27)	94.71(2)
C(16)-Ir(1)-N(3)	90.39(11)	C(16)-Ir(1)-O(1)	84.46(10)
C(27)-Ir(1)-N(3)	174.82(10)	C(16)-Ir(1)-N(5)	94.93(11)
C(27)-Ir(1)-N(1)	89.56(11)	C(27)-Ir(1)-O(1)	90.67(11)
Ángulo de torsión(°)			
N(7)-C(20)-C(21)-C(26)		-35.9(5)	
Puentes de hidrogeno (Å)			
D-H...A	d(D-H)	d(H...A)	d(D...A)
N(7)-H(7N)...O(1)	0.922(18)	1.78(3)	2.518(3)

Tabla A8. Datos cristalográficos para el complejo 5.

Fórmula	$C_{32}H_{37}BIrN_7O$	
Peso molecular	738.70	
Temperatura	100(2) K	
Longitud de onda	0.71073 Å	
Sistema cristalino	Monoclínico	
Grupo espacial	P2(1)/c	
Dimensiones de la celda unidad	$a = 18.4844(3)$ Å	$\alpha = 90^\circ$
	$b = 10.4000(2)$ Å	$\beta = 119.1270(10)^\circ$
	$c = 18.0720(3)$ Å	$\gamma = 90^\circ$
Volumen	$3034.79(9)$ Å ³	
Z	4	
Densidad (calculada)	1.617 Mg/m ³	
Coefficiente de absorción	4.438 mm ⁻¹	
F(000)	1472	
Dimensiones del cristal	0.20 x 0.16 x 0.14 mm ³	
Intervalo de toma de datos	2.95 a 30.57°	
Reflexiones medidas	27066	
Reflexiones independientes	8882 [R(int) = 0.0341]	
Índices R finales [$I > 2\sigma(I)$]	R1 = 0.0286, wR2 = 0.0616	
Índices R (todos los datos)	R1 = 0.0398, wR2 = 0.0658	

Complejo 11

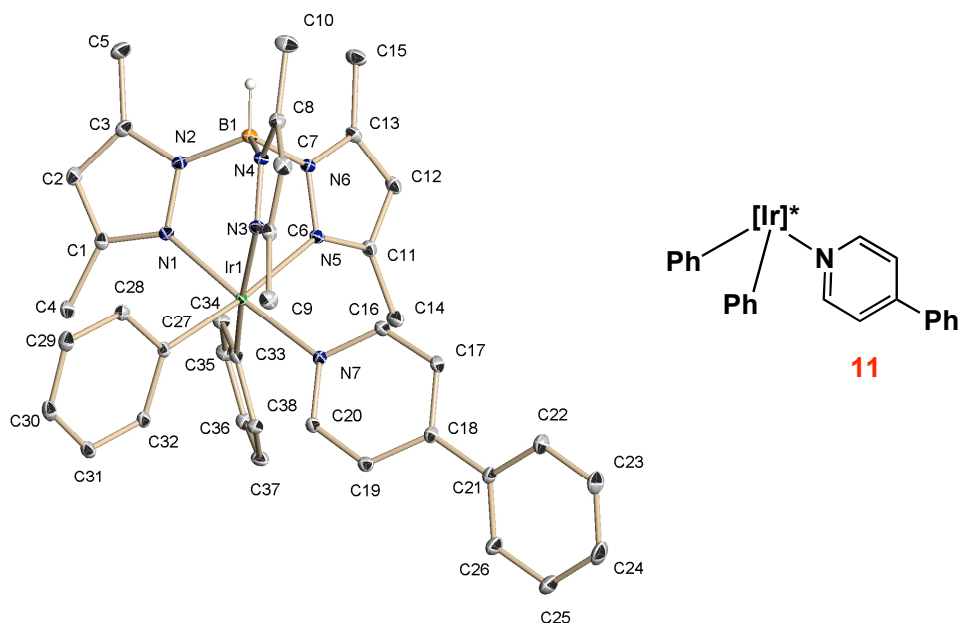


Tabla A9. Distancias (Å) y ángulos de enlace (°) seleccionados para 11.

Longitudes de enlace (Å)			
Ir(1)—N(1)	2.0496(15)	N(7)—C(20)	1.349(2)
Ir(1)—N(3)	2.1629(5)	N(7)—C(16)	1.355(2)
Ir(1)—N(5)	2.1656(14)	C(16)—C(17)	1.381(3)
Ir(1)—N(7)	2.0704(3)	C(17)—C(18)	1.398(2)
Ir(1)—C(27)	2.0484(17)	B C(18)—C(19)	1.399(2)
Ir(1)—C(33)	2.0496(17)	C(19)—C(20)	1.380(2)
Ángulos de enlace (°)			
N(1)—Ir(1)—N(3)	87.13(6)	C(27)—Ir(1)—C(33)	95.83(7)
N(3)—Ir(1)—N(5)	86.97(6)	C(33)—Ir(1)—N(1)	90.71(6)
N(7)—Ir(1)—N(5)	90.86(6)	C(27)—Ir(1)—N(7)	86.72(6)
C(27)—Ir(1)—N(3)	92.50(6)	C(33)—Ir(1)—N(7)	94.18(6)
C(27)—Ir(1)—N(7)	94.22(6)		
Ángulo de torsión(°)			
C(17)—C(18)—C(20)—C(21)			29.8(3)

Tabla A10. Datos cristalográficos para el complejo **11**.

Fórmula	$C_{41}H_{48}BIn_7$ [$C_{38}H_{41}BIn_7, 0.5(C_6H_{14})$]
Peso molecular	841.87
Temperatura	100(2) K
Longitud de onda	0.71073 Å
Sistema cristalino	Monoclínico
Grupo espacial	P2(1)/c
Dimensiones de la celda unidad	$a = 13.1552(4)$ Å $\alpha = 90^\circ$ $b = 17.2781(5)$ Å $\beta = 107.2930(10)^\circ$ $c = 17.3334(5)$ Å $\gamma = 90^\circ$
Volumen	$3761.74(19)$ Å ³
Z	4
Densidad (calculada)	1.487 Mg/m ³
Coefficiente de absorción	3.588 mm ⁻¹
F(000)	1700
Dimensiones del cristal	$0.38 \times 0.34 \times 0.21$ mm ³
Intervalo de toma de datos	2.86 a 30.56°
Reflexiones medidas	87835
Reflexiones independientes	11452 [R(int) = 0.0332]
Índices R finales [$I > 2\sigma(I)$]	R1 = 0.0188, wR2 = 0.0436
Índices R (todos los datos)	R1 = 0.0242, wR2 = 0.0458

Complejo 13

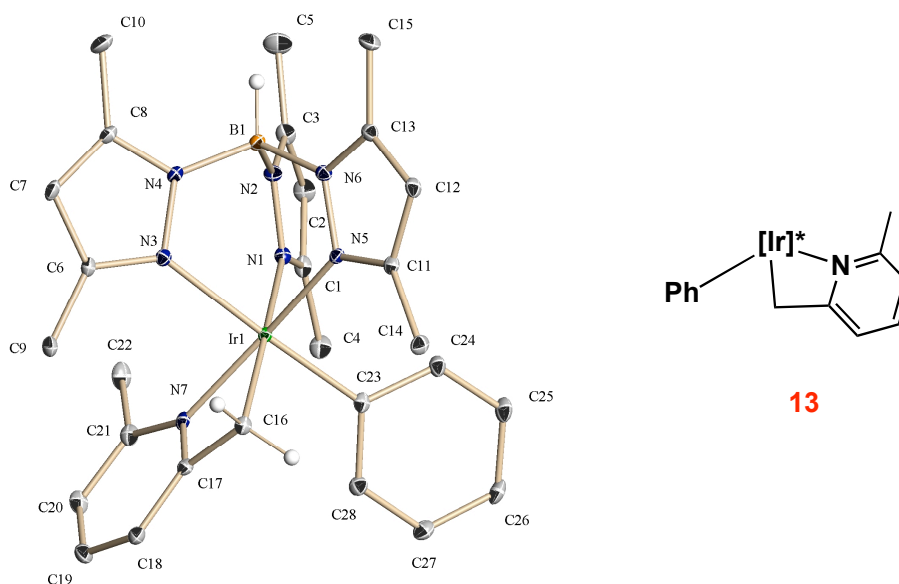


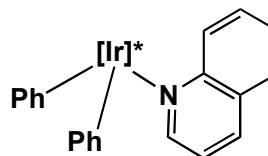
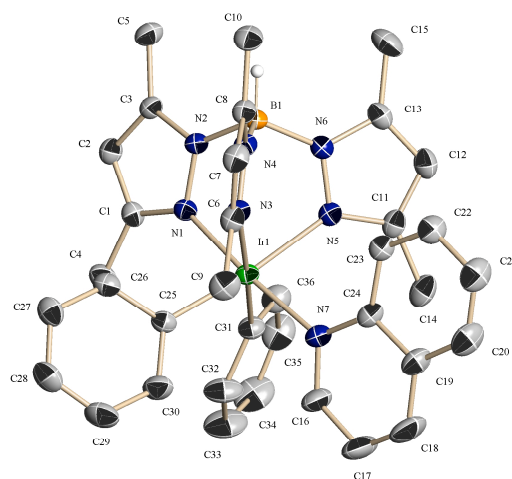
Tabla A11. Distancias (Å) y ángulos de enlace (°) seleccionados para **13**.

Longitudes de enlace (Å)			
Ir(1)—N(1)	2.150(3)	Ir(1)—C(23)	2.042(4)
Ir(1)—N(3)	2.193(3)	Ir(1)—C(16)	2.098(4)
Ir(1)—N(5)	2.053(3)	C(16)—C(17)	1.497(5)
Ir(1)—N(7)	2.055(3)	C(21)—C(22)	1.490(6)
Ángulos de enlace (°)			
N(7)—Ir(1)—C(16)	66.36(13)	C(23)—Ir(1)—C(16)	87.37(14)
N(7)—C(17)—C(16)	105.2(3)	C(23)—Ir(1)—N(5)	92.85(13)
N(7)—C(21)—C(22)	120.8(4)	C(23)—Ir(1)—N(7)	93.05(13)
N(5)—Ir(1)—C(16)	101.61(13)		

Tabla A12. Datos cristalográficos para el complejo **13**.

Fórmula	$\text{C}_{60}\text{H}_{76}\text{B}_2\text{Ir}_2\text{N}_{14}\text{O}$ [$2(\text{C}_{29}\text{H}_{35}\text{BIrN}_7)$, $\text{C}_2\text{H}_6\text{O}$]	
Peso molecular	1415.37	
Temperatura	173(2) K	
Longitud de onda	0.71073 Å	
Sistema cristalino	Triclínico	
Grupo espacial	P-1	
Dimensiones de la celda unidad	$a = 8.1599(7)$ Å	$\alpha = 94.853(3)^\circ$
	$b = 10.6163(10)$ Å	$\beta = 93.693(3)^\circ$
	$c = 18.4205(19)$ Å	$\gamma = 98.286(2)^\circ$
Volumen	$1568.7(3)$ Å ³	
Z	1	
Densidad (calculada)	1.498 Mg/m ³	
Coefficiente absorción	4.288 mm ⁻¹	
F(000)	706	
Dimensiones de cristal	$0.27 \times 0.18 \times 0.17$ mm ³	
Intervalo de toma de datos	1.95 a 25.55°	
Reflexiones medidas	27555	
Reflexiones independientes	5690 [$R(\text{int}) = 0.0896$]	
Índices R finales [$I > 2\sigma(I)$]	$R1 = 0.0602$, $wR2 = 0.1510$	
Índices R (todos los datos)	$R1 = 0.0776$, $wR2 = 0.1719$	

Compuesto 14



14

Tabla A13. Distancias (Å) y ángulos de enlace (°) seleccionados para **14**.

Longitudes de enlace (Å)			
Ir(1)—N(1)	2.052(3)	N(7)—C(24)	1.411(5)
Ir(1)—N(3)	2.161(3)	N(7)—C(16)	1.329(5)
Ir(1)—N(5)	2.156(3)	C(16)—C(17)	1.403(7)
Ir(1)—N(7)	2.127(3)	C(17)—C(18)	1.349(8)
Ir(1)—C(25)	2.061(3)	C(18)—C(19)	1.420(7)
Ir(1)—C(31)	2.065(3)	C(19)—C(20)	1.435(5)
Ángulos de enlace (°)			
N(1)—Ir(1)—C(25)	89.51(2)	C(31)—Ir(1)—N(3)	174.86(12)
N(1)—Ir(1)—C(31)	86.84(12)	C(25)—Ir(1)—N(3)	88.14(11)
C(31)—Ir(1)—N(7)	93.15(14)	C(25)—Ir(1)—N(7)	95.48(13)
C(31)—Ir(1)—N(5)	90.47(14)	N(7)—Ir(1)—N(5)	87.59(11)

Tabla A14. Datos cristalográficos para el complejo **14**.

Fórmula	$C_{73}H_{80}B_2Cl_2Ir_2N_{14}$ [$2(C_{36}H_{39}BIrN_7)$, CH_2Cl_2]	
Peso molecular	1630.43	
Temperatura	293(2) K	
Longitud de onda	0.71073 Å	
Sistema cristalino	Monoclínico	
Grupo espacial	$P2_1/c$	
Dimensiones de la celda unidad	$a = 19.4731(9)$ Å	$\alpha = 90^\circ$
	$b = 10.9707(5)$ Å	$\beta = 112.2210(10)^\circ$
	$c = 18.3367(8)$ Å	$\gamma = 90^\circ$
Volumen	$3626.4(3)$ Å ³	
Z	2	
Densidad (calculada)	1.493 Mg/m ³	
Coefficiente de Absorción	3.791 mm^{-1}	
F(000)	1628	
Dimensiones del cristal	$0.46 \times 0.41 \times 0.13\text{ mm}^3$	
Intervalo de toma de datos	2.40 a 30.53°	
Reflexiones medidas	63801	
Reflexiones independientes	11062 [$R(\text{int}) = 0.0300$]	
Índices R finales [$I > 2\sigma(I)$]	$R1 = 0.0329$, $wR2 = 0.0750$	
Índices R (todos los datos)	$R1 = 0.0519$, $wR2 = 0.0846$	

Complejo 15

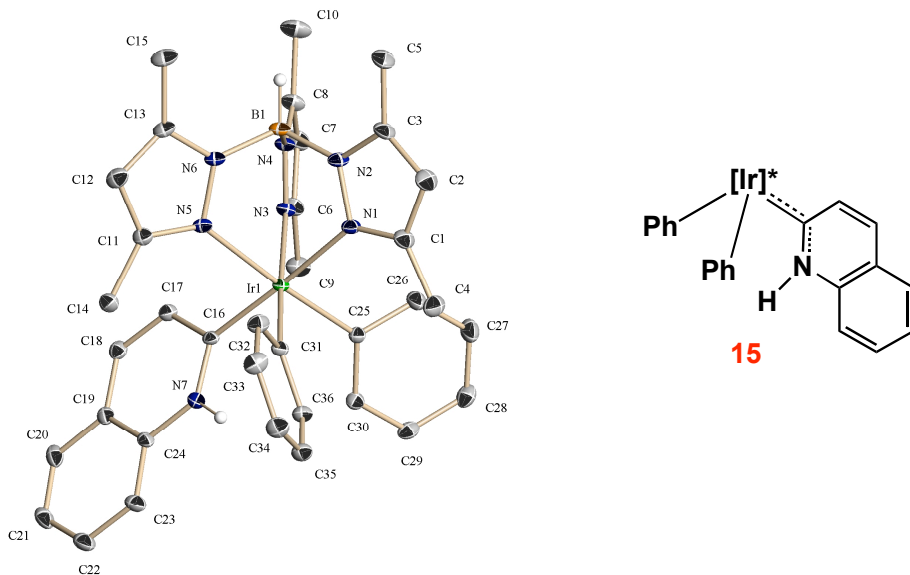


Tabla A15. Distancias (Å) y ángulos de enlace (°) seleccionados para 15.

Longitudes de enlace (Å)			
Ir(1)—N(1)	2.142(8)	Ir(1)—C(16)	1.978(9)
Ir(1)—N(3)	2.159(8)	Ir(1)—C(25)	2.054(9)
Ir(1)—N(5)	2.169(8)	Ir(1)—C(31)	2.061(9)
N(7)—C(24)	1.381(11)	N(7)—C(16)	1.354(11)
Ángulos de enlace (°)			
C(16)-Ir(1)-N(1)	86.7(3)	C(16)-Ir(1)-C(25)	93.4(4)
N(7)-C(16)-Ir(1)	121.7(7)	C(16)-Ir(1)-C(31)	92.0(4)
C(16)-Ir(1)-N(5)	88.0(3)	C(25)-Ir(1)-C(31)	94.1(4)
C(31)-Ir(1)-N(1)	86.7(3)	N(5)-Ir(1)-N(3)	85.4(3)

Tabla A16. Datos cristalográficos para el complejo **15**.

Fórmula	$C_{36}H_{39}BIrN_7$	
peso molecular	772.75	
Temperatura	100(2) K	
Longitud de onda	0.71073 Å	
Sistema cristalino	Monoclínico	
Grupo espacial	$P2_1/n$	
Dimensiones de la celda unidad	$a = 8.4825(4)$ Å	$\alpha = 90^\circ$
	$b = 20.2384(8)$ Å	$\beta = 102.4690(10)^\circ$
	$c = 19.5234(8)$ Å	$\gamma = 90^\circ$
Volumen	$3272.6(2)$ Å ³	
Z	4	
Densidad (calculada)	1.568 Mg/m ³	
Coefficiente de absorción	4.117 mm ⁻¹	
F(000)	1544	
Dimensiones del cristal	0.21 x 0.20 x 0.19 mm ³	
Intervalo de toma de datos	2.94 a 30.55°	
Reflexiones medidas	26487	
Reflexiones independientes	9887 [R(int) = 0.0321]	
Índices R finales [$I > 2\sigma(I)$]	R1 = 0.0289, wR2 = 0.0596	
Índices R (todos los datos)	R1 = 0.0452, wR2 = 0.0645	

Complejo 20

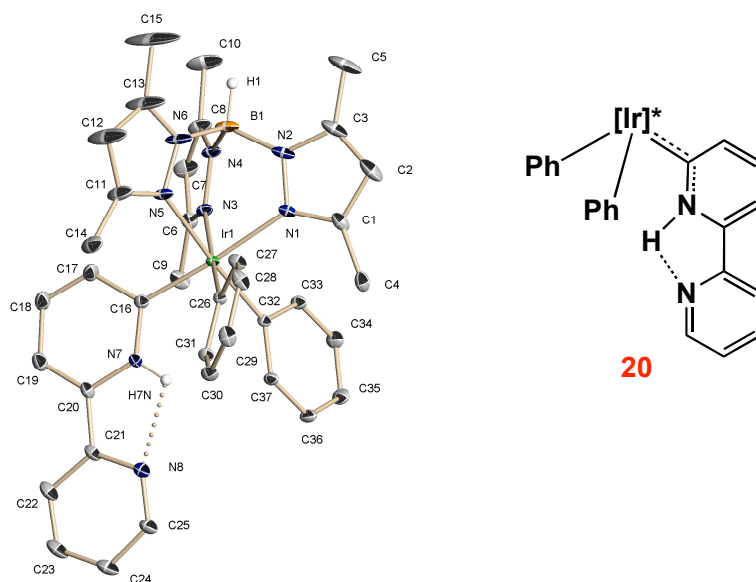


Tabla A17. Distancias (Å) y ángulos de enlace (°) seleccionados para **20**.
Longitudes de enlace (Å)

Ir(1)—N(1)	2.127(3)	C(16)—C(17)	1.434(5)
Ir(1)—N(3)	2.167(3)	C(17)—C(18)	1.364(6)
Ir(1)—N(5)	2.163(3)	C(25)—N(8)	1.333(5)
Ir(1)—C(16)	1.974(4)	C(21)—N(8)	1.337(5)
Ir(1)—C(26)	2.060(3)	C(20)—N(7)	1.367(4)
Ir(1)—C(32)	2.063(2)	C(16)—N(7)	1.362(4)

Ángulos de enlace (°)

C(26)-Ir(1)-N(1)	86.79(10)	C(16)-Ir(1)-C(26)	94.38(10)
C(16)-Ir(1)-N(5)	90.44(14)	C(16)-Ir(1)-C(32)	93.19(10)
N(7)-C(16)-Ir(1)	124.70(3)	C(26)-Ir(1)-C(22)	94.93(13)
N(1)-Ir(1)-N(3)	85.39(12)	C(32)-Ir(1)-N(1)	88.50(13)

Ángulo de torsión(°)

N(7)-C(20)-C(21)-N(8)	5.7(5)
-----------------------	--------

Puentes de hidrogeno (Å)

D-H...A	d(D-H)	d(H...A)	d(D...A)
N(7)-H(7N)...N(8)	0.88	2.18	2.609(4)

Tabla A18. Datos cristalográficos para el complejo **20**.

Fórmula	$C_{37}H_{40}BIrN_8$		
Peso molecular	799.78		
Temperatura	136(2) K		
Longitud de onda	0.71073 Å		
Sistema cristalino	Triclínico		
Grupo espacial	P-1		
Dimensiones de la celda unidad	$a = 8.6033(4)$ Å	$\alpha = 91.5240(10)^\circ$	
	$b = 10.1856(5)$ Å	$\beta = 99.3170(10)^\circ$	
	$c = 22.8839(12)$ Å	$\gamma = 102.1720(10)^\circ$	
Volumen	$1930.53(17)$ Å ³		
Z	2		
Densidad (calculada)	1.376 Mg/m ³		
Coefficiente de absorción	3.493 mm ⁻¹		
F(000)	800		
Dimensiones del cristal	$0.46 \times 0.33 \times 0.32$ mm ³		
Intervalo de toma de datos	2.71 a 30.58°		
Reflexiones medidas	56043		
Reflexiones independientes	11771 [R(int) = 0.0295]		
Índices R finales [$I > 2\sigma(I)$]	R1 = 0.0370, wR2 = 0.0811		
Índices R (todos los datos)	R1 = 0.0382, wR2 = 0.0815		

Complejo 21

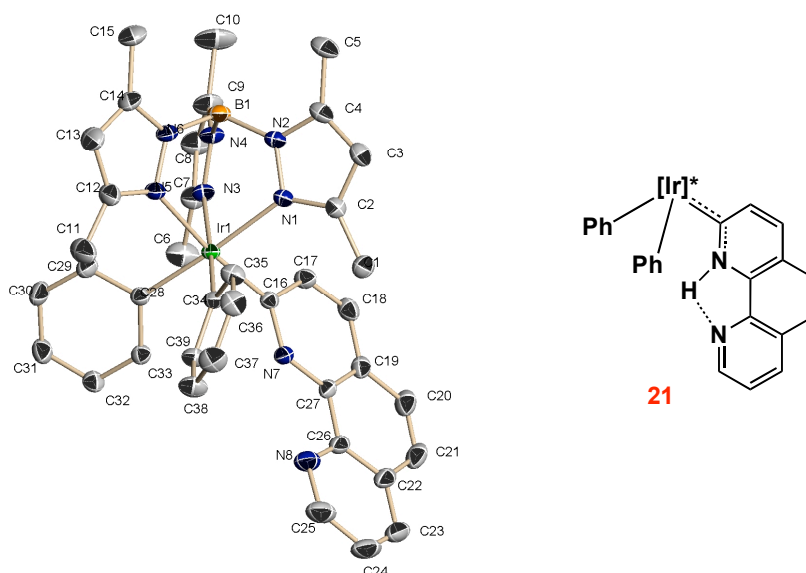


Tabla A19. Distancias (Å) y ángulos de enlace (°) seleccionados para 21.

Longitudes de enlace (Å)			
Ir(1)—N(1)	2.1642(18)	C(16)—C(17)	1.426(3)
Ir(1)—N(3)	2.1637(17)	C(17)—C(18)	1.364(6)
Ir(1)—N(5)	2.1448(17)	C(25)—N(8)	1.321(3)
Ir(1)—C(16)	1.974(2)	C(26)—N(8)	1.356(4)
Ir(1)—C(28)	2.052(2)	C(27)—N(7)	1.359(3)
Ir(1)—C(34)	2.053(3)	C(16)—N(7)	1.359(3)
Ángulos de enlace (°)			
C(16)-Ir(1)-N(1)	86.77(7)	C(16)-Ir(1)-C(21)	94.46(8)
C(34)-Ir(1)-N(5)	88.11(8)	C(16)-Ir(1)-C(34)	93.61(8)
N(7)-Ir(1)-C(16)	124.20(20)	C(28)-Ir(1)-C(34)	93.36(8)
C(28)-Ir(1)-N(3)	92.41(8)	N(7)-C(26)-C(27)	118.8(2)
Puentes de hidrogeno (Å)			
D-H...A	d(D-H)	d(H...A)	d(D...A)
N(7)-H(7N)...N(8)	0.876	2.308	2.726

Tabla A20. Datos cristalográficos para el complejo **21**.

Fórmula	$C_{39}H_{40}BIrN_8$	
Peso molecular	823.80	
Temperatura	273(2) K	
Longitud de onda	0.71073 Å	
Sistema cristalino	Monoclínico	
Grupo espacial	P2(1)/c	
Dimensiones de la celda unidad	$a = 8.6897(3)$ Å	$\alpha = 90^\circ$
	$b = 20.2130(6)$ Å	$\beta = 102.0930(10)^\circ$
	$c = 20.1292(6)$ Å	$\gamma = 90^\circ$
Volumen	$3457.13(19)$ Å ³	
Z	4	
Densidad (calculada)	1.583 Mg/m ³	
Coefficiente de absorción	3.903 mm ⁻¹	
F(000)	1648	
Dimensiones del cristal	0.27 x 0.22 x 0.16 mm ³	
Intervalo de toma de datos	1.44 a 33.10°	
Reflexiones medidas	63240	
Reflexiones independientes	13022 [R(int) = 0.0320]	
Índices R finales [$I > 2\sigma(I)$]	R1 = 0.0284, wR2 = 0.0546	
Índices R (todos los datos)	R1 = 0.0382, wR2 = 0.0571	

Complejo 24

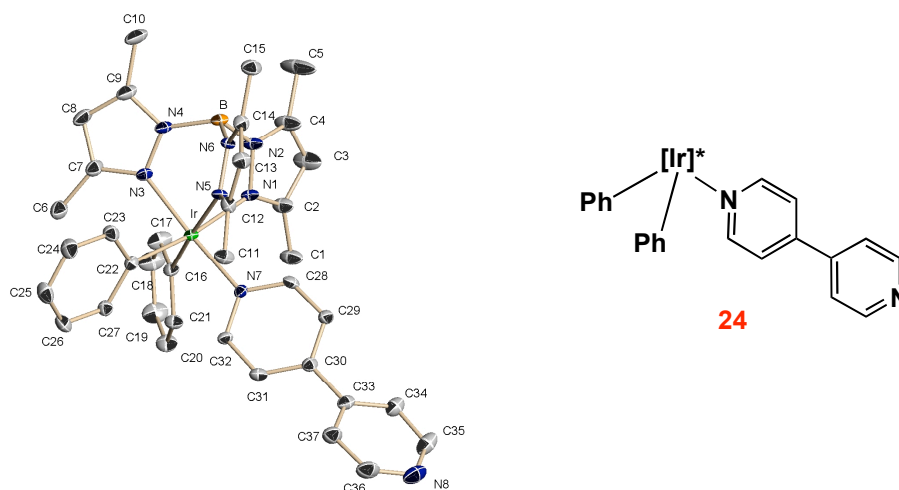


Tabla A21. Distancias (Å) y ángulos de enlace (°) seleccionados para **24**.

Longitudes de enlace (Å)			
Ir(1)—N(1)	2.169(5)	N(7)—C(28)	1.348(2)
Ir(1)—N(3)	2.052(5)	N(7)—C(32)	1.363(2)
Ir(1)—N(5)	2.164(4)	Ir(1)—C(22)	2.046(17)
Ir(1)—N(7)	2.069(3)	Ir(1)—C(16)	2.050(17)
Ángulos de enlace (°)			
N(3)-Ir(1)-N(5)	88.94(8)	C(22)-Ir(1)-C(16)	94.71(11)
N(3)-Ir(1)-N(1)	87.63(8)	C(22)-Ir(1)-N(3)	85.63(9)
N(5)-Ir(1)-N(1)	85.34(8)	C(16)-Ir(1)-N(3)	91.73(10)
C(16)-Ir(1)-N(1)	88.38(10)	C(22)-Ir(1)-N(7)	94.61(9)
Ángulo de torsión(°)			
C(29)-C(30)-C(33)-C(34)	-34.9(4)		

Tabla A22. Datos cristalográficos para el complejo **24**.

Fórmula	$C_{37}H_{40}BrN_8$	
Peso molecular	799.78	
Temperatura	273(2) K	
Longitud de onda	0.71073 Å	
Sistema cristalino	Monoclínico	
Grupo espacial	P2(1)/n	
Dimensiones de la celda unidad	$a = 8.8477(3)$ Å	$\alpha = 90^\circ$
	$b = 18.6297(5)$ Å	$\beta = 99.1270(10)^\circ$
	$c = 20.5562(6)$ Å	$\gamma = 90^\circ$
Volumen	$3345.38(17)$ Å ³	
Z	4	
Densidad (calculada)	1.588 Mg/m ³	
Coefficiente de absorción	4.031 mm ⁻¹	
F(000)	1600	
Dimensiones del cristal	0.17 x 0.19 x 0.12 mm ³	
Intervalo de toma de datos	1.48 a 36.23°	
Reflexiones medidas	73676	
Reflexiones independientes	12399 [R(int) = 0.1680]	
Índices R finales [$I > 2\sigma(I)$]	R1 = 0.0389, wR2 = 0.0959	
Índices R (todos los datos)	R1 = 0.0483, wR2 = 0.0975	

Complejo 25

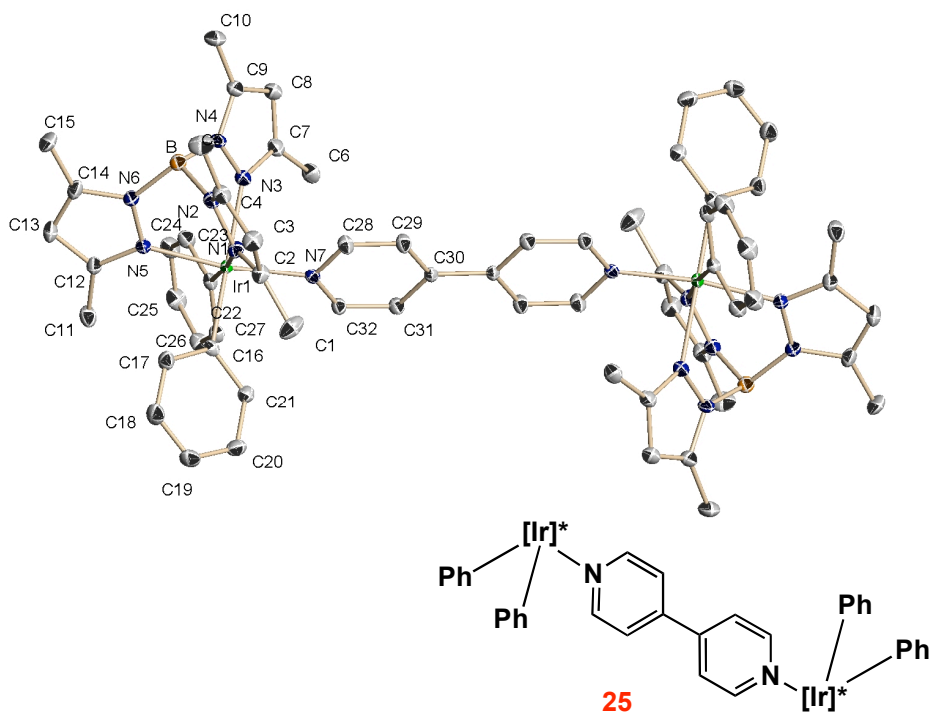


Tabla A23. Distancias (Å) y ángulos de enlace (°) seleccionados para **25**.

Longitudes de enlace (Å)			
Ir(1)—N(1)	2.154(2)	N(7)—C(28)	1.347(3)
Ir(1)—N(3)	2.171(2)	N(7)—C(32)	1.360(3)
Ir(1)—N(5)	2.055(18)	C(28)—C(29)	1.401(3)
Ir(1)—N(7)	2.066(13)	C(29)—C(30)	1.391(3)
Ir(1)—C(16)	2.050(2)	C(30)—C(31)	1.391(3)
Ir(1)—C(22)	2.059(2)	C(31)—C(32)	1.386(3)
Ángulos de enlace (°)			
C(16)—Ir(1)—N(5)	92.11(8)	N(5)—Ir(1)—N(7)	172.34(7)
C(16)—Ir(1)—C(22)	93.44(8)	C(22)—Ir(1)—N(3)	87.45(7)
N(5)—Ir(1)—C(22)	87.42(9)	N(7)—Ir(1)—N(3)	85.14(7)
C(22)—Ir(1)—N(7)	94.80(8)	C(16)—Ir(1)—N(1)	86.53(7)

Tabla A24. Datos cristalográficos para el complejo **25**.

Fórmula	$C_{33}H_{38}BCl_2IrN_7$		
Peso molecular	806.61		
Temperatura	273(2) K		
Longitud de onda	0.71073 Å		
Sistema cristalino	Monoclínico		
Grupo espacial	C2/c		
Dimensiones de la celda unidad	$a = 36.4221(6)$ Å	$\alpha = 90^\circ$	
	$b = 10.6726(2)$ Å	$\beta = 110.1720(10)^\circ$	
	$c = 18.2274(3)$ Å	$\gamma = 90^\circ$	
Volumen	$6650.7(2)$ Å ³		
Z	8		
Densidad (calculada)	1.611 Mg/m ³		
Coefficiente de absorción	4.210 mm^{-1}		
F(000)	3208		
Dimensiones del cristal	$0.35 \times 0.32 \times 0.22\text{ mm}^3$		
Intervalo de toma de datos	2.00 a 30.55°		
Reflexiones medidas	84445		
Reflexiones independientes	10085 [R(int) = 0.0906]		
Índices R finales [$I > 2\sigma(I)$]	R1 = 0.0273, wR2 = 0.0786		
Índices R (todos los datos)	R1 = 0.0301, wR2 = 0.0795		

Complejo 27

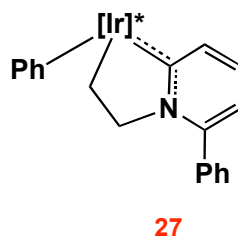
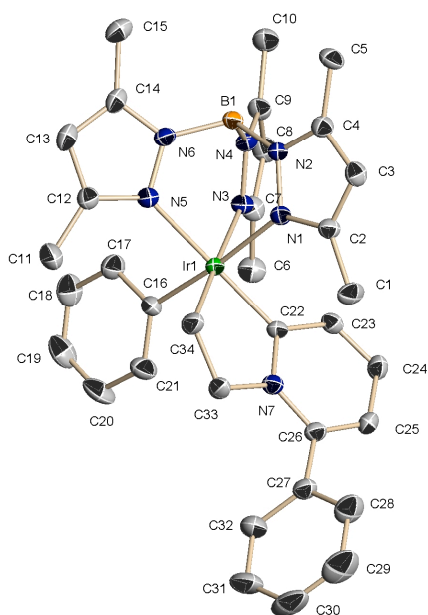


Tabla A25. Distancias (Å) y ángulos de enlace (°) seleccionados para **27**.

Longitudes de enlace (Å)			
Ir(1)—N(1)	2.163(2)	N(7)—C(33)	1.500(4)
Ir(1)—N(3)	2.172(2)	N(7)—C(22)	1.383(4)
Ir(1)—N(5)	2.142(2)	N(7)—C(26)	1.375(4)
Ir(1)—C(22)	1.949(3)	C(22)—C(23)	1.413(4)
Ir(1)—C(16)	2.042(3)	C(23)—C(24)	1.370(4)
Ir(1)—C(34)	2.063(3)	C(24)—C(25)	1.401(4)
C(33)—C(34)	1.534(4)	C(25)—N(26)	1.372(4)
Ángulos de enlace (°)			
N(1)—Ir(1)—N(3)	85.50(9)	C(22)—Ir(1)—C(16)	93.21(12)
N(5)—Ir(1)—N(3)	87.28(9)	C(22)—Ir(1)—C(34)	81.95(12)
N(5)—Ir(1)—N(1)	86.42(9)	C(16)—Ir(1)—C(34)	93.58(12)
Ángulo de torsión(°)			
C(25)—C(26)—C(27)—C(28)	57.0(4)		

Tabla A26. Datos cristalográficos para el complejo **27**.

Fórmula	$C_{34}H_{39}BIrN_7$	
Peso molecular	748.73	
Temperatura	173(2) K	
Longitud de onda	0.71073 Å	
Sistema cristalino	Triclínico	
Grupo espacial	P-1	
Dimensiones de la celda unidad	$a = 11.8571(2)$ Å	$\alpha = 70.6210(10)^\circ$
	$b = 11.8919(2)$ Å	$\beta = 69.7480(10)^\circ$
	$c = 14.0694(3)$ Å	$\gamma = 86.0300(10)^\circ$
Volumen	1753.41(6) Å ³	
Z	2	
Densidad (calculada)	1.418 Mg/m ³	
Coefficiente de absorción	3.839 mm ⁻¹	
F(000)	748	
Dimensiones del cristal	0.23 x 0.17 x 0.10 mm ³	
Intervalo de toma de datos	1.63 a 32.16°	
Reflexiones medidas	17251	
Reflexiones independientes	10972 [R(int) = 0.0244]	
Índices R finales [$I > 2\sigma(I)$]	R1 = 0.0327, wR2 = 0.0698	
Índices R (todos datos)	R1 = 0.0405, wR2 = 0.0717	

Complejo 30

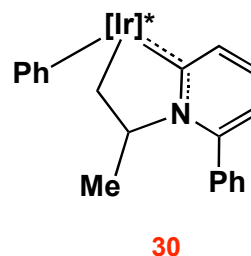
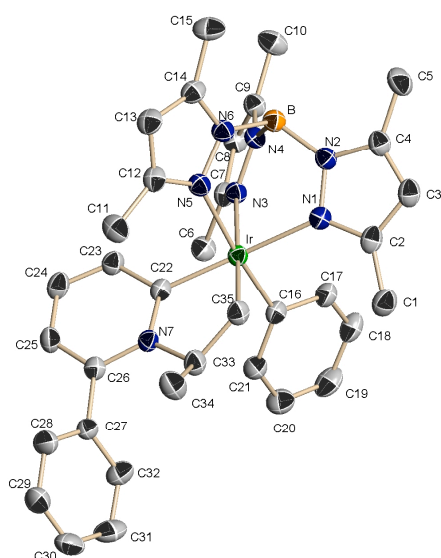


Tabla A27. Distancias (Å) y ángulos de enlace (°) seleccionados para **30**.

Longitudes de enlace (Å)			
Ir(1)—N(1)	2.143(4)	N(7)—C(26)	1.385(6)
Ir(1)—N(3)	2.178(4)	N(7)—C(33)	1.506(6)
Ir(1)—N(5)	2.191(4)	N(1)—C(22)	1.390(6)
Ir(1)—C(16)	2.041(5)	C(22)—C(23)	1.422(6)
Ir(1)—C(22)	1.949(5)	C(23)—C(24)	1.362(7)
Ir(1)—C(35)	2.056(5)	C(24)—C(25)	1.393(8)
C(33)—C(34)	1.525(8)	C(25)—C(26)	1.362(7)
Ángulos de enlace (°)			
N(1)—Ir(1)—N(3)	86.54(15)	C(22)—Ir(1)—C(16)	93.48(19)
N(1)—Ir(1)—N(5)	85.95(15)	C(22)—Ir(1)—C(35)	89.28(19)
N(3)—Ir(1)—N(5)	85.51(15)	C(16)—Ir(1)—C(35)	93.7(2)
C(22)—Ir(1)—N(5)	89.59(17)	C(16)—Ir(1)—N(1)	91.68(7)
Ángulo de torsión(°)			
N(7)—C(26)—C(27)—C(32)	-61.8(7)		

Tabla A28. Datos cristalográficos para el complejo **30**.

Fórmula	$C_{38}H_{46}BIrN_7$	
Peso Molecular	803.83	
Temperatura	273(2) K	
Longitud de onda	0.71073 Å	
Sistema cristalino	Monoclínico	
Grupo espacial	P2(1)/c	
Dimensiones de la celda unidad	$a = 12.0761(3)$ Å	$\alpha = 90^\circ$
	$b = 12.0451(3)$ Å	$\beta = 90.2150(10)^\circ$
	$c = 24.7165(6)$ Å	$\gamma = 90^\circ$
Volumen	$3595.18(15)$ Å ³	
Z	4	
Densidad (calculada)	1.485 Mg/m ³	
Coefficiente de absorción	3.751 mm ⁻¹	
F(000)	1620	
Dimensiones del cristal	$0.29 \times 0.13 \times 0.15$ mm ³	
Intervalo de toma de datos	1.65 a 28.28°	
Reflexiones medidas	72284	
Reflexiones independientes	8901 [R(int) = 0.0260]	
Índices R finales [$I > 2\sigma(I)$]	R1 = 0.0434, wR2 = 0.1095	
Índices R (todos los datos)	R1 = 0.0479, wR2 = 0.1129	

Complejo 35

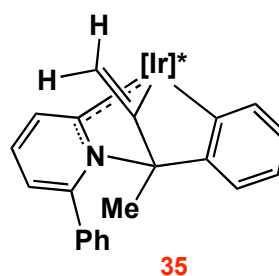
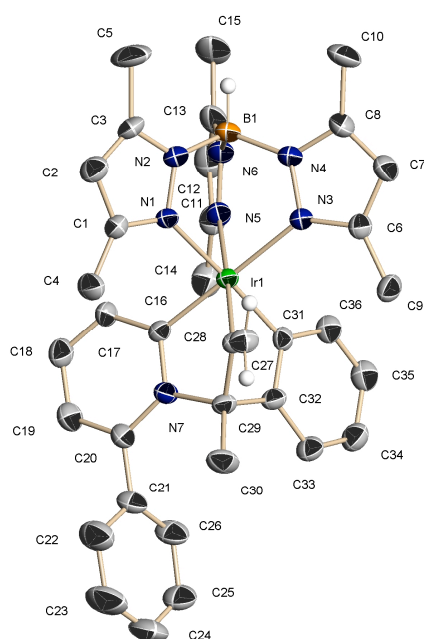


Tabla A29. Distancias (Å) y ángulos de enlace (°) seleccionados para **35**.

Longitudes de enlace (Å)			
Ir(1)—N(1)	2.131(7)	C(28)—C(29)	1.540(11)
Ir(1)—N(3)	2.159(6)	C(27)—C(28)	1.351 (11)
Ir(1)—N(5)	2.153(8)	C(29)—C(30)	1.505 (11)
Ir(1)—C(16)	1.948(8)	N(7)—C(16)	1.391(9)
Ir(1)—C(28)	1.998(8)	N(7)—C(20)	1.358(10)
Ir(1)—C(31)	2.008(9)	C(16)—C(17)	1.382 (10)
N(7)—C(29)	1.545(10)	C(17)—C(18)	1.334(12)
C(32)—C(29)	1.555(5)	C(18)—C(19)	1.433(13)
Ángulos de enlace (°)			
N(1)—Ir(1)—N(3)	87.1(3)	C(16)—Ir(1)—C(31)	86.7(3)
N(5)—Ir(1)—N(3)	84.4(3)	C(16)—Ir(1)—N(1)	91.8(3)
N(1)—Ir(1)—N(5)	85.4(3)	C(28)—Ir(1)—N(1)	97.1(3)
C(16)—Ir(1)—C(28)	79.9(3)	C(16)—Ir(1)—N(5)	96.2(3)
Ángulo de torsión(°)			
N(7)—C(20)—C(21)—C(26)	-70.6(15)		

Tabla A30. Datos cristalográficos para el complejo **35**.

Fórmula	$C_{36}H_{39}BrIrN_7$	
Peso molecular	772.75	
Temperatura	173(2) K	
Longitud de onda	0.71073 Å	
Sistema cristalino	Monoclínico	
Grupo espacial	$P2_1/n$	
Dimensiones de la celda unidad	$a = 18.5154(8)$ Å	$\alpha = 90^\circ$
	$b = 20.2030(8)$ Å	$\beta = 111.322(2)^\circ$
	$c = 19.3104(9)$ Å	$\gamma = 90^\circ$
Volumen	$6728.9(5)$ Å ³	
Z	8	
Densidad (calculada)	1.526 Mg/m ³	
Coefficiente de absorción	4.004 mm ⁻¹	
F(000)	3088	
Dimensiones del cristal	0.10 x 0.09 x 0.08 mm ³	
Intervalo de toma de datos	1.52 a 26.44°	
Reflexiones medidas	70346	
Reflexiones independientes	13345 [R(int) = 0.1016]	
Índices R finales [$I > 2\sigma(I)$]	R1 = 0.0516, wR2 = 0.1044	
Índices R (todos los datos)	R1 = 0.1563, wR2 = 0.1380	

IV. Conclusiones

Conclusiones

- El fragmento insaturado $[\text{Tp}^{\text{Me}_2}\text{Ir}(\text{C}_6\text{H}_5)_2]$, generado *in situ*, reacciona con diversas piridinas sustituidas en la posición 2 con formación de los correspondientes carbenos N-heterocíclicos mediante un proceso de tautomería, que es resultado de una migración formal 1,2 de un átomo de hidrógeno. Las piridinas sustituidas en otras posiciones del anillo no experimentan esta reorganización y de los estudios mecanicistas realizados se concluye que la transformación es estrictamente intermolecular y que el grupo fenilo y su ácido conjugado, el benceno, actúan como aceptor-donador del átomo de hidrógeno.
- La formación de los aductos coordinados a través del átomo de nitrógeno de las piridinas sustituidas en la posición 2 se encuentra desfavorecida debido a la tensión frontal entre el sustituyente y los ligandos del fragmento insaturado $[\text{Tp}^{\text{Me}_2}\text{Ir}(\text{C}_6\text{H}_5)_2]$, y sólo se ha observado en algún caso, como producto cinético (por ejemplo con la 2-picolina). Estos aductos son menos estables termodinámicamente que los correspondientes carbenos y se transforman en ellos mediante calentamiento de sus disoluciones a temperaturas adecuadas.
- Diversos experimentos de intercambio con piridina deuterada confirman la labilidad de los enlaces Ir–N de todos los aductos-N, tanto los que forman carbenos como los que no, por lo que esta propiedad no es condición suficiente para la formación de carbenos N-heterocíclicos. Por lo tanto, la formación de los carbenos N-heterocíclicos con las piridinas sustituidas en la posición 2 no se debe a la labilidad de los correspondientes aductos, sino a su menor estabilidad termodinámica en comparación con sus carbenos isómeros.

- Las polipiridinas bpy, phen y terpy reaccionan con el fragmento insaturado $[\text{Tp}^{\text{Me}_2}\text{Ir}(\text{C}_6\text{H}_5)_2]$, para formar los correspondientes carbenos N-heterocíclicos, lo que corresponde a un nuevo modo de coordinación, previamente desconocido, como ligandos carbeno mododentados, que se unen al centro metálico a través del átomo de carbono adyacente al uno de nitrógeno.
- Los carbenos N-heterocíclicos derivados de las piridinas sustituidas en la posición 2 reaccionan con etileno y propeno, con eliminación de una molécula de benceno, dando lugar a complejos metalacíclicos que provienen de la formación de nuevos enlaces C–N e Ir–C. En el caso del propeno se observa la formación de dos diastereoisómeros, en equilibrio termodinámico, cuyas proporciones varían dependiendo del grupo R en el fragmento piridínico. La reacción con los complejos carbeno con propeno es reversible.
- Los carbenos N-heterocíclicos derivados de las piridinas sustituidas en la posición 2, reaccionan con acetileno, para dar origen a una mezcla de compuestos, de la cual es posible aislar dos especies. En una de ellas se observa la incorporación y acoplamiento de dos moléculas de acetileno, mientras que en la otra se observa la adición de una molécula de agua al triple enlace. En ambos casos se observa la eliminación de una molécula de benceno, del mismo modo que ocurre en las reacciones con el etileno y el propeno.

Conclusions

- The unsaturated fragment $[\text{Tp}^{\text{Me}_2}\text{Ir}(\text{C}_6\text{H}_5)_2]$ generated *in situ* reacts with several 2-substituted pyridines, giving rise to the formation of the corresponding N-heterocyclic carbenes. These complexes result from a tautomerization process consisting formally in a 1,2 hydrogen shift. Pyridines with substituents in other positions of the ring other than 2 do not undergo tautomerization. The mechanistic studies performed allow us to conclude that it is an intermolecular process where the phenyl group and its conjugated acid, benzene, act respectively as hydrogen accepting and transferring agents.
- The formation of N-bound adducts for 2-substituted pyridines is disfavoured due to F-strain effects between the 2-substituent and the ligands of the unsaturated fragment $[\text{Tp}^{\text{Me}_2}\text{Ir}(\text{C}_6\text{H}_5)_2]$. The N-bound adducts have been observed only in a few cases, as kinetic products (for instance with 2-picoline). These adducts are less stable than their carbene tautomers and are cleanly converted to the latter at suitable temperatures.
- Several exchange experiments with deuterated pyridine confirm the lability of the Ir–N bond of all N-bound adducts, regardless of whether or not they may transform into corresponding carbenes. Therefore, the generation of carbenes cannot be ascribed to this property and for 2-substituted pyridines carbene formation is due to their superior thermodynamic stability with N-bound adducts.
- Polypyridines bpy, phen and terpy react with $[\text{Tp}^{\text{Me}_2}\text{Ir}(\text{C}_6\text{H}_5)_2]$ to generate the corresponding N-heterocyclic carbenes. This constitutes a

new, previously unknown, coordination mode, as monodentate ligands, that bind to the metal centre through a carbon atom adjacent to nitrogen.

- The N-heterocyclic carbenes derived from 2-substituted pyridines, react with ethylene and propene, with elimination of a benzene molecule, generating metallacyclic complexes that result from the formation of new C–N and Ir–C bonds. In the case of propene, two diastereoisomers are formed, (in thermodynamic equilibrium), with their ratio depending on the substituent in the pyridinic fragment. With propene the reaction is reversible, whereas for ethylene it is not.
- The N-heterocyclic carbenes derived from 2-substituted pyridines, react with acetylene to generate a mixture of compounds from which it is possible to isolate two compounds. One of them is the result of the incorporation and coupling of two acetylene molecules, whereas the other results from the addition of one water molecule to the triple bond. In both cases, formation of the final products is accompanied with elimination of benzene.

